The Role of Transglutaminase 2 isoforms in Breast Carcinogenesis

A thesis submitted to the University of Manchester for the degree of Doctor of Philosophy in the Faculty of Biology, Medicine, and Health

2022

Nuha Alshahrani

Division of Pharmacy and Optometry
School of Health Sciences
Faculty of Biology, Medicine, and Health
University of Manchester

[Blank page]

Table of Contents

Word Count: 37,592

List of figures

List of Tables

List of Abbreviations

AI	Aromatase inhibitor
ALDH	Aldehyde dehydrogenase
ANA	Anastrozole
Arg580	Arginine 580
Asp	Aspartate
ATRA	All-trans-retinoic acid
BC	Breast cancer
BSA	Bovine serum albumin
cdks	Cyclin-dependent kinases
CRABP	Cellular retinoic acid-binding proteins
CYP	Cytochrome P450
Cys	Cysteine
DEX	Dexamethsone
DMSO	Dimethyl sulfoxide
DOX	Doxorubicin
E-cad	E-cadherin
E2	ß-estradiol
EM	Energy metabolism
EMT	Epithelial-mesenchymal transition
ER	Estrogen receptor
ER	Endoplasmic reticulum
FRET	Fluorescence resonance energy transfer
GPCR	G protein-coupled receptor
GS	Growth signals
GTP	Guanosine triphosphate
h	Hour
HAT	Histone acetyltransferase activity
HDAC	Histone deacetylase
HDACI	Histone deacetylase inhibitor
HER2	Human epidermal growth factor receptor 2

His	Histidine
IkBα	Nuclear factor of kappa light polypeptide gene enhancer in B-cells inhibitor, alpha
LBD	Ligand binding domain
MCF.7	Michigan cancer foundation-7
MET	Mesenchymal-epithelial transition
MTT	3-(4,5-dimethylthiazol-2-yl)-2,5-diphenyl tetrazolium bromide
N-cad	N-cadherin
ND	Neurodegenerative diseases
NF-κB	Nuclear factor kappa-light-chain-enhancer of activated B cells
PA	Protein aggregation
PDI	Protein disulfide isomerase
PLC-δ1	Phospholipase C-δ1
PR	Progesterone receptor
pRb	Retinoblastoma protein
R580	Arginine 580
RA	Retinoic acid
RALDH	Retinaldehyde dehydrogenases
RAR	Retinoic acid receptor
RAREs	Retinoic-acid responsive elements
RBP	Retinol-binding proteins
RLX	Raloxifen
ROS	Reactive oxygen species
RXRs	Retinoid X receptors
SAHA	Suberoylanilide hydroxamic acid
SERM	Selective oestrogen receptor modulator
siRNA	Small interfering Ribonucleic Acid
SRB	Sulforhodamine B
SRC-1	Steroid receptor co-activator 1
TG2	Transglutaminase 2 protein
Tgase	Transglutaminase

TGM2	Transglutaminase 2 gene
TMX	Tamoxifen
TNF	Tumour necrosis factor
TSA	Trichostatin A
VEGF	Vascular endothelial growth factor

Abstract

Background: The formation of cancer stem cells is an important factor for breast cancer growth, metastasis, and response to treatment, hence prognosis. Elevated levels of the Ca^{2+} dependent enzyme transglutaminase 2 (TG2) have been identified in cancer cells displaying resistance to anti-cancer treatment or those isolated from metastatic sites, implying TG2's involvement in these processes. TG2 is a multifunctional enzyme with different activities, including transamidase, GTPase, protein disulfide isomerase, and protein kinase. The various enzymatic activities and functions of TG2 may be referred to alternative splicing of TG2 mRNA. This study aims to investigate the role of the TG2 different isoforms in breast carcinogenesis by assessing their contribution to various carcinogenic processes, including transformation to cancer stem cells and acquisition of the EMT phenotype. **Methods:** The protein levels of the different TG2 isoforms have been investigated in the ERα positive MCF-7 and T47D and the triple negative MDA-MB-231 and MDA-MB-468 breast cancer cell lines. The transamidase activity was measured by TG2-CovTest. The ability of the different TG2 isoforms to confer stemness to these cells has been evaluated following mammosphere formation and expression level of the cancer stem cell (CSC) markers CD44 and CD24 in the presence or absence of the different TG2 isoforms. EMT has been evaluated by following the protein expression of the epithelial marker E-cadherin and the mesenchymal markers N-cadherin and vimentin. **Results:** MDA-MB-231, expresses both the TG2-L and TG2-S isoforms. MCF-7 and T47D also express both isoforms but to a very lower extent compared to MDA-MB-231, whereas MDA-MB-468 expresses only the TG2-S isoform. ZDON increased the $CD44^{+}/CD24^{-/low}$ phenotype and ALDH activity. NC9 induced the $CD44^{+}/CD24^{-/low}$ phenotype and increased ALDH activity to a higher extent than ZDON. In MDA-MB-231, silencing of the TG2 gene expression by siRNA significantly reduced $CD44^{+}/ CD24^{-/low}$ phenotype, ALDH activity and mesenchymal marker vimentin. **Conclusion:** Human breast cancer cell lines express two TG2 isoforms, which exhibit differential roles in CSC and EMT. The $CD44^{+}/CD24^{-/low}$ phenotype is linked to high basal expression of TG2-L in MDA-MB-231. The GTP-binding domain (GTPase activity) of TG2 plays an important role in promoting its carcinogenic effects, whereas its transamidase activity is not essential. The catalytic-binding domain (transamidase activity) reduces the oncogenic effect of TG2, reduces stemness traits, and EMT phenotype.

Declaration

that no portion of the work referred to in the thesis has been submitted in support of an application for another degree or qualification of this or any other university or other institute of learning.

Copyright statement

Acknowledgements

First and foremost, I would like to praise Allah the Almighty, the most gracious, and the most merciful for His blessing given to me during my study and in completing this thesis. May Allah's blessing goes to His Final Messenger, Mohammed, (peace be upon him), his family and his companions.

I would like to express my sincere gratitude to my supervisor, Dr Constantinos Demonacos. His guidance, inspiring supervision, motivation, and immense knowledge helped me in all the time of research and writing of this thesis. His presence and support helped me navigate my way through this study. I was able to grow and learn through every part of this journey with the advantage of his advice. I wish to express my sincere gratitude and appreciation to Prof. Marija Krstic Demonacos for her important and helpful input and advice during the research group meetings.

I must express my heartfelt appreciation to my dear mother Aysha and father Saeed for their unwavering support and encouragement during my studies. I am immensely thankful for their emotional support, continuous care, patience, encouragement, and unconditional love, which provided me with the most strength to accomplish this PhD journey. This achievement would not have been possible without their assistance.

A special thanks to Dr Gareth Howell at Flow cytometry core facility for his help and input.
I am also thankful to my lab members, Dr Rasheed, Hend, Kawther, Najla, and Abdul Hameed. A special thanks to Kawther for her inspiring talks and Najla for her care and thoughtfulness. And I cannot forget my gratitude to the Experimental Oncology group: Dr Mai for her valuable advice in the lab, Dr Heather, Alex, Amira, and Dr Abid.

PhD life is filled with so many peaks and troughs, and I am thankful to my friends, Khaleda, Alya, Mohra, Alya Basak and Ala'a, who shared this experience with me. I appreciate our time spent together. Every part of it made a beautiful impact throughout these years. I am also thankful for the fond memories at the Stopford building for coffee and talks with Dr Reem, Dr Maryam, Dr Amal, Sarah, Muna, and Sajwa. Where we shared our ups and downs, our

experiences, our new achievements and much more. Such simple moments gave me comfort and ease.

My life in Manchester would not have been as lovely and unforgettable had it not been for my amazing neighbors, Jawaher, Amna, and Andria. Being far from home and from your loved ones is tough, but having such wonderful people close to me gave me the strength to live through it. Especially Amna, who I cannot thank enough for sharing every moment of my journey with me through the good and the bad. When I think back to the sorrowful moments, I remember your presence and how much comfort and strength it gave me. You hold a warm and beautiful memory that will forever be engraved in my mind.

Thank you again to my parents, who worked countless hard hours and endured countless hardships to ensure that my sister and I could have a comfortable life and access to an education that they couldn't have. No words will ever be enough to express the gratitude and respect that I hold for you. Your determination and love for learning inspired me to be the person that I am today, to always push myself to be better and to never waste an opportunity. Thank you for always keeping me in your prayers and encouraging me at every chance. Thank you to my family, Maram, Abdulaziz, Ohood, Sarah, Jana, Rasil and our little Saeed. The happiness your presence gives me is indescribable. You always kept me in your thoughts and prayers and reminded me that I would always have someone to fall back on. And thank you to my father-in-law and my sisters-in-law, Fayza, Fawzya, and Fareda. I will always remember your prayers, love, and support, and to my beloved mother-in-law, who left this world during my PhD journey; may your soul rest in peace and may we be reunited in heaven.

An exceptionally warm thanks to my dearest husband. I don't know how to thank you because I have no words big enough to express my gratitude for all you have done for me during these years. You gave me your love, your support, your kind words, your advice, your guidance, and everything I could ever need. Your presence felt like a constant warm and peaceful embrace that made me push through my troubles and hardships. Thank you from the bottom of my heart.

Finally, I am very grateful to The Ministry of Education in Saudi Arabia and The Saudi Cultural Bureau in London for the financial support and funding for the project.

Dedication

I dedicate my thesis to my beloved parents, for their endless love, support, and encouragement.

Chapter 1

Introduction

1. Chapter 1: Introduction

1.1 Cancer

1.1.1 Brief overview

Cancer is defined as a cellular disease characterised by uncontrolled cell proliferation (Warburg, 1956). Cancer is a major cause of human mortality, and the number of diagnosed cases consistently increases due to environmental conditions and modern life habits. Cancer is associated with genetic mutations and DNA damage, leading to deregulation of cell proliferation, differentiation, and cellular homeostasis. Genes involved in carcinogenesis mainly exhibit their effects via direct regulation of cell proliferation, programmed cell death (apoptosis, necroptosis, etc.), or repair of damaged DNA (Fearon and Dang, 1999). Hence, genes regulating cancer can be categorized into two classes: tumour suppressor genes, such as Retinoblastoma (RB) and p53 protein; and oncogenes, like Ras (Hyland, 2008). Therefore, a focus on these genes could provide a potential target for the treatment of cancer. p53 is a tumour suppressor gene that contributes to cellular functions, including apoptosis, DNA damage repair, cell cycle control, metabolic reprogramming, invasion and metastasis, and regulation of immune response (Lane, 1993; Silva *et al.*, 2014). However, inactivation of this gene by single point mutations has been found in more than 50% of tumours. p53 mutations are found as aggregates in different tumour cell lines. These mutations inactivate the p53 transcriptional activity, thereby dysregulating the expression of genes targeted by this tumour suppressor, leading to defects in pathways such as apoptosis and providing a survival advantage to cancer cells (Kim and An, 2016).

1.1.2 The hallmarks of cancer

Hanahan and Weinberg described the characteristic features of cancer cells that facilitate the development of carcinogenesis based on research which has identified the tumour acquired biological capabilities shared among most types of human cancers (Hanahan and Weinberg, 2000, 2011). In 2000, six essential alterations called "cancer hallmarks" were identified, including self-sufficiency in growth signals, insensitivity to anti-growth signals, evading apoptosis, limitless replicative potential, sustained angiogenesis, and tissue invasion and metastasis (Hanahan and Weinberg, 2000). In 2011, two enabling and two emerging

characteristics were added to the six previously identified hallmarks, which are genome instability and mutation, tumour promoting inflammation, reprogramming energy metabolism, and evading immune destruction (Hanahan and Weinberg, 2000, 2011). A recent review published in 2022 by Hanahan reported two new hallmark capabilities , including phenotypic plasticity and disruption of differentiation. Additionally, two characteristics that enable the acquisition of hallmark capabilities were added: non-mutational epigenetic reprogramming and polymorphic microbiomes (Figure 1.1) (Hanahan, 2022).

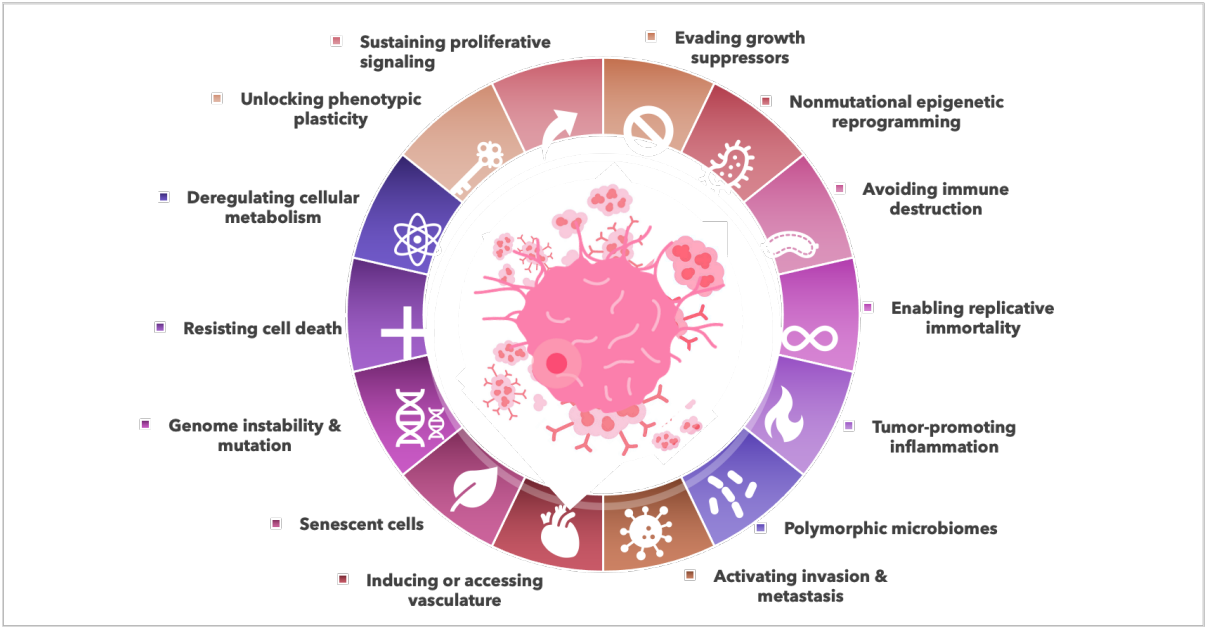

Figure 1-1 The hallmarks of cancer

1.1.2.1 Self-sufficiency in growth signals

Normal cells require mitogenic growth signals (GS) that stimulate cellular growth, proliferation, and differentiation. These GS are transmitted into the cell via receptors that possess transmembrane domains that allow the transmission of signals for the surrounding environment inside the cell. These receptors include extracellular matrix components (ECM), diffusible growth factors, and cell-to-cell adhesion/interaction molecules (Hanahan and Weinberg, 2000, 2011). Normal cells are unable to proliferate in the absence of stimulatory signals. In contrast, cancer cells are less dependent on exogenous GS, present in the normal

tissue microenvironment, and release their own signals which, in turn, change the tissue microenvironment and allow them to acquire independence from exogenous growth factors and self-regulate their growth (Hanahan and Weinberg, 2000, 2011). Three molecular strategies have been identified for achieving GS autonomy in cancer cells. First, cancer cells can alter the level of extracellular growth signals. Unlike normal cells, which release growth factors (GFs) created by one cell type to stimulate the proliferation of another type, cancer cells generate their own GFs to stimulate others of their kind. Consequently, this creates a positive feedback signaling loop, termed autocrine stimulation (Hanahan and Weinberg, 2000). Second, cancer cells modify the cell surface receptors that transduce signals from outside of the cell into it. In normal cells, GF binds to GF receptors and activates intracellular phosphorylation reactions via tyrosine kinase enzymes that trigger signaling cascades that regulate cellular growth and differentiation. Overexpression of cell surface receptors allows sustained proliferation of cancer cells by transforming them to be hyper-responsive to GF signals that normally do not stimulate signaling cascades at that stage (Hanahan and Weinberg, 2000). Third, cancer cells cause alterations of components of the downstream cytoplasmic circuits, converting them to constitutively active growth signals. For instance, Ras, a protein involved in cellular signal transduction, is found to be mutated and structurally altered in about 25% of human cancers. This alteration enables Ras to produce GS without stimulation of normal upstream regulators (Hobbs, Der and Rossman, 2016).

1.1.2.2 Insensitivity to anti-growth signals

The cell cycle is a complex process that controls cellular growth, proliferation, and expansion. Various regulatory proteins are involved in the direction of the cell cycle via a series of actions inside the cell. These actions are strictly time-regulated, taking place at a precise time during one of the four phases of the cell cycle resulting in the division of one parental cell into two identical daughter cells (Collins, Jacks and Pavletich, 1997). The cell cycle is divided into four phases: the Gap1 (G1), synthesis (S), Gap2 (G2), and mitosis (M) phases. The G1 and G2 phases are indicated by gaps that occur between the DNA synthesis (S) phase and the mitosis (M) phase. In the gap 1 (G1) phase, the cell increases in size, preparing for DNA synthesis. In the synthesis (S) phase, the DNA is replicated, and the cells continue to grow, preparing for mitosis in the gap 2 (G2) phase. The mitosis (M) phase indicates the end of cell growth, and

the cell divides into two daughter cells. In addition to those four phases, the G0 phase is the quiescence phase, during which the cells have left the cell cycle but have the potential to divide (Collins, Jacks and Pavletich, 1997). The transition from one phase of the cell cycle to the next and the prevention of one phase from returning to the previous phase are monitored by checkpoints, defined as biochemical pathways, that ensure the order and timing of cell cycle transitions and the completion of critical processes. There are three major checkpoints in the cell cycle: the G1 checkpoint, which determines whether the cells are ready to enter the synthesis phase, the G2 checkpoint, which checks whether the DNA has been replicated accurately and there are no mutations introduced; and the M phase checkpoint, which ensures the chromosome is attached to the spindle (Figure 1.2) (Collins, Jacks and Pavletich, 1997).

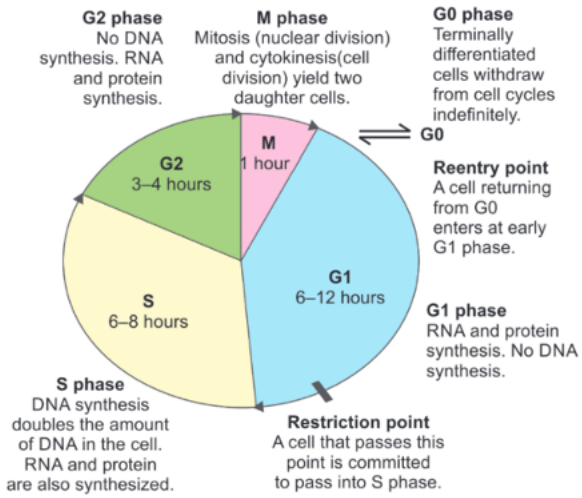

Figure 1-2 The cell cycle and checkpoints (Ray *et al.*, 2020)

In addition to those checkpoints, there are two groups of intracellular molecules that regulate the cell cycle by promoting cell progression to the next phase (positive regulation) or by terminating the cell cycle (negative regulation). In positive regulation, molecules such as cyclins and cyclin-dependent kinases (Cdks) are activated at specific time points during the cell cycle to regulate cell cycle progression, and their inactivation prevents mitosis (Collins, Jacks and Pavletich, 1997; Lim and Kaldis, 2013). In negative regulation, many tumour suppressor genes are involved in halting the progression of the cell cycle (Hanahan and Weinberg, 2011).

In normal cells, anti-proliferative signals – growth inhibitors – maintain cellular quiescence and tissue homeostasis. These inhibitors exhibit their effect in one of two ways: by forcing the cells out of the active proliferative cycle into the quiescent (G0) state, or by inducing the cells to enter a post-mitotic state where the cells are unable to undergo mitosis (Hanahan and Weinberg, 2000). In contrast, as cancer cells can sustain proliferative signals, they can also evade programs that negatively regulate cell proliferation. Many of these programs depend on the actions of tumour suppressor genes. However, those genes are found to be inactivated in cancer cells, such as the retinoblastoma protein (pRb) and the p53 tumour suppressor (Weinberg, 1995; Hanahan and Weinberg, 2000, 2011).

1.1.2.3 Evading apoptosis

Apoptosis is defined as a programmed cell death pathway in the event of DNA damage that is beyond repair (Hanahan and Weinberg, 2000). Cancer cells evade apoptotic signals and have acquired resistance to this mechanism. Several physiological stresses can trigger apoptosis, which results during the course of tumorigenesis or as a result of anti-cancer treatment (Hanahan and Weinberg, 2011). The main regulator of the intrinsic pathway of apoptosis is a family of proteins known as the Bcl-2 (B-cell leukemia) family. These proteins are divided into two groups: pro-apoptotic proteins, such as Bax, Bad, Bid, Bok, Bik and Bak and anti-apoptotic proteins, such as Bcl-2, Bcl-XL, Bcl-W, Mcl-1, and A1. While normal cells are controlled by counterbalancing pro-apoptotic and anti-apoptotic proteins of the Bcl-2 family, cancer cells produce excessive amounts of anti-apoptotic proteins which, in turn, downregulate the pro-apoptotic proteins and resist apoptosis (Hanahan and Weinberg, 2011). In normal cells, the p53 tumour suppressor gene detects damaged DNA and activates mechanisms of DNA damage repair or induces pro-apoptotic proteins to initiate apoptosis in the event that the DNA damage is extensive. However, this protein is mutated in more than 50% of cancer cases, thus facilitating cancer progression (Rivlin *et al.*, 2011).

1.1.2.4 Limitless replicative potential

Normal cells undergo a limited number of successive cell cycle rounds and divisions, known as the Hayflick Limit (Hanahan and Weinberg, 2000). Telomerase is a reverse transcriptase enzyme that catalyses the addition of short DNA fragments to the lagging strand in order to

complete replication.The biological significance of the telomere is that it protects chromosomes from recombination, end-to-end fusion and serves as a molecular clock that controls the replicative capacity of human cells and their entry into senescence. Normal cells proliferate a limited number of times. The gradual shortening of telomeres after the completion of each replication cycle monitors the replicative history of cells. This mechanism prevents the development of cancer in aged cells by limiting the number of cell divisions. The cell detects the very short telomeres as DNA damage and enters the processes of cellular senescence, growth arrest, or apoptosis. Cancer cells become immortalised by telomere extension, mostly due to the activation of telomerase, which induces limitless replication (Hanahan and Weinberg, 2000, 2011; Hiyama and Hiyama, 2007).

1.1.2.5 Tissue invasion and metastasis

Cancer cells can escape from their site or organ of origin to invade surrounding tissue, travelling to a distant site to form new colonies. The new colonies, known as metastasis, are the main cause of death in more than 90% of cancer patients. E-cadherin is a cell-to-cell adhesion molecule that acts as a suppressor of invasion and metastasis in epithelial cells. However, the function of E-cadherin and other adhesion molecules is lost in many types of cancer, thus the cell-cell contacts are weakened, and cells acquire characteristic features that allow them to survive without needing to be bound to other cells in the tissue and become competent to migrate to distant sites (Hanahan and Weinberg, 2000, 2011). The attainment of these characteristics takes place through the biological process called epithelial-mesenchymal transition (EMT) and during this procedure, epithelial cells are transformed into mesenchymal cells (Mani *et al.*, 2008)

1.2 Breast cancer

1.2.1 Brief overview of Breast Cancer

According to the GLOBOCAN 2020 data, breast cancer is the most diagnosed cancer in women worldwide, with an estimated 2.3 million new cases each year, and it is the 5th cause of cancer death (Sung *et al.*, 2021). Although the exact mechanisms by which breast cancer originates are not clear, different risk factors contribute to its development and progression.

Breast cancer is a heterogeneous disease with different morphological and biological characteristics that affect the clinical behaviour and treatment outcomes. Thus, breast cancer classification aids in accurately diagnosing, describing the cancer's aggressiveness, and predicting the metastatic potential to other organs and the outcome of treatment. Breast cancers are classified histologically depending on their tumour cell type, extracellular secretion, architectural features, and immunohistochemical profile.

1.2.2 Classification of breast cancer

Histological classification

More than 20 different histological types of invasive carcinoma have been identified, including invasive ductal carcinoma no specific type (IDC-NST) (around 70% to 80% of all invasive cancers), invasive lobular carcinomas (around 10%), in addition to the less common histological types, such as micropapillary, papillary, tubular, medullary, mucinous, cribriform, metaplastic, and apocrine carcinomas (Tsang and Tse, 2020).

Molecular classification:

Breast cancer can also be classified into five molecular subtypes based on mRNA gene expression levels, including luminal, HER2-enriched, basal-like, normal breast-like (Perou *et al.*, 2000; Bernard *et al.*, 2009), and claudin-low breast cancer (Herschkowitz *et al.*, 2007). Luminal breast cancers are further classified into luminal A and B subtypes. Both subtypes are ER-positive tumours that account for over 70% of all breast cancer cases in Western countries. Luminal A subtype is defined as ER-positive and/or PR-positive and HER2-negative, whereas luminal B subtype expresses ER and may also express PR and/or HER2 (Tsang and Tse, 2020).

Immunophenotype classification:

ER, PR, and HER2 are the key predictive biomarkers, used in diagnosis and clinical decision-making for hormonal or anti-HER2 therapy.

Estrogen mediates its effect through two receptor proteins, ERα and ERβ, which are encoded by the ERS1 and the ERS2 genes, respectively (Jordan, 2004). In normal tissues, the function of ERβ is uncertain. In breast cancer, ERα and ERβ have opposing effects. ERα is highly

expressed in ER-positive breast cancers and is linked to with progression (Leygue *et al.*, 2000). On the other hand, only low levels of ERβ have been found and the loss of its expression in breast cancer has been linked to enhanced proliferation (Lazennec *et al.*, 2001; Huang *et al.*, 2014).

The active form of the estrogen hormone, 17 β-estradiol interacts with the ERα to regulate the reproductive system, bone metabolism, cardiovascular and nervous system. The link between estrogen and breast cancer was first identified by George Beatson in 1896 after breast cancer progression was observed to slow in a patient subjected to ovariectomy (Beatson, 1896). ER-positive breast cancer expressing ERα, which accounts for 70% of all breast cancer cases, is sensitive to anti-estrogen therapy (Robertson, 1996).

Based on hormone receptor status, breast cancer can be classified into three groups namely: i) Hormone receptor positive (estrogen receptor (ER^+) or progesterone receptor (PR^+)), ii) human epidermal receptor 2 positive ($HER2^+$), and iii) triple-negative breast cancer (TNBC) (ER^-, PR^-, $HER2^-$), which further classified into six molecular subtypes (Lehman's classification); basal-like 1 (BL-1), basal-like 2 (BL-2), mesenchymal (M), mesenchymal stem cell-like (MSL), immunomodulatory (IM), and luminal androgen receptor (LAR) (Lehmann *et al.*, 2011). Hormone receptor positive is the most common type of breast cancer, accounting for 60–70% of cases in developed countries, primarily in pre-menopausal women. In ER^+ breast cancer, two treatment approaches have been used, including: i) estrogen receptor blocking by anti-estrogens such as tamoxifen. ii) or prevention of hormone production from the ovaries (Reinert and Barrios, 2015). The standard treatment in $HER2^+$ patients is the use of anti-HER2 monoclonal antibodies such as trastuzumab. Triple negative breast cancer (TNBC) represents 10–20% of all breast cancers and its treatment is very challenging in comparison to other types of breast cancer. Chemotherapy is the most extensively used treatment for this group of patients. Combination of chemotherapy with humanized monoclonal antibody against vascular endothelial growth factor (VEGF) such as the bevacizumab is also used (Li *et al.*, 2015).

Histopathological grading classification

Grading classification of breast cancers includes microscopic evaluation of histologic differentiation in the form of tubule formation, nuclear pleomorphism, and proliferation as indicated by the mitotic index. The Nottingham grading system is the most extensively used to classify diverse types of breast cancer. Grade 1 relates to scores between 3 and 5, Grade 2 corresponds to a score of 6 or 7, and Grade 3 refers to a score of 8 or 9 (Ivshina *et al.*, 2006).

1.2.3 p53 and breast cancer:

Genetic mutations in cancer can be inherited and affect all cell types or can be acquired (somatic), which is more common in breast cancers and affects only the cancer cells (Bland *et al.*, 2017). p53 is a tumour suppressor protein that regulates tissue homeostasis by controlling cell proliferation proteins, and its inhibition at the gene or protein level facilitates oncogenesis and cancer progression. Mutations in the TP53 gene, which encodes the p53 protein, result in the accumulation of inactive mutant p53 protein, giving malignant cells with mutated p53 a survival advantage and resistance to antigrowth signals (Hanahan and Weinberg, 2011). A major p53 target is p21, which inhibits cell cycle progression at the G1/S transition by inhibiting the kinase activity of cyclin D and cdk4/6 to allow for DNA damage repair to take place. In addition to various apoptotic target genes, including PUMA, Bax, and Noxa (El-Deiry *et al.*, 1993; Vousden and Prives, 2009; Berger *et al.*, 2012).

1.2.4 Treatment of breast cancer

The therapy of breast cancer has developed to incorporate molecular diversity, with a greater emphasis on biologically tailored medications and therapies with minimal adverse effects. BC has been controlled with several strategies, including surgery, chemotherapy, radiation, and endocrine therapy, depending on the tumor's stage, hormone receptor status, and disease progression. Two endocrine treatment strategies have been used in ER+ breast cancer: i) blocking the oestrogen receptor with anti-estrogen, in which selective oestrogen receptor modulators (SERMs) and down regulators (SERDs) are used. ii) lowering the amount of circulating oestrogen accessible to the receptors, in which ovarian suppression in pre-menopausal women and aromatase inhibitors in post-menopausal women are used (Lumachi, 2015). SERMs, such as tamoxifen and raloxifene, act as competitive inhibitors of estrogen

(Dunn and Ford, 2001; Vogel *et al.*, 2003). The aromatase enzyme directs the production of oestrogen to produce progesterone and androgens. This enzyme's activity is inhibited by aromatase inhibitors (AIs), which suppress oestrogen levels in the blood (Budillon, Carbone and Di Gennaro, 2013).

1.2.5 Drug resistance

Chemo-therapeutic resistance and metastasis of primary tumours to distant sites are the major challenges to successful treatment of cancer (Verma and Mehta, 2007). Most anticancer drugs exert their effect by activating apoptosis; hence, deregulation of the apoptotic pathway results in chemo-resistance. Several modifications that generate resistance to apoptosis have been recognised. These include three mechanisms: (a) activation of pro-survival signal transduction pathways; for instance, those mediated by Ras or nuclear factor kappa B (NF-κB); (b) inactivation of apoptotic pathways, such as mutation or silencing of p53 and pRb; or (c) overexpression of pro-survival proteins such as Bcl-2 (Fesik, 2005). Recently, elevated levels of the multifunctional enzyme transglutaminase 2 (TG2) have been reported in cancer cells that display resistance against anti-cancer treatment or have been isolated from metastatic sites (Chen et al., 2004; Verma et al., 2006). Epigenetic and proteomic studies in breast cancer cells revealed that high TG2 expression is primarily associated with doxorubicin resistance. Moreover, numerous pathways and transcription factors regulate TG2 expression in the case of the generation of reactive oxygen species, which have a major role in cancer (Chen et al., 2004; Mehta et al., 2004; Budillon, Carbone and Di Gennaro, 2013). Thus, TG2 inhibition could be a possible target with beneficial clinical outcomes. However, more studies are needed to illuminate the correlation between TG2 and cancer progression, which could provide promising results for novel approaches in the treatment of cancer.

1.3 Transglutaminase

In the 1950s, the term transglutaminase was first introduced by Clarke et al. to define transamidation activity in guinea pig liver. Transglutaminase is a family of enzymes that catalyse Ca^{2+}-dependent post-translational modifications of proteins through the formation of an isopeptide bond (protein cross-linking) (York and Clarke, 1957; Clarke *et al.*, 1959). The

isopeptide bond is an amide bond formed via transamidation of γ-carboxamide group of glutamine residue and the ε-amino group of lysine residue, resulting in a ε-(γ-glutamyl) lysine linked product. The resulting product, usually with a high molecular mass, is highly resistant to chemical and proteolytic degradation (Figure 1.3) (Catalogus, 1968). In addition to crosslinking, transglutaminases mediate incorporation of primary amines, or site-specific deamidation of glutamine residues in the lack of substrates (Kanchan, Fuxreiter and Fésüs, 2015).

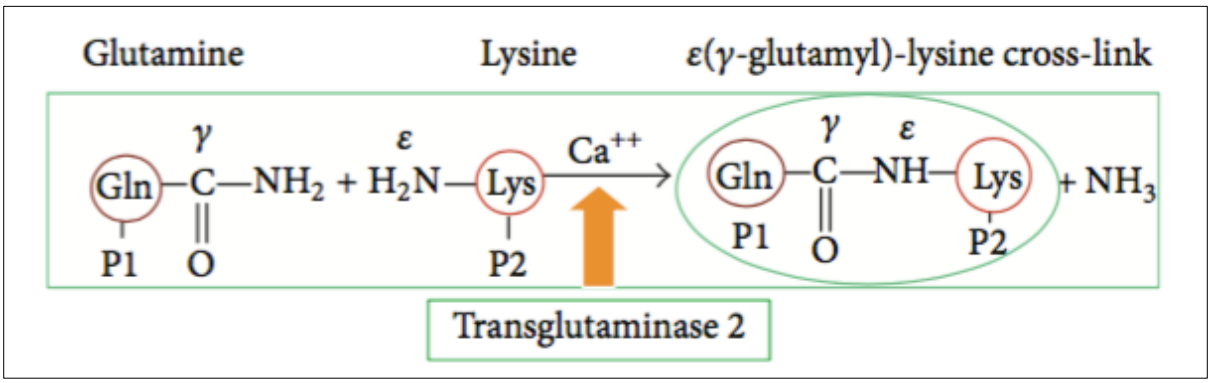

Figure 1-3 Glutamine (P1) and lysine (P2) residues of proteins are linked together by TG2 in the presence of Ca^{2+} leading to the formation of ε(γ-glutamyl)-lysine cross-link. (Shrestha *et al.*, 2014)

Transglutaminase 2 (TG2) was the first discovered member of this family, and then additional proteins presenting transglutaminase activity have been identified in micro-organisms, plants, vertebrates, and invertebrates (Griffn, Casadio and Bergamini, 2002). In human, nine enzymes (TG1–7, factor XIII, and band 4.2 of the transglutaminase (TG) family have been recognized. While eight of them are catalytically active, band 4.2 is inactive (Griffn, Casadio and Bergamini, 2002; Mehta and Eckert, 2005). The transglutaminase activity of these enzymes is activated by Ca^{2+}, while it is inhibited by GTP binding in three of them (TG2, TG3 and TG5) (Badarau, Collighan and Griffin, 2013; Kanchan, Fuxreiter and Fésüs, 2015). Transglutaminase enzymes are distributed in different human organs and cells with structurally and functionally related properties (Grenard, Bates and Aeschlimann, 2001; Griffn, Casadio and Bergamini, 2002). The transglutaminase primary sequences are different. However, they share an identical amino acid sequence at their active site apart from band

4.2, where cysteine amino acid is replaced with alanine and the protein turns catalytically inactive (Figure 1.4) (Mehta and Eckert, 2005)

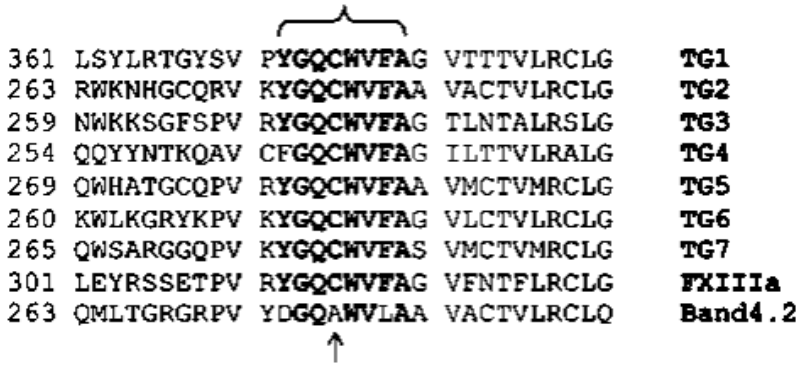

Figure 1-4 The transglutaminase protein catalytic sites. The arrow indicates alanine replaced cysteine residue in band 4.2 protein (Eckert et al., 2014)

1.3.1 Transglutaminase 2

Transglutaminase 2 (TG2, tissue transglutaminase, transglutaminase C, tTG, $G_{\alpha h}$) is the most studied and biologically characterised member of the transglutaminase family. It is expressed in different tissues and cell compartments and is implicated in several diseases, including celiac sprue (Molberg *et al.*, 2001), Alzheimer's disease, Huntington's disease, and some types of cancer (Grosso and Mouradian, 2012; Badarau, Collighan and Griffin, 2013).

1.3.1.1 Transglutaminase 2 structure

Most transglutaminase family members share the same structure. However, the TG2 structure possesses some specific features, making it a multifunctional protein with both intracellular and extracellular functions (Huang, Xu and Liu, 2015). The crystal structure of TG2 shows four domains: (a) N-terminal β-sandwich domain (spanning the 1-139 amino acids), (b) catalytic core domain (containing Cys277, His335 and Asp358) (140 to 454 amino acids), and (c) two C-terminal β-barrel 1 (479 to 585 amino acids) and β-barrel 2 (586-687 amino acids) domains (Fesus and Piacentini, 2002a; Mehta, Kumar and Kim, 2010; Jang *et al.*, 2014). Each one of these domains possesses numerous and unique functions of TG2, in which the N-terminal domain contributes to cell adhesion and migration functions because it contains binding sites for fibronectin (FN) and promotes cell attachment to the extra cellular matrix (ECM). In an extended active form of TG2 induced by calcium, the catalytic core

domain regulates the transamidation activity of TG2 through its six calcium binding sites. The ß1 barrel domain is involved in the binding and hydrolysis of GTP/ATP. However, the ß2 barrel stimulates phospholipase C and is implicated in TG2 mediated pro-inflammatory actions. The ß1, ß2, and catalytic core domain together act as a G-protein in regulating signal transducing pathways (Figure 1.5) (Fesus and Piacentini, 2002a; Mehta, Kumar and Kim, 2010; Kanchan, Fuxreiter and Fésüs, 2015).

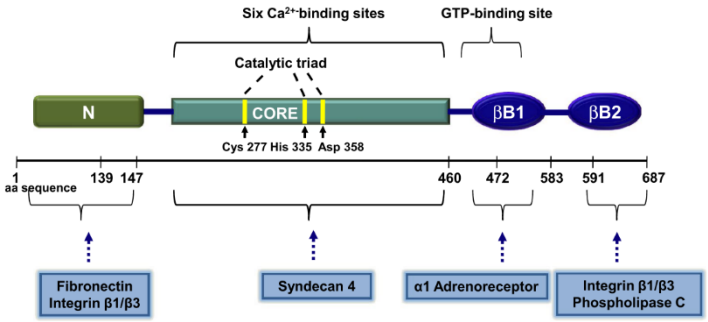

Figure 1-5 Schematic representation of the structural domains of transglutaminase 2. (Lai and Greenberg, 2013; Martucciello et al., 2018)

1.3.1.2 Transglutaminase 2 gene expression

TG2 expression is controlled by the TG2 promoter and encoded by the TGM2 gene. The entire gene of TG2 (TGM2) is localised on chromosome 20 within the band 20q11-12 and contains 13 exons and 12 introns (Fraij and Gonzales, 1997; Mehta, Kumar and Kim, 2010). The main variant, TGM2-L (TG2 full length), that was first identified by Gentile et al, encodes a polypeptide of 687 amino acid residues with a molecular mass of around 79 kDa (Gentile *et al.*, 1991), while the short form (TGM2-S) encodes a polypeptide of 548 amino acid residues with a molecular mass of 62 kDa (Fraij *et al.*, 1992). Another TG2 variant encoding for a 349 amino acid residue polypeptide with a molecular mass of 38 kDa has also been reported (Fraij and Gonzales, 1996). Recently, two more alternatively spliced TGM2 variants (tTGv1 and tTGv2) have been identified in human leukocytes, vascular smooth muscle, and endothelial cells (Figure 1.6) (Lai *et al.*, 2007). However, the full length (TGM2-L) and short form (TGM2-S) are the most extensively studied TGM2 variants, and only these two isoforms have been detected in this study.

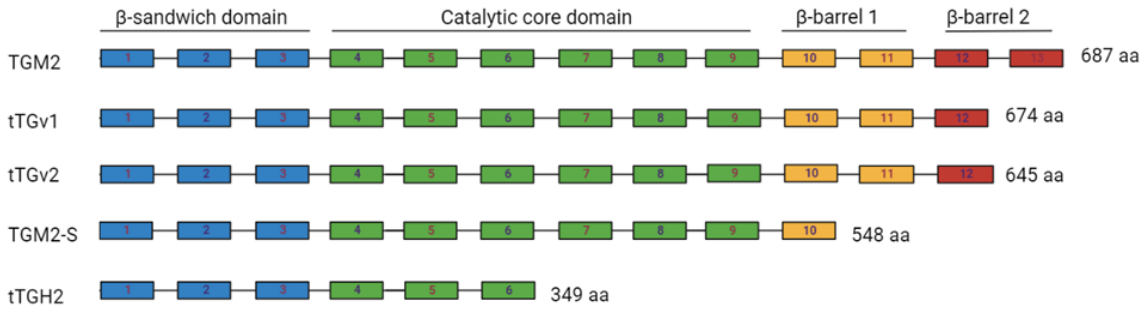

Figure 1-6 Schematic representation of TG2 intron and exon structure in different TGM2 isoforms.

TG2 expression is mainly controlled at the transcriptional level by several factors including the transforming growth factor (TGF)-β1 (Ritter and Davies, 1998), nuclear factor-κ B (NF-κB) (Park *et al.*, 2009), glucocorticoid receptor (Campisi *et al.*, 2008), interleukin (IL)-1 (Johnson *et al.*, 2001), IL-6 (Suto, Ikura and Sasaki, 1993), hypoxia-inducible factor-1 (Jang *et al.*, 2010), tumour necrosis factor (TNF)-α (Kuncio *et al.*, 1998), epidermal growth factor (EGF) (Antonyak *et al.*, 2004) and retinoic acid receptor (RAR) that binds to the TG2 promoter and regulates its gene expression (Griffn, Casadio and Bergamini, 2002). RA-induced TG2 expression is mediated via a tripartite response element located in the TG2 gene promoter, approximately at 1720 bp (RRE-1) and 1731 bp (RRE-2) (Figure 1.7) (Nagy *et al.*, 1996). It is well known that retinoids, particularly RA, induce TG2 expression at both the mRNA and protein levels in various cell lines (Davies *et al.*, 1985; Mehta and Lopez-Berestein, 1986; Zhang *et al.*, 1995).

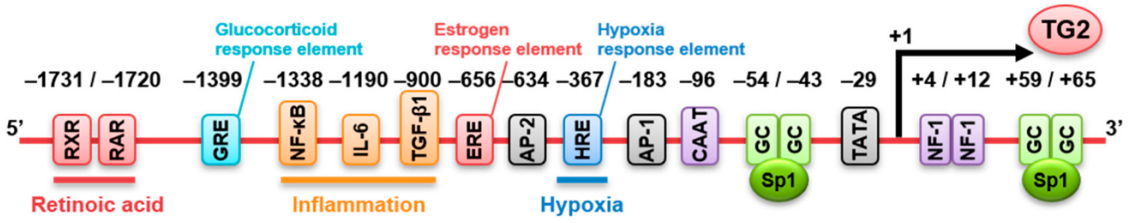

Figure 1-7 Regulatory elements of human TG2 gene expression. (Tatsukawa and Hitomi, 2021)

Retinoids, such as b-carotene, retinol, retinal, isotetrinoin, and retinoic acid, are natural derivatives and metabolised products of vitamin A. They have potent antiproliferative

properties and are physiological carcinogen suppressors. Retinoic acid is the most biologically active and naturally occurring member of the family of retinoids. Three stereoisomers of retinoic acid have been known: the all-trans-retinoic acid (ATRA), 9-cis, and 13-cis-RA (Connolly, Nguyen and Sukumar, 2013). ATRA, which is termed simply as retinoic acid (RA), in addition to synthetic retinoids, bexarotene and fenretinide, play an important role in many biological activities, such as proliferation, differentiation, and embryonic development (Lotan, Lotan and Sacks, 1990; Freemantle, Spinella and Dmitrovsky, 2003). RA mediates cellular growth and differentiation via nuclear receptor interactions. In blood circulation, retinol binds to the retinol-binding proteins (RBPs), which aid intracellular transfer through interaction with the RBP receptor. Inside the cell, retinol binds to cellular retinol-binding protein (CRBP) in the cytoplasm and converts to retinal by alcohol dehydrogenases (ADHs), and then irreversibly converts to RA by the retinaldehyde dehydrogenases (RALDHs) (Theodosiou, Laudet and Schubert, 2010; Conserva *et al.*, 2019). Synthesized RA binds to cellular retinoic acid-binding proteins 1 or 2 (CRABP1 or CRABP2). RA bound to CRABP1 is transferred to CYP26 to be degraded, while RA bound to CRABP2 is relocated to the nucleus and regulates gene expression by binding to the RA receptors (RARs) and the retinoid X receptors (RXRs), each of which contains α, β, and γ subtypes. Upon RA binding, RARs form heterodimers with RXRs (RAR-RXR) before they can act as transcriptional regulators by binding to retinoic-acid responsive elements (RAREs) located in the regulatory regions of the targeted genes (Figure 1.8) (Bastien and Rochette-Egly, 2004; Di Masi *et al.*, 2015). Expression of RAR and RXR is controlled by the receptors themselves, nuclear ERα, or other subtypes in the same family (Klein *et al.*, 1996; Ross-Innes *et al.*, 2010). ATRA and fenretinide bind particularly to RARS, while 13-cis RA and bexarotene bind to RXRS, and 9-cis RA binds to RARS or RXRS (Klein *et al.*, 1996; Theodosiou, Laudet and Schubert, 2010).

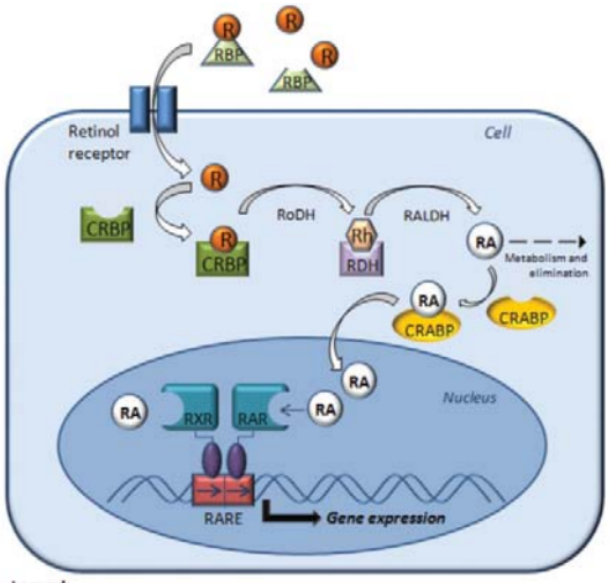

Figure 1-8 Pathways for the synthesis and mechanism of action of RA. (Afornali *et al.*, 2013)

In the absence of RA, the RAR-RXR heterodimer is bound to RAREs and associated with co-repressors forming a repressor complex with histone deacetylases. The co-repressors include silencing mediator of retinoid and thyroid signaling (SMRT) and nuclear receptor co-repressor (N-CoR) that mediate increased chromatin condensation and block gene transcription (Chen, Umesono and Evans, 1996; Marlétaz *et al.*, 2006). Binding of RA to the RAR ligand binding domain (LBD) destabilises the LBD and induces a conformational change. Subsequently, the co-repressor is released, and coactivators with histone acetyltransferase activity (HAT) bind to RAR. The co-activators such as steroid receptor co-activator 1 (SRC-1) mediate histone acetylation, leading to chromatin de-condensation and transcription activation (Figure 1.9) (Shiohara *et al.*, 1996; Marlétaz *et al.*, 2006).

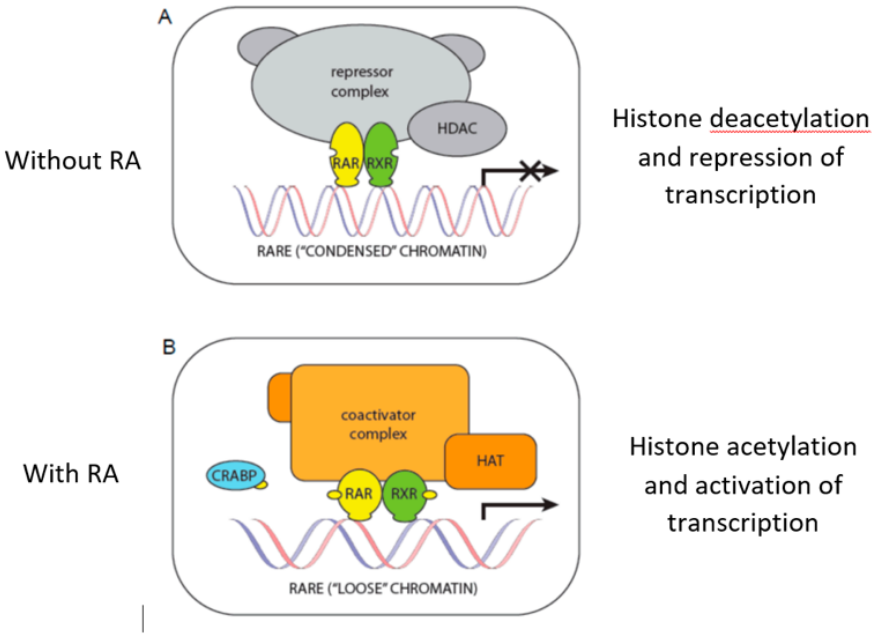

Figure 1-9 Transcriptional regulation by retinoids. Modified from (Chlapek *et al.*, 2018)

1.3.1.3 Transglutaminase 2 activities

TG2 is a multifunctional enzyme which is attributed to four main reasons including: (i) The diverse enzymatic activities of TG2, functioning as transamidating and GTPase enzyme (Antonyak *et al.*, 2006; Kumar *et al.*, 2012). (ii) The conformational changes (open vs closed conformations), which depend on the cellular microenvironment (Di Venere *et al.*, 2000; Ha *et al.*, 2018). (iii) The genetic background of model of study, cell lines vs animal model (Mehta and Eckert, 2005) and (iv) Its structurally different isoforms originating from alternative splicing, leading to the formation of proteins that lack functional domains (Antonyak *et al.*, 2006).

1.3.1.3.1 Transamidase activity

TG2 belongs to the transglutaminase family, and thus it catalyses various types of Ca^{2+}-dependent post-translational modifications of proteins by transamidation or deamidation of polypeptide-bound glutamines based on the substrate. These reactions include: i) Protein cross-linking by isopeptide bond or primary amine: TG2-mediated transamidation reaction via crosslinking between γ-carboxamide of a glutamine residue and the ε-amino group of a lysine residue to form ε-(γ-glutamyl) lysine isopeptide bonds (Figure 1.10:C) or a primary

amine acting as a crosslinker between two proteins (Figure 1.10:D). ii) Protein amination: TG2-mediated transamidation reaction by amine incorporation such as polyamines and histamine into the glutamine residue of the acceptor protein (Figure 1.10:B). iii) Protein deamidation: TG2-catalyzed deamidation reaction via reaction of glutamine substrate with water to generate glutamic acid (Figure 1.10:A) (Nurminskaya and Belkin, 2012). Among different TG2 enzymatic activities, transamidation, or the crosslinking of glutamine and lysine residues, is the most significant reaction catalysed by TG2.

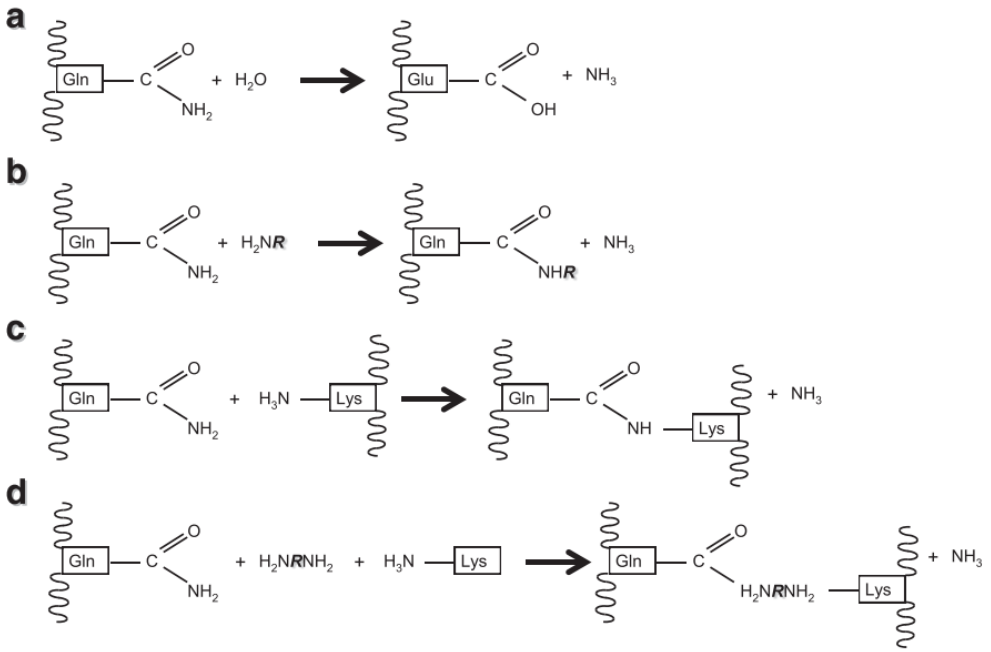

Figure 1-10 Reactions catalyzed by the transamidase activity of TG2. (Gundemir *et al.*, 2012)

1.3.1.3.2 GTPase and G protein activity

TG2 has several other enzymatic functions that are Ca^{2+} independent. TG2 ability to bind and hydrolyze GTP to GDP was first identified in 1987 (Achyuthan and Greenberg, 1987). A link between GTPase activity and G protein-coupled receptor (GPCR) function was established later in 1994, when it was discovered that TG2 and a guanosine triphosphate (GTP)-binding protein, termed $G_{\alpha h}$ are the same protein. TG2 functions as a G protein ($G_{\alpha h}$) which is associated with the α1 adrenergic receptor signaling transduction pathway that activates phospholipase C-δ1 (PLC-δ1). PLC-δ1 activation promotes hydrolysis of phosphatidyl- inositol 4,5-bisphosphate (PIP2) to diacylglycerol (DAG) and inositol 1,4,5-triphosphate (IP3), resulting

in an increase in intracellular Ca^{2+} which activates the transamidation reaction (Figure 1.12) (Nakaoka *et al.*, 1994).The GTPase activity of TG2/ $G_{\alpha h}$ is deactivated by elevated intracellular Ca^{2+} levels. TG2 also mediates signaling by different GPCRs, including thromboxane and oxytocin receptors.

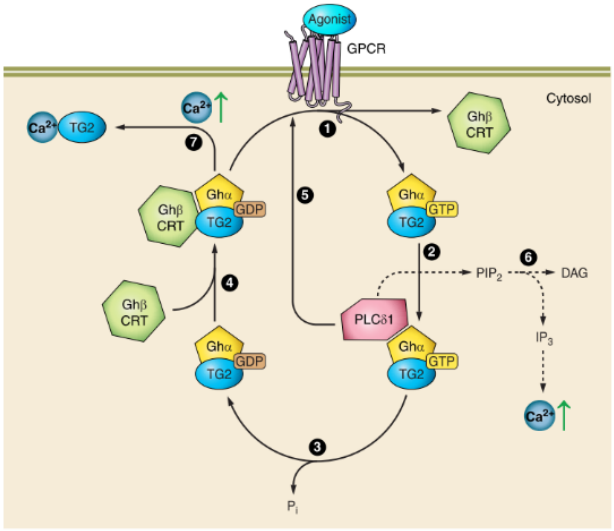

Figure 1-7 TG2 GTPase activity and TG2/ Gαh signaling. (Eckert *et al.*, 2014)

1.3.1.3.3 Kinase activity

Another enzymatic function of TG2 was reported in 2004, when TG2 was discovered to have an intrinsic serine/threonine kinase activity that phosphorylates insulin-like growth factor-binding protein (IGFBP-3) and (IGFBP-5) at multiple serine residues, on the cell membrane of breast cancer cells. Ca^{2+} was found to inhibit TG2 protein kinase activity, although it stimulates its transamidation activity (Mishra and Murphy, 2004). TG2 has also been reported to phosphorylate histones H1-4 (Mishra *et al.*, 2006), p53 tumour suppressor protein (Mishra and Murphy, 2006), and retinoblastoma protein (Mishra, Melino and Murphy, 2007). In vitro, TG2 intrinsic kinase activity has been proven, but it is still controversial in vivo (Mishra and Murphy, 2004, 2006).

1.3.1.3.4 Protein disulfide isomerase activity

TG2 was found to have protein disulfide isomerase (PDI) activity that is implicated in mitochondrial-dependent apoptosis. The PDI activity of TG2 is Ca^{2+} independent and, unlike

other TG2 activities, it is not inhibited by GTP. Also, it is mediated by a different domain than that used in transglutaminase activity (Hasegawa *et al.*, 2003).

1.3.1.4 Regulation of TG2 conformation and activity

The function of TG2 depends on its conformation. Transamidation activity of TG2, which requires Cys277 to attack γ-glutamyl residues on acyl donor substrates, is regulated by conformational changes in which binding of Ca^{2+} to the TG2 catalytic domain reveals an open active conformation, while binding to GTP or GDP occurs with the inactive closed conformation. In the GTP/GDP binding, access to the transamidation active site in the catalytic core domain is blocked, and the TG2 cysteine residue forms a hydrogen bond with the GTP tyrosine residue. On the other hand, Ca^{2+} binding modifies the protein conformation since the ß1 and ß2 domains are moved away from the catalytic domain, facilitating accessibility to the active site (Figure 1.12) (Fesus and Piacentini, 2002a; Liu, Cerione and Clardy, 2002).

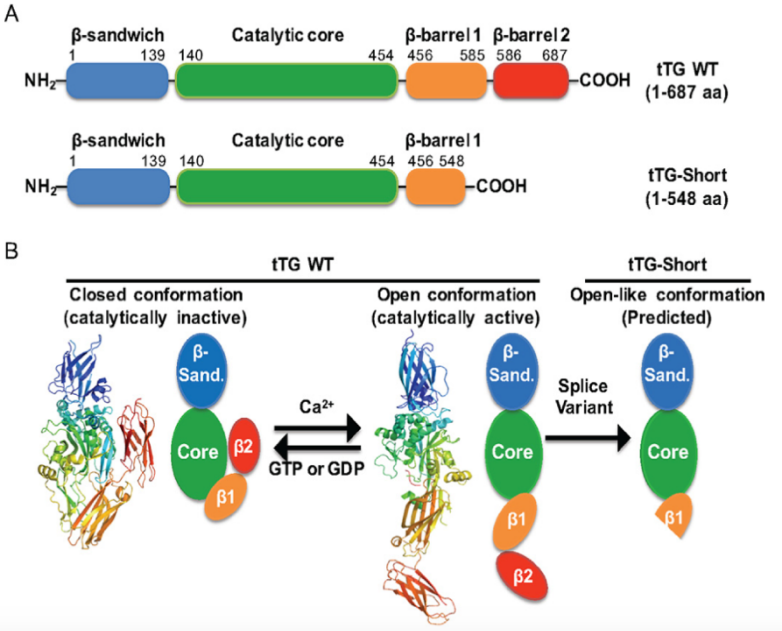

Figure 1-8 TG2 structure conformation. (Singh *et al.*, 2016)

TG2 is primarily a cytosolic protein, but it is also found in the nucleus, mitochondria, and on the cell surface (Piacentini et al., 2014) . Intracellular TG2 is usually found in a catalytically inactive state as a result of the high GTP, low free Ca^{2+}, and low redox potential (Fesus and

Piacentini, 2002a). It also serves as a scaffold protein and activates various signaling pathways under normal physiological conditions. However, under stress conditions, Ca^{+-2} levels are increased, resulting in TG2 acquiring an open active conformation, which catalyses protein crosslinking and apoptotic death (Mehta, Kumar and Kim, 2010; Agnihotri, Kumar and Mehta, 2013). On the other hand, extracellular TG2 is found to be in a catalytically active state due to low GTP and high calcium levels and serves as a stabiliser of the extra cellular matrix (ECM). Also, a high amount of extracellular TG2 remains inactive because of the intra-molecular disulfide bond (Figure 1.13) (Grenard, Bates and Aeschlimann, 2001; Mehta, Kumar and Kim, 2010; Agnihotri and Mehta, 2017).

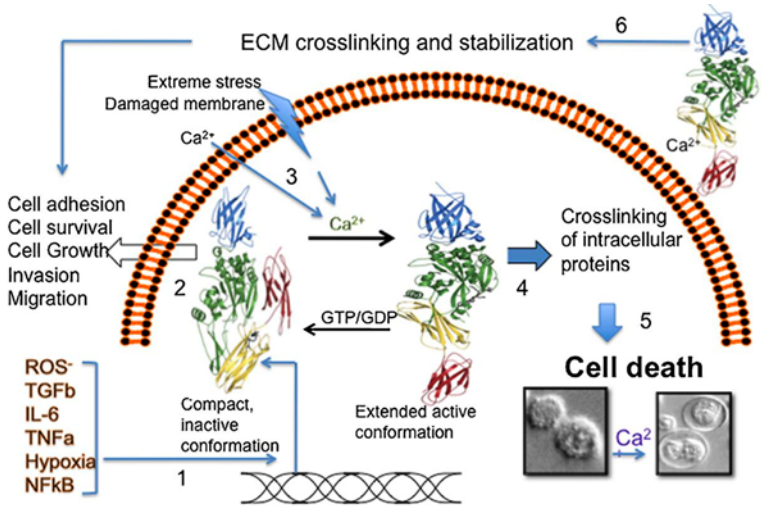

Figure 1-9 TG2 conformation and function depend on its location or other cellular contexts (Mehta et al., 2010)

1.3.1.5 Regulation of TG2 by Oxidative Stress

Reactive oxygen species (ROS) are defined as radicals, ions or molecules that are highly reactive as a result of the presence of a single unpaired electron in their outermost layer. ROS are classified into two groups: (i) free oxygen radicals, such as superoxide ($O_2^{\bullet -}$), nitric oxide ($NO^{\bullet}$), and hydroxyl radical ($^{\bullet}OH$); and (ii) non-radical ROS; for instance, hydrogen peroxide (H_2O_2) and singlet oxygen ($^1O_2$) (Liou and Storz, 2010). ROS are generated by endogenous or exogenous sources. The endogenous sources include mitochondrial dysfunction, cytochrome P450 enzymes, cyclooxygenases, and peroxisomes, while the exogenous sources include alcohol, smoking, environmental agents, ultraviolet radiation, and drugs, such as paracetamol

and doxorubicin (Nathan and Cunningham-bussel, 2013; Phaniendra, Jestadi and Periyasamy, 2015).

To maintain ROS homeostasis, various enzymatic and non-enzymatic antioxidant reactions take place to detoxify the excessive levels of ROS. Glutathione, flavonoids, and vitamins A, C, and E are examples of non-enzymatic molecules, whereas enzymatic antioxidants include superoxide dismutase (SOD), catalase, and thioredoxin (Liou and Storz, 2010; Hitomi, Kojima and Fesus, 2016). Under normal physiological conditions, ROS intracellular levels are important for maintaining many cellular processes; on the other hand, excessive ROS generation causes an imbalance between ROS and antioxidant detoxification systems, which in turn leads to oxidative stress and subsequently affects intracellular signaling (Figure 1.14) (Lebedeva, Eaton and Shadel, 2009; Nogueira and Hay, 2013). Furthermore, oxidative stress is associates with the progression of common disorders such as cancer, inflammatory and degenerative diseases. TG2 cellular levels are regulated by ROS and abnormal regulation of oxidative stress leads to the accumulation of increased TG2 cellular levels and TG2 involvement in the pathogenesis of these disorders (Phaniendra, Jestadi and Periyasamy, 2015). Three mechanisms have been identified to describe the response of TG2 to oxidative stress conditions. First, oxidative stress induces TG2 expression level, which leads to stimulation of redox responsive transcription factors, such as nuclear factor kappa B (NF-κB) (Verma and Mehta, 2007; Szondy *et al.*, 2017). Second, ROS increase TG2 by stimulating post-translational modifications (PTMs), like intramolecular disulfide-bond formation and the formation of TG2 protein aggregates (Georgopoulou and McLaughlin, 2001). Third, TG2 is increased by ROS mediated activation of intracellular calcium ion concentration or TGFβ, or by ROS mediated suppression of ribosomal proteins, such as L7a (RPL7a) and L13 (RPL13), which are endogenous TG2 inhibitors (Hitomi, Kojima and Fesus, 2016).

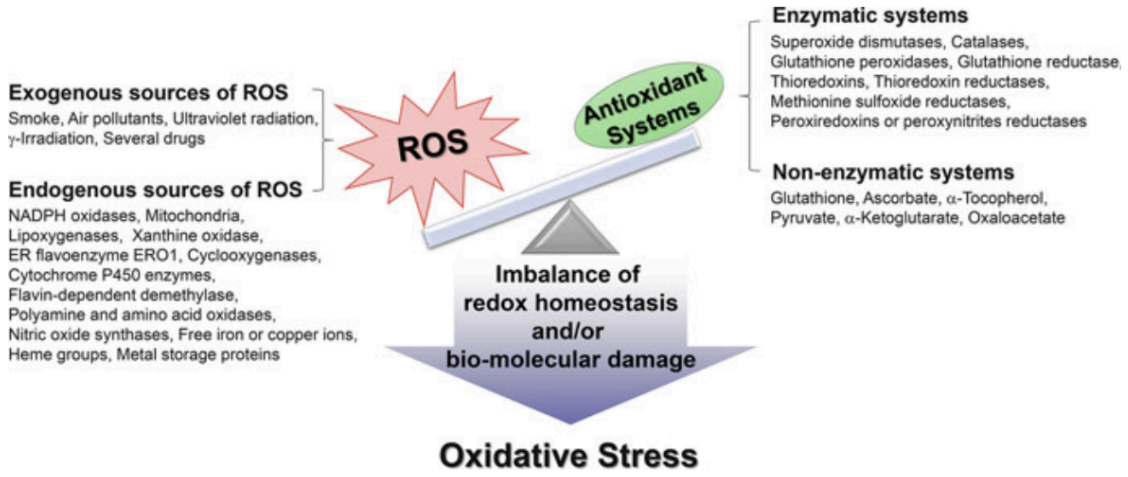

Figure 1-14 Imbalance between ROS generation and detoxification systems (Hitomi, Kojima and Fesus, 2016)

1.3.1.6 Roles of TG2 in cancer progression

Cancer progression shares many similar characteristics with inflammation and tissue injury. Chronic inflammation plays an important role at different stages of tumour progression. As TG2 is involved in many inflammatory processes, several studies have revealed increased TG2 expression levels as a hallmark of many types of cancer cells, such as breast carcinoma (Mehta *et al.*, 2004), pancreatic carcinoma (Verma *et al.*, 2006), and ovarian carcinoma (Hwang *et al.*, 2008). However, TG2 expression was found to be down-regulated in primary tumours and upregulated in secondary metastatic and chemo-resistant cancers, and its expression is a poor prognostic factor (Mangala *et al.*, 2007). Therefore, normal mammary and benign tumour tissues rarely express TG2, while TG2 is highly expressed in breast cancer cells, which subsequently increases cell survival, invasion, metastasis, and resistance to chemotherapy (Huang, Xu and Liu, 2015). Under chronic inflammatory conditions, high levels of TG2 in breast cancer cells decrease the expression of IκBα and enhance NF-κB activity.

1.3.1.6.1 TG2 in cell adhesion and metastasis

The interactions between cells and extracellular matrix (ECM) play an important role in regulating many cellular processes, including growth, survival, migration, and invasion. Several studies have demonstrated that TG2 stimulates cell adhesion (Mehta and Eckert,

2005; Zemskov *et al.*, 2006). This stimulation is carried out by two mechanisms. First, extracellular TG2 has a high affinity for fibronectin (FN), which is implicated in thrombosis, inflammation, tumour growth and angiogenesis (Zemskov *et al.*, 2006). The interaction between extracellular TG2 and FN plays an important role in cell-matrix adhesion, cell migration, and signalling. Second, TG2 has been found to be linked to integrin receptors, such as integrin β1 and β3 in order to maintain cell and extracellular matrix (ECM) interactions. Thus, TG2 activates cell adhesion, spreading, and migration (Mehta, Kumar and Kim, 2010; Onyekachi, Ebidor and Maxwell, 2015). EMT plays a vital role in chemo-resistance and is involved in the transformation of the early stages of a tumour into invasive and metastasizing. As TG2 is upregulated in cancer cells, it is implicated in tumour progression by regulating EMT. However, these effects are not only because of TG2 mediated EMT regulation, but also because TG2 induces resistance to apoptosis, which protects cells from doxorubicin-induced apoptosis and increases the cell's ability to metastasise (Mehta, Kumar and Kim, 2010; Huang, Xu and Liu, 2015).

1.3.1.6.2 TG2 in self-sufficiency of growth signals

In cancer cells, TG2 promotes cell growth and survival by activating transforming growth factor beta (TGFβ). Additionally, extracellular TG2 stimulates adhesion molecules (fibronectin and integrin) leading to ECM stabilisation and activation of cell survival signalling (Mehta, Fok and Mangala, 2006).

1.3.1.6.3 TG2 in tumour insensitivity to antigrowth signals

Nuclear TG2 regulates the retinoblastoma protein (pRb), which is a modulator of anti-proliferative signals. Hypo-phosphorylated pRb inhibits cell proliferation by recruiting E2F transcription factors into a multiprotein complex that maintains these factors in a transcriptional inactive state. E2F transcription gene targets are vital for the transition from the G1 to the S phase of the cycle. Therefore, inactive E2F transcription factors result in cell cycle arrest. The hyperphosphorylation of pRb mediated by TG2 results in the release of E2F transcription factors from the multiprotein complex and subsequent activation of genes involved in the transition from the G1 phase of the cell cycle to the S phase. TG2 kinase activity therefore exerts proliferative effects (Onyekachi, Ebidor and Maxwell, 2015).

1.3.1.6.4 TG2 in apoptosis

TG2 has a dual effect on apoptosis. Intracellular TG2 can act as anti-apoptotic factor, while extracellular TG2 serves as a pro-apoptotic factor (Mehta and Eckert, 2005). Intracellular nuclear TG2 exhibits its anti-apoptotic effects by interacting with NF-κB and stimulating this transcription factor to exert its anti-apoptotic effects. In contrast, extracellular TG2 enhances apoptosis by stabilising the ECM and by its interactions with FN and integrin, thus facilitating the crosslinking of dying cells and phagocytic cells, resulting in the induction of apoptosis. Extracellular TG2 also, reduces the migration and metastasis of cancer cells through interactions with the ECM (Odii and Coussons, 2014).

1.3.1.6.5 TG2 in genome instability and mutation

As mentioned previously, cancer is associated with many protein mutations. For instance, p53 which is found mutated in more than 50% of cancer cases. In 2006, a study by Mishra and Murphy demonstrated that inhibition of TG2 kinase activity will phosphorylate p53 at Ser^{15} and Ser^{20} residues, resulting in reduce p53 and MDM2 gene interactions. Since p53 mediates its apoptotic effects by inducing cell cycle arrest, this process requires destabilisation of p53-MDM2 interactions. As MDM2 binds to the N-terminal region of p53, thus, phosphorylation of serine residues in this region by TG2 disrupts this binding and facilitates p53 apoptotic effect. TG2 kinase activity increased in presence of low Ca^{2+} level in contrast to transamidating activity is increased by high Ca^{2+} level (Mishra and Murphy, 2006). However, this could be a promising target in the treatment of breast cancer and further studies are still needed to figure out the role of TG2 kinase activity and TG2 in general on p53.

1.3.1.6.6 TG2 in deregulating cellular energetics

Abnormal TG2 expression regulates metabolic reprogramming and enables metabolic alterations by different mechanisms, such as activating nuclear factor NF-κB, resulting in an increase in hypoxia inducible factor-1α (HIF-1α) cellular levels, which correlates with increased glucose uptake, increased lactate production, and decreased oxygen consumption by mitochondria (Kumar *et al.*, 2014).

1.3.1.6.7 TG2 in inflammation

Several studies have reported the involvement of TG2 in inflammatory conditions, such as wound healing, tissue repair, fibrosis, atherosclerosis, celiac disease, and auto-immune disease (Molberg *et al.*, 2001; Grosso and Mouradian, 2012; Huang, Xu and Liu, 2015; Szondy *et al.*, 2017). During the initial phases of cell injury, TG2 expression is regulated via various pro-inflammatory cytokines and growth factors. For instance, transforming growth factor beta 1 (TGF-β1) induces TG2 expression in keratinocytes and dermal fibroblasts through the TGF-β1 response element, which is localised in the TGM2 gene promoter (Mehta, Kumar and Kim, 2010). Another example is the tumour necrosis factor (TNF-α) that increases the TG2 synthesis in liver cells by activation of the nuclear factor of kappa light polypeptide gene enhancer in B-cells inhibitor, alpha (IκBα) phosphorylation. Normally, IκBα inhibits the function of NF-κB. Phosphorylated IκBα dissociates from NF-κB which is in turn activated and binds to the TGM2 gene promoter and stimulates TG2 expression (Kuncio *et al.*, 1998) (Mehta, Kumar and Kim, 2010). Interestingly, TG2 also exerts pro-inflammatory functions that stimulate the effect of TGF-β, which is a powerful inflammatory factor promoting inflammation. Activation of pro-inflammatory factors during inflammation stimulates TG2 expression levels. TGF-β and TNF-α up-regulate TG2 expression and worsen inflammatory diseases (Huang, Xu and Liu, 2015).

1.3.1.7 Transglutaminase 2 Inhibition

Elevated levels of TG2 are associated with various pathological conditions, such as neurodegenerative diseases, cancers, and inflammatory diseases. TG2 activity, including cross-linking, deamidation, and GTP-related activity is associated with those diseases (Griffn, Casadio and Bergamini, 2002; Song *et al.*, 2017; Szondy *et al.*, 2017). Thus, the development of potent TG2-specific inhibitors could be an efficient therapeutic approach for the treatment of these diseases. In the case of cancer, down-regulation of TG2 by small interfering RNA (siRNA) or its inhibition by small molecule compounds has been shown to reverse chemo-resistance, to induce apoptosis, and to inhibit invasion and metastasis in *in vitro* and *in vivo* animal models (Verma and Mehta, 2007; Hwang *et al.*, 2008). To date, numerous types of TG2 inhibitors have been discovered (Pietsch *et al.*, 2013).

TG2 inhibitors can be classified into three main classes based on their mechanism of action: competitive amine inhibitors, reversible inhibitors, and irreversible inhibitors (Siegel and Khosla, 2007; Badarau, Collighan and Griffin, 2013). The competitive amine inhibitors block the cross-linking activity by acting as competitive primary amine substrates incorporated into the γ-glutamyl residue. Competitive inhibitors are the most commonly applied TG2 inhibitors like cystamine since they are chemically stable, commercially available, and relatively non-toxic in living systems (Karpuj *et al.*, 2002; Siegel and Khosla, 2007). They are used in several in vitro studies, whereas they have limited applications *in vivo* since they trigger autoimmune responses, and they are non-specific to TG2, therefore they may bind to other transglutaminase members. Therefore, they are not promising compounds for drug development (Badarau, Collighan and Griffin, 2013). The reversible compound inhibitors block enzyme activity by inhibiting substrate access to the active site by competing for the TG2 cofactor (GTP and GDP) binding site (Siegel and Khosla, 2007; Badarau, Collighan and Griffin, 2013). The irreversible inhibitors block enzyme activity by covalently modifying the enzyme, thus blocking substrate binding. Furthermore, the majority of these irreversible inhibitors target the cysteine residue (Cys277) in the TG2 enzyme (Siegel and Khosla, 2007; Badarau, Collighan and Griffin, 2013).

ZDON is an example of an irreversible TG2 inhibitor discovered by Zedira GmbH. The company have tried to mimic the gluten peptides which are highly expressed in celiac disease and is considered as a good substrate for TG2, however Z-DON has shown inhibitory effect for TG1 and TG3 also, and has very high IC50 (Figure 1.15) (McConoughey *et al.*, 2010). ZDON irreversibly binds to the cysteine residue (Cys277) in the TG2 catalytic core domain, resulting in inhibition of TG2 transamidation activity (Schaertl *et al.*, 2010; Badarau, Collighan and Griffin, 2013). Binding of ZDON to the catalytic core domain of TG2 locks the TG2 in an open active conformation, potentially inhibiting the GTP binding.

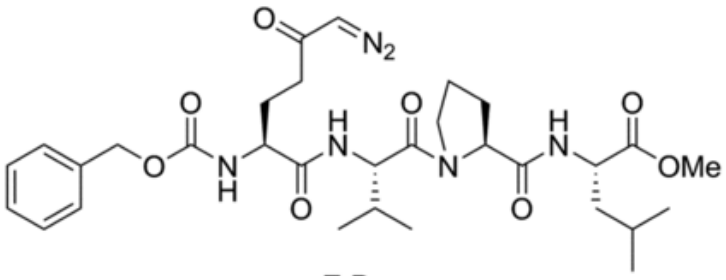

Figure 1-10 Z-DON chemical structure, TG2 irreversible inhibitor (Katt, Antonyak and Cerione, 2015)

Another irreversible inhibitor of TG2 is NC9, which inhibits both the transamidase and GTPase activity of TG2 (Figure 1.16). It covalently binds to the enzyme, causing it to adopt an open conformation and stabilising it at this conformation, resulting in GTP binding inhibition (Caron *et al.*, 2012; Akbar *et al.*, 2017).

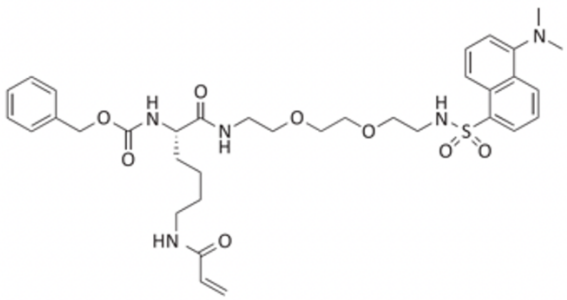

Figure 1-11 NC9 chemical structure, TG2 irreversible inhibitor (Keillor, Apperley and Akbar, 2015)

1.4 Aim and objectives:

Transglutaminase 2 (TG2) is a member of the transglutaminase family, catalysing Ca^{2+} dependent transamidation of proteins. It is a multifunctional protein with several functions, including transamidase, GTPase, protein disulfide isomerase, and protein kinase. The various enzymatic activities and functions of TG2 may be referred to alternative splicing of TG2 mRNA. Aberrant expression of TG2 in cancer cells could promote chemoresistance and cancer metastasis by inducing the EMT and CSC phenotype. The $CD44^{+}/CD24^{-/low}$ phenotype is strongly linked to highly aggressive cancer types and indicates metastasis and recurrence. Silencing of TG2 gene expression by using siRNA or inhibiting its functions by small molecule inhibitors in different cancer cells has been effectively used and shown to increase their sensitivity to chemotherapy-induced cell death and inhibition of invasion and metastasis, both in vitro and in vivo preclinical models. However, the role of TG2 in cancer is still controversial. It has been suggested that changing the TG2 conformational states from closed to open conformation induces cell death, while its closed impact conformation activates cell survival, invasion, migration, and adhesion.

Aim of the study:

It was hypothesised that different TG2 isoforms express differently and imply distinct roles in breast cancer progression. The study aimed to explore the role of TG2 isoforms (TG2-L and TG2-S) in breast cancer.

Objectives:

- Determination of the TG2 isoforms (TG2-L and TG2-S) expression in ER+ and triple negative breast cancer cell lines.
- Evaluation of the role of TG2 isoforms in cancer stem cells (CSCs) by assessing CSC features such as $CD44^{+}/CD24^{-/low}$ phenotype, high ALDH, and the ability to form mammosphere.
- Examine the role of TG2 isoforms in epithelial-mesenchymal transition and their role in cell migration.

Chapter 2

Materials and Methods

2. Chapter2: Materials and methods

2.1 Materials

2.1.1 Cell culture and treatments

In this study, four human breast cancer cell lines were used, including MCF-7, T47D, MDA-MB-231, and MDA-MB-468. The cells were purchased from the European Collection of Cell Cultures (ECACC). The characteristics of these cell lines are summarised in the below table (Table 2.1).

Table 2-1 Brest cancer cell lines and their molecular characteristics

Cell line	Description	ER	PR	HER2	p53
MCF.7 Michigan Cancer Foundation-7	A human breast cancer cell line established in 1970 from the pleural effusion of a 69-year-old Caucasian woman with metastatic mammary carcinoma.	Positive	Positive	Negative	Wild type
T47D	A human breast cancer cell line established from the pleural effusion of a 54- years old patient	Positive	Positive	Negative	Mutated
MDA-MB-231	human breast cancer cell line established from the pleural effusion of a Caucasian patient aged 51-year-old	Negative	Negative	Negative	Mutated
MDA-MB-468	A human breast cancer cell line established in 1977 from the pleural effusion of a patient aged 51-year-old	Negative	Negative	Negative	Mutated

All cell culture media, supplements, chemicals, and reagents were purchased from Sigma Aldrich (UK) unless otherwise stated. Heat-inactivated foetal bovine serum (FBS) was purchased from Gibco (UK). Solvents used, such as ethanol, methanol, isopropanol, glacial acetic acid and dimethyl sulphoxide (DMSO) were purchased from Fisher Chemicals (UK). ZDON and NC9 were purchased from Zedira (Germany).

2.1.2 siRNA reagents

All siRNA were purchased from Dharmacon (Horizon Discovery Ltd) as listed in the table below:

Table 2-2 siRNA reagents

Target Gene	siGENOME SMARTpool siRNA Cat#
TGM2	D-004971-01
	D-004971-02
	D-004971-03
	D-004971-04
Non-Targeting (control)	D-001206-13-05

2.1.3 SRB proliferation assay

Sulforhodamine B (SRB) and trichloroacetic acid (TCA) were purchased from Sigma Aldrich (UK). Tris base was purchased from Fisher Scientific (UK).

2.1.4 Antibodies

Antibodies used for immunoblotting or flow cytometry are listed in the table below.

Table 2-3 Antibodies used in western blotting or flow cytometry

Antibody	Application	Supplier
Monoclonal anti-TG2	WB	Abcam (CUB7402)
Monoclonal anti-catenins	WB	Proteintech (66379-1)
Monoclonal anti- vimentin	WB	Proteintech (60330-1)
Monoclonal anti- E-cadherin	WB	Proteintech (60335-1)
Monoclonal anti- N-cadherin	WB	Proteintech (66219-1)
Monoclonal anti-actin	WB	Santa Cruz (SC-517582)
Anti-mouse IgG-HRP	WB	Abcam (ab6789)
Monoclonal Antibody CD24	FC	Thermofisher scientific (17-0247-42)
Monoclonal Antibody CD44	FC	Thermofisher scientific (12-0441-82)
Mouse IgG2a kappa Isotype Control, APC	FC	Thermofisher scientific (17-4724-81)
Mouse IgG2a kappa Isotype Control, PE	FC	Thermofisher scientific (12-4724-81)

2.1.5 Mammosphere assay

Gibco™ DMEM/F-12 (No Phenol Red), EGF Recombinant Human Protein and B-27™ Supplement (50X), minus antioxidants were purchased from Gibco, Fisher Scientific (UK). Anti-adherence rinsing solution that was used for plate coating was purchased from STEMCELL Technologies (07010).

2.1.6 Western blot

Tetramethylethylenediamine (TEMED) was purchased from GE Healthcare (UK). PageRulerTM Plus Prestained Protein Ladder was purchased from ThermoFisher Scientific (UK). Immobilon-P 26.5x3.75m Roll PVDF 45um was purchased from Merck

Millipore (UK). Ammonium persulfate (APS), β-Mercaptoethanol, Phenylmethylsulfonyl fluoride (PMSF), and Protease inhibitors (PI) were purchased from Sigma-Aldrich (UK). SuperSignal™ West Pico PLUS Chemiluminescent Substrate was purchased from Thermo Fisher Scientific (UK).

2.1.7 Laboratory kits

Specific tissue transglutaminase colorimetric microassay kit (TG2-CovTest) was purchased from Covalab, Germany (cat: 00014867). ALDEFLUOR™ kit was purchased from STEM CELL. Protein quantification kit: Pierce™ BCA Protein Assay Kit from Thermo Fisher Scientific (UK).

2.2 Methods

2.2.1 Cell culture

2.2.1.1 Cell lines maintenance

Cell line cultures were grown in humidified incubators at 37 °C in an atmosphere of 5% CO_2. Cell culture processes were carried out in a Class II biological safety cabinet to provide a sterile environment. The cells were cultured in complete culture medium, containing Dulbecco's modified Eagle's medium (DMEM) supplemented with 10% fetal albumin serum (FBS).

2.2.1.2 Cell thawing and freezing

For thawing cells, cell vials were rapidly thawed in a 37 °C water bath. Then, the cell suspension was gently pipetted into 10 mL of complete DMEM and centrifuged at 1300 x g for 3 minutes to remove DMSO. The cell pellets were re-suspended in complete DMEM and dispensed into a T25 cm2 culture flask. Cells were incubated at 37°C in an atmosphere of 5% CO_2 and allowed to attach overnight. On the next day, the medium was replaced with fresh medium to remove DMSO, dead cells, and unattached cells. Cells were passaged 2-3 times when they were ~ 80% confluent to recover before starting the experiment.

For freezing cells, cells were trypsinised as described in section 2.2.1.3, Then, it was centrifuged at 1300 rpm for 3 minutes and re-suspended in freezing medium (50% DMEM, 40% FBS, and 10% dimethyl sulfoxide (DMSO)). DMSO used to prevent the formation of intracellular ice crystals. The solution was then transferred to cryovials and stored at -80°C.

2.2.1.3 Cell passaging

All cell lines were passaged in T75 cm^2 culture flasks when they were ~80 confluent. Cells were washed with phosphate-buffered saline (PBS) solution and 2 ml of 1x trypsin (EDTA) solution was added. The flask was re-incubated with trypsin at 37 °C for 3-5 minutes. The flask was tapped gently and checked under the microscope to make sure all cells were detached. The cell suspension was re-suspended in 7 ml of complete culture medium and mixed well by pipetting to prevent the formation of cell clumps. The cell suspension was then transferred to a new labelled flask containing 10 ml of fresh medium. Cells were left overnight in the incubator to adhere to the culture flask.

2.2.1.4 Cell counting and seeding

Cell counting is carried out before any experiments to determine the appropriate number of cells to be used. The concentration of the cell was determined using an automated cell counter by BIORAD. The cells were trypsinised and re-suspended in fresh medium before pipetting into a 15 ml centrifuge tube. Then, 10 µl of the cell suspension and 10 µl of Trypan Blue stain was pipetted into an Eppendorf tube. The mixture was gently mixed by pipetting up and down. 10 µl of the mixture was transferred to the cell counting slide, and the live cell count per ml was calculated. By using the below equation (Equation 1), After adding the calculated volume of cell suspension (A) into each plate to get the required cell number, the remaining volume was made up by adding fresh DMEM up to the total volume.

$$\text{Volume of cell suspension required } (\mathrm{A}) = \mathrm{B}/\mathrm{C} \qquad \text{Equation 1}$$

Where, A: volume of cell suspension required, B: number of cells required for experiment,

and C: live cell count: x cells/ml

2.2.1.5 Cell seeding densities

Cell seeding densities were optimised to achieve 80-90% confluency by end of the experiments as listed in the table below:

Table 2-4 Cell seeding densities

Cell line	6-well plate (cells/well)	12-well plate (cells/well)	96-well plate (cells/well)
MDA-MB-231	2×10^5	0.5×10^5(siRNA) 1×10^5(inhibitors)	2×10^3
MDA-MB-468	3×10^5	1.5×10^5	2×10^3
MCF.7	3×10^5	1.5×10^5	3×10^3
T47D	3×10^5	1.5×10^5	3×10^3

2.2.1.6 Cell treatment

All treatment stock concentrations were dissolved in DMSO and kept at -20°C, then diluted in DMEM up to the working concentration immediately before use. Throughout this study, samples treated with DMSO were used as a negative control. To avoid harming the cells, the amount of DMSO in these samples didn't go above 0.1–0.2% of the total volume. All drugs' stock, working concentrations, and incubation periods are listed in the table below.

Table 2-5 Treatment Scheduling

Drug	Stock conc.	Working conc.	Incubation period
SAHA	100 mM	0.5 μM	48 h
TSA	10 μM	0.05 μM	48 h
RA	1 mM	40 μM	48 h
ZDON	1 mM	70 μM	72 h
NC9	1 mM	30 μM	72 h

2.2.2 Small interfering Ribonucleic Acid (siRNA) transfection

TG2 protein expression was knocked down in MDA-MB-231 cell line using 25-50 nM siGENOME SMARTpool TGM2 siRNA. siGENOME SMARTpool non-targeting siRNA was used as a negative control. Western blot was used to confirm TG2 expression knockdown at the protein level. The individual SMARTpool siRNA target sequences are listed in the table 2.6. The target sequences were uploaded to the NCBI BLAST tool to confirm the sequence location on exons (Figure 2.1)

Table 2-6 Gene targeting sequences of siGENOME SMARTpool non-targeting siRNA (Horizon, Dharmacon)

Target Gene	Target Sequence	Exon
TGM2	GAACATGGGCAGTGACTTT	Exon 10
	CCGAGGAGCTGGTCTTAGA	Exon 1 & 2
	GCAACCTTCTCATCGAGTA	Exon 7
	GGTCAATGCCGACGTGGTA	Exon 9
Non-Targeting (control)	UAGCGACTAAACACATCAA	
	UAAGGCTATGAAGAGATAC	
	ATGTATTGGCCTGTATTAG	
	ATGAACGTGAATTGCTCAA	

Figure 2-1 TGM2 sequencing (NCBI's BLAST)

Following the manufacturer's protocol, the effect of DharmaFECT 1 transfection reagent was examined to avoid cytotoxicity. The SRB assay was used to determine cell viability. Cells were seeded in a 96-well plate and then treated with DharmaFECT 1 at three different concentrations for 48, 72, and 96 h. These concentrations were 0.5, 1, and 2%. At the end of the experiment, 80% cell viability should be maintained, according to the manufacturer's instructions. Only cells treated with 2% DharmaFECT 1 showed $<$ 80% cell viability compared to untreated control cells, while 1% DharmaFECT 1 showed $\geq$ 80% cell viability between 48-96 h and it was used for the following siRNA transfection experments (Figure 2.2).

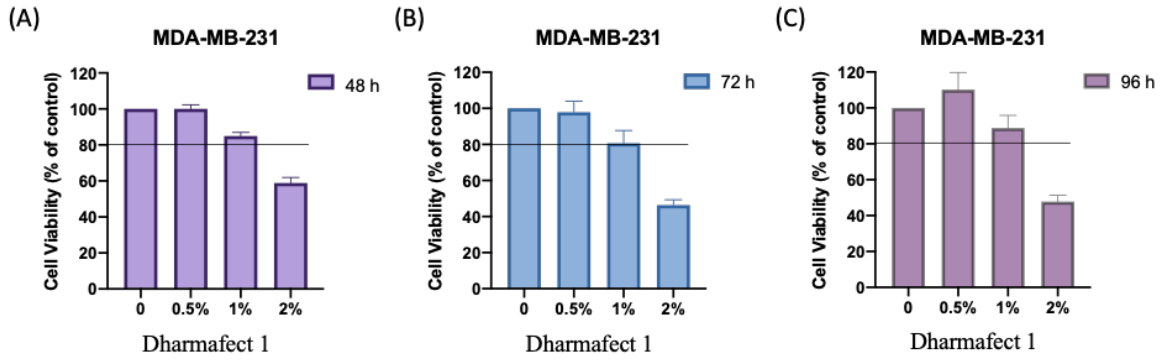

Figure 2-2 The cytotoxic effect of DharmaFECT 1 transfection reagent in MDA-MB-231 cell line using SRB proliferation assay. Cells were treated with a range of concentrations of DharmaFECT 1 for 48h (A), 72h (B), or 96h (C). DMSO was used as control (CTRL). Data are presented as the mean ± SEM of three independent experiments each one performed in triplicates. The black line indicates 80% cell viability

Optimizations of siTG2 concentration were also essential to achieve ≥ 70% expression silencing efficiency.

The stock concentrations of 5 µM of siGENOME SMARTpool TGM2 siRNA and 5 µM of siGENOME SMARTpool non-targeting siRNA were prepared using DNase/RNase-Free distilled water (Thermo Fisher, UK) and kept at -20°C, and were diluted to a 25 or 50 nM final concentration immediately before use.

Then, the working concentration of Dharmafect 1 transfection reagent (Dharmacon, UK) was prepared by adding serum-free medium without penicillin/streptomycin and l-glutamate, in which 2 µL transfection reagent in 198 µL serum-free medium was used per well. After calculating the required amount of transfection reagent, the Dhramfect reagent in serum-free medium was mixed by pipetting and incubated for 5 min at RT. Then, the transfection reagent was added to the working concentration of siTG2 and non-targeting siRNA at a concentration of 1:1 to prepare siRNA complex. The complex was then mixed properly and incubated for 20 min at RT. After that, 400 µL of siTG2 and non-targeting complexes were added to 6-well plate and 1600 µL of 2×10^5 cells in DMEM without penicillin/streptomycin was added to the wells. The wells were mixed by shaking the plate gently and the plate was incubated for 48, 72, or 96 h before collecting the samples. Then samples were submitted to a western blot to confirm the efficiency of silencing.

2.2.3 SRB assay

The Sulforhodamine B (SRB) assay is a technique used for cell density determination or drug cytotoxicity screening. It depends on the ability of SRB dye to bind to protein components of cells that have been fixed by trichloroacetic acid (TCA) to tissue-culture plates. SRB is a pink aminoxanthene dye with two sulfonic groups that bind to basic amino-acid residues of TCA in weak acid conditions and dissolve in basic conditions by Tris solution. The amount of pink dye released from stained cells is directly proportional to cell density (Vichai and Kirtikara, 2006).

Cells were seeded at appropriate densities (Table 2.4) in 200 µL of complete cell culture medium into 96-well plates, in triplicates. Cells were allowed to attach overnight at 37°C and 5% CO_2. On the following day, the medium was changed with 200 µl of fresh complete medium supplemented with different concentrations of SAHA, TSA, RA, ZDON, NC9, or DMSO as a control. Cells were incubated for time points of 24, 48, or 72 h. At the end of the incubation period, attached cells were fixed with 50µl of cold 50% (w/v) trichloroacetic acid (TCA) to each well, and incubated for 1 h at 4°C, followed by washing four times in tap water and allowed to dry at room temperature. Cells were then stained with 50µl 0.4% (w/v) SRB prepared in 1% (v/v) acetic acid for 30 minutes at room temperature and rinsed four times with 1% acetic acid to remove unbound dye and then dried at room temperature. 200 µl of 10 mM Tris base solution was added to each well to dissolve the bound dye and the plates were then placing on a shaker (Heidolph, Germany) for 10 min at room temperature. Absorbance was measured at 510 nm using a plate reader (µQuant Microplate Spectrophotometer, Biotek, UK) connected with Gen5 software (BioTek, UK), in which optical density (OD) values corresponded to the number of viable cells.

The percentage of viable cells at each drug concentration was calculated as a percent of the negative control (DMSO) using the following equation:

$$\text{Cell growth (\% of control)} = \frac{\text{Absorbance (sample)}}{\text{Absorbance (negative control)}} \times 100$$

The IC50 value was calculated by generating a dose-response curves from at least three independent experiments by plotting the drug concentrations versus the percentage of cell growth in GraphPad Prism 9.

2.2.4 Immunoblotting/ Western blot

2.2.4.1 Preparation of cell lysate

Cells were seeded in 6-well plates and treated the next day. After the required treatment time, the medium was removed and the cells were washed with 2 ml of cold PBS and lysed in 60 µl of RIPA lysis buffer, supplemented freshly with 1X protease inhibitor cocktail and 1mM phenylmethylsulphonyl fluoride (PMSF). Samples were kept on ice all the time. The mixture in the plate was scraped and lysates were collected into labelled Eppendorf tubes. Cells were centrifuged at 13,000 rpm for 15 minutes at 4°C. The supernatants were collected into fresh Eppendorf tubes and the pellet was discarded. Supernatants prepared were used to carry out immunoblotting experiments.

2.2.4.2 Determination of protein concentration

The total protein concentration in cell lysates was determined using a colorimetric bicinchoninic acid (BCA) assay. The assay is based on that amino acid residues in protein molecules can reduce copper from cupric (Cu+2) to cuprous (Cu+1) in an alkaline solution. BCA interacts with cuprous ion forming a stable complex with purple colour. The colour intensity is directly proportional to the sample's protein concentration (Smith *et al.*, 1985).

A standard curve was prepared using serial dilution of bovine serum albumin (BSA) in distilled water at concentrations of 2,4,8, and 16 mg/mL. In a 96-well plate, 5 µl of each protein standard, 5 µL sample lysate, and 5 µL distilled H20 (blank) were added in duplicate. BCA reagent was freshly prepared at a 1:50 ratio of BCA: 4% (w/v) copper sulphate solution. Then 195 µl was dispensed into each well. The plate was incubated at 37°C for 30 min and the absorbance was then read at 562 nm using a plate reader (µQuant Microplate Spectrophotometer, Biotek, UK) coupled with Gen5 software (BioTek, UK). A standard curve was created on Microsoft Excel by plotting the sample's absorbance against BSA standard concentrations (blank corrected). The protein concentration of each sample was calculated using the straight-line equation generated from the standard curve. (Figure 2.3)

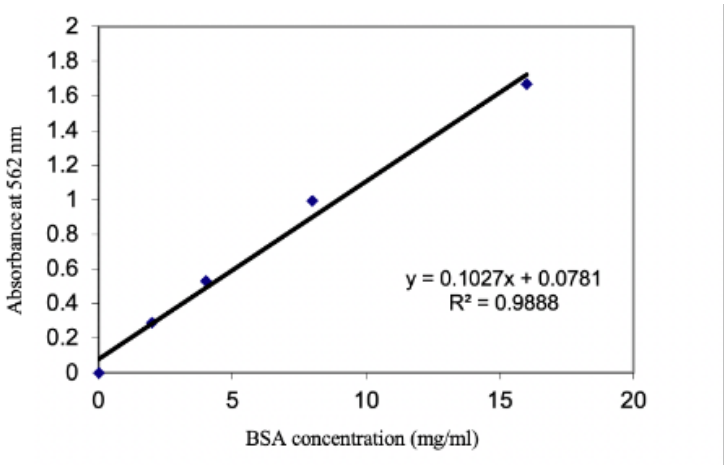

Figure 2-3 Standard curve of serially diluted BSA protein concentrations using BCA assay

2.2.4.3 Sodium dodecyl sulphate polyacrylamide gel electrophoresis (SDS-PAGE)

Gel electrophoresis is an analytical method for separating molecules based on their molecular masses in an electric field. A polyacrylamide gel is used as a supporting medium, and sodium dodecyl sulfate (SDS) is used to denature the proteins.

- Method

The gel casting apparatus (Mini-PROTEAN 3-Bio-Rad, UK) was set-up according to the manufacturer's guidelines. The SDS-PAGE gel contains both stacking and resolving gel. A 7.5% resolving gel was prepared by mixing the components as listed in Table 2.7 and pouring between the glass plates. A layer of isopropanol was added on top of the resolving gel to remove air bubbles and polymerise for 45-60 min at room temperature. Isopropanol was removed and a stacking gel was prepared, with the components listed in Table 2.7. The gel was poured onto the top of the resolving gel and a 10 well comb was inserted between them.

The gel was left to polymerise in the casting apparatus, then fitted into the electrophoresis mini buffer tank (Bio-Rad) and the tank was filled with SDS-PAGE running buffer (25mM Tris, 190mM Glycine, 35mM SDS). The comb was removed, and the wells were washed with distilled water before samples were loaded (20 µg of proteins). For sample preparation, 4x SDS loading buffer (Bio-rad) was added to the protein extracts, which were prepared as described in section 2.2.4.1. Before loading the sample onto SDS-PAGE, the mixture was boiled at 95°C for 10 minutes to denature the protein, then centrifuged at 13,000 rpm for 30 seconds. Molecular markers (5 µl) were also loaded into the first well. Electrophoresis was

run at 80 V until the samples entered the resolving gel, and then the voltage was changed to 110 V.

Table 2-7 Constituents of three 7.5% polyacrylamide resolving and stacking gels

7.5% GEL		
Solutions	**Resolving**	**Stacking**
Distilled Water	13.3 ml	6.73 ml
Acrylamide	7.0 ml	1.67 ml
Tris pH 8.95 (1.5 M)	7.0 ml	___
Tris pH 6.95 (1 M)	___	1.25 ml
EDTA (0.2 M)	280 µl	100 µl
SDS (10%)	280 µl	100 µl
APS (10%)	157 µl	157 µl
TEMED	17 µl	17 µl

2.2.2.4 Western blotting

Blotting is a technique used to transfer of DNA, RNA, or protein samples, after separation by gel electrophoresis, to a membrane followed by subsequent detection on the membrane. It is known as Southern and northern blot for detecting of DNA and RNA, respectively. In 1981, the western blot was first introduced by Burnette to detect proteins by probing with specific antibody to the targeted protein. It is a qualitative and semi quantitative method for the protein detection (Towbin, Staehelin and Gordon, 1979; Burnette, 1981).

- Method

Following gel electrophoresis, proteins were transferred to a PVDF membrane (Millipore,UK) by wet transfer. The Bio-Rad Western transfer apparatus was set up according to the manufacturer's instructions. The buffer tank was filled with western transfer buffer (20% methanol, 25mM Tris, 192mM glycine). The transfer reaction was performed at 0.4 Amp for 90 minutes with an ice pack, while the ice pack was changed after 45 minutes to maintain the western transfer reaction temperature.

- Immunodetection of proteins

After transfer, membranes were blocked in 5% low fat milk in PBS for 1 hour on shaker at room temperature to reduce non-specific antibodies binding on non-target protein. The membrane was then incubated with primary antibody (Table 2.8) in 2.5% milk in PBS on shaker overnight at 4^{o}C. The next day, membrane was washed three times with PBS-0.1% Tween-20 for 10 minutes and incubated for 1 h with anti-ß–actin antibody. The membrane washed again three times with PBS-0.1% Tween-20, then, incubated for 1 h at room temperature with secondary antibody (Anti-Mouse IgG HRP Conjugate) at dilution 1:2500 in 2.5% milk in PBS, and washed again three times with PBS-0.1% Tween-20. SuperSignal™ West Pico PLUS Chemiluminescent Substrate (Thermo Fisher Scientific, UK) was used to visualise the proteins of interest on the membranes using the Chemi DocTM MP imaging system (Bio-Rad, UK).

Table 2-8 Antibodies used in western blotting

Antibody	Dilution	Molecular weight (kDa)
Monoclonal anti-TG2	1:3000	TG2-L: 79 and TG2-S: 62
Monoclonal anti-catenins	1:5000	92
Monoclonal anti- vimentin	1:5000	55
Monoclonal anti- E-cadherin	1:3000	120
Monoclonal anti- N-cadherin	1:3000	130
Monoclonal anti-actin	1:2500	42
Anti-mouse IgG-HRP	1:2500	-

- Densitometry

The protein bands observed on membranes were quantified by using Image J software. Each band was measured three times and then normalised to its corresponding -actin's band.After that, the average of the three readings of each experiment was measured and normalised to the control, which was calculated as 1.

2.2.5 Transglutaminase 2 enzymatic activity assay (TG2-CovTest)

TG2 transamidase activity was measured using a specific TG2 colorimetric microassay kit (TG2-CovTest), which is used for biological samples with minimal or no interference with other transglutaminase family members. The TG2-CovTest uses biotinylated T26 peptide (Biotin-pepT26), which is embedded in the kit plate's wells, as the first substrate (an amine-acceptor/acyl-donor) and (an amine-donor/acyl-acceptor) as a second substrate. In a sample containing TG2, the γ carboxamide of the glutaminyl residue of the biotin-pepT26 is incorporated into the amine substrate to form biotinylated isopeptide bound. The amount of biotin incorporated is related to the TG2 activity and is reflected by the absorbance of the reaction mixture at 450 nm.

According to the manufacturer's protocol, treated cells were collected and lysed with RIPA buffer and protein quantified using the BCA assay. A 150 µl of 1X wash buffer was dispensed in microtiter strips (96-well plate) coated with amine substrate and incubated for 15 min at 37^0C. Then, the 1X wash buffer was removed and 50 µL of cold assay mixture was dispensed. 10 µL of EDTA was added to the negative control tube. Then, 25µL of cold protein sample (25 µg protein) was added to the test wells and incubated for 30 min at 37 ^{0}C with gentle shaking. The wells were then washed once with 200 µL/well of 1X wash buffer. A 100 µL of freshly prepared SAv-HRP solution was added into each well and incubated at 37 ^{0}C for 15 minutes with gentle shaking. At the end of the incubation period, the wells were washed three times with 200 µL of 1X wash buffer, and 100 µL of HRP substrate was dispensed into each well and incubated at room temperature for 5 minutes. A 100 µL of blocking reagent was added into each well, and the optical density was measured at 450 nm using a plate reader (µQuant Microplate Spectrophotometer, Biotek, UK) connected with Gen5 software (BioTek, UK). The yellow colour intensity is proportional to the TG2 activity.

2.2.6 Mammosphere assay

In 1992, an in vitro neurosphere assay was discovered after a population of stem cells in neural tissue formed neurospheres (Reynolds and Weiss, 1992). Later, sphere-forming assays have been adopted and developed for use with a variety of different tissue types to assess stem cell activity and self-renewal that termed mammosphere- forming assay (Al-Hajj *et al.*, 2003; Shaw *et al.*, 2012).

To isolate single cells and generate primary mammospheres from human breast cancer cell lines, treated cells were collected from wells and washed twice in 1x PBS and trypsinised. Then, cells were centrifuged at 580 g for 2 minutes at room temperature. The supernatant was discarded, and the cells were resuspended in 1 ml of mammosphere medium (DMEM/F12 medium without serum supplemented with 1X B27, EGF (20 ng/ml), and 1% P/S immediately before use). A 25 G needle was used to syringe the cell suspension three to five times, to ensure a single cell suspension had formed. To achieve ultra-low attachment conditions, each well was pre-treated with 1 mL of anti-adherence rinsing solution and washed once with sterile PBS. Cells counted and 5×10^3 cells plated out in 6-well plate containing 2 ml of mammosphere medium supplemented with the proper treatment (SAHA, TSA, RA, ZDON, or NC9). Cells incubated at 37°C and 5 % CO_2 for 7 days without moving or disturbing the plates and without replenishing the medium. After 7 days, the number of mammospheres formed was counted (at 4x magnification) which are ≥ 30 µm (for MDA-MB-468 and MDA-MB-231 cell lines) or ≥ 50 µm (for MCF.7 and T47D cell lines) using a microscope fitted with a graticule. Images taken using an Inverted Phase Contrast Microscope (Optika) at 10x objective using the Optika® Vision Pro Software (Optika). Assays were performed in triplicate and repeated three times independently.

Mammosphere forming efficiency (%) is calculated using the following equation:

$$\text{Mammosphere forming efficiency } (\%) = \frac{\text{number of mammospheres per well}}{\text{number of cells seeded per well}} \times 100$$

2.2.7 Flow cytometry

2.2.7.1 Sample preparation

Cells were seeded in 6 well plates as describing in (Table 2.4) and incubated overnight at 37°C, 5% CO_2. The cells were then treated as stated in treatment scheduling (Table 2.5). At the end of the treatment period, the medium was removed from the plate and the wells were washed with PBS, then cells were harvested in 500 µL Accutase solution (Sigma, Cat# A6964), resuspended in 500 µL medium, transferred to a new Eppendorf tube, and then centrifuged at 300 g for 5 min at 4°C. Cells were then washed once in cold PBS and centrifuged again. Next, $5x10^5$ cells were resuspended in 1 mL of cold blocking buffer (1% (w/v) BSA in PBS) and incubated for 10 minutes at RT then centrifuged at 300 g for 5 min at 4°C.

2.2.7.2 Cell staining

For detection of surface antigens (CD24 and CD44), immunolabelling was performed by diluting each antibody (at a concentration suggested by the manufacturer) in 100 µL of cold blocking buffer. The fluorescently conjugated diluted antibodies, CD24 monoclonal antibody and CD44 monoclonal antibody were added to the cell pellet and stained for 30 minutes at 4°C. The same concentration of antibody corresponding isotype control (negative control) was added to the control tubes, mouse IgG2a kappa isotype control (APC), or mouse IgG2a kappa isotype control (PE). After the incubation period, the cells were centrifuged and washed twice with 500 µL of cold blocking buffer. Then, cells were fixed in 2% (w/v) Paraformaldehde in PBS for 10 minutes at RT, washed twice, and resuspended in cold PBS, prior to being run on Fortessa X20 flow cytometer (BD Biosciences, Flow Cytometry Facility, University of Manchester).

2.2.7.3 Data collection

For each sample, 10,000 events were acquired using FACSDiva software (BD, ver 6.1.2). Analysis was performed by first creating a Side scatter (SSC-A) vs Forward scatter (FSC-A) plot to gate out cell debris. Cell clumps and doublets were then gated out using FSC-H vs FSC-A to determine the main population of single cells (Figure 2.4).

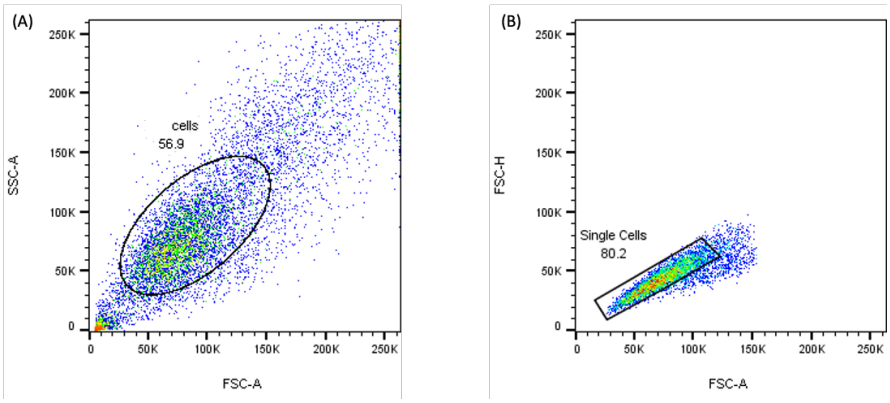

Figure 2-4 Example of gating out cell debris and doublets in flow cytometry. (A) Representative image showing the gating out of cell debris SSC-A/FSC-A. (B) the gating out of cell doubles FSC-H/FSC-A

2.2.7.4 Data analysis

The data were further analysed by FlowJo_V10.6.1 software and presented as histograms or quadrants. The APC fluorescence intensity is directly proportional to the level of CD24 cellular expression, and the PE fluorescence intensity is directly proportional to the level of CD44 cellular expression. Negative control (isotype) was used to optimise the experiment protocol and antibody concentration, while unstained control cells were used to identify auto-fluorescent cells and non-specific staining (Figure 2.5:A). Cells single stained with the cell surface markers CD24 (APC conjugated) or CD44 (PE conjugated) were used to set the gating (Figure 2.5: B and C). CD44/CD24 phenotype was presented as quadrant (Figure 2.5:D). The median fluorescence intensity (MFI) of each sample was divided by the MFI of the unstained sample to determine the extent of CD44 or CD24 expression. Populations of cells could then be distinguished based on their phenotype expression of CD24/CD44 (Figure 2.6).

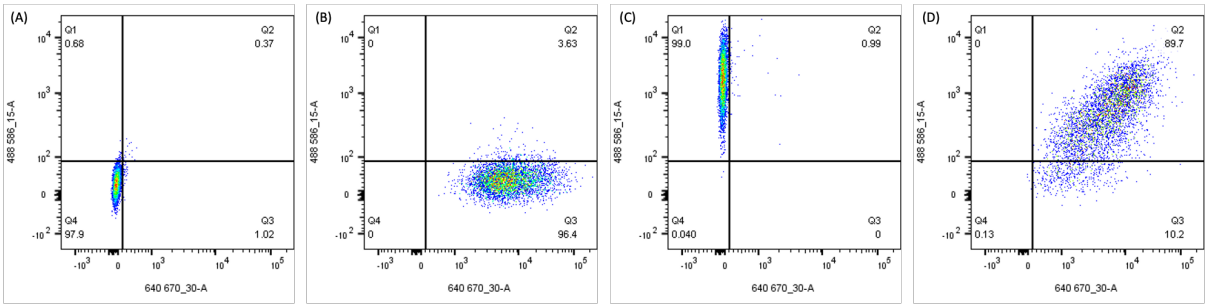

Figure 2-5 Flow cytometry gating strategy for dual colour fluorescence by FlowJo software. Cells were unstained (A), stained with antibodies which recognise the cell surface marker CD24 (APC conjugated) (B), stained with antibodies which recognise the cell surface marker CD44 (PE conjugated) (C), or double stained with CD24 and CD44 antibodies (D).

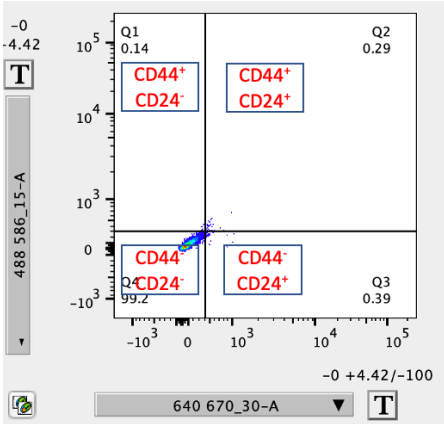

Figure 2-6 Flow cytometry analysis of expression of CD24 and CD44 to sort CD44/CD24 phenotype

2.2.8 ALDH activity

To identify and isolate stem cells, cells can be stained with antibodies against cell surface stemmnes markers. Alternatively, internal cellular enzymes can also be used. Cells expressing high levels of ALDH can be identified using a flow cytometer or isolated by cell sorting for further research. Storms et al. developed ALDEFLUOR™ kit to detect ALDH expression in cells (Storms *et al.*, 1999). The ALDH enzyme converts BODIPY-aminoacetaldehyde, a fluorescent substrate for ALDH, which has disseminated into live cells, into a fluorescing BODIPY-aminoacetate, which is trapped inside the cell. The emitted fluorescence is directly proportional to the ALDH activity in the cells and is measured using a flow cytometer. The ALDH activity can be inhibited using diethylaminobenzaldehyde (DEAB), which allows for the setting of background fluorescence.

Cells were seeded in 6-well plates then treated and incubated for the required time. Cells were then collected by trypsinisation and washed with PBS. Cells were centrifuged for 5 minutes at 250 x g, supernatant was removed, cell pellets were resuspended in 1 ml ALDEFLUOR assay buffer, then 0.5 ml aliquot incubated for 45 minutes with 5 µl ALDEFLUOR, a fluorescent substrate for ALDH enzyme; and 0.5 ml aliquot incubated with 5 µl ALDEFLUOR and 5 µl DEAB, an inhibitor of ALDH, as a negative control to set the fluorescence background. The level of enzyme activity which is directly linked to ALDH expression determined by

Fortessa X20 flow cytometer (BD Biosciences, Flow Cytometry Facility, University of Manchester). Data acquired using FACSDiva software (BD, ver 6.1.2) then further analysed by FlowJo_V10.6.1 software. Cells were gated on forward and side scatter and then gated for ALDEFLUOR based on FITC intensity. A549 cells were used as a positive control. Unstained cells from each cell line used to set the machine background. The experiment was repeated twice for each cell lines. For the analysis of the results, the percentage of gated cells were used.

2.2.9 Scratch assay

The in vitro scratch assay (wound healing assay) is a well-established method of assessing cell migration (Liang, Park and Guan, 2007). Cells were seeded in 12-well plates and incubated with the treatments for the required time. A 200µl sterile pipette tip was used to create a scratch across the cell monolayer, which was 90% confluent and washed once in PBS to remove debris. Cells were incubated in low serum 0.5% FBS supplemented medium at 37°C and 5% CO_2. Images were taken at time points: 0, 24, and 48 h for MCF.7 cells and at 0, 6, and 24 h for MDA-MB-231 cells using an Inverted Phase Contrast Microscope (Optika) at 4x objective using the Optika® Vision Pro Software (Optika). Two images were taken per well for two independent wells from three independent experiments. The scratch gap area of these images analysed on ImageJ software and the average of measurements was calculated. Percentage of cell migration was calculated as percent wound closure with reference to time point 0 h using the following equation, then control sample was arbitrarily set as 100.

$$\%\ \text{Wound closure} = \frac{\text{Distance}_{0\ (\text{h})} - \text{Distance}_{\text{time}\ (\text{h})}}{\text{Distance}_{0\ (\text{h})}} \times 100$$

2.2.10 Statistical analysis

Each experiment was repeated at least three times independently and the data are presented as mean ± SEM. Initial data management was performed using Microsoft Excel. All data shown were analysed using GraphPad Prism 9. The difference between two groups was analysed using student T-test, while the differences between more than two groups were analysed using one-way analysis of variance (ANOVA) with Dunnett or Tukey's post-hoc test. The p-values were represented as follows: *p<0.05, **p<0.01, ***p<0.001, ****p<0.0001, or n.s indicates not significant.

Chapter 3

TG2 protein levels in breast cancer cell lines

3. Chapter3: TG2-L and TG2-S isoforms' protein levels in breast cancer cell lines

3.1 Introduction

The expression of TG2 is frequently up-regulated in cancer cells that are resistant to chemotherapy and radiotherapy or form isolated metastatic sites (Mehta, 1994; Mehta *et al.*, 2004). TG2 biological activity depends on the cell type and cellular context and its subcellular localization, thus it can act either as an anti-apoptotic (Cao *et al.*, 2008; Jang *et al.*, 2010) or pro-apoptotic protein (Hsieh *et al.*, 2013). The expression of different TG2 isoforms has been reported in neuronal tumours. In particular a TG2 splice variant named TG2-S in addition to the well-known TG2-L variant has been identified in this type of cancer (Tee *et al.*, 2010).

Vorinostat (suberoylanilide hydroxamic acid, SAHA) is a potent histone deacetylase (HDAC) inhibitor that blocks the catalytic site of these enzymes (Marks and Breslow, 2007). In 2006, SAHA was first approved by the FDA for the treatment of cutaneous manifestations in cutaneous T cell lymphoma in patients with progressive or recurrent disease whom have received or currently on two prior systemic therapies (Olsen *et al.*, 2007). It has also been used for its anticancer effect in vitro in laryngeal cancer cells and lung carcinoma cells (Zhao *et al.*, 2014; Grabarska *et al.*, 2017). Promising anticancer effects of SAHA have been identified in a phase I clinical trial in patients with advanced cancer (Kelly *et al.*, 2005).Further clinical studies used SAHA as a monotherapy or in combination with other systemic therapies conducted in patients with haematological or solid malignancies. These studies demonstrated that SAHA has a potential anticancer activity and symptomatic improvement in different types of tumours with low side effect profile (Siegel *et al.*, 2009).However, some patients were insensitive or resistant to HDAC inhibitor therapy, thus a better understanding of the factors affecting the efficacy of treatment is needed.

Another HDAC inhibitor is Trichostatin A (TSA) (Yoshida *et al.*, 1990). It is an organic antifungal antibiotic derived from Streptomyces hygroscopicus that selectively inhibits mammalian enzymes of the class I and II HDAC families (Tsuji *et al.*, 1976). TSA has shown antitumor effects as monotherapy or combination with gemcitabine and cisplatin on urothelial

carcinoma of bladder cell lines inducing apoptosis and cell cycle arrest (Yeh *et al.*, 2016). In addition, it has been shown to sensitise cisplatin-resistant ovarian cancer cells (Hulin-Curtis *et al.*, 2018).

In clinical practice, retinoids have been approved by the US FDA for the treatment of acute promyelocytic leukemia, cutaneous T-cell lymphoma, and different dermatologic disorders (MS *et al.*, 1997; Orfanos *et al.*, 1997; Duvic *et al.*, 2001). The therapeutic effectiveness of retinoids in acute leukaemia has attracted attention to using them for personalised therapy of solid malignancies, including breast cancer. Although the therapeutic and chemo-preventive effects of retinoid treatment on solid tumors are still controversial, several retinoids are now in clinical trials to treat or prevent breast cancer progression, either alone or in combination with interferons and estrogen antagonists (Veronesi *et al.*, 2006; Recchia *et al.*, 2009). However, limited studies are available that explain the possible effects of retinoids, particularly the RA role in breast cancer progression and metastasis.

The TG2 gene expression was found to be up regulated by different HDAC inhibitors, such as the SAHA and TSA, and by RA in cancer cells isolated from different organs (Fraij and Gonzales, 1996; Lai *et al.*, 2007; Marks and Breslow, 2007; Olsen *et al.*, 2007). SAHA, TSA, and RA treatments were used in this project to examine whether they modulate the expression of the different TG2 isoforms TG2-L, and/or TG2-S in breast cancer cells. The biological functions and functional significance of the TG2 isoforms and their contribution to breast carcinogenesis would be possible then to study in breast cancer cells.

Although TG2 expression in breast cancer has been studied, limited data is available on its isoforms' expression and their influence on different biological activities. To shed light on the function of the TG2 different isoforms in breast cancer and given that the ERα and potentially the p53 transcription factors (Shankar *et al.*, 2020) are involved in the differential expression of the TG2 isoforms the MCF-7, T47D, MDA-MB-468, and MDA-MB-231 cells bearing variable expression of ERα and p53 (Wasielewski *et al.*, 2006) were used to explore the expression of TG2 isoforms in these cells. MCF-7 cells are wild-type ERα and p53 cells whereas T47D are wild-type ERα and mutant p53 cells. MDA-MB-468 and MDA-MB-231 cells are ERα defective and express mutated p53. Wild-type p53 cells are more sensitive to anti-cancer treatment

induced apoptosis than mutant p53 cell lines (Lowe *et al.*, 1993; Miller *et al.*, 2005). Given that treatment of human lung adenocarcinoma cells with the TG2 inhibitor KCC009 sensitises the cells to radiotherapy in a p53-independent manner (Huaying *et al.*, 2016) it was of interest to investigate whether this is the case for breast cancer cells.

3.2 Aim and objectives

The aims of the research presented in this chapter are: (i) to screen the TG2 isoforms' expression profile in four different breast cancer cell lines with different genetic backgrounds and validate these cells as a model to study the TG2 expression and its role in breast cancer progression and (ii) to determine the transamidase enzymatic activity of the different TG2 isoforms (Fesus and Piacentini, 2002b; Mishra and Murphy, 2004).

Objectives:

- To investigate the nature and the levels of expression of different TG2 isoforms in MCF.7, T47D, MDA-MB-468 and MDA-MB-231 breast cancer cell lines
- To determine the transamidase enzymatic activities of the different TG2 isoforms expressed in MCF.7, T47D, MDA-MB-468 and MDA-MB-231 breast cancer cell lines

3.3 Results

3.3.1 Characterisation of the TG2 isoforms' basal protein expression in breast cancer cell lines

The TG2 protein expression in different breast cancer cell lines was assessed using western blot analysis. Considerable variation in the TG2-L and TG2-S protein levels in MDA-MB-231, MDA-MB-468, MCF.7, and T47D breast cancer cell lines was observed. In MDA-MB-231 cells, two TG2 isoforms were detected namely the TG2-L (~79 kDa) and the TG2-S (~62 kDa) expressed at high levels. Low protein levels of both isoforms were detected in the MCF.7 and T47D cells, whereas in the MDA-MB-468 cells low levels of only the TG2-S isoform were recorded (Figure 3.1).

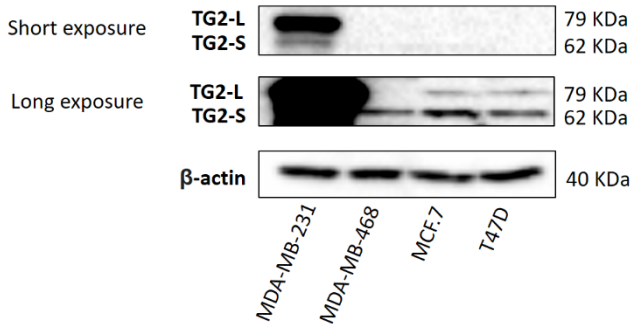

Figure 3-1 TG2 protein levels in MDA-MB-231, MDA-MB-468, MCF.7, and T47D Breast cancer cell lines. Whole cell lysates from MDA-MB-231, MDA-MB-468, MCF.7, and T47D breast cancer cell lines were subjected to Western blot analysis. One representative out of three independent repeats is presented in the figure.

3.3.2 The cytotoxic effect of SAHA, TSA, and RA in MCF.7, T47D, and MDA-MB-468 cells

To determine cell viability and establish the drug concentration that could induce the TG2 expression with no toxic effect on the cells, the SRB assay was employed as described in the Materials and Methods section. Cells were incubated with increasing concentrations of SAHA (0.1-20 µM), TSA (0.001-5 µM), or RA (0.1-200 µM) for 24, 48, and 72h.

Following the detection of TG2-L and TG2-S basal expression levels in the breast cancer cell lines used in this project, the MCF.7, T47D, and MDA-MB-468 cell lines which do not express

or express low TG2-L protein levels were treated with a range of different concentrations or SAHA, TSA, or RA which are known inducers of TG2 gene expression (SAHA (Ling *et al.*, 2012), TSA (Liu *et al.*, 2007), and RA (Ou *et al.*, 2000; Shimada *et al.*, 2001)). To optimize the concentrations to be used in the subsequent experiments, the cell cytotoxicity of SAHA, TSA, or RA was followed.

The effect of SAHA on cell cytotoxicity in MCF-7, T47D, and MDA-MB-468, cells was investigated using a range of different SAHA concentrations (0.01, 0.5, 1, 10, and 20μM) to treat these cells for 24, 48, and 72 h. MCF-7 cells exhibited higher sensitivity to SAHA, compared to T47D and MDA-MB-468 (Figure 3.2). This effect was both time and dose dependent (Figure 3.2A, 3.2B, and 3.2C). At the highest concentration used (20 μM), significant cell cytotoxicity was observed after 24 h of treatment of MCF-7 (68.34%) T47D (42.34%), and MDA-MB-468 (44.5%) cells (Figure 3.2A). Cell cytotoxicity 48 hours after SAHA treatment was 81% for MCF-7, 67.67% for T47D, and 63.5% for MDA-MB-468 (Figure 3.2B), and it was 90% for MCF-7, 73% for T47D, and 84% for MDA-MB-468 cells after 72 h treatment (Figure 3.2C).

The concentration selected to be used in the subsequent experiments was 0.5 μM for 48 h, as this concentration did not cause a significant reduction in cell viability (more than 80% of the cells were viable), but did induce TG2 expression, as confirmed by western blot.

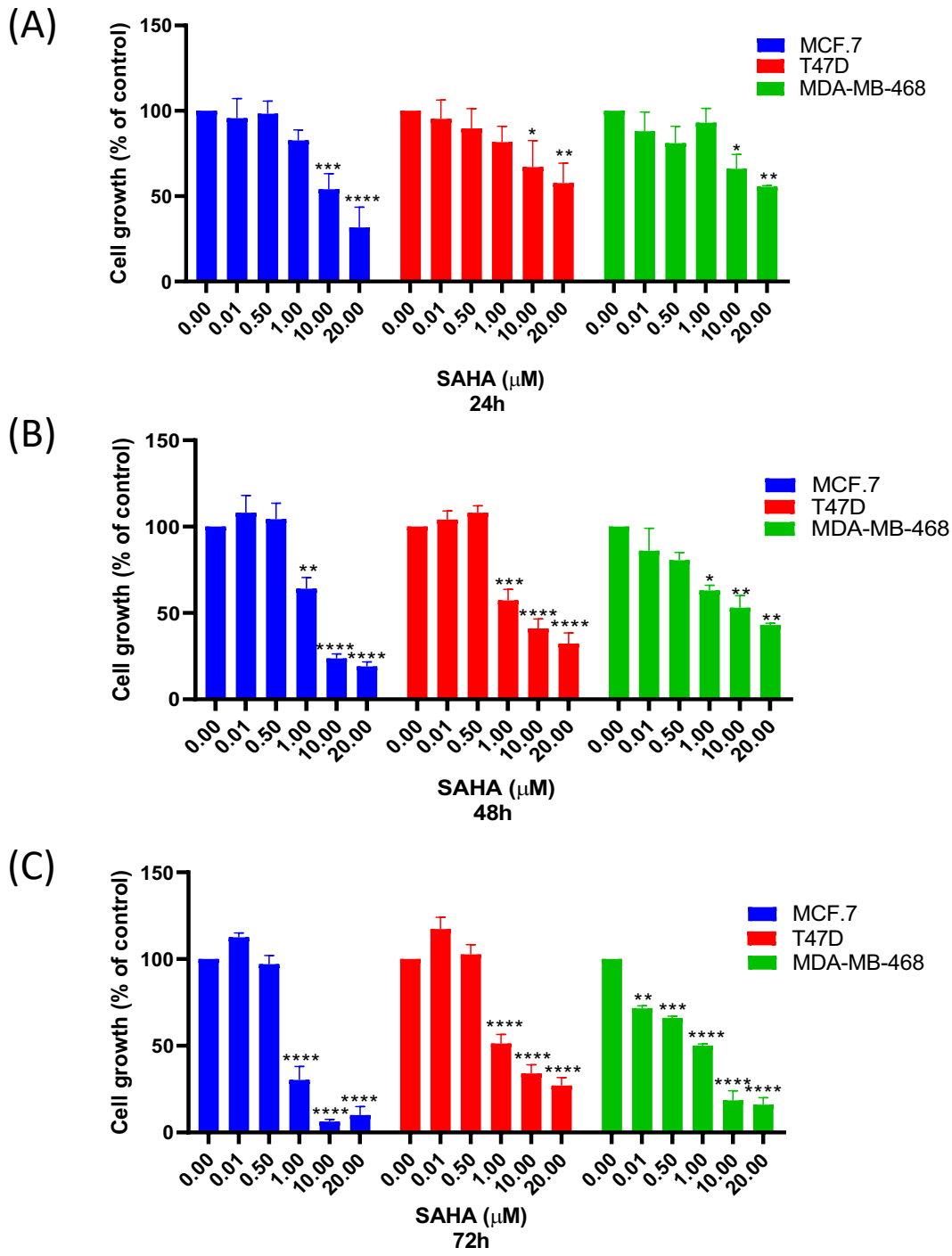

Figure 3-2 The cytotoxic effect of SAHA on MCF.7, T47D, and MDA-MB-468 cells using SRB proliferation assay. Cells were treated with a range of concentrations of SAHA for 24h (A), 48h (B), or 72h (C). DMSO was used as control (CTRL). Data are presented as the mean ± SEM of three independent experiments each one performed in triplicates. Statistical analysis was performed using One-way ANOVA followed by Dunnett's multiple comparisons test. **p<0.01, ***p<0.005 and ****p<0.0001.

Similarly to SAHA, 72h of incubation of MCF.7 cells revealed the highest sensitivity to TSA even with low concentrations (Figure 3.3). The cell viability upon incubation with 0.05µM TSA for 48 hours was 81.33% for MCF.7, 83.33% for T47D, and 76% for MDA-MB-468 cells (Figure 3.3B). This concentration was selected for subsequent experiments to induce the TG2 protein levels.

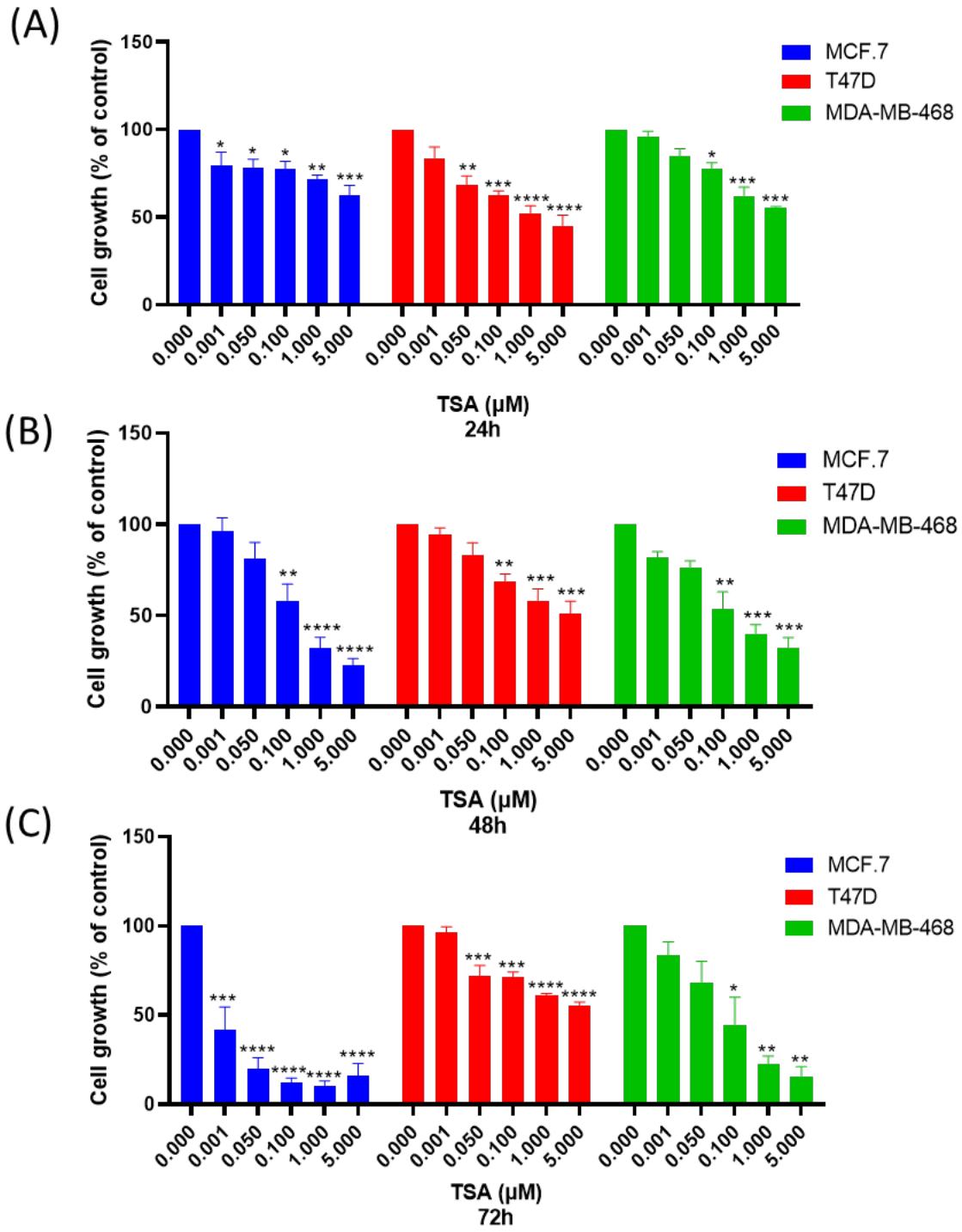

Figure 3-3 The cytotoxic effect of TSA in MCF.7, T47D, and MDA-MB-468 cells using SRB proliferation assay. Cells were treated with a range of TSA concentrations for 24h (A), 48h (B), or 72h (C). DMSO was used as control (CTRL). Data are presented as the mean ± SEM of three independent experiments each one performed in replicates. Statistical analysis was performed using One-way ANOVA followed by Dunnett's multiple comparisons test. **p<0.01, ***p<0.005 and ****p<0.0001.

Treatment of breast cancer cells with 0.1–10 µM RA for 24h, induced cell survival in MCF.7, and MDA-MB-468 cells. Cell viability in T47D was not significantly reduced following RA treatment with the same concentrations (Figure 3.4A). RA cytotoxicity significantly increased following 48h and 72h incubation, with higher RA concentrations (100 and 200 µM) (Figure 3.4B and 3.4C). The concentration selected for subsequent experiments was 40 µM RA to induce TG2 protein levels.

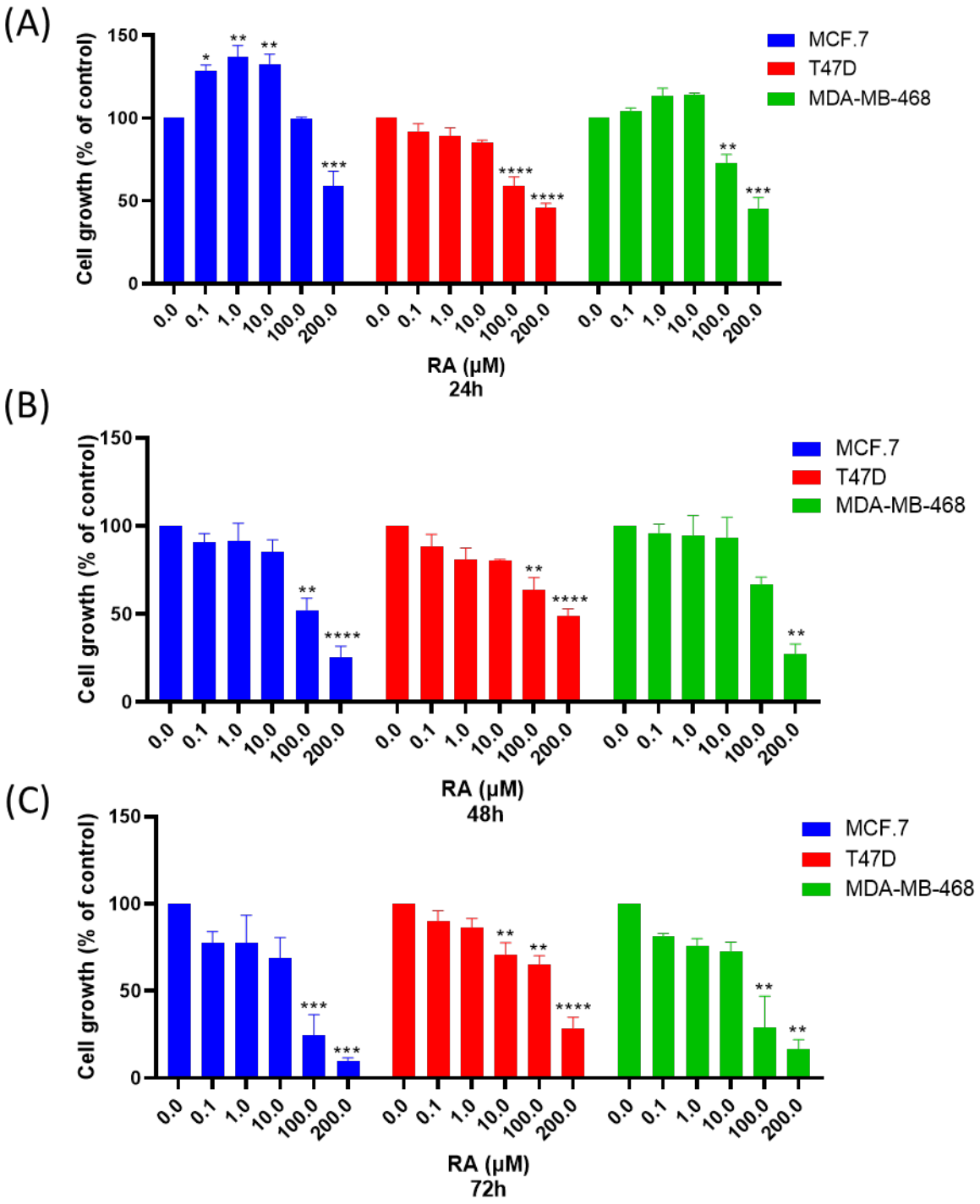

Figure 3-4 The cytotoxic effect of RA in MCF.7, T47D, and MDA-MB-468 cells using SRB proliferation assay. Cells were treated with a range of concentrations of RA for 24h (A), 48h (B), or 72h (C). DMSO was used as control (CTRL). Data are presented as the mean ± SEM of three independent experiments each one carried out in triplicates. Statistical analysis was performed using One-way ANOVA followed by Dunnett's multiple comparisons test. **p<0.01, ***p<0.005 and ****p<0.0001.

3.3.3 TG2 isoforms' protein levels in MCF-7, T47D, and MDA-MB-468 cells treated with SAHA, TSA, and RA

The protein levels and the cellular activities associated with each one of the different TG2 isoforms have not been investigated in breast cancer cells. To shed light on the role of the TG2 isoforms and the potential differential effects on breast cancer progression 3 x 10^5 MCF.7, T47D, and MDA-MB-468 cells were seeded in a 6 well plate and treated with SAHA (0.5 μM), TSA (0.05 μM), or RA (40 μM) for 48 h to induce the expression of the different TG2 isoforms. To confirm the treatment with these compounds induced the expression of different isoforms, the protein levels of the TG2 isoforms were analyzed using Western blot as described in the Materials and Methods section (Chapter 2).

This analysis indicated that the TG2-L and TG2-S isoforms' protein levels increased in the treated compared to the untreated MCF.7 cells (Figure 3.5). Both SAHA and TSA treatment did not significantly affect the TG2-L and TG2-S protein levels. However, RA treatment resulted in a significant increase of the TG-L isoform and exerted minor effect on TG2-S protein levels. The TG2-L isoform showed greater induction than the TG2-S isoform, but only RA-treated cells presented significant changes compared to control cells (Figure 3.5C).

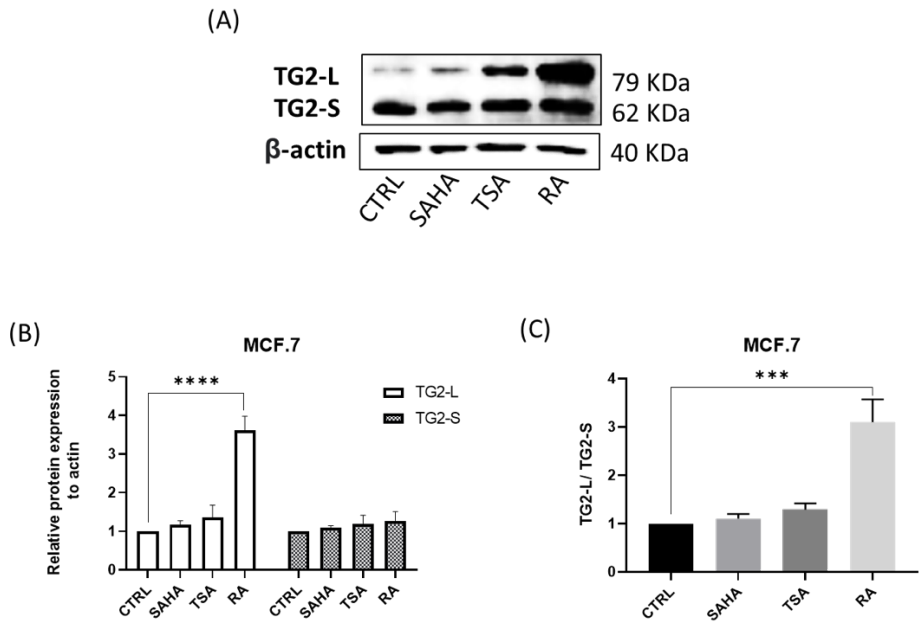

Figure 3-5 Protein levels of TG2 isoforms in MCF.7 cells. MCF.7 cells were treated with DMSO (CTRL), 0.5 µM SAHA, 0.05 µM TSA, or 40 µM RA for 48 hours. Cells were then lysed, and cellular extract (20 µg protein) was analyzed by Western blotting. A) Representative western blot indicating the protein levels of the TG2-L, TG2-S, and β-actin. B) Densitometric analysis of TG2-L (white bars) and TG2-S (grey bars) expression normalized to β-actin. C) The ratios of TG2-L / TG2-S protein expression. Bars represent the mean ± SEM of at least three independent experiments. Statistical analysis was performed using One-way ANOVA followed by Dunnett's multiple comparisons test. Statistical significance is denoted by ***p<0.005 and ****p<0.0001.

Similarly to MCF.7, the western blot of the TG2 isoforms' profiles in T47D indicated that both TG2 isoforms were induced in cells treated with SAHA, TSA, and RA. None of these changes were statistically significant, apart from the TG2-L which was significantly increased in cells treated with RA, compared to control cells (Figure 3.6A and 3.6B). The TG2-L isoform showed greater induction than the TG2-S isoform, but none of these differences were significant. (Figure 3.6C)

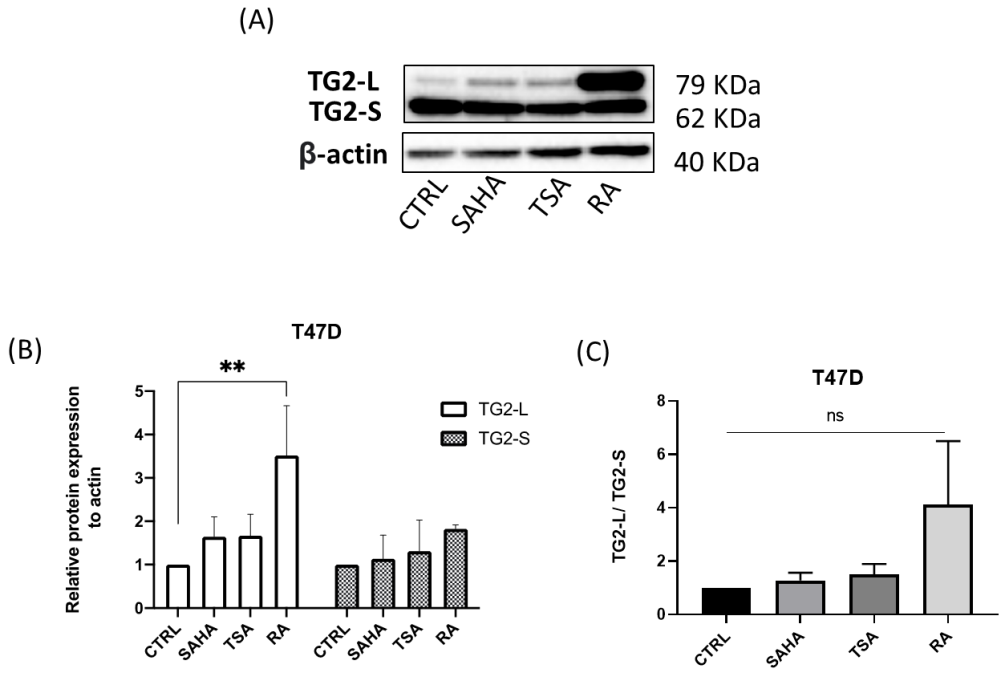

Figure 3-6 Protein levels of the TG2 isoforms in T47D cells. T47D cells were treated with DMSO (CTRL), 0.5 µM SAHA, 0.05 µM TSA, or 40 µM RA for 48 hours. Cells were then lysed, and cellular extract (20 µg protein) was analyzed by Western blotting. A) Representative western blot indicating the TG2-L, TG2-S, and β-actin. B) Densitometric analysis of TG2-L (white bars) and TG2-S (grey bars) expression normalized to β-actin and then expressed as percentages of the control. C) The ratios of TG2-L / TG2-S protein expression.Bars represent the mean ± SEM of at least three independent experiments. Statistical analysis was performed using One-way ANOVA followed by Dunnett's multiple comparisons test. Significance is denoted by **p<0.01

In MDA-MB-468 cells the TG2-L isoform was not detected. Treatment with SAHA, TSA, and RA did not affect the TG2-L protein levels in these cells, but non significantly reduced TG2-S (Figure 3.7).

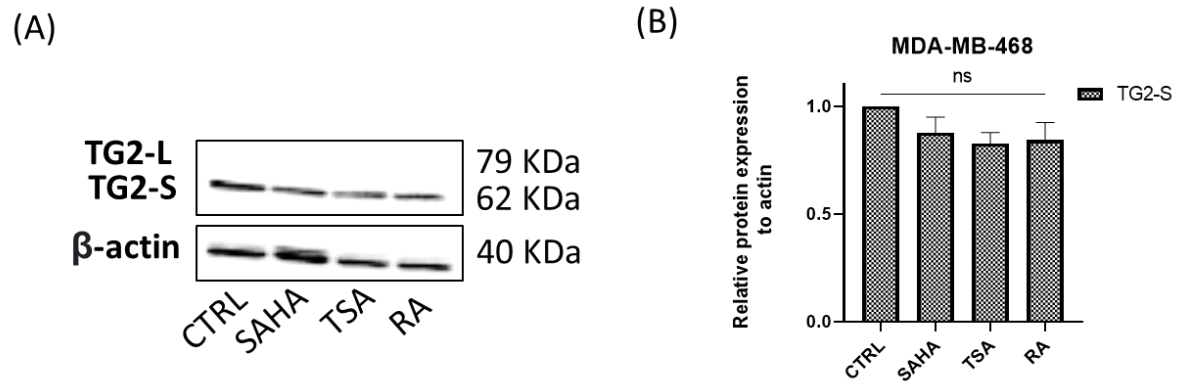

Figure 3-7 Protein levels of TG2 isoforms in MDA-MB-468 cells. MDA-MB-468 cells were treated with DMSO (CTRL), 0.5 µM SAHA, 0.05 µM TSA, or 40 µM RA for 48 hours. Cells were then lysed, and cellular extract (20 µg protein) was analyzed by Western blotting. A) Representative western blot for TG2-L, TG2-S, and β-actin. B) Densitometric analysis of TG2-L and TG2-S expression normalized to β-actin. Bars represent the mean ± SEM of six independent experiments. Statistical analysis was performed using One-way ANOVA followed by Dunnett's multiple comparisons test.

3.3.4 Assessment of TG2 transamidase activity in MCF.7 and T47D cells treated with SAHA, TSA, or RA

The transamidase enzymatic activity of the long and short TG2 isoforms was examined in whole cell lysate using the TG2-specific colorimetric assay kit (TG2 CovTest) as described in the Materials and Methods section. Briefly the TG2 enzyme present in the cell lysates of the treated cells forms biotinylated isopetide bond with the biotin-pepT26 substrate embedded in the kit plate's wells. The biotin incorporated is equivalent to the transglutaminase activity and is reflected by the absorbance of the reaction mixture at 450nm. Cellular extract (20µg total protein) from either untreated or treated for 48h with 1 µM SAHA, 0.1 µM TSA, or 50 µM RA, was loaded on the kit's 96 well plate and the absorbance at 450nm was measured.

Induction of the TG2 transamidase activity was observed in both cell lines, MCF.7 and T47D, treated with SAHA, TSA, and RA (Figure 3.8 and 3.9). RA-treated MCF.7 cells exhibited higher activity compared to the untreated, TSA-treated and SAHA-treated cells. The induction in transamidase activity was compatible with the increased TG2-L and TG2-S protein levels in the RA-treated MCF.7 and T47D cells. SAHA and TSA-treated T47D cells displayed statistically significant higher transamidase activity compared to the untreated and RA-treated cells. RA represented the highest induction, followed by TSA and SAHA.

Analysis of relative transamidase activity to TG2-L protein expression showed higher transamidase activity in control cells (DMSO-treated cells) compared to SAHA-, TSA-, and RA-treated cells relative to protein expression and these changes were only significant in RA-treated cells (Figure 3.8B and 3.9B).

TG2-S protein expression showed different transamidase activity in control cells (DMSO-treated cells) compared to SAHA-, TSA-, and RA-treated cells relative to protein expression, but none of these changes were significant (Figure 3.8C and 3.9C). Indeed, SAHA, TSA, and RA induced TG2-L and TG2-S protein expression and demonstrated higher transamidase activity. However, these treated cells in compared to control cells showed lower transamidase activity relative to the protein expression in the same sample. This suggests that SAHA, TSA, and RA induced the transamidase activity in a way irrelevant to the changes in protein expression.

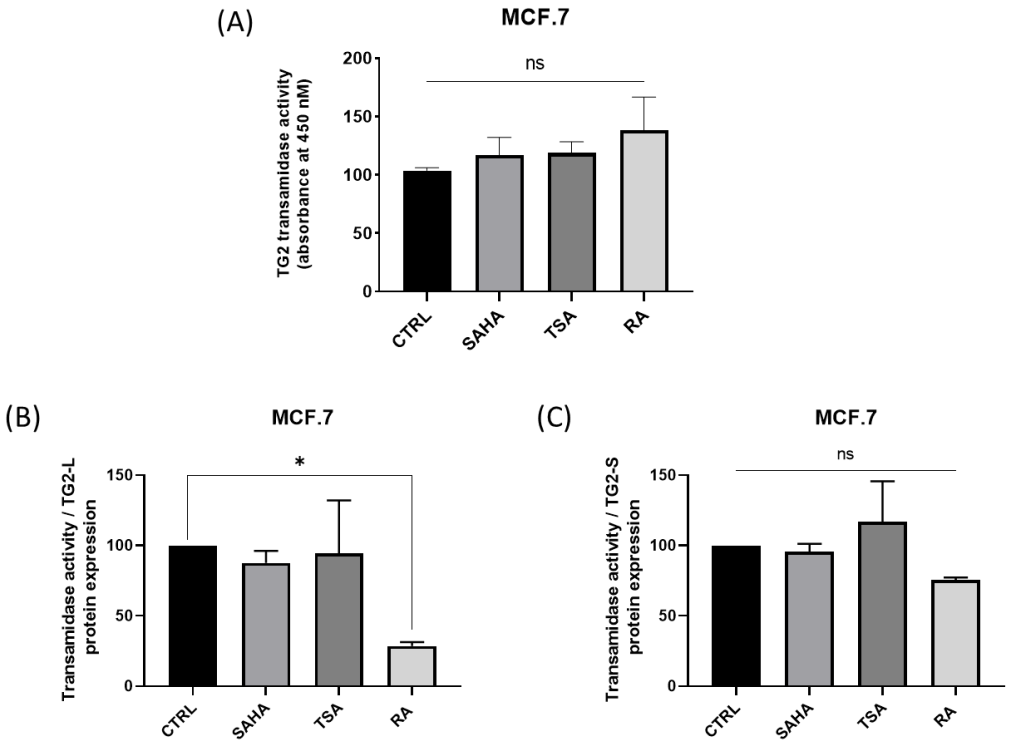

Figure 3-8 TG2 transamidase activity in MCF.7 cells. Cells were treated with DMSO, SAHA, TSA, or RA for 48 h, and the TG2-transamidase activity was estimated using the colorimetric microassay kit (TG2 CovTest). A) The plotted data represents the mean ± SEM of transamidase activity from three independent experiments, each performed in triplicates. B) TG2 transamidase activity was normalised to TG2-L protein expression. C) TG2 transamidase activity was normalised to TG2-S protein expression. Statistical analysis was performed using One-way ANOVA followed by Dunnett's multiple comparison test. Statistical significance is denoted by *p≤0.05.

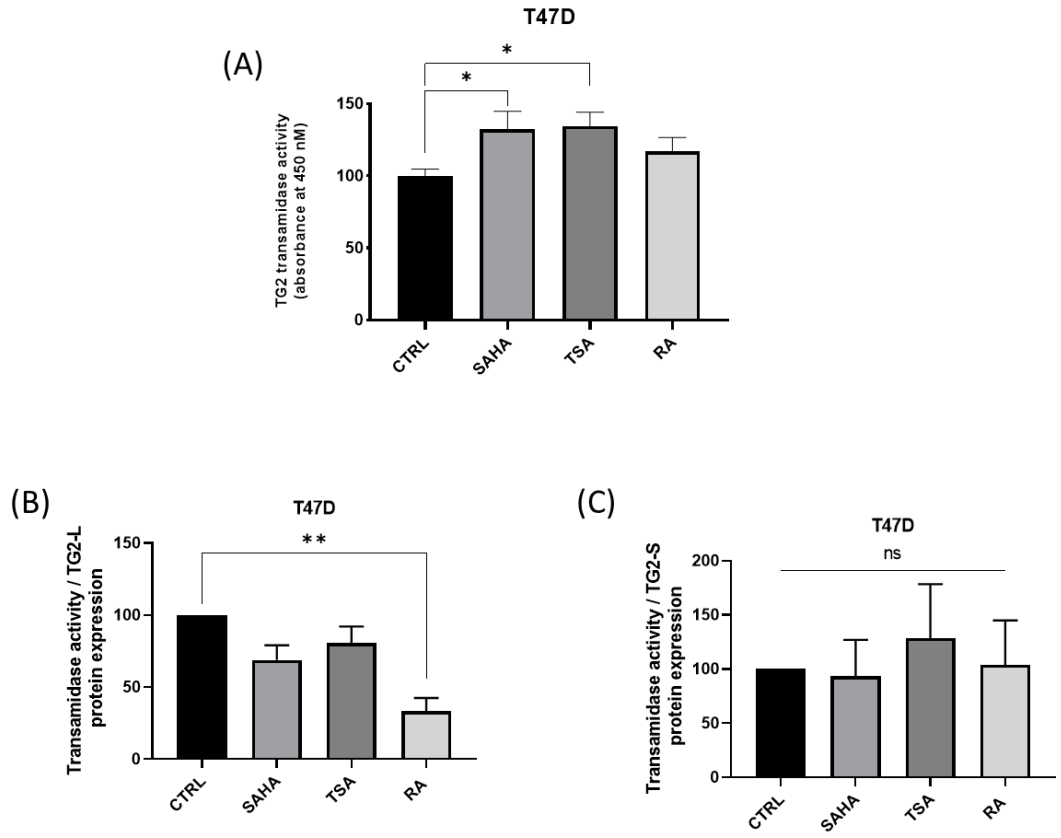

Figure 3-9 TG2 transamidase activity in T47D cells. Cells were treated with DMSO, SAHA, TSA, or RA for 48 h, and the TG2-transamidase activity was estimated using the colorimetric microassay kit (TG2 CovTest). A) The plotted data represents the mean ± SEM of transamidase activity from three independent experiments, each performed in triplicates. B) TG2 transamidase activity was normalised to TG2-L protein expression. C) TG2 transamidase activity was normalised to TG2-S protein expression. Statistical analysis was performed using One-way ANOVA followed by Dunnett's multiple comparison test. Statistical significance is denoted by *p≤0.05 and **p<0.01.

3.3.5 Assessment of TG2 transamidase activity in MDA-MB-468 cells treated with SAHA, TSA, or RA

The triple-negative cell line MDA-MB-468 cells treated for 48h with SAHA, TSA, or RA exhibited reduced TG2-S protein levels compared to untreated cells (Figure 3.10). Reduced TG2 transamidase activity was observed under all treated conditions compared to the untreated cells following the same pattern as that of the TG2-S protein levels (Figure 3.12).

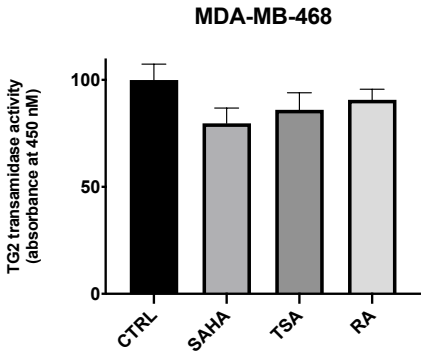

Figure 3-10 TG2 transamidase activity in MDA-MB-468 cells. MDA-MB-468 cells were left untreated or treated with SAHA, TSA, or RA for 48h and the TG2-transamidase activity was estimated using the colorimetric microassay kit (TG2 CovTest). Data plotted are the mean ± SEM of three independent experiments each performed in triplicates (C). Statistical analysis was performed using One-way ANOVA followed by Dunnett's multiple comparison test.

3.4 Discussion

TG2 has been shown to have a dual function in cancer, raising the possibility that different TG2 isoforms mediate different effects. To investigate the potentially different roles of the TG2 isoforms in the process of breast carcinogenesis, a model in which the different TG2 isoforms are differentially expressed had to be developed. To this direction the MC.7, T47D and MDA-MB-468 cells that express one TG2 isoform (Figure 3.4) were treated with the HDAC inhibitors SAHA and TSA and the vitamin A1 metabolite RA which are known inducers of the expression of the different TG2 isofroms.

3.4.1 The cytotoxic effect of SAHA, TSA, and RA in MCF.7, T47D, and MDA-MB-468 cells

To optimize the concentration and the duration of the treatment with SAHA, TSA, and RA, the SRB proliferation assay was employed. SAHA has relatively low toxicity in normal cells, but it has high growth-inhibitory activity for different tumours, including breast cancer, prostate cancer, and ovarian cancer (Butler *et al.*, 2000; Chen *et al.*, 2013; Min *et al.*, 2015; Grabarska *et al.*, 2017). SAHA suppresses proliferation in both ER-positive (MCF.7 and T47D) and ER-negative (MDA-MB-468) cell lines at low concentrations. Those effects were dose and time dependent. The most remarkable antiproliferative effect of SAHA on breast cancer cells was observed in the MCF.7 cell line, whereas MDA-MB-468 cells were the most resistant to SAHA treatment among all analyzed cell lines. Consistent with our findings, previous reports

indicate that SAHA inhibits cell proliferation in a dose- and time-dependent manner regardless of breast cancer cell subtypes. However, T47D is more sensitive to SAHA than MCF.7 and MDA-MB-468 cells were the most resistant cell line (Wawruszak *et al.*, 2019). Increasing concentrations of TSA ranging from 0.1 to 1 μM for 24, 48, or 72 hours significantly decrease cell viability of MCF.7, T47D, and MDA-MB-468 cells assessed by MTT assay (Chen et al.). Also, MCF.7 and T47D cells are more sensitive to TSA than MDA-MB-468 cells, in accordance with our findings, indicating that MCF.7 cells were more sensitive to TSA, followed by T47D and then MDA-MB-468. These results suggest that different breast cancer subtypes exhibit variable sensitivity to the HDACIs, SAHA, and TSA.

RA has been reported to exert growth inhibitory activity, which makes it a potential agent for the treatment of human cancers. Although natural retinoids have limited effects in the majority of cancers, synthetic retinoids like all-trans-N-(4-hydroxyphenyl) retinamide (fenretinide) have shown promising results in the treatment of breast cancer, endometrial cancer, and other human malignancies (Costa *et al.*, 1994; Puduvalli *et al.*, 1999; Mittal *et al.*, 2014). Our findings indicate that RA exerts significant cytotoxic effects in cells treated with high concentration $\geq$ 100 μM. Centritto et al. evaluated the growth-inhibitory effects of RA using SRB assay in luminal A MCF.7 and T47D cells ($ER^+/PR^+/HER^-$) and in triple negative MDA-MB-468 cells, in addition to other breast cancer cell lines and concluded that luminal A cells were more sensitive to RA than MDA-MB-468 cells (Centritto *et al.*, 2015). Among the different RA receptor subtypes, RAR-α is the main retinoid receptor variant mediating the anti-tumour activity of the retinoic acid in mammary cells (Centritto *et al.*, 2015). ER-negative breast cancer cell lines express lower levels of RAR-α than ER-positive and most of them are more resistant to RA-mediated growth inhibition (Alexander *et al.*, 1992). In conclusion, RA showed lower cytotoxicity in MDA-MB-468 cells compared to MCF.7 and T47D cells.

Mutated p53 induces cell survival of breast cancer cells as it has been shown that silencing of the mutated p53 in MDA-MB-468 and T47D cells triggers apoptosis (Lim *et al.*, 2009). These observations taken together with the results shown in this thesis suggest that wild-type p53 expressed in MCF.7 sensitises these cells to SAHA, TSA, and RA treatment compared to mutant p53 expressed in T47D and MDA-MB-468 cells. However, this observation requires

statistical validation by including a larger number of cell lines with mutated and wild-type p53 in future experiments.

3.4.2 Protein levels of TG2 isoforms in MCF.7, T47D, and MDA-MB-468 cells treated with SAHA, TSA, or RA

Our findings revealed that the triple negative MDA-MB-231 cells express a high level of TG2-L and a low level of TG2-S isoforms, while TG2-L was not detectable in the untreated or treated with SAHA, TSA, or RA MDA-MB-468 cells. In addition, low TG2-S protein levels were detected in untreated MDA-MB-468 cells and were further downregulated upon SAHA, TSA, or RA treatment. Untreated MCF.7 and T47D showed low TG2-L and TG2-S protein levels, whereas SAHA, TSA, or RA treated MCF.7 and T47D cells exhibited up-regulation of the protein levels of the two isoforms after 48 hours of incubation with these compounds. The induction of TG2-L in these two cell lines was significantly increased in RA-treated cells compared to the untreated control cells.

The basal protein expression of both TG2-L and TG2-S isoforms has not been studied so far in breast cancer cell lines. Ai et al. conducted a study on seven breast cancer cell lines, including MDA-MB-231, MDA-MB-435, MDA-MB-468, T47D, BT-549, MCF.7, and SK-BR-3) and two non-tumour (MCF-10A and 184B5) cell lines. The study concluded that TG2 high expression is displayed by the MDA-MB-231 cells while TG2 was not detectable in the MDA-MB-468 cells and low TG2 protein levels were recorded in MCF.7 and T47D cells (Ai *et al.*, 2008). These observations are consistent with the results presented in this thesis in regards with the TG2-L isoform, but the TG2-S isoform was not monitored in the Ai et al. study. Other studies have reported that MDA-MB-231 cells express high TG2 protein levels and the TG2-L isoform is not detectable in the MCF.7 and T47D cells (Mehta *et al.*, 2004). These discrepancies between the findings reported in this thesis and those described in previously published articles could be attributed to different antibodies used in these studies.

It should also be noted that HDAC inhibitors do not induce TG2 gene expression or protein levels in normal non-malignant cells in which the baseline TG2 expression is low or

undetectable. These results have been observed in peripheral blood lymphocytes (PBLs), human normal keratinocytes HaCaT cells (Carbone *et al.*, 2017), human mammary epithelial cells (MCF.10A1), human lung fibroblasts (MRC-5), and human umbilical vein epithelial cells (HUVEC) (Liu *et al.*, 2007). These findings indicate that HDAC inhibitors induce TG2 expression only in cancer cells and not in normal non-malignant cells. Carbone et al. reported that cancer cells express higher TG2 protein levels, coinciding with resistance to the histone deacetylase (HDAC) inhibitor SAHA upon 48 h treatment with this compound (Carbone *et al.*, 2017).

HDAC inhibitors have shown promising anticancer effects in preclinical trials, and many of them are currently at different stages of clinical trials for the treatment of different types of malignancies. SAHA is used in clinical trials to treat cutaneous lymphoma. However, many patients develop resistance to HDAC inhibitors' induced cell growth inhibition. One of the proposed mechanisms mediating this resistance is the upregulation of TG2 (Carbone *et al.*, 2017).

In neuroblastoma cell lines CHP134, SK-N-DZ, and BE(2)-C, the two isoforms of TG2 mRNA and protein levels have been detected and treatment of the cells with 1.2 µM SAHA for 72 h up-regulated the expression of both isoforms (Ling *et al.*, 2012). These results are in line with those presented in this thesis since high TG2 protein levels were detected by western blot analysis in the MCF-7 and T47D cellular extracts of cells treated with 0.5 µM SAHA for 48h.

cDNA microarray gene profiling of hepatoma cells demonstrated that TG2 is a common transcriptionally induced target in various cell lines treated with TSA (Chiba *et al.*, 2004). It has also been reported that treatment of MDA-MB-468 and MCF-7 with 0.1 µM TSA for 6h or 24h does not induce cell death but significantly up-regulates TG2 gene expression (Liu *et al.*, 2007). However, western blot analysis in the present study revealed that 0.05 µM TSA for 48 h up-regulated both TG2 isoforms' expression without a significant reduction in cell viability of MCF-7 or T47D cells. Down-regulation of TG2-S protein levels was detected in MDA-MB-468 cells treated with the same concentration of TSA.

Finally up regulation of the TG2 protein levels were detected in the RA treated MCF-7 and T47D cells whereas downregulation of the TG2-s protein levels was detected in the RA treated

MDA-MB-468 cells. ERα has been shown to modulate RARα transcriptional activity in ERα-positive breast cancer cells (Lu *et al.*, 2005) and RAR-α was found to be down-regulated in ERα-negative breast cancer cells (Rishi *et al.*, 1996) providing justification for the observed results in the RA treated ERα negative MDA-MB-468 cells.

3.4.3 Assessment of TG2 transamidase activity in MCF-7, T47D, and MDA-MB-468 cells treated with SAHA, TSA, or RA

The TG2 transamidase activity assessed in the MCF-7 and T47D cells treated with SAHA, TSA, or RA indicated compatibility between TG2 enzymatic activity and induction of TG2 protein levels compared to the untreated cells. The same trend was observed in MDA-MB-468 where reduced TG2-S protein levels in SAHA, TSA, and RA treated cells coincided with down-regulated TG2 transamidase activity suggesting that TG2 protein levels are linked to its transamidase activity in breast cancer cells.

Studies exploring the binding affinity of the TG2-S versus the TG2-L to GTP nucleotide have indicated that TG2-S binds to GTP with lower affinity suggesting that the short TG2 isoform might lack the GTP binding domain, or it adopts a conformation similar to the open-state (Singh *et al.*, 2016). Indeed the TG2-S isoform lacks the GTP-binding Arg-580 residue, and consequently displays less than 5% of transamidase activity (Tee *et al.*, 2010; Lai and Greenberg, 2013). It has also been shown that the transamidation activity of the TG2 isoforms bearing weaker GTP- binding is compromised (Monsonego *et al.*, 1997; Begg, Carrington, *et al.*, 2006) suggesting that the TG2 transamidation activity could be determined by the differential TG2-S protein levels in MCF-7, T47D and MDA-MB-468 cells upon treatment with SAHA, TSA, or RA.

Retinoic acid has been shown to increase the TG2 transamidase activity in human tumour cells such as cervix adenocarcinoma cells (HeLa-TV) and neuroblastoma cells (SK-N-BE-2) by six and twelve fold, respectively (Piacentini *et al.*, 1991). The GTP-binding activity of TG2 has also been studied in RA treated HeLa cells indicating that RA stimulates GTP-binding to TG2 (Singh and Cerione, 1996) suggesting that induced TG2 transamidase activity in RA treated

cells results from the stimulation of the GTPase activity complementing the increased TG2 protein levels in the RA treated cells. Thus, MDA-MB-468, which are RAR-α defective and express only the TG2-S isoform, showed reduced transamidase activity upon SAHA, TSA and RA treatment.

3.5 Conclusion

MDA-MB-231, MCF-7, and T47D express both the TG2-L and TG2-S isoforms, whereas MDA-MB-468 expresses only the TG2-S isoform. Increased protein levels of the TG2-L and TG2-S isoforms occur in the SAHA-, TSA-, and RA-treated MCF-7 and T47D cells compared to untreated cells, and TG2 transamidase activity has been induced in all treated cells. TG2-S protein levels decreased in the SAHA-, TSA-, and RA-treated MDA-MB-468 compared to untreated cells. As TG2-S expression was reduced in MDA-MB-468-treated cells, transamidase activity also decreased relative to untreated cells.

Chapter 4

TG2 Down-regulation in high TG2-L and low TG2-S expressing cell line

4. Chapter 4: TG2 Down-regulation in high TG2-L and low TG2-S expressing cell line

4.1 Introduction

TG2 is a multifunctional protein possessing several enzymatic activities including transamidase, protein disulphide isomerase, and guanine and adenine nucleotide binding activities. Conformational changes and diverse TG2 subcellular localization determine the enzymatic activity of this multifunctional protein under specific cellular microenvironmental conditions (Gundemir *et al.*, 2012). TG2 is alternatively spliced producing mainly two variants, the TG2-L and the TG2-S which have different characteristics and exert divergent biological functions (Antonyak *et al.*, 2006). In the breast cancer cells studied in this thesis, the two structurally different TG2 protein isoforms were found to be expressed in high levels in MDA-MB-231 cells and lower in MCF-7 and T47D whereas the MDA-MB-468 cells express only the TG2-S variant. Given that the TG2-S variants lack some domains such as the GTP binding site (Antonyak *et al.*, 2006) together with the fact that each domain affects the enzymatic function of the others as it has been shown for the GTP-binding activity affecting the TG2 transamidase activity conferring to cancer cells survival advantage, activation of cancer stem cell, and EMT (Kumar *et al.*, 2012) it was of interest to further investigate the role of each isoform in breast cancer.

4.2 Aim and objectives

The aim of the research described in this chapter was to investigate the contribution of the transamidation and GTP binding activities of TG2 to breast carcinogenesis. To study the involvement of each domain to pathways leading to breast cancer development, the TG2 gene expression was silenced in MDA-MB-231 cells with small interfering RNA (siRNA) or the ZDON or the NC9 TG2 inhibitors known to hinder specific enzymatic TG2 activities were used to treat breast cancer cells.

Objectives:

- Silencing the TG2 gene expression in MDA-MB-231 cells
- Determine the cytotoxicity and optimise the concentration of ZDON and NC9 to be used to treat breast cancer cells.
- To determine the enzymatic activities of the different TG2 isoforms expressed in MDA-MB-231 breast cancer cell lines treated with the TG2 inhibitors (ZDON and NC9) or siRNA.

4.3 Results

4.3.1 Silencing of the TG2 gene expression

The optimal concentration and time of siRNA transfection to achieve 70% reduction of TG2 gene expression were studied. According to the manufacturer's instructions, TG2 gene silencing is measured at the mRNA level 24 to 48 hours after transfection, whereas silencing efficiency at the protein level is measured 48 hours or more after transfection. Hence, different siRNA concentrations and different transfection times were used to determine the most appropriate conditions to silence TG2 gene expression. 200,000 cells seeded in a 6 well plate and transfected with scramble-non targeting, used as a negative control, or siRNA targeting TG2. Cell lysates were then collected 48h, 72h, or 96h post-transfection. The TG2 protein levels were then followed by western blot analysis (Figure 4.1A). The TG2 band intensity was normalised to that of the corresponding β-actin, and relative comparisons were made between the siTG2 conditions and the scramble control.

The results indicated that the TG2-S isoform was more sensitive to siRNA targeting TG2 compared to the TG2-L. However, cells transfected with 50 nM of TG2 siRNA for 96h presented ≥ 30% downregulation of TG2-L protein levels and ≥ 70% reduction of the TG2-S protein levels compared to those monitored in scramble siRNA transfected cells. Therefore, this condition was used in the subsequent experiments as the most efficient (Figure 4.1B).

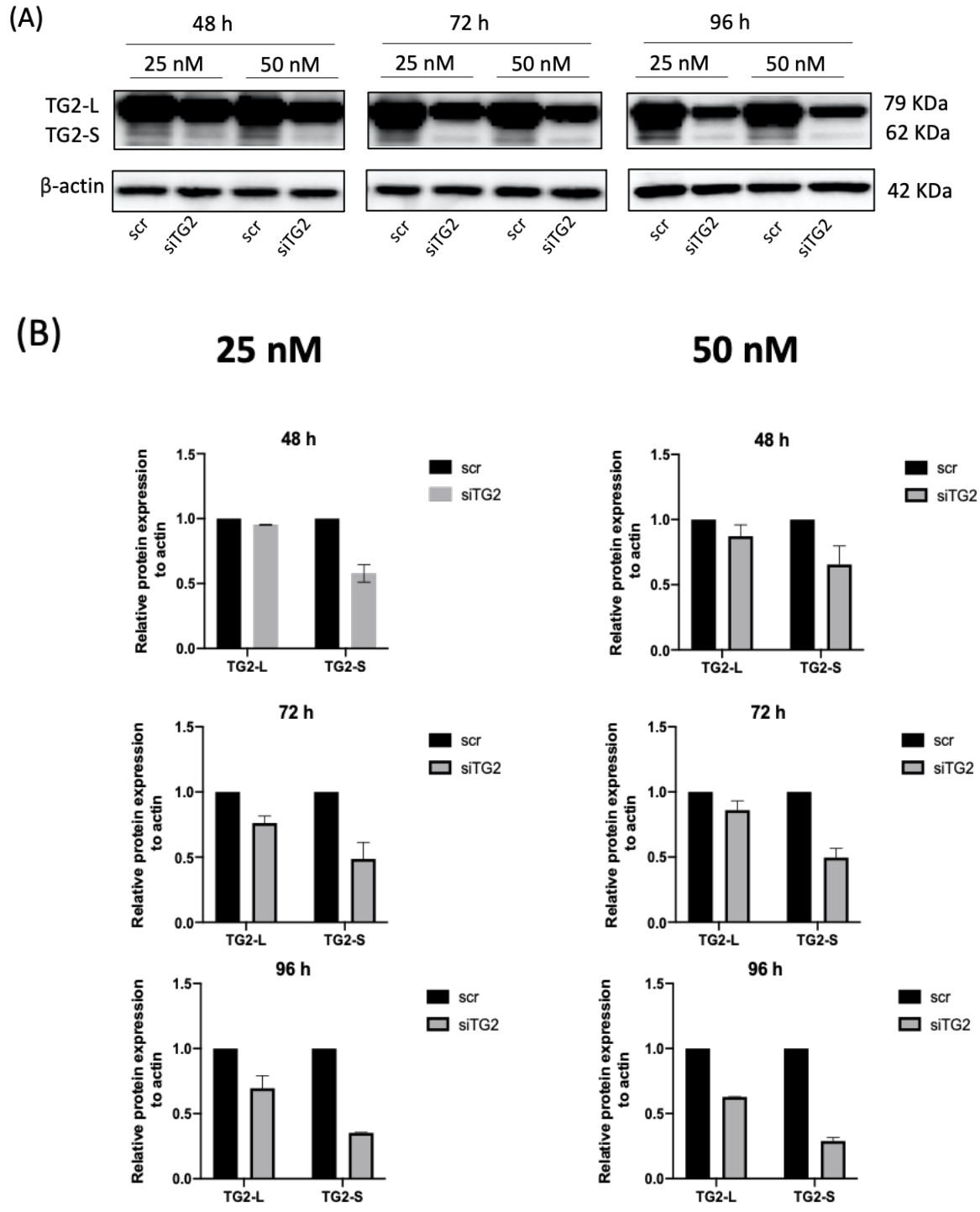

Figure 4-1 Silencing of TG2 gene expression in MDA-MB-231 cells. MDA-MB-231 cells were transfected with 25nM or 50nM of scramble or siRNA targeting TG2 for 48h, 72h, or 96 hours. Cell lysates were collected and the TG2 protein levels were followed by western blot. A) Representative western blot indicating the protein levels of the TG2-L, TG2-S, and β-actin. B) Densitometric analysis of the TG2 protein levels in scramble (black bars) or TG2 siRNA (grey bars) transfected cells normalized to β-actin. Bars represent the mean ± SEM of two independent experiments.

4.3.2 The effect of TG2 silencing on cell viability

We examined whether TG2 silencing would affect cell viability by conducting SRB assay in the presence and absence of TG2. The results showed that TG2 silencing reduced cell viability in a time-dependent manner.

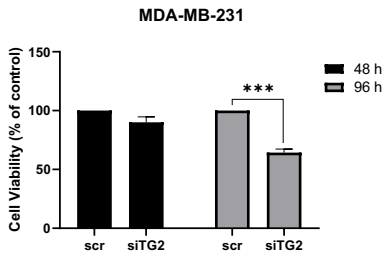

Figure 4-2 Effect of TG2 silencing on cell viability using SRB assay. MDA-MB-231 cells were transfected with 50nM scramble or TG2 siRNA for 48 or 96 hours. Bars represent the mean ± SEM of at least three independent experiments. Statistical analysis was performed using t-test. Significance is denoted by ***p<0.005

4.3.3 The cytotoxic effect of ZDON and NC9 in MDA-MB-231 cells

To determine drug cytotoxicity and establish the drug concentration that inhibits 50% of cell growth (IC50), the SRB assay was performed as described in the Materials and Methods section. The inhibitory concentration (IC50) was calculated from a dose response curve by plotting the cell survival (%) against a range of concentrations of ZDON and NC9.

4.3.3.1 The cytotoxic effect of ZDON in MDA-MB-231 cells

To evaluate the cytotoxicity of ZDON, MDA-MB-231 cells were treated with a range of different ZDON concentrations (1, 10, 50, 100, 200 µM) for 24, 48, and 72 h and cell viability was assessed using the SRB assay and the dose-response curves were used to calculate the ZDON IC50 (Figure 4.3A). The results demonstrated that cell viability was reduced after 24, 48, and 72h of treatment, and the ZDON IC50 values were 163.267 $\pm$ 5.212 µM at 24h, 97.64 $\pm$ 9.137 µM at 48h, and 70.22 $\pm$ 9.197 µM at 72h (Figure 4.3B). The ZDON effect was dose- and time-dependent.

(A)

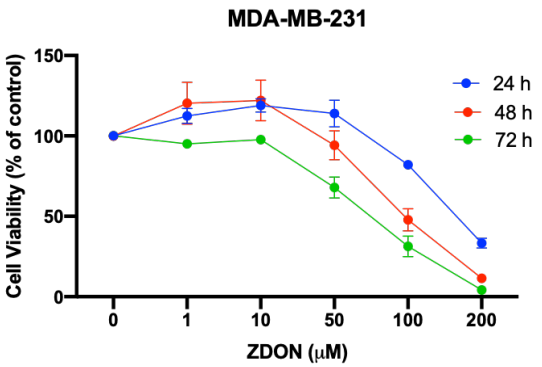

(B)

MDA-MB-231
ZDON IC50 ± SEM

24 h	48 h	72 h
163.267 ± 5.212	97.64 ± 9.137	70.22 ± 9.197

Figure 4-3 The cytotoxic effect of ZDON in MDA-MB-231 cells using SRB assay. Cells were treated with a range of ZDON concentrations for 24h, 48h, or 72h (A). DMSO was used as control (CTRL). IC50 values are the mean ± SEM obtained from dose- response curves of three independent experiments each one performed in triplicates (B).

4.3.3.2 The cytotoxic effect of NC9 in MDA-MB-231 cells

The SRB assay was also used to determine the cytotoxicity of NC9 in MDA-MB-231. Cells were treated with a range of different NC9 concentrations (1, 10, 50, 100, 200 µM) for 24h, 48h, and 72h and cell viability was assessed using the SRB assay, and the dose-response curves were used to calculate the IC50 (Figure 4.4A). Reduced cell viability was observed after 24h, 48h, and 72 h of treatment, and the NC9 IC50 values were 44.96 ± 1.409 µM at 24h, 33.57 ± 2.517 µM at 48h, and 31.41 ± 2.15µM at 72h (Figure 4.4B). The NC9 effect on MDA-MB-231 cell viability was dose- and time-dependent. The results demonstrated that MDA-MB-231 cells were more sensitive to NC9 treatment compared to that of ZDON.

(A)

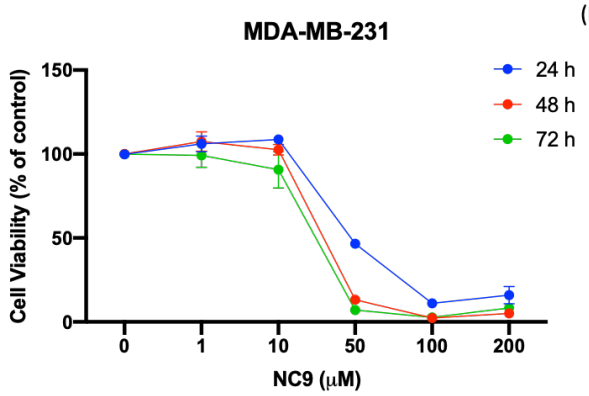

(B)

MDA-MB-231
NC9 IC50 ± SEM

24 h	48 h	72 h
44.96 ± 1.409	33.57 ± 2.517	31.41 ± 2.15

Figure 4-4 The cytotoxic effect of NC9 in MDA-MB-231 using SRB assay. Cells were treated with a range of concentrations of NC9 for 24h, 48h, or 72h (A). DMSO was used as control (CTRL). IC50 values are the mean ± SEM obtained from dose-response curves of three independent experiments each one performed in triplicates (B).

4.3.4 TG2 isoforms' protein levels in MDA-MB-231

Western blot was used to study the protein levels of the TG2 isoforms in whole cell lysates. Cells were treated for 72h with ZDON (70 µM) or NC9 (30 µM) (based on the estimation of the IC50 for each one of these compounds), or cells were transfected with 50 nM of non-targeting scramble or 50 nM of TG2 siRNA for 96h. The protein levels of each TG2 isoform (TG2-L or TG2-S) in ZDON- or NC9-treated samples were compared to control cells (treated with DMSO) and siTG2 transfected samples were compared to scramble transfected samples.

4.3.4.1 Silencing of TG2 gene expression in MDA-MB-231 cells

MDA-MB-231 cells were transfected with 50 nM of non-targeting scramble or 50 nM of TG2 siRNA for 96h. Following TG2 siRNA transfection as described in the Materials and Methods section the TG2-L and TG2-S protein levels were determined using western blot and a specific anti-TG2 antibody. TG2 siRNA significantly reduced the TG2-S protein levels (by 90%) in MDA-MB-231, while the TG2-L protein levels were reduced to a lesser extent (34%) compared to those detected in the scramble transfected cells (Figure 4.5).

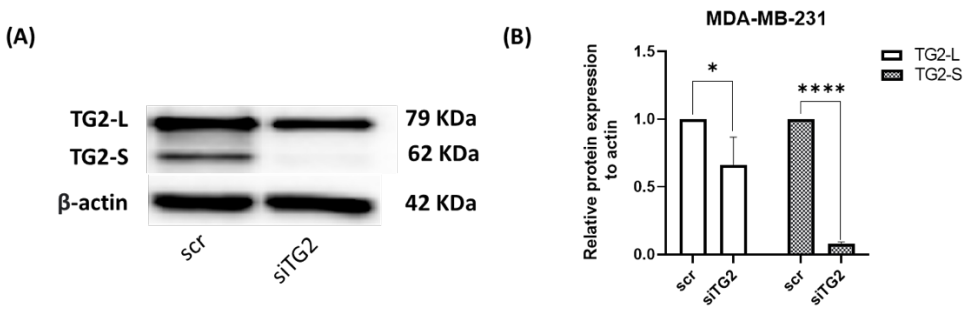

Figure 4-5 Silencing of TG2 gene expression in MDA-MB-231 cells. MDA-MB-231 cells were transfected with 50 nM scramble or TG2 siRNA for 96 hours. Cells were then lysed, and equal protein cellular extract (20 µg) was analyzed by Western blot analysis. A) Representative western blot indicating the protein levels of the TG2-L, TG2-S, and β-actin. B) Densitometric analysis of TG2-L (white bars) and TG2-S (grey bars) protein levels normalized to β-actin. Bars represent the mean ± SEM of at least three independent experiments. Statistical analysis was performed using t-test. Significance is denoted by *p≤0.05 and ****p<0.0001.

4.3.4.2 TG2 protein levels in ZDON or NC9 treated MDA-MB-231 cells

To further characterise the effect of transamidase and GTP binding activities on each other and on isoform expression, cells were incubated with two different TG2 inhibitors, ZDON (70 µM) or NC9 (30 µM), for 72h, and the whole cell lysate from the not treated or treated cells was subjected to western blot analysis.

The results demonstrated that ZDON has no effect on TG2-L protein levels but induced the TG2-S expression by 35%. NC9 stimulated 27% induction in the TG2-L isoforms, while it reduced the TG2-S expression by 39%. However, none of these changes were significant (Figure 4.6A, B).

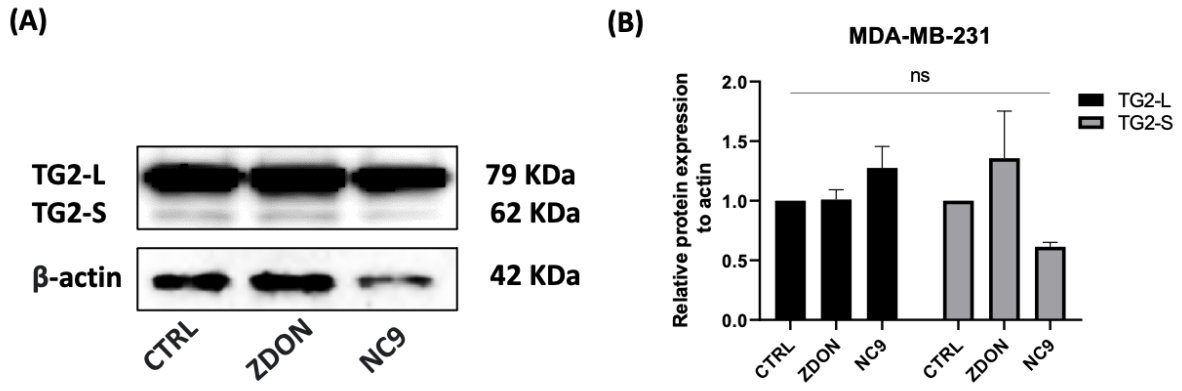

Figure 4-6 Protein levels of TG2 isoforms in MDA-MB-231 cells. MDA-MB-231 cells were treated with DMSO (CTRL), ZDON (70 µM) or NC9 (30 µM) for 72 hours. Cells were then lysed, and cellular extract (20 µg protein) was analyzed by Western blotting. A) Representative western blot indicating the protein levels of the TG2-L, TG2-S, and β-actin. B) Densitometric analysis of TG2-L (black bars) and TG2-S (grey bars) expression normalized to β-actin. Bars represent the mean ± SEM of at least three independent experiments. Statistical analysis was performed using One-way ANOVA followed by Dunnett's multiple comparisons test.

4.3.5 Transamidase activity of TG2 isoforms

The transamidase enzymatic activity of the long and short TG2 isoforms was examined in whole cell lysate using the TG2-specific colorimetric assay kit (TG2 CovTest) as described in the Materials and Methods section. Briefly the TG2 enzyme present in the cell lysates of the treated cells forms biotinylated isopetide bond with the biotin-pepT26 substrate embedded in the kit plate's wells. The biotin incorporated is equivalent to the TG2 activity and is reflected by the absorbance of the reaction mixture at 450 nm. Cellular extract (20 µg total protein) from cells transfected with siRNA, and from untreated or treated for 72 h with ZDON (70 µM) or NC9 (30 µM) was loaded on the kit's 96 well plate and the absorbance at 450 nm was measured.

4.3.5.1 Assessment of TG2 transamidase activity in TG2 silenced MDA-MB-231 cells

To evaluate whether modulation of TG2 expression levels in the MDA-MB-231 cells leads to a change in transamidase activity, the TG2 enzymatic activity was monitored in the scramble transfected cells and compared to that exhibited by the TG2 silenced cells. MDA-MB-231 cells

were transfected with 50 nM scramble or TG2 siRNA for 96 h, the cell lysates were collected and the TG2 transamidase activity examined assessed using the TG2-specific colorimetric microassay kit (TG2 CovTest).

Western blot results indicated ≥ 30% reduction of TG2-L protein levels and ≥ 90% decrease of the TG2-S protein levels compared to those detected in the lysates of the scramble transfected cells. The TG2 transamidase enzymatic activity was reduced by 25% in the TG2 siRNA transfected cells compared to that recorded in the scramble transfected cells (Figure 4.7A).

Although cells transfected with siTG2 significantly decreased transamidase activity compared to scramble transfected cells, the analysis of relative transamidase activity to TG2-L and TG2-S protein expression showed higher transamidase activity in siTG2 transfected cells compared to scramble transfected cells relative to protein expression, and these changes were only significant in transamidase activity relative to TG2-S isoform's expression (Figure 4.7B and 4.7C).

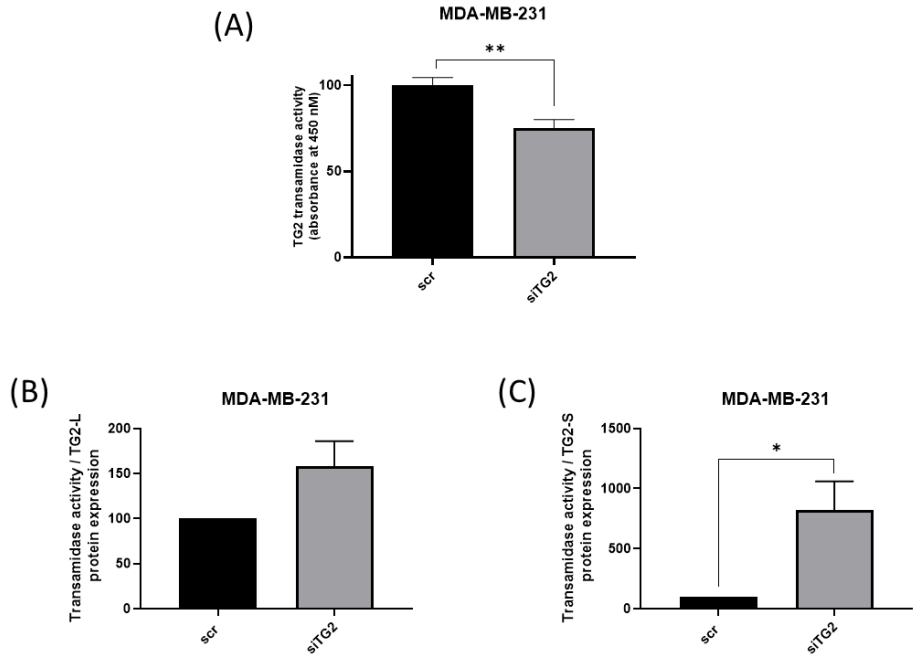

Figure 4-7 **TG2 transamidase activity in TG2 silenced MDA-MB-231 cells.** MDA-MB-231 cells were transfected with 50 nM scramble or TG2 siRNA for 96 hours and the TG2-transamidase activity was estimated using the colorimetric microassay kit (TG2 CovTest). A) The plotted data represents the mean ± SEM of transamidase activity from three independent experiments, each performed in triplicates. B) TG2 transamidase activity was normalised to TG2-L protein expression. C) TG2 transamidase activity was normalised to TG2-S protein expression. Statistical analysis was performed using t-test. Statistical significance is denoted by *p≤0.05 and **p<0.01.

4.3.5.2 Assessment of TG2 transamidase activity in ZDON or NC9 treated MDA-MB-231 cells

MDA-MB-231 cells were treated with DMSO (CTRL), ZDON (70 μM) or NC9 (30 μM) for 72 hours. And the TG2 transamidase activity examined in whole cell lysates using the TG2-specific colorimetric microassay kit (TG2 CovTest). Reduction of the TG2 transamidase activity was observed in cells treated with either ZDON or NC9 compared to the DMSO treated cells (CTRL) (Figure 4.8A). NC9-treated MDA-MB-231 cells exhibited statistically significant reduction (30%) of TG2 transamidase activity compared to ZDON-treated cells, which reduced TG2 transamidase activity by 20% but this reduction was not statistically significant.

Although cells transfected with siTG2 significantly decreased transamidase activity compared to scramble transfected cells, the analysis of relative transamidase activity to TG2-L and TG2-S protein expression showed higher transamidase activity in siTG2 transfected cells compared to scramble transfected cells relative to protein expression, and these changes were only significant in transamidase activity relative to the TG2-S isoform's expression (Figure 4.7B and 4.7C).

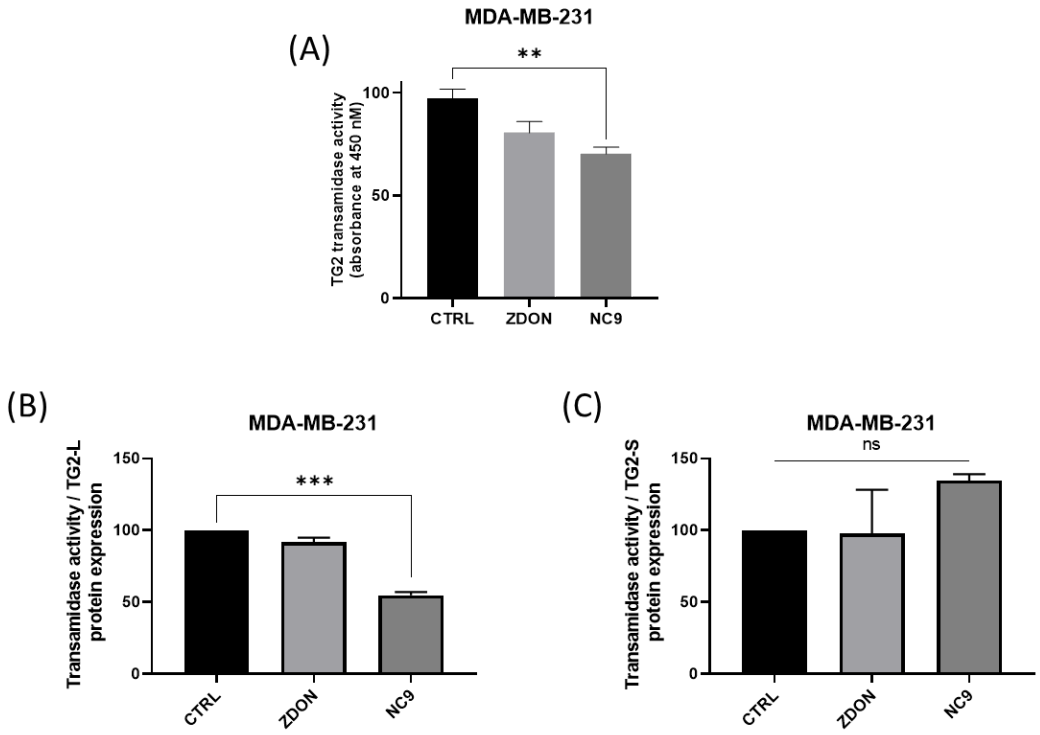

Figure 4-8 TG2 transamidase activity in ZDON or NC9 treated MDA-MB-231 cells. MDA-MB-231 cells were treated with DMSO (CTRL), ZDON (70 µM) or NC9 (30 µM) for 72 hours and the TG2-transamidase activity was estimated using the colorimetric microassay kit (TG2 CovTest). A) The plotted data represents the mean ± SEM of transamidase activity from three independent experiments, each performed in triplicates. B) TG2 transamidase activity was normalised to TG2-L protein expression. C) TG2 transamidase activity was normalised to TG2-S protein expression. Statistical analysis was performed using One-way ANOVA followed by Dunnett's multiple comparison test. Statistical significance is denoted by **p<0.01 and ***p<0.005.

4.4 Discussion

To evaluate the correlation between TG2 protein levels and biological activity in breast cancer cells, the TG2 protein levels were first analyzed in different human breast cancer cells including the luminal (MCF-7 and T47D), the basal A (MDA-MB-468), and the basal B (MDA-MB-231) cells. Low TG2-L and TG2-S protein levels were identified in the luminal (MCF-7 and T47D) cells and high TG2-L and TG2-S in the basal B (MDA-MB-231) cells, but only TG2-S was detectable in the basal A (MDA-MB-468) cells.

4.4.1 The effect of TG2 silencing on cell viability

The siRNA target sequences used in this study are present on exons 1, 2, 7, 9, and 10. However, different silencing effects on TG2 isoforms have been shown in our results. In MDA-MB-231 cells, TG2 siRNA significantly reduced the TG2-S protein levels ≥ 90%, while the TG2-L protein levels were reduced to a lesser extent ≥ 30% compared to those detected in the scramble transfected cells. TG2-L contains exons 1-13, while TG2-S contains exons 1-10 (Malkomes *et al.*, 2021). This explains the higher sensitivity of TG2-S to the siRNA transfection.

It has been shown that over-expression of TG2-S induces cytotoxicity, while over-expression of TG2-L induces cell proliferation (Antonyak *et al.*, 2006). In addition, cell proliferation is inhibited when TG2-L is suppressed in neuroblastoma cell lines (Ling *et al.*, 2012). To investigate whether similar effects of the two isoforms apply for breast cancer cells the SRB proliferation assay was used and results indicated that cell viability was down regulated in a time dependent manner. TG2 silencing reduced the TG2-L protein levels by 34% whereas the TG2-S protein levels were reduced by 90% in the TG2 siRNA transfected cells suggesting that the effect on cell viability was mainly due to the TG2-S silencing.

4.4.2 Assessment of TG2 transamidase activity in TG2 silenced MDA-MB-231 cells

TG2 is a multifunctional enzyme exerting both transamidase and GTPase activities. Ca^{2+} binding activates transamidase activity and represses GTP binding, while GTP binding repress transamidase activity (Figure 1.12) (Achyuthan and Greenberg, 1987). Therefore, the TG2 transamidase activity depends on whether its GTP binding is turned on or not. The alternative splicing of the TG2 gene produces structurally different isoforms that exert similar or opposite functions. Both the TG2-L and TG2-S isoforms bear transamidase catalytic domain (Cys-277, His-355, and Asp-358), whereas the TG2-S isoform lacks the GTP-binding Arg-580 residue and hence displays reduced by 5% transamidase activity (Antonyak *et al.*, 2006). Alanine (Ala) substitution for Arginine (Arg-580) in the GTP-binding site improves TG2's sensitivity to calcium activation and induces transamidase activity (Begg, Carrington, *et al.*, 2006; Begg, Holman, *et al.*, 2006).

The NC9 inhibitor reacts with the Cys-277 located within the TG2 transamidation catalytic domain and directly inhibits the TG2 transamidase activity. NC9 also indirectly inhibits the GTPase activity by interacting with the transamidase domain, thereby stimulating the extended/open conformation of the protein and leading to the blockade of the GTP binding site (Kerr *et al.*, 2017).

A study conducted by Jeong et al. concluded that TG2 was degraded by calcium-mediated ubiquitination, resulting in a decrease in TG2 levels (Jeong *et al.*, 2009). ZDON-treated cells showed higher TG2-L and TG2-S protein expression compared to control cells, while NC9-treated cells showed only an induction in TG2-L expression. Both inhibitors bind to the catalytic core domain, resulting in inhibition of Ca^{2+} binding. This explains higher TG2 levels in cells treated with inhibitors compared to cells where Ca^{2+} can bind and degrade TG2, subsequently decreasing its level.

4.5 Conclusion

Transfection of MDA-MB-231 with 50 nM siRNA for 96 h knocked-down the expression of TG2-L by approximately 30% and TG2-S by approximately 90% and significantly reduced the transamidase activity. Cell viability was significantly reduced after TG2 know-down, implying that TG2 plays a role in drug-induced cell death and may contribute to treatment resistance.

Results shown in this thesis indicate that NC9 induced the TG2-L protein levels while it reduced the TG2-S protein levels. In addition, the TG2 transamidase activity was reduced in the NC9 treated compared to the untreated control cells. These results are compatible with the notion that NC9 mediated induction of TG2-L protein levels induces GTP-binding, thus leading to the inhibition of the TG2 transamidase activity. The TG2 ZDON inhibitor (Badarau, Collighan and Griffin, 2013) on the other hand, had no effect on TG2-L protein levels while stimulating TG2-S. Furthermore, ZDON reduced the TG2 transamidase activity but to a lesser extent compared to that exhibited by the NC9, lending support to the previously described model.

Chapter 5

TG2 and Breast Cancer Stem Cells

5. Chapter 5: TG2 and Cancer Stem Cells

5.1 Introduction

Stem cells are distinguished by their ability to self-renew and differentiate into different mature cell types. This theory has been developed from embryonic stem cells (ESCs) and adult stem cells to cancer stem cells (CSCs), in which ESCs can give rise to any type of cell in the body (pluripotent stem cells) while adult stem cells can be used as regenerative therapies. Adult stem cells can be isolated from organs such as the prostate, liver, skin, and mammary gland, and grown to organoid structures with the final aim to be used to repair damaged tissues (Zakrzewski *et al.*, 2019). CSCs are defined as a subpopulation of stem-like cells within tumours that have stem cell and cancer cell features. Two different hypotheses have been suggested for the origin of CSCs: i) CSCs originate from normal stem cells that have acquired genetic mutations or environmental changes. ii) CSCs develop from normal somatic cells that acquire stem-like features from genetic alterations, such as cancer cells developing stem-like properties that acquire mesenchymal characteristics and express stem-cell markers (Mani *et al.*, 2008; Yu *et al.*, 2012). CSCs are hypothesised to be resistant to chemotherapy and radiotherapy, resulting in the recurrence and metastasis of cancer and they can also initiate a tumour when implanted into immune-deficient mice (Yu *et al.*, 2012).

The role of stem cells in cancer was first recognised in 1994, when a human patient's acute myeloid leukemia-initiating cell population was isolated and injected into immune-deficient mice. These cells express $CD34^+/CD38^-$ cell surface markers (Lapidot *et al.*, 1994). In the last few years, different cell surface markers have been uncovered known as cancer hallmarks for CSCs, including CD44, CD24, CD133, CD29, CD90, aldehyde dehydrogenase 1 (ALDH1), and epithelial-specific antigen (ESA). The expression of the CSC markers is tissue dependent. Breast CSCs express $CD44^+/CD24^{-/low}$ and $ALDH^+$ (Al-Hajj *et al.*, 2003; Ginestier *et al.*, 2007), $CD133^+$ is expressed in colon (O'Brien *et al.*, 2007), brain (Choi *et al.*, 2014), and lung CSCs (Eramo *et al.*, 2008), $CD34^+CD38^-$ in leukemia (Guzman and Jordan, 2004), $CD44^+$ by head and neck CSCs (Prince *et al.*, 2007), $CD90^+$ by liver CSCs (Yang *et al.*, 2008), and $CD44^+/CD24^+/ESA^+$ by pancreatic CSCs (Wang *et al.*, 2016). In 2003, a small subpopulation of cancer cells was identified in breast cancer expressing the $CD44^+/CD24^{-/low}$ antigenic phenotype. These cells

are highly abundant in tumour-initiating cells compared to the tumour cells with the $CD44^{low}/CD24^{high}$ phenotype in the same sample (Al-Hajj *et al.*, 2003).

The ALDH enzymes are a family of enzymes that are composed of 19 isoforms that are localised in the cytoplasm, mitochondria, or nucleus. It is widely assumed that the ALDH activity of CSCs arises from the ALDH1A1 isoform found in humans (Marcato *et al.*, 2011). An increase in ALDH activity is a CSC marker and can be detected by the aldefluor assay. The ALDH enzymes are associated with different biological processes, such as aldehyde detoxification, in which aldehydes generated from oxidative degradation of membrane lipids, amino acids, carbohydrates, or neurotransmitter catabolism are oxidised to carboxylic acids by ALDH (Marchitti *et al.*, 2008). ALDH also mediates ester hydrolysis and antioxidant activity via generation of NADPH. The main ALDH function associated with stemness properties is oxidation of all-trans-retinal and 9-cis-retinal to produce RA. RA cell signaling is inhibited by N,N-diethylaminobenzaldehyde (DEAB) a specific ALDH inhibitor (Marcato *et al.*, 2011).

High levels of TG2 are associated with tumour initiation and increased metastasis by regulating epithelial-to-mesenchymal transition (EMT) and stemness-related processes (Kang *et al.*, 2018). Reduced cell adhesion, migration, invasiveness and cancer cell-stemness have been reported in renal cell carcinoma in which TG2 expression had been silenced (Bagatur *et al.*, 2018). The TG2 GTP-binding domain but not the catalytic domain has been suggested to mediate the epithelial-to-mesenchymal transition in mammary epithelial cells (Kumar *et al.*, 2012). Two TG2 isoforms are expressed in breast cancer cell, namely the TG2-L which has both catalytic and GTP-binding domains therefore this isoform exerts transamidase as well as GTPase activities, while the TG2-S lacks the GTP-binding domain (Arg580). This provided the foundation of our hypothesis that the expression of two different TG2 isoforms exhibit different functions in CSCs and therefore the expression of the TG2-L or the TG2-S isoform could be used as a prognostic marker for metastatic breast cancer. Furthermore, the regulation of their expression or enzymatic activities could be an efficient therapeutic strategy in the different types of breast cancer expressing diverse TG2 isoforms.

5.2 Aims and objectives

The aim of the research presented in this chapter is to characterize the role of the different TG2 isoforms in the process of CSC formation in breast cancer.

Objectives:

- To explore the importance of transamidase, GTPase, kinase and protein disulphide isomerase activities of TG2 in mammosphere formation of breast cancer cells
- Evaluate the relative contribution of the transamidase, GTPase, kinase and protein disulphide isomerase activities of TG2 on the levels of the CD44 and CD24 cell surface markers.
- Determine the effect of the transamidase, GTPase, kinase and protein disulphide isomerase activities of TG2 on ALDH enzymatic activity.

5.3 Results

5.3.1 Mammosphere-forming ability of breast cancer cell lines

In order to test the ability of breast cancer cells to form mammospheres in suspension culture on non-adherent plates we used the mammosphere formation assay as described originally by Shaw et.al, with some modifications (Shaw *et al.*, 2012). Briefly, MCF-7, T47D, and MDA-MB-468 cells were treated with SAHA (0.5 µM), TSA (0.05 µM), or RA (40 µM) for 48 h. Additionally, the role of the TG2 was assessed in MDA-MB-231 cells treated with ZDON (70 µM) or NC9 (30 µM) for 72 h, or the TG2 gene expression was silenced in these cells by siRNA transfection targeting specifically TG2. Cells were collected and re-seeded in a coated plate, to achieve ultra-low attachment condition, in DMEM:F12 medium without serum, supplemented with fresh 1X B27, EGF (20ng/ml), and 1% P/S. Cells incubated for seven days in a humidified atmosphere at 37°C and 5% CO_2 then mammospheres were counted under light microscope and images were taken using an Inverted Phase Contrast Microscope (Optika) at 10x objective using the Optika® Vision Pro Software (Optika). Three independent experiments were performed each one in triplicates.

A small population of stem-like cancer cells within a tumour promotes carcinogenesis and confers on tumour cells the ability to self-renew and form new tumours (Al-Hajj *et al.*, 2003).

The sphere formation assay of suspended cells, which are grown in serum-free medium supplemented with growth factors in an ultra-low attachment plate, is an assay allowing the identification of cancer stem cell-like cells (CSCs) (Cioce *et al.*, 2010). It was first applied to neuron cells and then was adapted to mammary cells and is called mammosphere formation assay.

5.3.1.1 Mammosphere-forming ability of MCF-7 cells

MCF-7 cells formed well- rounded, compact, and clearly defined edge mammospheres in CSCs specific culture medium. At day seven of incubation the mammospheres formed that had a diameter ranging between 30µm and 50µm were counted and the percentage of mammosphere formation efficiency (MFE %) was determined as indicated in the Materials and Methods section. Increased MFE was observed in cells treated with SAHA or TSA (Figure 5.1, SAHA, TSA) compared to untreated cells (Figure 5.1, CTRL, lower panel). This increase was statistically significant only in cells treated with TSA. Also, the morphology of the monolayer and the cells forming the mammospheres were similar to that in untreated cells. Treatment of MCF-7 cells with RA, on the other side, resulted in decreased MFE compared to that measured in untreated cells but this change was not statistically significant. Moreover, the monolayer cells presented more extended atractoid shape and mammospheres formed large loose aggregates rather than compact entities as it was the case for the mammospheres formed in untreated, SAHA, and TSA treated cells (Figure 5.1A and B). Overall, the number of mammospheres was higher in cells incubated with SAHA or TSA compared to untreated cells and lower in cells treated with RA (Figure 5.1C).

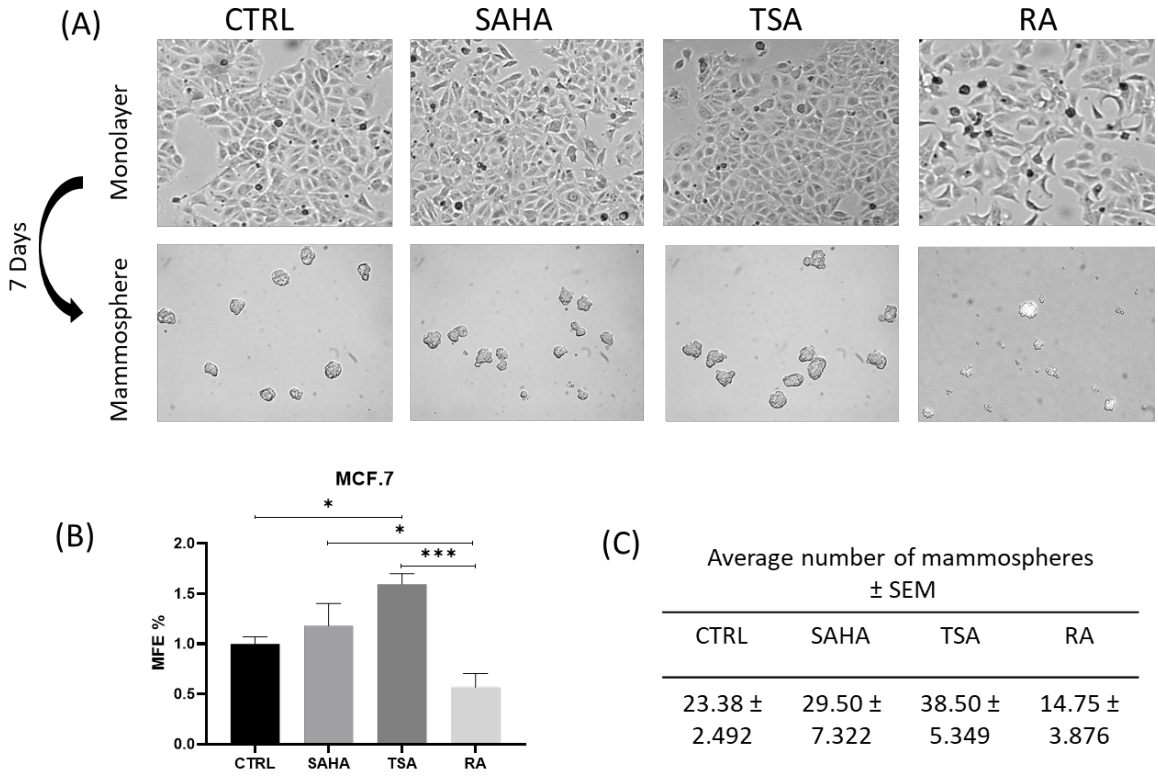

(C)

Average number of mammospheres ± SEM			
CTRL	SAHA	TSA	RA
23.38 ± 2.492	29.50 ± 7.322	38.50 ± 5.349	14.75 ± 3.876

Figure 5-1 Mammosphere formation by MCF-7 cells. (A) MCF-7 cells' monolayer representing the cells growing in adhesion and mammospheres' formation after 7 days of incubation in CSCs medium. (B) Mammosphere forming efficiency (MFE %) of untreated cells (black bars) or treated with SAHA (grey bar) TSA (dark grey bar) or RA (light grey bar). The MFE was calculated by dividing the number of mammospheres per well in the different treatments by the number of seeded cells. This number was arbitrarily set to 100 for the untreated cells. (C) Number of mammospheres sized between 30 µm and 50 µm at day 7 of incubation in CSCs medium. Data plotted are the mean ± SEM of three independent experiments each performed in triplicates. Statistical analysis was performed using One-way ANOVA followed by Tukey's multiple comparison test. Significance is denoted by *p<0.05 and ***p<0.005

5.3.1.2 Mammosphere-forming ability of T47D cells

T47D cells formed rounded or curled sheet- like mammospheres following incubation in CSCs specific culture medium. Compared to MCF-7, the mammospheres formed by T47D cells showed higher mobility and ability to split apart and rejoin during moving the plate. At day seven the mammospheres formed with diameter ranging between 30µm and 50µm were counted and the percentage of mammosphere formation efficiency (MFE %) was determined as indicated in the Materials and Methods section. Mammospheres formed in the absence of

any treatment (Figure 5.2, CTRL). Increased MFE was observed in cells treated with TSA (Figure 5.2, TSA) compared to untreated cells. The morphology of the monolayer and the cells forming the mammospheres were similar in cells treated with SAHA or TSA compared to those formed by the untreated cells. Treatment of T47D cells with SAHA or RA, on the other side, resulted in decreased MFE compared to that measured in untreated cells but these changes were only statistically significant in cells treated with RA. Moreover, mammospheres formed by cells treated with RA were small-scale rounded aggregates rather than curled sheets as it was the case for the mammoshperes formed in untreated, SAHA, and TSA treated cells (Figure 5.2A and B). Overall, the number of mammospheres was higher in cells incubated with TSA compared to untreated cells and lower in cells treated with SAHA or RA (Figure 5.2C).

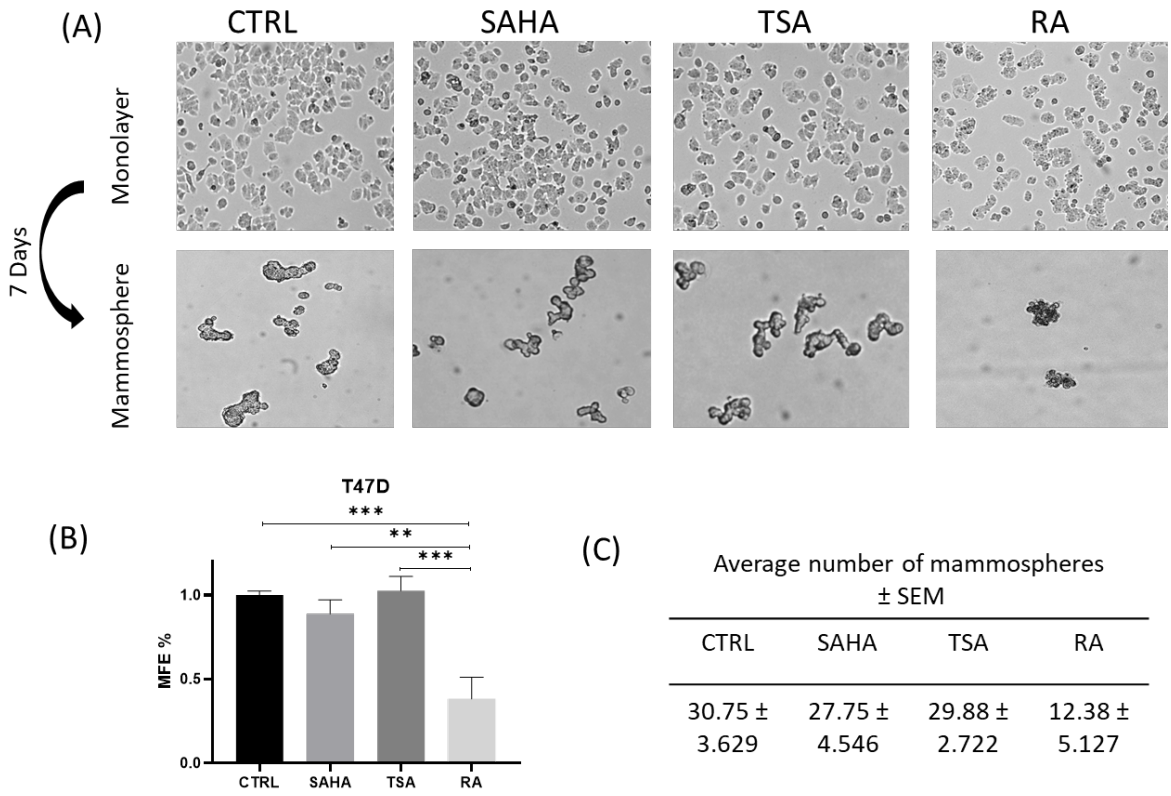

Figure 5-2 Mammosphere formation by T47D cells. (A) T47D cells' monolayer representing the cells growing in adhesion and mammospheres' formation after 7 days of incubation in CSCs medium. (B) Mammosphere forming efficiency (MFE %) of untreated cells (black bar) or treated with SAHA (grey bar), TSA (dark grey bar), or RA (light grey bar). The MFE was calculated by dividing the number of mammospheres per well in the different treatments by the number of seeded cells. This number was arbitrarily set to 100 for the untreated cells. (C) Number of mammospheres sized between 30 µm and 50 µm at day 7 of incubation in CSCs medium. Data plotted are the mean ± SEM of three independent experiments each

performed in triplicates. Statistical analysis was performed using One-way ANOVA followed by Tukey's multiple comparison test. Significance is denoted by **p<0.01 and ***p<0.005.

5.3.1.3 Mammosphere-forming ability of MDA-MB-468 cells

MDA-MB-468 cells formed loose grape-like mammospheres in CSCs specific culture medium. These mammospheres lacked cell–cell adhesion. The mammospheres formed at day seven following incubation in CSCs which had diameter 30µm were counted and the percentage of mammosphere formation efficiency (MFE %) was determined as indicated in the Materials and Methods section. Increased MFE was observed in cells treated with SAHA, TSA, or RA (Figure 5.3A, SAHA, TSA, RA) compared to untreated cells (Figure 5.3A, CTRL). This increase was not statistically significant. Overall, the number of mammospheres was higher in cells incubated with SAHA, TSA, or RA compared to untreated cells (Figure 5.3C).

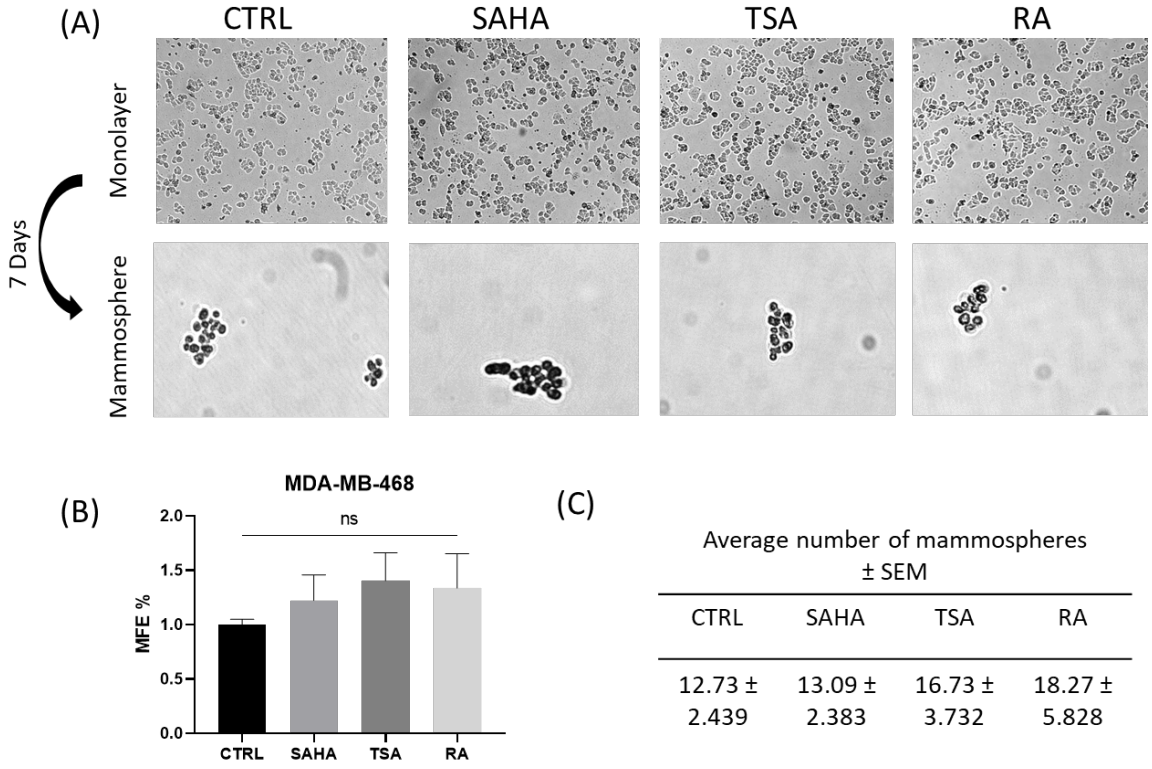

Figure 5-3 Mammosphere formation by MDA-MB-468 cells. (A) MDA-MB-468 cells' monolayer representing the cells growing in adhesion and mammospheres' formation after 7 days of incubation in CSCs medium. (B) Mammosphere forming efficiency (MFE %) of untreated cells (black bars) or treated with SAHA (grey bar) TSA (dark grey bar) or RA (light

grey bar). The MFE was calculated by dividing the number of mammospheres per well in the different treatments by the number of seeded cells. This number was arbitrarily set to 100 for the untreated cells. (C) Number of mammospheres sized between 30 µm and 50 µm at day 7 of incubation in CSCs medium. Data plotted are the mean ± SEM of three independent experiments each performed in triplicates. Statistical analysis was performed using One-way ANOVA followed by Tukey's multiple comparison test, ns indicates non-significant.

5.3.1.4 Mammosphere-forming ability of MDA-MB-231 cells

MDA-MB-231 cells formed loosely adhered clumps grape- like mammospheres in CSCs specific culture medium. The mammospheres formed at day seven following incubation in CSCs which had diameter $\geq$ 30µm were counted and the percentage of mammosphere formation efficiency (MFE%) was determined as indicated in the Materials and Methods section. Mammospheres formed in the absence of any treatment (Figure 5.2, CTRL). Increased MFE was observed in cells treated with ZDON (Figure 5.4, ZDON) compared to untreated cells. Decreased MFE compared to that measured in untreated cells was observed in NC9 treated cells, but this change was not statistically significant, however, MFE% of ZDON treated cells was statistically significant compared to cells treated with NC9 (Figure 5.4: A and B). The number of mammospheres was higher in cells treated with ZDON compared to that counted in untreated cells and lower in cells treated with NC9 (Figure 5.4C)

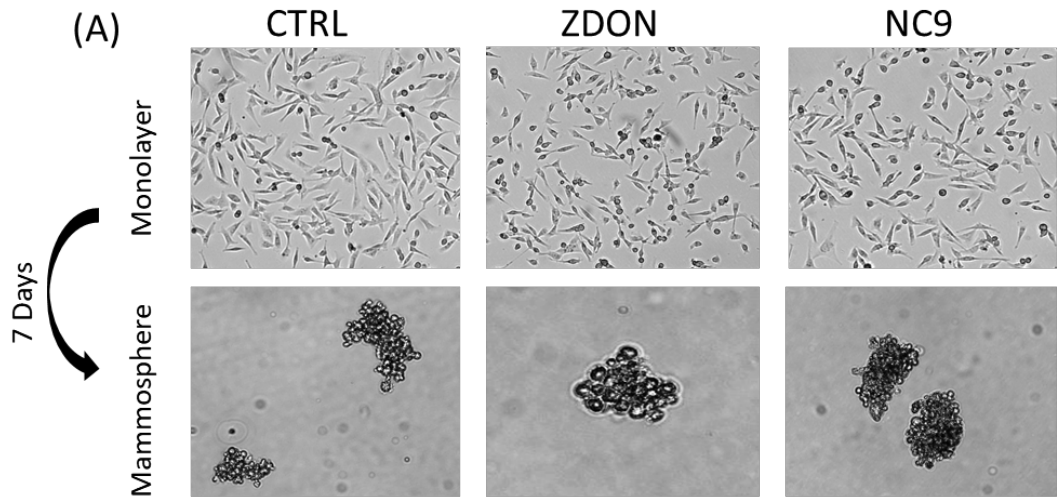

(B)

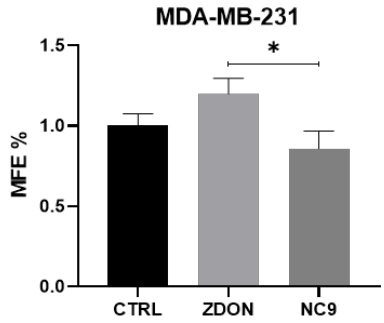

(C)

Average number of mammospheres ± SEM		
CTRL	ZDON	NC9
23. 75 ± 2.603	28.13 ± 3.073	21.00 ± 3.505

Figure 5-4 Mammosphere formation by MDA-MB-231 cells. (A) MDA-MB-231 cells' monolayer representing cells growing in adhesion and mammospheres' formation after 7 days of incubation in CSCs medium. (B) Mammosphere forming efficiency (MFE %) of untreated cells (black bars) or treated with ZDON (light grey bar) or NC9 (dark grey bar). The MFE was calculated by dividing the number of mammospheres per well in the different treatments by the number of seeded cells. This number was arbitrarily set to 100 for the untreated cells. (C) Number of mammospheres sized ≥ 30 µm at day 7 of incubation in CSCs medium. Data plotted are the mean ± SEM of three independent experiments each performed in triplicates. Statistical analysis was performed using One-way ANOVA followed by Tukey's multiple comparison test. Significance is denoted by *p<0.05.

MDA-MB-231 cells transfected with siRNA targeting TG2 for 96h were collected and re-seeded in CSCs specific culture medium. At day seven of incubation in CSCs medium the cells that formed mammospheres sized ≥ 30 µm and appeared to form mass grape-like aggregates were counted and the percentage of mammosphere formation efficiency (MFE%) was determined as indicated in the Materials and Methods section. Decreased MFE by 25% was observed in cells transfected with siRNA targeting TG2 (Figure 5.5B, siTG2) compared to

scramble transfected cells (Figure 5.5, scr), but this change was not statistically significant. The number of mammospheres was lower in cells transfected with siTG2 compared to scramble transfected cells (Figure 5.5C).

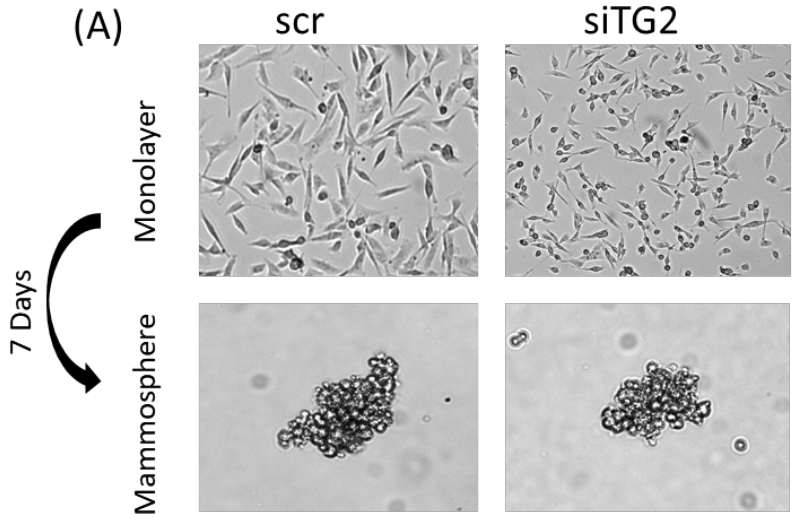

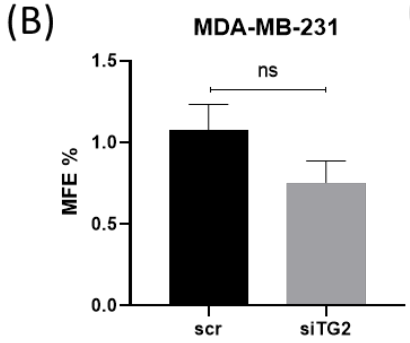

(C)

Average number of mammospheres ± SEM	
scr	siTG2
20.88 ± 5.269	14.00 ± 2.940

Figure 5-5 Mammosphere formation in TG2 silenced MDA-MB-231 cells. (A) Scramble or TG2 silenced MDA-MB-231 cells' monolayer representing cells growing in adhesion and mammospheres' formation after 7 days of incubation in CSCs medium. (B) Mammosphere forming efficiency (MFE%) of scramble transfected (black bars) or siTG2 transfected (grey bar). The MFE was calculated by dividing the number of mammospheres per well in the different treatments by the number of seeded cells. This number was arbitrarily set to 100 for the untreated cells. (C) Number of mammospheres sized ≥ 30 µm at day 7 of incubation in CSCs medium. Data plotted are the mean ±SEM of three independent experiments each performed in triplicates. Statistical analysis was performed using t-test, ns indicates non-significant.

5.3.2 CD24 and CD44 cellular levels in breast cancer cells

Cancer stem cell formation is associated with the ability of cells to form mammospheres and this correlates with the expression of the CD44 and CD24 stem cell markers (Al-Hajj *et al.*, 2003). Basal breast cancer cell lines are found to express a high level of total CD44 compared to luminal subtypes (Olsson *et al.*, 2011). To investigate the association between mammosphere formation and CD44, CD24 expression, the CD44 and CD24 protein levels were assessed in MCF-7, T47D, and MDA-MB-468 cells untreated or treated with SAHA, TSA, or RA, and in MDA-MB-231 untreated or treated with ZDON, NC9, or transfected with siTG2.

MCF-7, T47D, and MDA-MB-468 cells were treated with SAHA (0.5 µM), TSA (0.05 µM), or RA (40 µM) for 48h. MDA-MB-231 cells were treated with ZDON (70 µM) or NC9 (30 µM) for 72h or transfected with siRNA (siTG2) or a non-targeting siRNA control (scramble) for 96h. To detect CD44 and CD24 expression in breast cancer cells, cells were harvested using dissociation buffer, cell pellet was blocked using 1% BSA for 10 minutes. Single-cell suspension was incubated with PE-mouse anti-human CD44 and APC-mouse anti-human CD24 antibodies (Invitrogen) at 4˚C for 30 min. After washing twice with PBS containing 1% BSA (wash buffer), the cells were fixed in 2% paraformaldehyde solution at room temperature for 10 minutes. Then 10,000 events were acquired using a Fortessa X20 flow cytometer. Data analysis was performed by using FlowJo v10.6.1 software. The intensity of APC fluorescence is directly proportional to the level of CD24 cellular expression, while the intensity of PE fluorescence is proportional to the level of CD44 cellular expression. The median fluorescence intensity (MFI) of CD24 and CD44 in each sample was divided by the MFI of the unstained control (negative control).

MDA-MB-231 cells were found to have a very high level of CD44 and a very low level of CD24 expression compared to MCF-7 and T47D (Vikram *et al.*, 2020). In this thesis, MCF-7, T47D, MDA-MB-468, and MDA-MB-231 cells exhibited basal CD24 expression levels of 79.93%, 60.52%, 222.35%, and 1.74%, respectively (Figure 5.6A). However, the CD44 expression was 27.07%, 3.92%, 24.59%, and 238.58% in MCF-7, T47D, MDA-MB-468, and MDA-MB-231, respectively (Figure 5.6B). This suggests that the MDA-MB-231 cells exhibited the highest

CD44 level and the lowest CD24 level, while the MDA-MB-468 cells exhibited the highest CD24 level and T47D cells the lowest CD44 level.

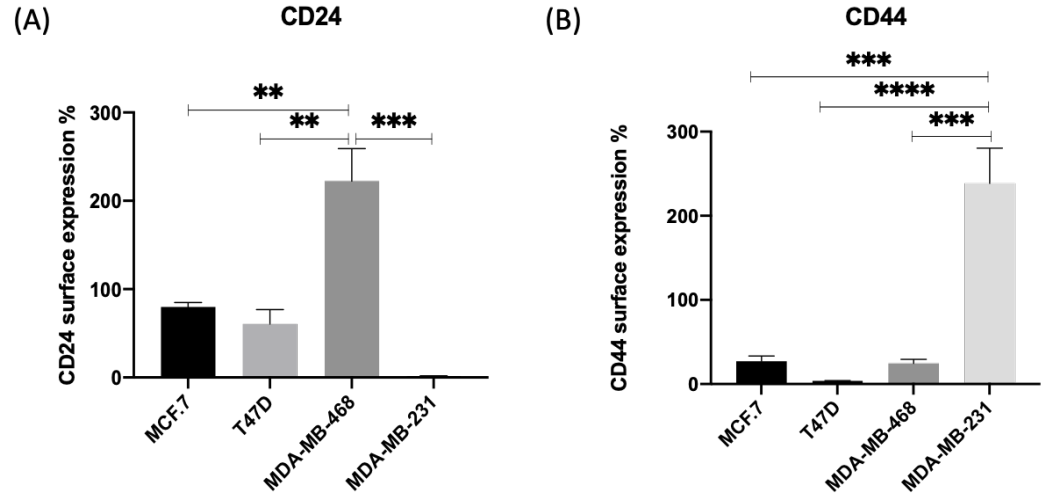

Figure 5-6 CD24 and CD44 protein basal levels in breast cancer cells. (A) CD24 expression in MCF-7, T47D, MDA-MB-468, and MDA-MB-231 is represented by the median fluorescence intensity (MFI) of APC-labelled cells. (B) CD44 expression in MCF-7, T47D, MDA-MB-468, and MDA-MB-231 is represented by the median fluorescence intensity (MFI) of PE-labelled cells. The bars represent fold change (mean ± SEM, n=3) between the MFI of the sample and the MFI of unstained cells. Statistical analysis was performed using One-way ANOVA followed by Tukey's multiple comparison test. Significance is denoted by **p<0.01, ***p<0.005 and ****p<0.0001.

5.4.2.1 CD24 and CD44 cellular levels in MCF-7 cells

The CD24 or CD44 protein levels in untreated MCF-7 cells was set to 100% and the protein levels of these markers in MCF-7 cells treated with either SAHA, TSA, or RA was determined accordingly. The CD24 protein levels in MCF-7 cells treated with SAHA were 104.7%, with TSA 103.8%, and RA 55.7% compared to control cells. Similarly, the protein levels of the CD44 marker in MCF-7 cells treated with SAHA was 137.4% with TSA 331%, and RA 90.6%.

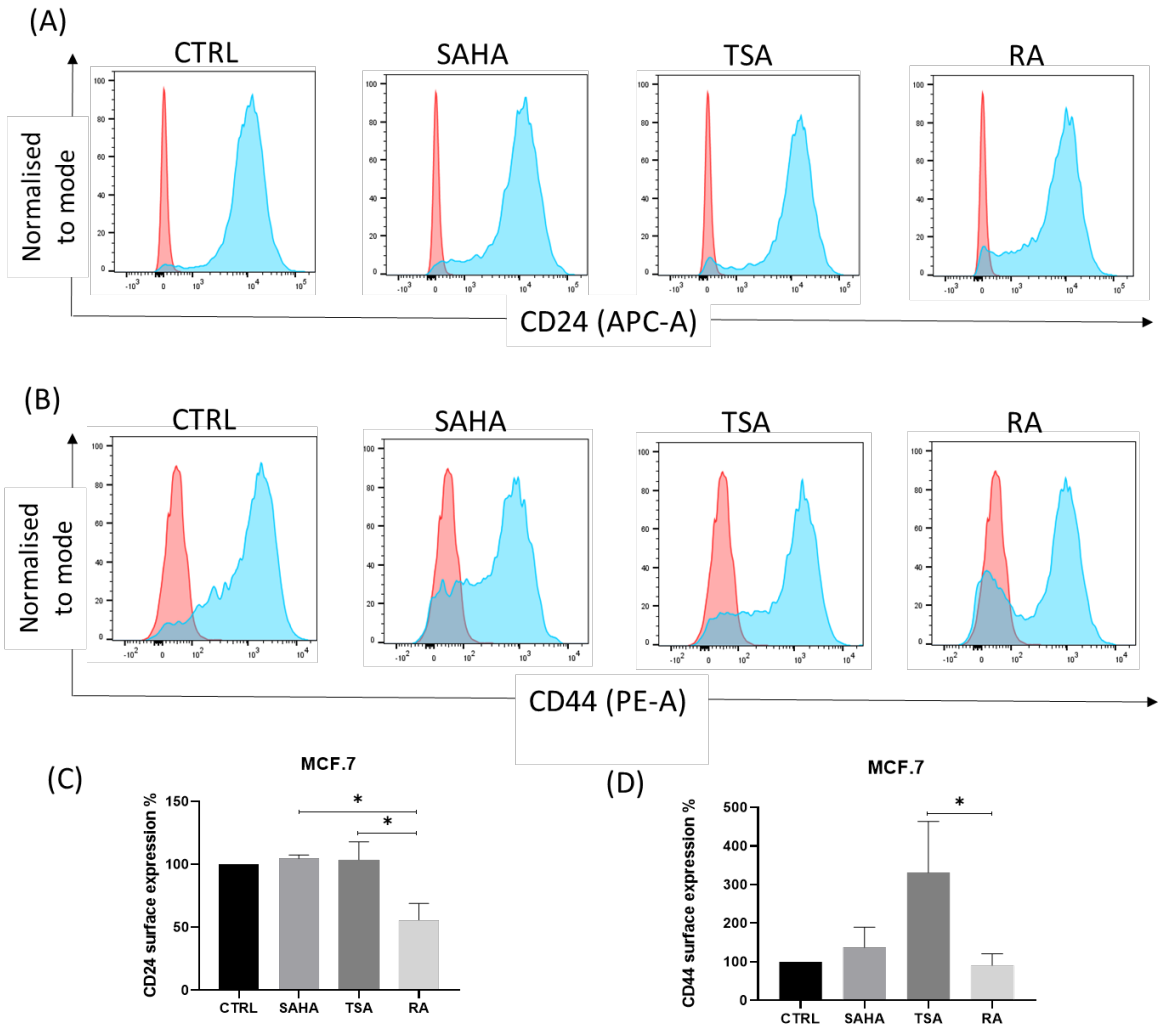

Figure 5-7 CD24 and CD44 protein levels in MCF-7 cells. (A) Representative flow cytometry histograms of CD24 expression in untreated MCF-7 cells or treated with SAHA, TSA, or RA. (B) Representative flow cytometry histograms of CD44 protein levels in untreated MCF-7 cells or treated with SAHA, TSA, or RA. CD24 (C) and CD44 (D) positive MCF-7 cells untreated (black bars) or treated with SAHA (grey bars), TSA (dark grey bars), or RA (light grey bars). The median fluorescence intensity (MFI) of untreated MCF-7 cells was arbitrarily set to 100 and the MFI of treated cells was normalized accordingly. The average ± SEM of three independent experiments is presented in (C) and (D). Statistical analysis was performed using One-way ANOVA followed by Tukey's multiple comparisons test. Significance is denoted by *p<0.05.

5.3.2.2 CD24 and CD44 protein levels in T47D cells

The CD24 or CD44 protein levels in untreated T47D cells was set to 100% and the protein levels of these markers in T47D cells treated with either SAHA, TSA, or RA was determined accordingly. The CD24 protein levels in T47D cells treated with SAHA were 129.09%, with TSA

109.66%, and RA 83.39% compared to control cells (Figure 5.8C). Similarly, the expression of the CD44 marker in T47D cells treated with SAHA was 71.57%, with TSA 2960.77%, and RA 62.1% (Figure 5.8D). Statistically significant induced CD44 protein levels were detected in TSA treated T47D cells.

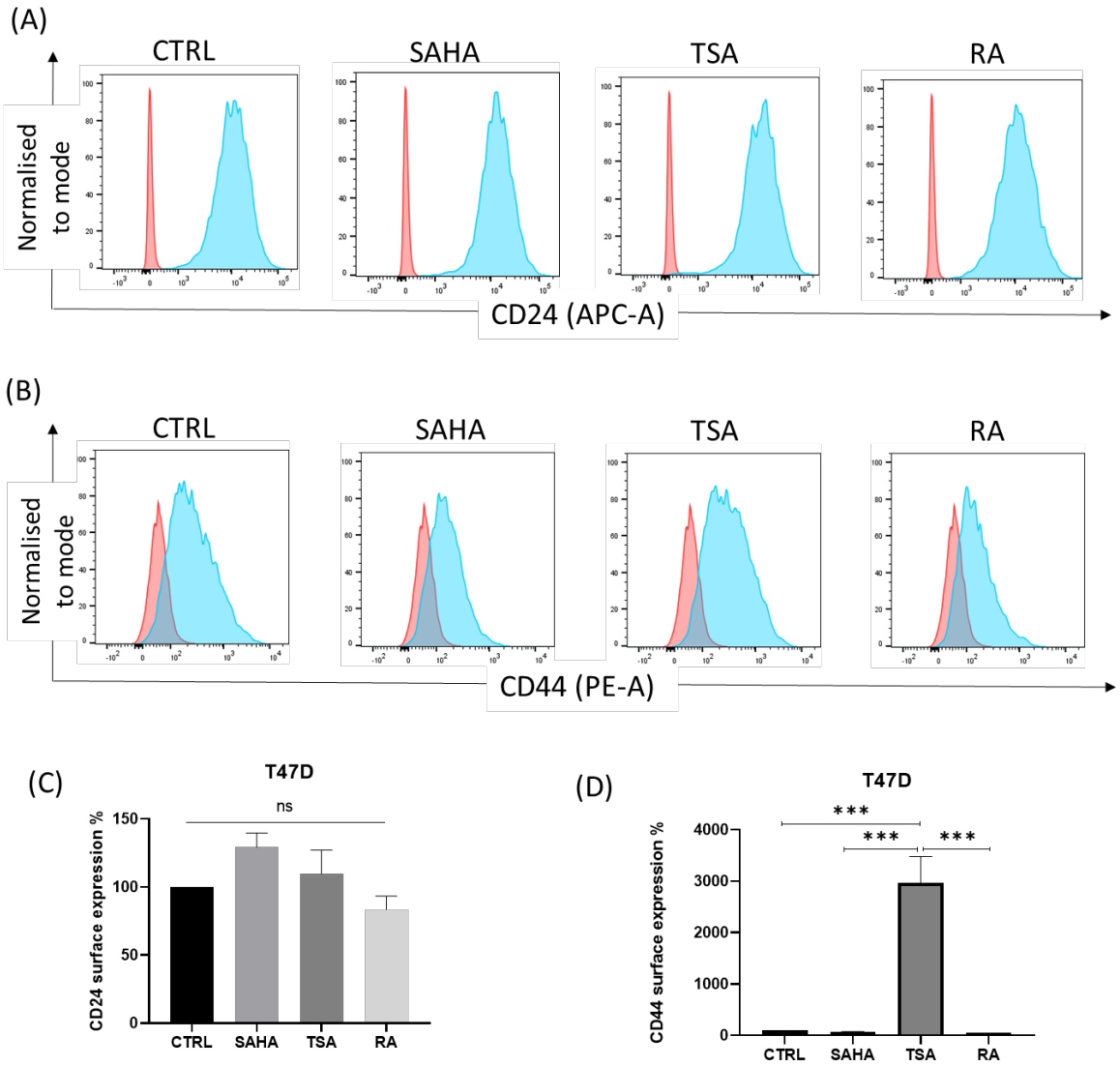

Figure 5-8 CD24 and CD44 protein levels in T47D cells. (A) Representative flow cytometry histograms of CD24 protein levels in untreated T47D cells or treated with SAHA, TSA, or RA. (B) Representative flow cytometry histograms of CD44 protein levels in T47D cells untreated or treated with SAHA, TSA, or RA. CD24 (C) and CD44 (D) positive T47D cells untreated (black bars) or treated with SAHA (grey bars), TSA (dark grey bars), or RA (light grey bars). The median fluorescence intensity (MFI) of untreated T47D cells was arbitrarily set to 100 and the MFI of treated cells was normalized accordingly. The average ± SEM of three independent experiments is presented in (C) and (D). Statistical analysis was performed using One-way ANOVA followed by Tukey's multiple comparisons test. Significance is denoted by ***p<0.005 and ns indicates non-significant.

5.3.2.3 CD24 and CD44 protein levels in MDA-MB-468 cells

The CD24 or CD44 protein levels in untreated MDA-MB-468 cells was set to 100% and the expression of these markers in MDA-MB-468 cells treated with either SAHA, TSA, or RA was determined accordingly. The CD24 protein levels in MDA-MB-468 cells treated with SAHA were 154.7%, with TSA 117.75%, and RA 106.63% compared to control cells, but these changes were not statistically significant (Figure 5.9C). The expression of the CD44 marker in MDA-MB-468 cells treated with SAHA was 110.79%, with TSA 527.13%, and RA 103.15%. Statistically significant induction of CD44 protein levels was detected in TSA treated MDA-MB-468 cells compared to untreated cells, SAHA-, and RA-treated cells (Figure 5.9D).

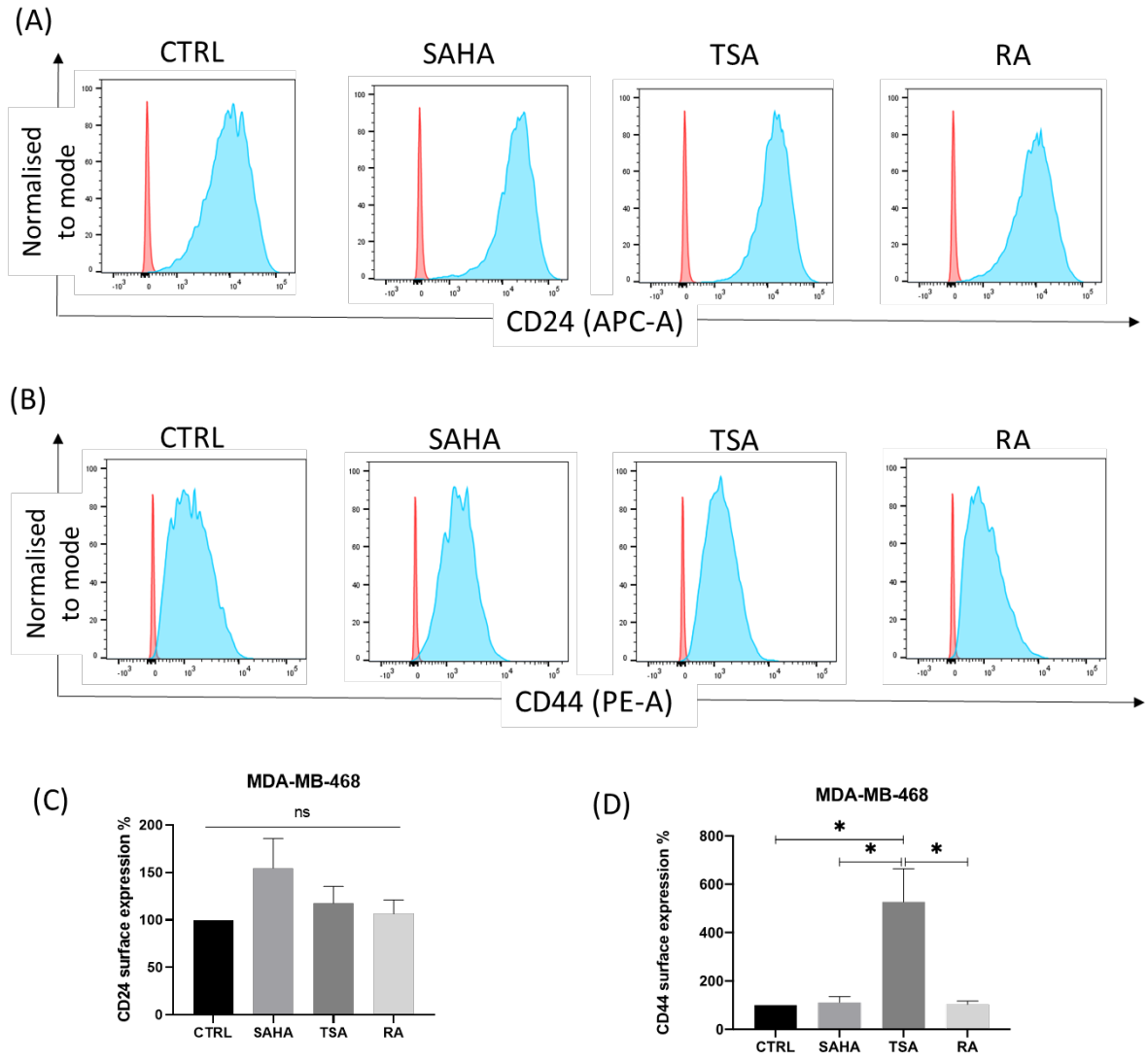

Figure 5-9 CD24 and CD44 protein levels in MDA-MB-468 cells. (A) Representative flow cytometry histograms of CD24 protein levels in untreated MDA-MB-468 cells or treated with SAHA, TSA, or RA. (B) Representative flow cytometry histograms of CD44 expression in

untreated MDA-MB-468 cells or treated with SAHA, TSA, or RA. CD24 (C) and CD44 (D) positive MDA-MB-468 cells untreated (black bars) or treated with SAHA (grey bars), TSA (dark grey bars), or RA (light grey bars). The median fluorescence intensity (MFI) of untreated MDA-MB-468 cells was arbitrarily set to 100 and the MFI of treated cells was normalized accordingly. The average ± SEM of three independent experiments is presented in (C) and (D). Statistical analysis was performed using One-way ANOVA followed by Tukey's multiple comparisons test. Significance is denoted by *$p<0.05$ and ns indicates non-significant.

5.3.2.4 CD24 and CD44 protein levels in MDA-MB-231 cells

The CD24 or CD44 protein levels in untreated MDA-MB-231 cells was set to 100% and the protein levels of these CSCs markers in MDA-MB-231 cells treated with either ZDON or NC9 were determined accordingly. The CD24 protein levels in MDA-MB-231 cells treated with ZDON were 87.38% and with NC9 78.47% compared to control cells. The protein levels of the CD44 marker in MDA-MB-231 cells treated with ZDON was 74.25% and with NC9 34.26%. Statistically significant reduction of CD44 protein levels was detected in NC9 treated MDA-MB-231 cells compared to untreated cells (Figure 5.10D).

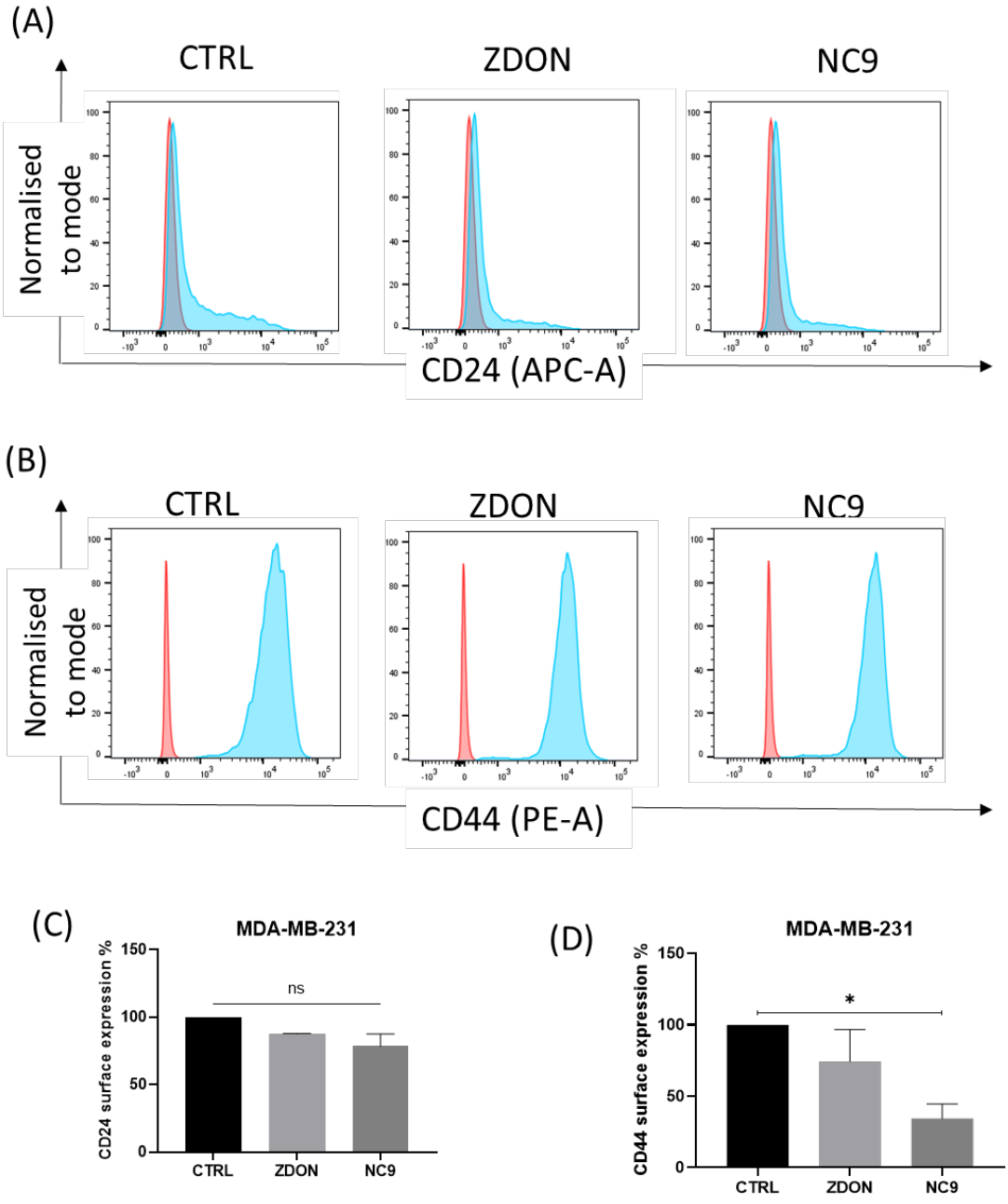

Figure 5-10 CD24 and CD44 protein levels in MDA-MB-231 cells. (A) Representative flow cytometry histograms of CD24 expression in untreated MDA-MB-231 cells or treated with ZDON or NC9. (B) Representative flow cytometry histograms of CD44 expression in untreated MDA-MB-231 cells or treated with ZDON or NC9. CD24 (C) and CD44 (D) positive MDA-MB-231 cells untreated (black bars) or treated with ZDON (grey bars) or NC9 (dark grey bars). The average fluorescence intensity (MFI) of untreated MDA-MB-231 cells was arbitrarily set to 100 and the MFI of treated cells was normalized accordingly. The average ± SEM of three independent experiments is presented in (C) and (D). Statistical analysis was performed using One-way ANOVA followed by Tukey's multiple comparisons test. Significance is denoted by *p<0.05 and ns indicates non-significant.

The CD24 or CD44 protein levels in MDA-MB-231 cells transfected with non-targeting control (scramble) was set to 100% and the protein levels of these markers in MDA-MB-231 cells transfected with siTG2 was determined accordingly. The CD24 protein levels in MDA-MB-231 cells transfected with siTG2 was *98.9%* compared to control cells (scramble) (Figure 5.11C). However, the expression of the CD44 marker was 80.58% in the TG2 silenced MDA-MB-231 cells (Figure 5.11D).

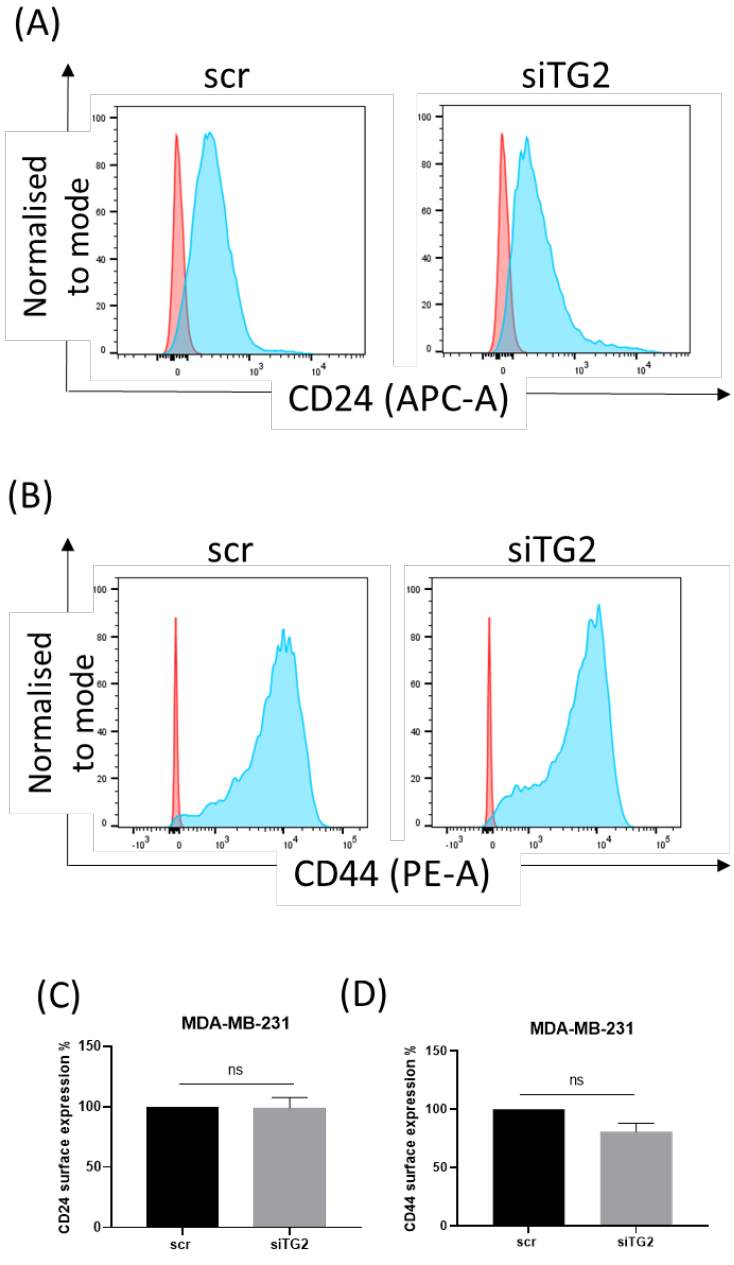

Figure 5-11 CD24 and CD44 protein levels in TG2 silenced MDA-MB-231 cells. (A) Representative flow cytometry histograms of CD24 expression in MDA-MB-231 cells transfected with scramble or siTG2. (B) Representative flow cytometry histograms of CD44 expression in MDA-MB-231cells transfected with scramble or siTG2. CD24 (C) and CD44 (D) positive cells MDA-MB-231 cells transfected with scramble (black bars) or siTG2 (grey

bars). The average fluorescence intensity (MFI) of the scramble transfected MDA-MB-231 cells was arbitrarily set to 100 and the MFI of the siTG2 transfected cells was normalized accordingly. The average ± SEM of three independent experiments is presented in (C) and (D). Statistical analysis was performed using t-test, ns indicates non-significant.

5.3.3 CD44/CD24 phenotype profile in breast cancer cell lines

Breast cancer tissues have been shown to hold a subpopulation of $CD44^+/CD24^-$ tumour cells that exhibit stem cell–like characteristics (Al-Hajj *et al.*, 2003). Patients with $CD44^+/CD24^-$ phenotype present poor prognosis and 10-years lower median age compared to patients with $CD44^+/CD24^+$ or $CD44^-/CD24^+$ phenotypes (Giatromanolaki *et al.*, 2011). The $CD44^+/CD24^-$ phenotype is linked mainly to the triple negative breast cancer subtype. Basal-mesenchymal (MDA-MB-231) but not luminal (MCF-7 or T47D) cell lines were found to fit mostly to high $CD44^+/CD24^-$ phenotype (Sheridan *et al.*, 2006).

Given these observations we aimed to investigate the association of CD44/CD24 status to the TG2 expression in the different types of breast cancer cells. After CD24 and CD44 detection in each cell line, cells were phenotyping based on four distinctive quadrants defined by these two markers as: $CD44^+/CD24^-$, $CD44^-/CD24^+$, $CD44^+/CD24^+$, and $CD44^-/CD24^-$.

5.3.3.1 CD44/CD24 phenotype in MCF-7 cells

Given that elevated CD44 and reduced CD24 protein levels is one of the characteristics of cancer stem cells (Al-Hajj *et al.*, 2003), and that SAHA, TSA, or RA treatment induced expression of different TG2 isoforms (Chapter 3), the potential differential effect of these isoforms in the CD44 and CD24 levels was investigated. The population of MCF-7 cells treated with SAHA exhibiting $CD44^+/CD24^+$ phenotype was 100.26 % and $CD44^-/CD24^+$ was 121.91 % of the cellular population. The percentage of the TSA treated MCF-7 cells displaying $CD44^+/CD24^+$ phenotype was 103.33 % and $CD44^-/CD24^+$ 118.50 %. MCF-7 cells treated with RA exhibited $CD44^+/CD24^+$ in 91.39% of the population and $CD44^-/CD24^+$ in 100.47% of the population (Figure 5.12). However, none of these changes were statistically significant.

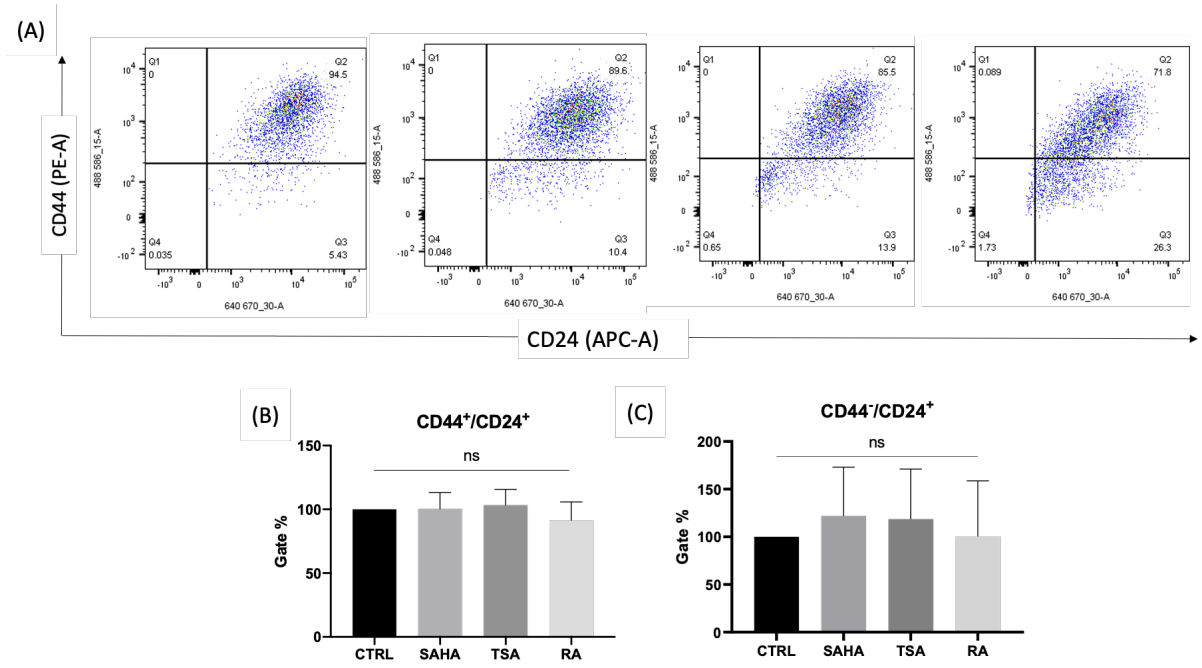

Figure 5-12 CD44/CD24 phenotype in MCF-7 cells. (A) Representative flow cytometry plots indicating the CD44/CD24 sub-population in untreated MCF-7 cells or treated with SAHA, TSA, or RA. Quadrant 1 corresponds to $CD44^+/CD24^-$ cells, quadrant 2 corresponds to $CD44^+/CD24^+$, quadrant 3 corresponds to $CD44^-/CD24^+$, and quadrant 4 corresponds to $CD44^-/CD24^-$. (B) The percentage of $CD44^+/CD24^+$ sub-population of untreated MCF-7 cells was arbitrarily set to 100 and the percentage of treated cells was normalized accordingly. (C) The percentage of $CD44^-/CD24^+$ sub-population of untreated MCF-7 cells was arbitrarily set to 100 and the percentage of treated cells was normalized accordingly. The average ± SEM of three independent experiments is presented in (B) and (C). Statistical analysis was performed using One-way ANOVA followed by Tukey's multiple comparisons test, ns indicates non-significant.

5.3.3.2 CD44/CD24 phenotype in T47D cells

The population of T47D cells treated with SAHA exhibiting $CD44^+/CD24^+$ phenotype was 66.47% and that exhibiting $CD44^-/CD24^+$ was 154.2% of the cellular population. The percentage of the TSA treated T47D cells displaying $CD44^+/CD24^+$ phenotype was 104.6% and $CD44^-/CD24^+$ 105.5%. T47D cells treated with RA exhibited $CD44^+/CD24^+$ in 62.51% of the population and $CD44^-/CD24^+$ in 149.3% of the population (Figure 5.13A). Cells treated with TSA exhibited statistically significant higher $CD44^+/CD24^+$ sub-population compared to SAHA or RA treated cells (Figure 5.13B).

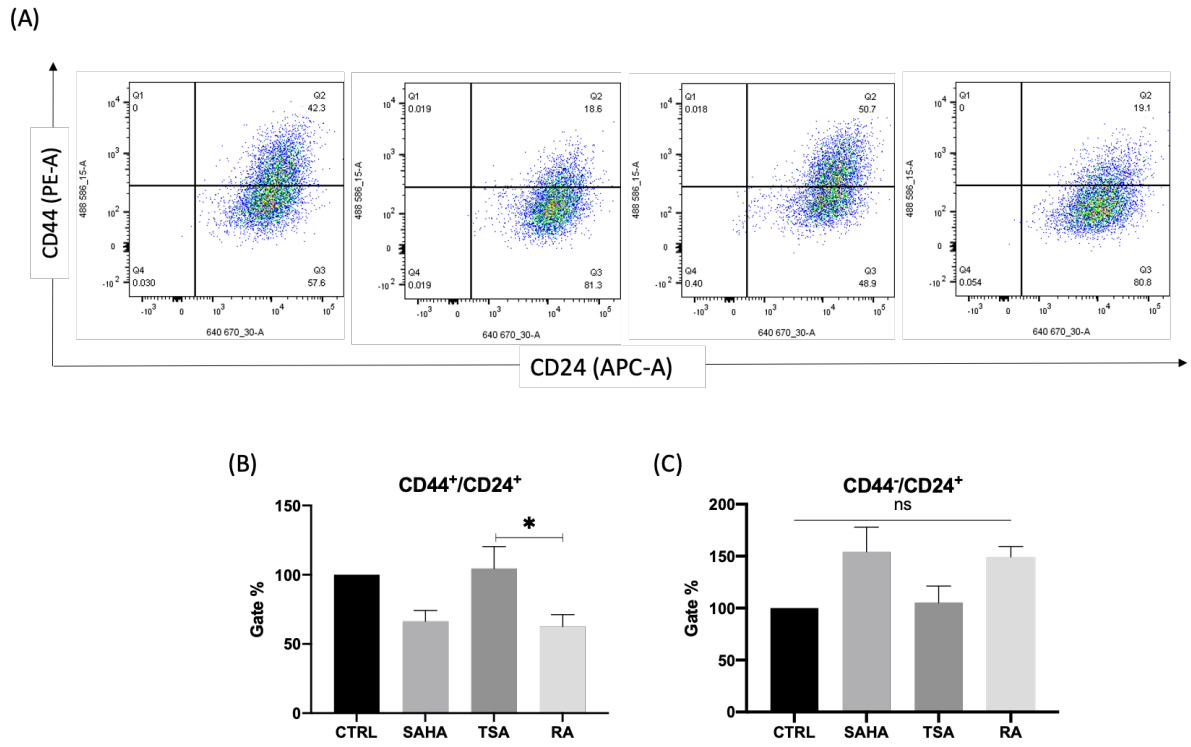

Figure 5-13 CD44/CD24 phenotype in T47D cells. (A) Representative flow cytometry plots indicating the CD44/CD24 sub-population in untreated T47D cells or treated with SAHA, TSA, or RA. Quadrant 1 corresponds to $CD44^+/CD24^-$ cells, quadrant 2 corresponds to $CD44^+/CD24^+$, quadrant 3 corresponds to $CD44^-/CD24^+$, quadrant 4 corresponds to $CD44^-/CD24^-$. (B) The percentage of $CD44^+/CD24^+$ sub-population of untreated T47D cells was arbitrarily set to 100 and the percentage of treated cells was normalized accordingly. (C) The percentage of $CD44^-/CD24^+$ sub-population of untreated T47D cells was arbitrarily set to 100 and the percentage of treated cells was normalized accordingly. The average ± SEM of three independent experiments is presented in (B) and (C). Statistical analysis was performed using One-way ANOVA followed by Tukey's multiple comparisons test. Significance is denoted by *$p<0.05$ and ns indicates non-significant.

5.3.3.3 CD44/CD24 phenotype in MDA-MB-468 cells

Untreated MDA-MB-468 cells exhibited almost 100% of cells expressing $CD44^+/CD24^+$. The population of MDA-MB-468 cells treated with SAHA, TSA, or RA exhibiting $CD44^+/CD24^+$ phenotype was 100.87%, 100.69%, and 101.45%, respectively (Figure 5.14A). No significant changes were reported (Figure 5.14B).

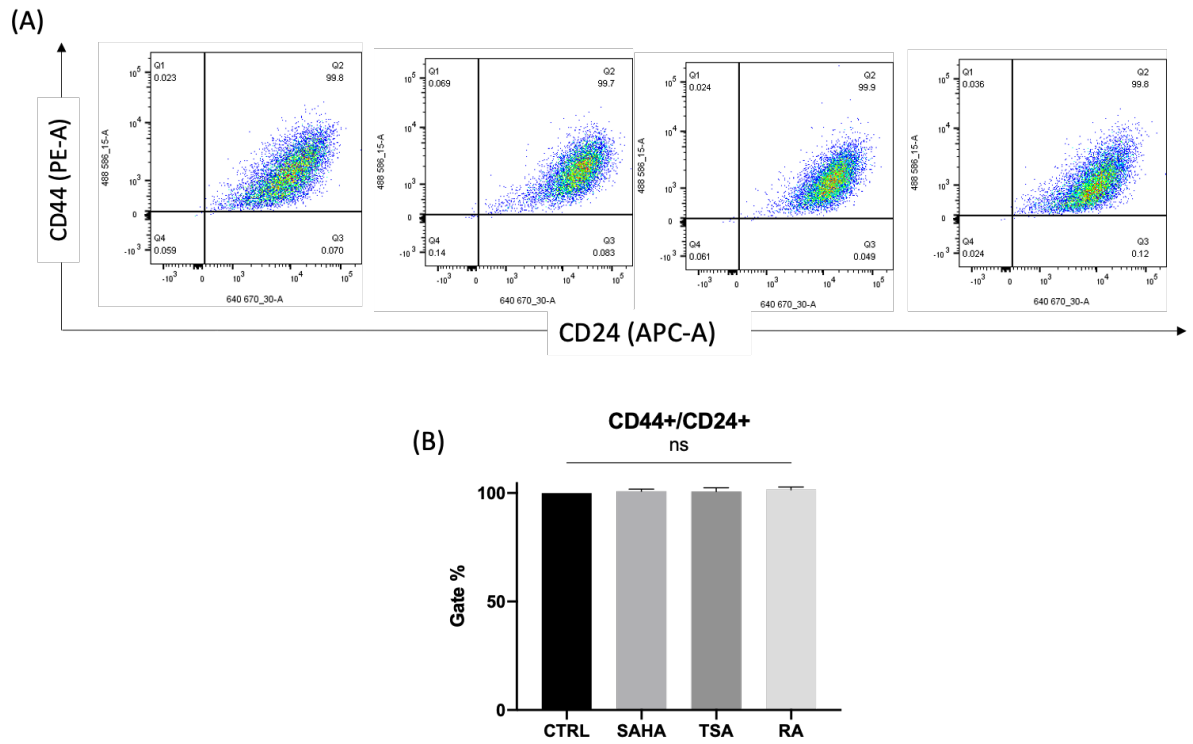

Figure 5-14 CD44/CD24 phenotype in MDA-MB-468 cells. (A) Representative flow cytometry plots indicating the CD44/CD24 sub-population in untreated MDA-MB-468 cells or treated with SAHA, TSA, or RA (A). Quadrant 1 corresponds to $CD44^+/CD24^-$ cells, quadrant 2 corresponds to $CD44^+/CD24^+$, quadrant 3 corresponds to $CD44^-/CD24^+$, quadrant 4 corresponds to $CD44^-/CD24^-$. (B) The percentage of $CD44^+/CD24^+$ sub-population of untreated MDA-MB-468 cells was arbitrarily set to 100 and the percentage of treated cells was normalized accordingly. The average ± SEM of three independent experiments is presented in (B). Statistical analysis was performed using One-way ANOVA followed by Tukey's multiple comparisons test, ns indicates non-significant.

5.3.3.4 CD44/CD24 phenotype in MDA-MB-231 cells

Unlike MCF-7, T47D, and MDA-MB-468 cells, most of MDA-MB-231 cells exhibited $CD44^+/CD24^-$ phenotype. The population of MDA-MB-231 cells treated with ZDON exhibiting $CD44^+/CD24^-$ phenotype was 113.05% and $CD44^+/CD24^+$ was 68.72% of the cellular population. The percentage of the NC9 treated MDA-MB-231 cells displaying $CD44^+/CD24^-$ phenotype was 112.8% and $CD44^+/CD24^+$ 68.72% of the population (Figure 5.15A). The reduction of the $CD44^+/CD24^+$ sub-population was statistically significant in cells treated with ZDON or NC9 compared to untreated cells (Figure 5.15C).

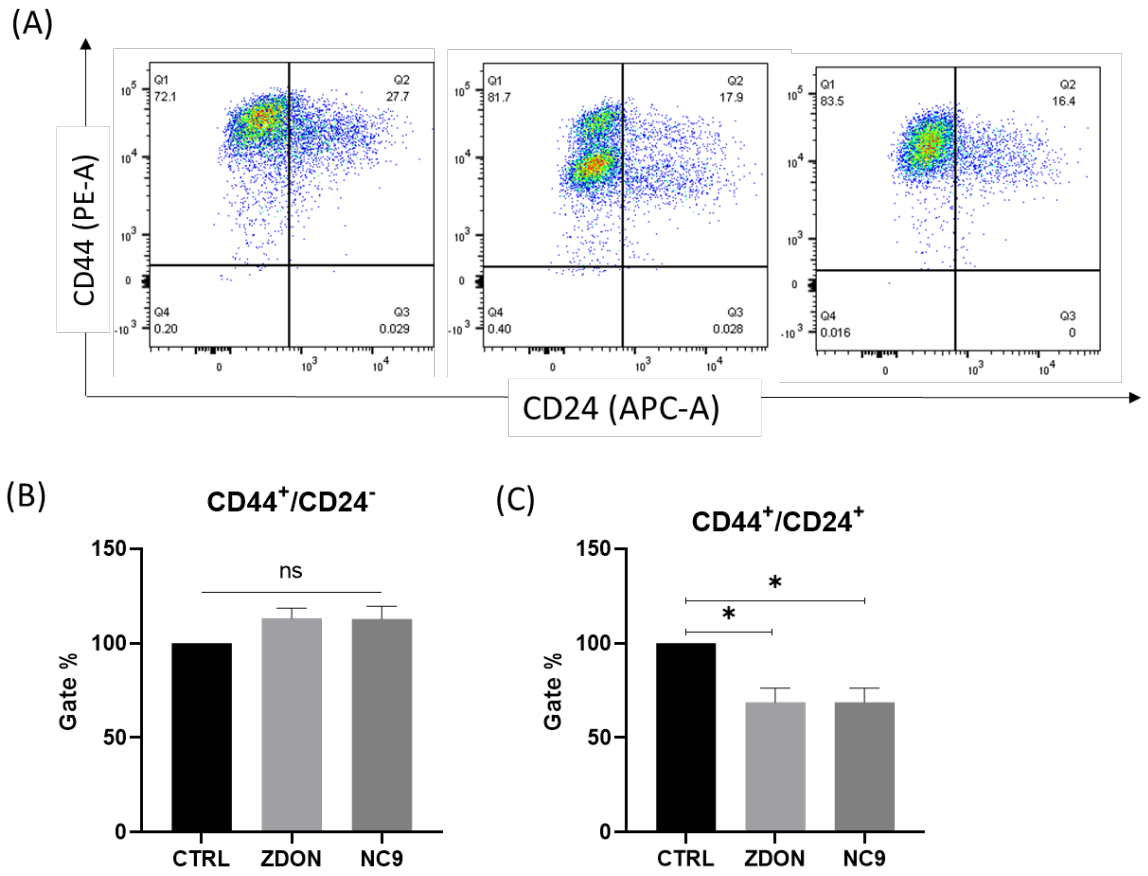

Figure 5-15 CD44/CD24 phenotype in MDA-MB-231 cells. (A) Representative flow cytometry plots indicating the CD44/CD24 sub-population in untreated MDA-MB-231 cells or treated with ZDON, or NC9. Quadrant 1 corresponds to $CD44^+/CD24^-$ cells, quadrant 2 correspond to $CD44^+/CD24^+$, quadrant 3 corresponds to $CD44^-/CD24^+$, quadrant 4 corresponds to $CD44^-/CD24^-$. (B) The percentage of $CD44^+/CD24^+$ sub-population of untreated MDA-MB-231 cells was arbitrarily set to 100 and the percentage of treated cells was normalized accordingly. The average ± SEM of three independent experiments is presented in (B) and (C). Statistical analysis was performed using One-way ANOVA followed by Tukey's multiple comparisons test. Significance is denoted by *$p<0.05$ and ns indicates non-significant.

The population of MDA-MB-231 cells transfected with siTG2 exhibiting $CD44^+/CD24^-$ phenotype was 93.05% which is statistically significant lower compared to that found in the cells transfected with the non-targeting (scramble) siRNA (Figure 5.16B). $CD44^+/CD24^+$ was

150.50% of the cellular population compared to that of the cells transfected with the non-targeting (scramble) (Figure 5.16C).

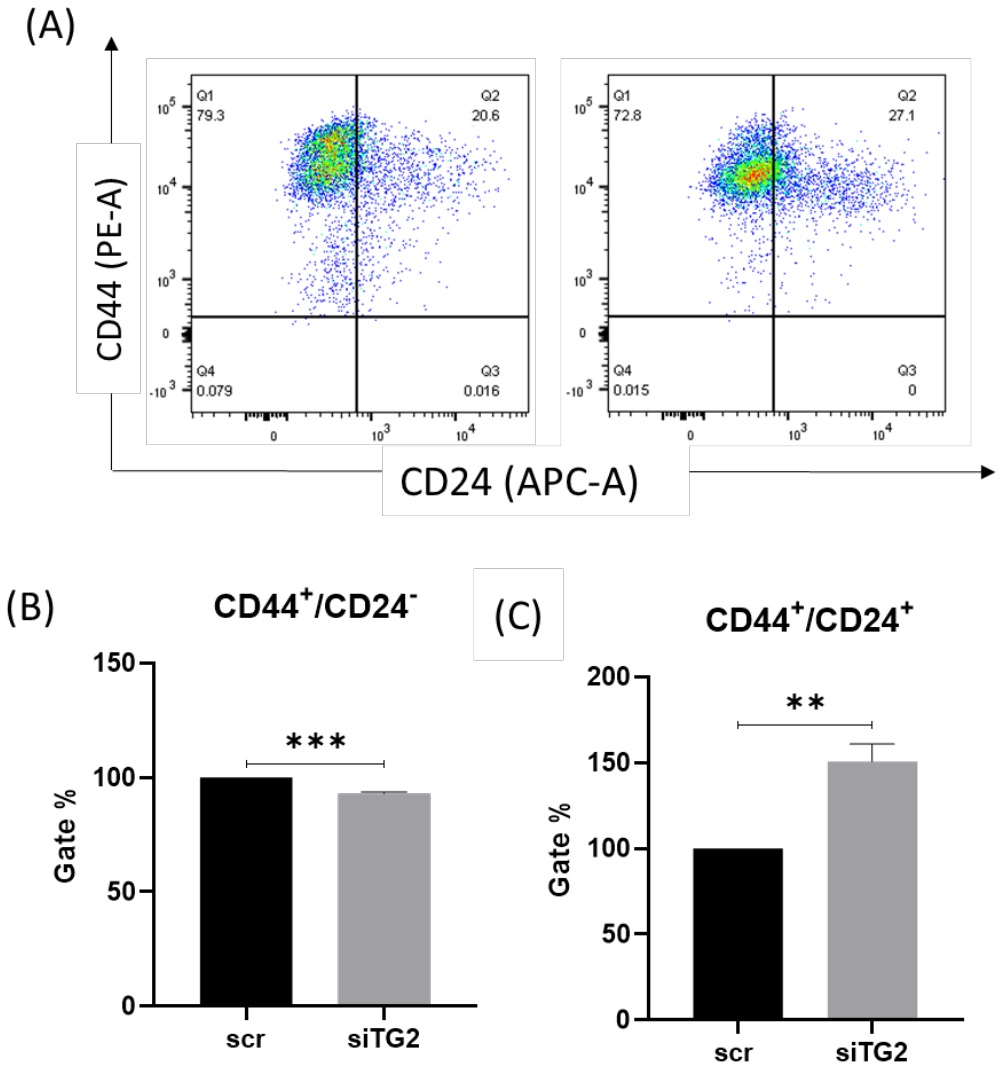

Figure 5-16 CD44/CD24 phenotype in MDA-MB-231 cells. (A) Representative flow cytometry plots indicating the CD44/CD24 sub-population in MDA-MB-231 cells transfected with non-targeting siRNA (scramble) or siTG2. Quadrant 1 corresponds to $CD44^+/CD24^-$ cells, quadrant 2 corresponds to $CD44^+/CD24^+$, quadrant 3 corresponds to $CD44^-/CD24^+$, quadrant 4 corresponds to $CD44^-/CD24^-$. (B) The percentage of $CD44^+/CD24^-$ sub-population of scramble transfected MDA-MB-231 cells was arbitrarily set to 100 and the percentage of cells transfected with siTG2 was normalized accordingly. (C) The percentage of $CD44^+/CD24^+$ sub-population of scramble transfected MDA-MB-231 cells was arbitrarily set to 100 and the percentage of cells transfected with siTG2 was normalized accordingly. The average ± SEM of three independent experiments is presented in (B) and (C). Statistical analysis was performed using One-way ANOVA followed by Tukey's multiple comparisons test. Significance is denoted by **p<0.01 and ***p<0.005.

5.3.4 Analysis of ALDH activity in breast cancer cells

ALDH activity is an indicator of cancer stem cells (CSC) and can be measured by the aldefluor assay (Marcato *et al.*, 2011). In this study, MCF-7, T47D, and MDA-MB-468 cells were treated with SAHA (0.5 μM), TSA (0.05 μM), or RA (40 μM) for 48h. MDA-MB-231 cells treated with ZDON (70 μM) or NC9 (30 μM) for 72h, or transfected with siRNA (siTG2) or a non-targeting siRNA control (scramble) for 96h and the ALDH activity was assessed under these conditions. Cell pellets were re-suspended in 1 ml buffer, and 500μl aliquot was incubated for 45 minutes with 5 μl of the fluorescent substrate for ALDH enzyme ALDEFLUOR. Another 0.5 ml aliquot was incubated with 5 μl ALDEFLUOR and 5 μl of the ALDH inhibitor DEAB, as a negative control. The level of the enzyme activity that is directly linked to ALDH expression was determined by flow cytometry analysis as described in the material and methods section. $ALDH^+$ expression was defined relative to DEAB gate.

5.3.4.1 Analysis of ALDH activity in MCF-7 cells

The percentage of ALDH$^+$ cells in SAHA-, TSA-treated cells were increased by 476.49% and 452.57%, respectively. Compared to control, RA-treated cells showed very high non-significant increase in ALDH+ cells (Figure 5.17).

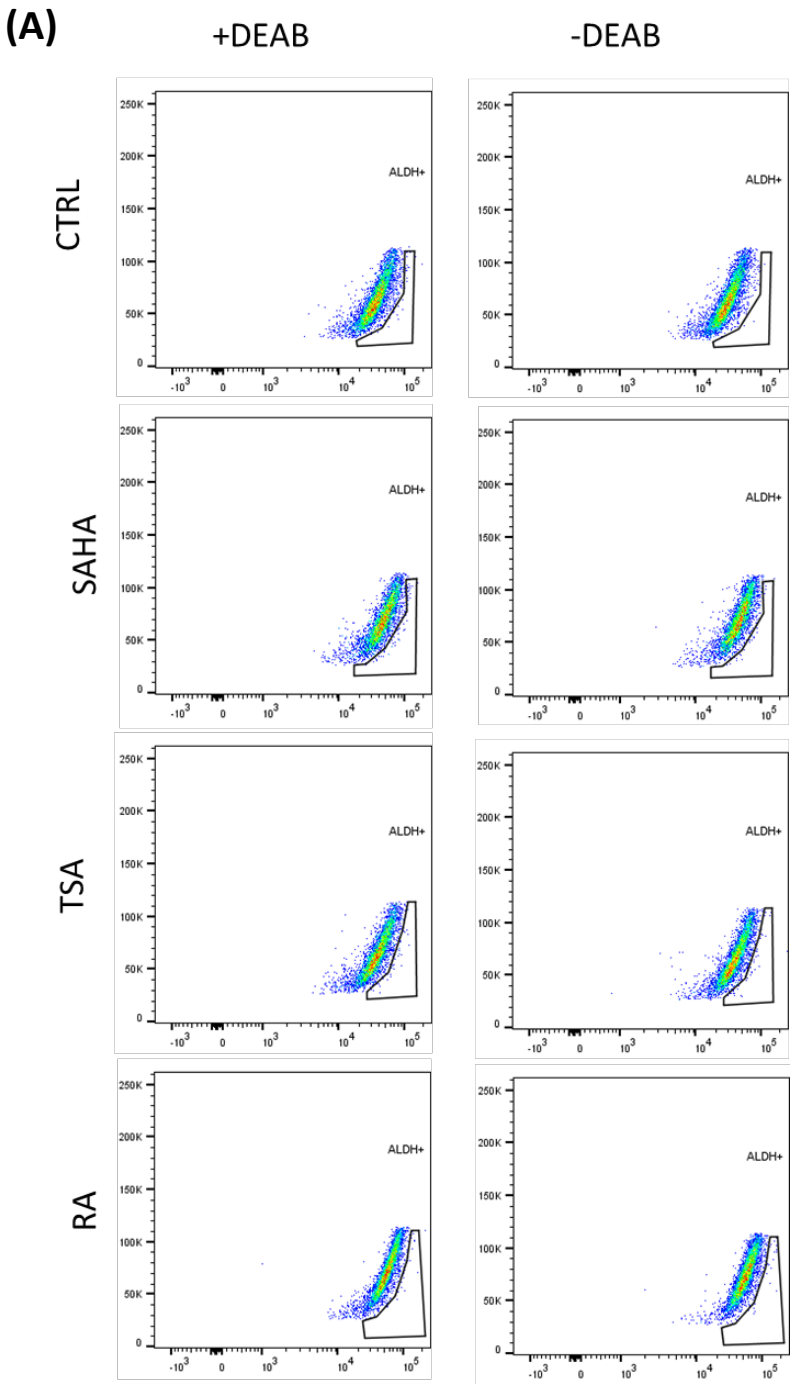

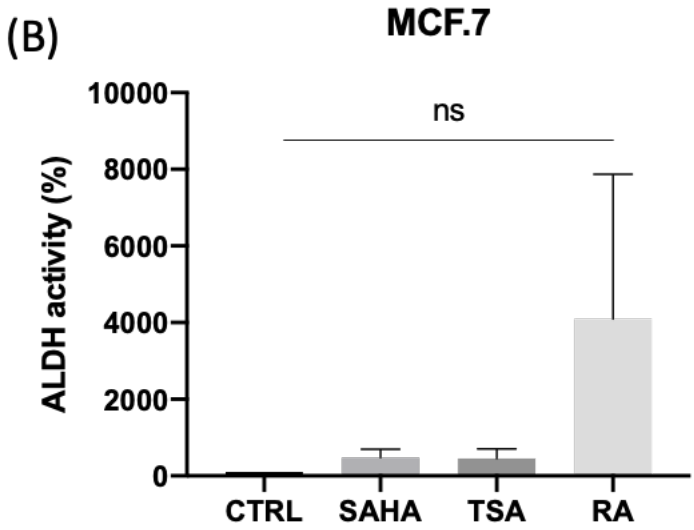

Figure 5-17 ALDH activity in MCF-7 cells. (A) Flow cytometry plots demonstrating the gating in the presence of DEAB which was used as negative control (left panels) and $ALDH^+$ activity in the absence of DEAB (right panels) in untreated MCF-7 cells or treated with SAHA, TSA, or RA. (B) The average ± SEM of at least three independent experiments is presented. Statistical analysis was performed using One-way ANOVA followed by Tukey's multiple comparisons test, ns indicates non-significant.

5.3.4.2 Analysis of ALDH activity in T47D cells

The percentage of ALDH$^+$ cells in SAHA- and TSA-treated cells were non-significantly increased by 198.8% and 144.3%, respectively, while they decreased by 76% in RA-treated cells compared to control (Figure 5.18B).

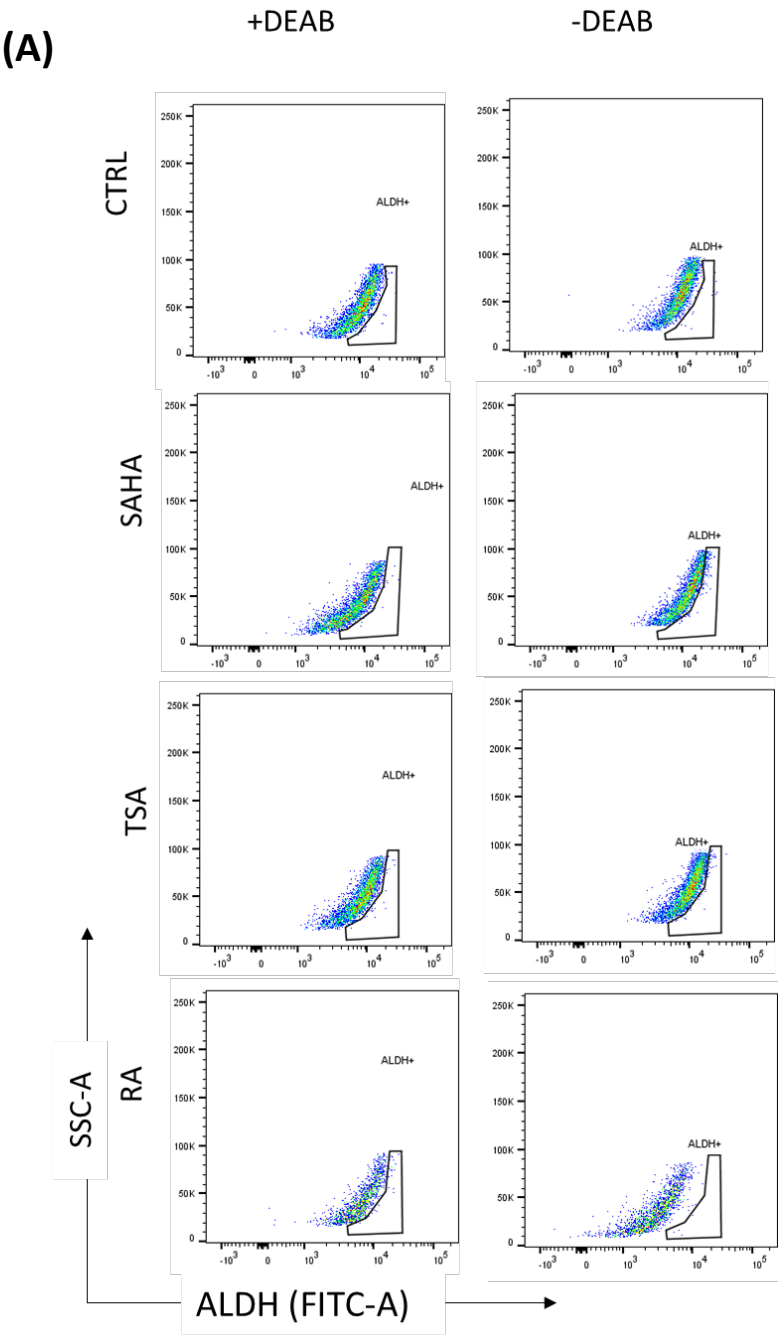

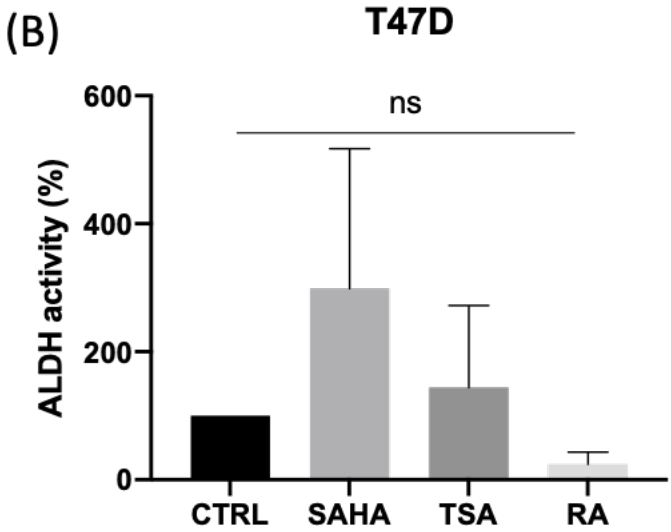

Figure 5-18 ALDH activity in T47D cells. (A) Flow cytometry plots demonstrating the gating in the presence of DEAB which was used as negative control (left panels) and $ALDH^+$ activity in the absence of DEAB (right panels) in untreated T47D cells or treated with SAHA, TSA, or RA. (B) The average ± SEM of at least three independent experiments is presented. Statistical analysis was performed using One-way ANOVA followed by Tukey's multiple comparisons test. ns indicates non-significant.

5.3.4.3 Analysis of ALDH activity in MDA-MB-468 cells

The percentage of ALDH$^+$ cells in SAHA-, TSA-, and RA-treated cells were 2382%, 700.55%, and 711.47%, respectively, compared to control cells (Figure 5.19).

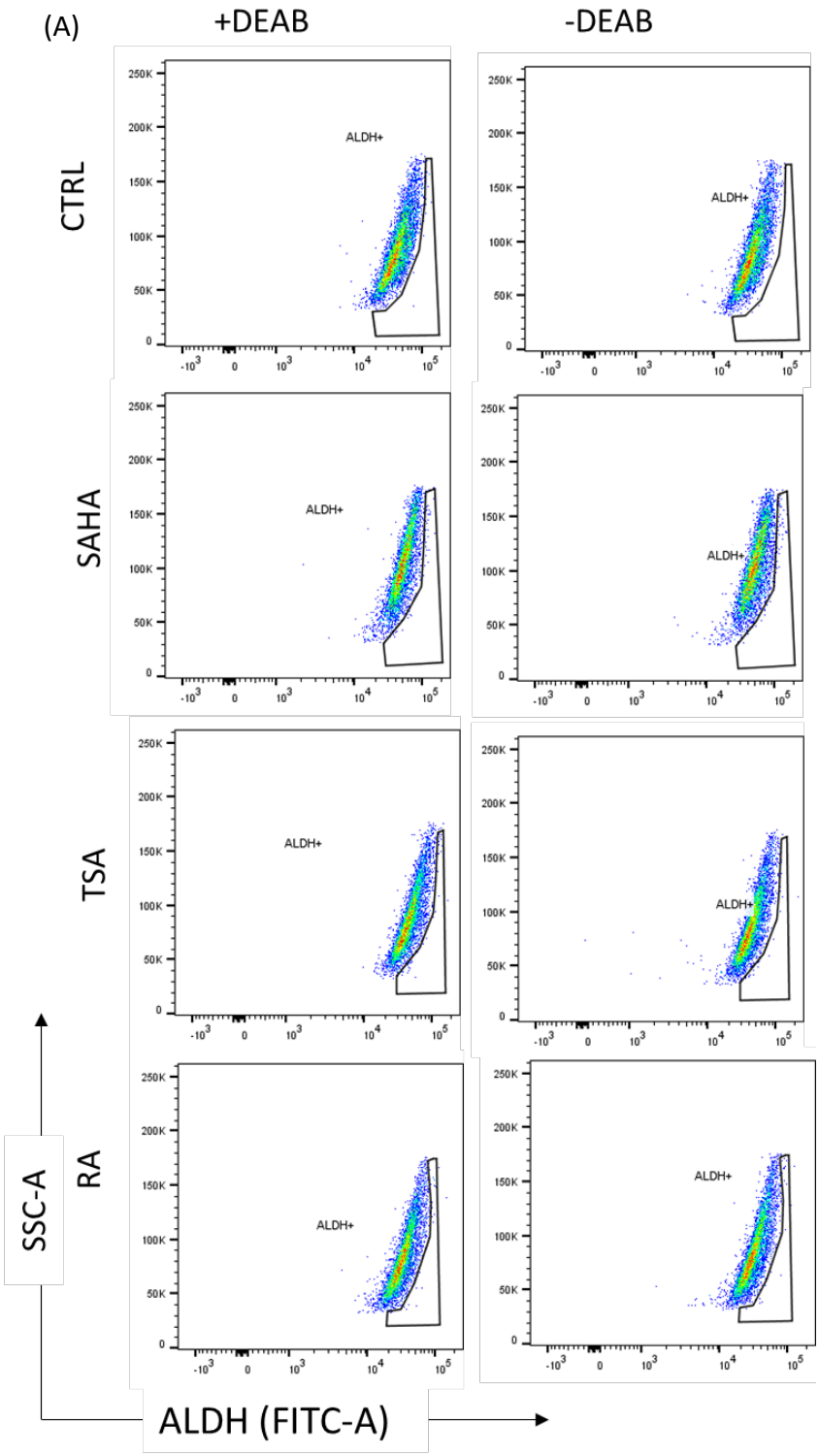

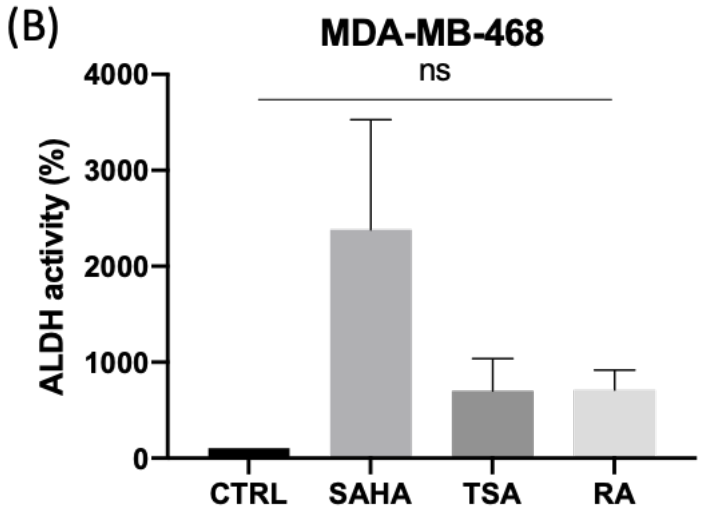

Figure 5-19 ALDH activity in MDA-MB-468 cells. (A) Flow cytometry plots demonstrating the gating in the presence of DEAB which was used as negative control (left panels) and $ALDH^+$ activity in the absence of DEAB (right panels) in untreated MDA-MB-468 cells or treated with SAHA, TSA, or RA. (B) The average ± SEM of at least three independent experiments is presented. Statistical analysis was performed using One-way ANOVA followed by Tukey's multiple comparisons test, ns indicates non-significant.

5.3.4.4 Analysis of ALDH activity in MDA-MB-231 cells

The percentage of ALDH$^+$ cells in ZDON and NC9-treated cells were non significantly increased by 19.23% and 43.72%, respectively, compared to control cells (Figure 5.20).

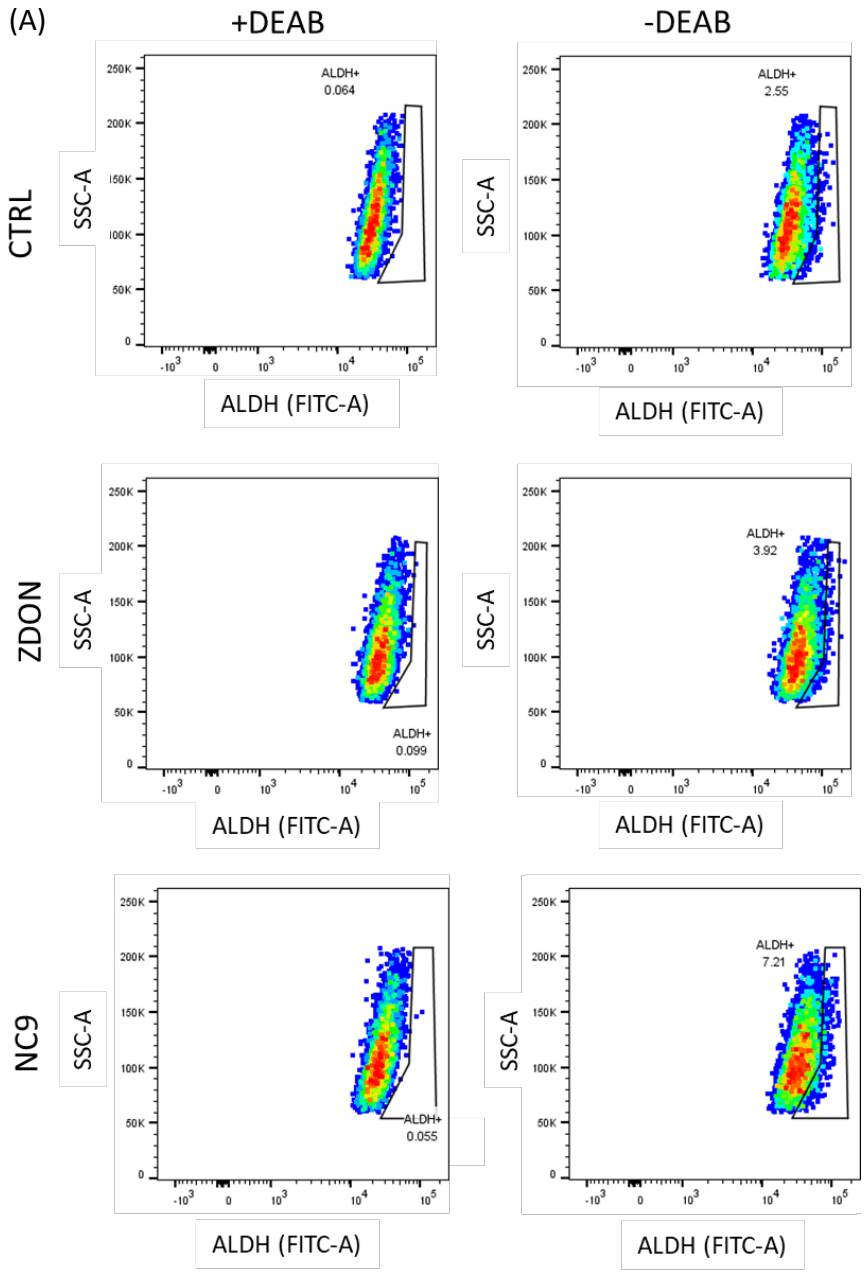

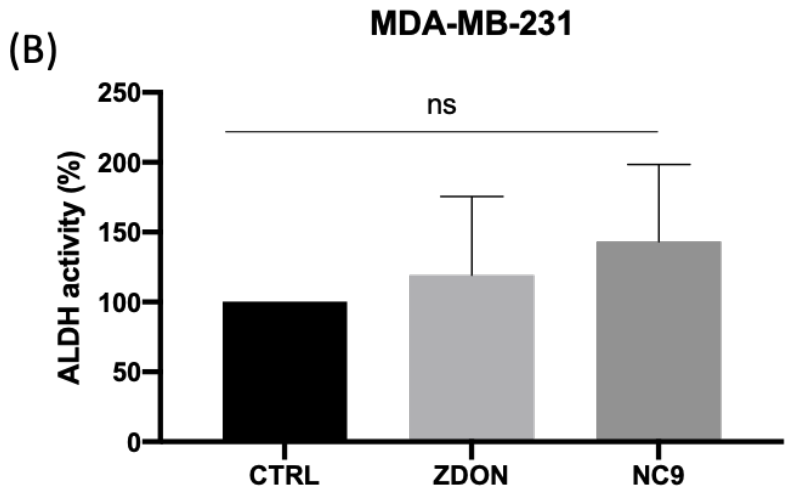

Figure 5-20 ALDH activity in MDA-MB-231 cells. (A) Flow cytometry plots demonstrating the gating in the presence of DEAB which was used as negative control (left panels) and $ALDH^+$ activity in the absence of DEAB (right panels) in untreated MDA-MB-231 cells or treated with ZDON or NC9. (B) The average ± SEM of at least three independent experiments is presented. Statistical analysis was performed using One-way ANOVA followed by Tukey's multiple comparisons test. ns indicates non-significant.

The percentage of ALDH$^+$ cells in MDA-MB-231 cells transfected with siTG2 was significantly decreased by 70.25% compared to non-targeting siRNA (scramble) (Figure 5.21).

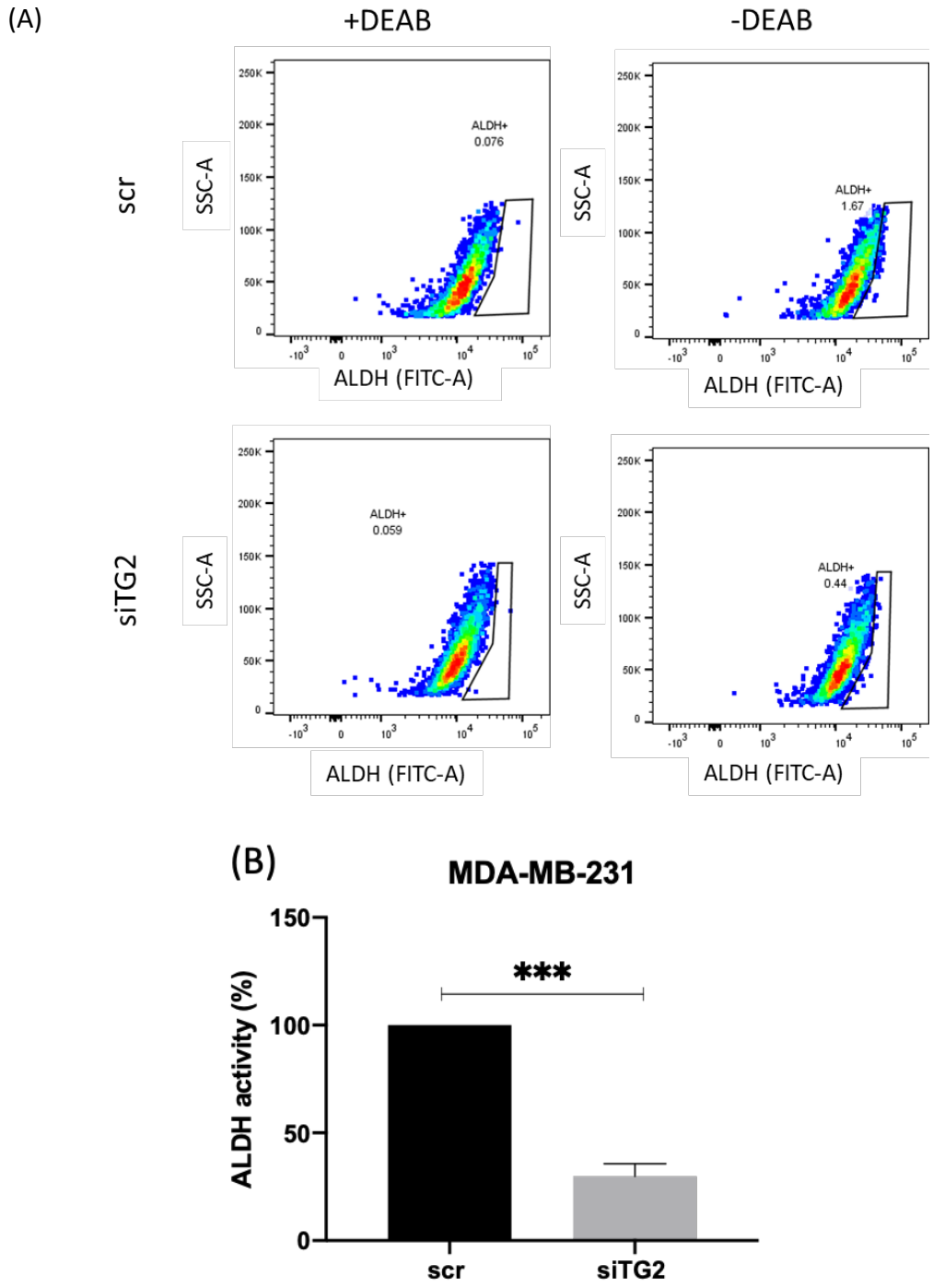

Figure 5-21 ALDH activity in MDA-MB-231 cells. (A) Flow cytometry plots demonstrating the gating in the presence of DEAB which was used as negative control (left panels) and ALDH$^+$ activity in the absence of DEAB (right panels) in MDA-MB-231 cells transfected with non-targeting siRNA (scramble) or siTG2. (B) The average ± SEM of at least three independent experiments is presented. Statistical analysis was performed using t-test. Significance is denoted by ***p<0.005.

5.4 Discussion:

CSCs are defined as cancer initiating cells with self-renewal ability and differentiation resulting in cancer progression and treatment resistance. Different therapeutic approaches have been proposed to target CSCs and have shown promising results in cancer treatment (Chen, Huang and Chen, 2013). The most frequent method used to identify and isolate CSCs is the expression of CSC surface markers. High CD44, negative or low CD24, and high ALDH expression are indicators of CSCs in breast cancer (Sheridan *et al.*, 2006; Marcato *et al.*, 2011; Chekhun *et al.*, 2013). Another approach to investigate stem cell activity in tumour tissues and cell lines is to isolate single cells from the samples and then test their ability to grow as mammospheres in non-adherent conditions and serum free media (Shaw *et al.*, 2012; Lombardo *et al.*, 2015). As TG2 has been linked to CSCs we investigated the role of its different isoforms in the process of CSCs development following the mammosphere forming efficiency and the expression of stemness markers under different conditions in which the different TG2 isoforms are expressed. In our study, we assessed four breast cancer cell lines: MCF.7, T47D, MDA-MB-468, and MDA-MB-231 for their mammosphere forming ability, CSC markers' expression (CD44 and CD24), and functional activity of ALDH enzyme.

5.4.1 Role of the different TG2 isoforms in mammosphere formation

Mammosphere formation assays can be used to assess stemness features in-vitro by counting the number of mammospheres formed from single cells. The ability of mammospheres to form several new generations in serial non-adherent passages were used to determine the self-renewal ability of the breast cancer cells (Shaw *et al.*, 2012).

All cell lines tested in the present study had the ability to grow as mammospheres in non-adherent conditions. MCF-7 formed well-rounded, compact, and clearly defined edge mammospheres, while T47D formed rounded or curled sheet-like mammospheres. Both MCF-7 and T47D cells are luminal and ERα positive cell lines. The TNBC cell lines MDA-MB-231 and MDA-MB-468 formed loose grape-like mammospheres. In agreement with our findings, different studies have shown similar mammosphere structures formed by breast cancer cell lines (Iglesias *et al.*, 2013; Lombardo *et al.*, 2015; Bailey *et al.*, 2018).

Mammosphere formation efficiency (MFE) was lower in MCF-7 and T47D cells treated with RA than in control cells treated with DMSO, although RA-induced TG2-L and TG2-S as confirmed by western blot analysis. These results could be explained by the fact that RA induces cell differentiation, resulting in a significant decrease in CSCs' features and a subsequently decreased mammosphere formation efficiency (MS *et al.*, 1997; Ginestier *et al.*, 2009). Consistent with our findings, Ginestier et al. who used the SUM149 and SUM159 basal cell lines, the $HER2^+$ cell line HCC1954, and the normal human mammary epithelial cell line 184A1, reported that RA-treated cells induce differentiation as confirmed by a reduction in mammosphere forming efficiency of these cells (Ginestier *et al.*, 2009).

Only the TG2-S isoform was found to be expressed in MDA-MB-468 cells and SAHA, TSA, and RA treatment reduced TG2-S expression compared to control untreated cells (Chapter 3), which was confirmed by the reduction of TG2 transamidase activity observed in these cells using the transamidase activity assay. Interestingly, MDA-MB-468 cells displayed increased but not statistically significant mammosphere formation efficiency, supporting our hypothesis that the TG2 transamidase activity reduces the acquisition of stemness features.

NC9, inhibits the TG2 transamidase activity and locks the enzyme in its open conformation thereby compromising its GTPase activity whereas ZDON inhibits the TG2 transamidase activity and possibly the GTPase activity (Caron *et al.*, 2012; Akbar *et al.*, 2017; Kerr *et al.*, 2017). Our results showed that MDA-MB-231 was the only cell line that endogenously expressed both isoforms at high levels compared to the other cell lines tested. Reduced mammosphere formation efficiency was observed in NC9 treated MDA-MB-231 cells whereas increased MFE was exhibited by ZDON treated MDA-MB-231 cells. A significant reduction of mammosphere formation was observed in NC9-treated cells compared to ZDON-treated cells, suggesting the TG2 GTPase activity might confer stemness features to the MDA-MB-231 cells since its inhibition decreased the mammosphere formation efficiency of these cells.

The TG2-L isoform has the catalytic active site (Cys277) where Ca^{2+} binding occurs to trigger the TG2 transamidase activity as well as the GTP-binding active site (Arg580) where GTP binds to activate the TG2 GTPase activity. The TG2-S isoform lacks the GTP-binding site (Arg580) suggesting that the TG2-S isoform exerts only transamidase activity (Singh *et al.*,

2016). Binding of Ca^{2+} to the catalytic site Cys277 of TG2 activates its transamidase activity and locks the TG2 in its open catalytically active conformation, whereas binding of GTP to the active site Arg580 stimulates the TG2 GTPase activity and locks TG2 in its closed conformation (Tatsukawa *et al.*, 2016; Tatsukawa and Hitomi, 2021).

Silencing of the TG2 gene expression in MDA-MB-231 cells by siRNA resulted in > 30% reduction in TG2-L protein levels and > 90% reduction in TG2-S protein levels. TG2 silenced MDA-MB-231 cells showed reduced mammospheres formation efficiency compared to the cells expressing TG2, which lends support to our hypotheses that the TG2 GTP-binding domain might at least in part play an important role in the formation of breast cancer CSCs. In accordance with our hypothesis, Kumar et al. demonstrated that transamidase-binding-deficient (Cys277 mutated) cells induce EMT and confer CSC properties to mammary epithelial cells, while GTP-binding-deficient (Arg580 mutated) cells do not induce EMT (Kumar *et al.*, 2012). Moreover, studying the self-renewal ability of cells by evaluating the mammosphere forming ability through serially passaged cells cultured as mammospheres demonstrated that TG2-WT and transamidase-binding-deficient (Cys277 mutated) cells were equally capable of promoting the self-renewal ability, while GTP-binding-deficient (Arg580 mutated) cells demonstrated a significant decrease in the number of mammospheres formed in each passage (Kumar *et al.*, 2011, 2012).

In the present study, passaging of mammospheres was not used because of the small number of mammospheres formed from the first passage and low cell viability, in which cells were insufficient to be re-seeded in CSCs medium, particularly in the case of MDA-MB-231 and MDA-MB-468 cells. There was a little chance to grow MCF-7 and T47D cells, but not all conditions were applicable as RA-treated cells had very low viability. Thus, only one passage of mammosphere was used to count the mammospheres formed in each cell line, but the self-renewal ability through different passages was not tested. Furthermore, the grown mammospheres could not be used in any further experiments, such as western blot or flow cytometry, to determine the level of TG2 expression in those mammospheres or to test the expression of stemness markers CD44, CD24, or ALDH because of the low cell viability of the formed mammospheres.

Consistent with our findings, Iglesias et al. found that only MCF-7 and T47D cells grow successfully for several non-adherent passages, and the number of viable cells also increases. On the other hand, MDA-MB-231 and MDA-MB-468 develop cell aggregates that can be easily distributed by moving the plate and the cell viability was substantially decreased on their second passage, hence, any further passage in suspension culture was not possible (Iglesias *et al.*, 2013).

5.4.2 Role of TG2 in the expression of the CD44 and CD24 cell surface markers

Human breast cancer cells injected to immunocompromised mice demonstrated that only a small subset of cells within a tumour are tumorigenic and have the capacity to form new tumours while the majority of the injected cells are non-tumorigenic and do not proliferate. The expression of cell surface markers CD44 and CD24 has been used to distinguish and isolate these tumorigenic cells from non-tumorigenic cells (Al-Hajj *et al.*, 2003). Breast cancer cells have phenotypically diverse mixed subpopulations, but only the $CD44^{+}/CD24^{-/low}$ phenotype is able to initiate new tumours in mice which contained additional populations with the same phenotype ($CD44^{+}/CD24^{-/low}$) (Al-Hajj *et al.*, 2003; Sheridan *et al.*, 2006). EMT has been proposed to facilitate cancer cell migration and invasion and enable cells to acquire self-renewal ability by stimulating a stem cell phenotype (Mani *et al.*, 2008). A stem cell phenotype $CD44^{+}/CD24^{-/low}$ can result from TG2-induced EMT (Kumar *et al.*, 2010).

MCF-7 cells were 95% $CD44^{+}/CD24^{+}$ and 5% $CD44^{-}/CD24^{+}$, whereas T47D cells had a lower percentage of $CD44^{+}/CD24^{+}$ (42%), and a higher percentage of $CD44^{-}/CD24^{+}$ (58%) sub-population. Interestingly, almost 100% of the weakly metastatic MDA-MB-468 cells were $CD44^{+}/CD24^{+}$. MCF-7 cells were found to have both $CD44^{+}/CD24^{+}$ and $CD44^{-}/CD24^{+}$ subpopulations, whereas MDA-MB-468 had only the $CD44^{+}/CD24^{+}$ sub-population. $CD44^{-}/CD24^{+}$ and $CD44^{+}/CD24^{+}$ subpopulations of MDA-MB-231 have been reported (Croker *et al.*, 2009; M Robertson and Chu, 2012). Li et. al. described similar phenotypes in MDA-MB-231 and MDA-MB-468, but they found that the majority of MCF-7 cells were $CD44^{-}/CD24^{+}$ (Li *et al.*, 2017).

Treatment of SUM159 and MDA-MB-231 cells with the HDACIs SAHA and valproic acid expanded the $CD44^{+}/CD24^{+}$ sub-population compared to control untreated cells which originally had a higher percentage of $CD44^{+}/CD24^{-}$ sub-population than $CD44^{+}/CD24^{+}$ (Jolly *et al.*, 2017). Results described in this thesis indicate that SAHA- and TSA- treatment of MCF-7 cells shifted the originally higher percentage of $CD44^{+}/CD24^{+}$ observed in control cells to the $CD44^{-}/CD24^{+}$ phenotype. Interestingly, RA treatment of MCF-7 and T47D cells reduced the subpopulation of cells with $CD44^{+}/CD24^{+}$ phenotype. In line with our findings, Ginestier et al. demonstrated that RA treatment induces breast CSCs differentiation, resulting in a significant reduction of the breast CSC population (Ginestier *et al.*, 2009).

MDA-MB-231 is a highly metastatic, invasive, and poorly differentiated TNBC cell line. The $CD44^{+}/CD24^{-/low}$ phenotype was only evident in the MDA-MB-231 cells, suggesting that $CD44^{+}/CD24^{-/low}$ is associated with the aggressive mesenchymal-like cell characteristics of these cells. It is also worth noting that MDA-MB-231 was the only cell line of those tested in the present study that expressed considerably high levels of TG2-L and TG2-S compared to the other cell lines tested (MCF-7, T47D, and MDA-MB-468), suggesting that TG2 expression is associated with the CSCs $CD44^{+}/CD24^{-/low}$ phenotype.

Silencing of TG2 gene expression using siRNA significantly reduced $CD44^{+}/CD24^{-/low}$ phenotype and significantly induced $CD44^{+}/CD24^{+}$ phenotype. In line with our findings, Kumar et al. reported that the 97% of $CD44^{+}/CD24^{-/low}$ sub-population of MDA-MB-231 cells was reduced to 72% after silencing of TG2 gene expression with TG2-shRNA and the number of mammospheres was also decreased compared to control transfected cells (Kumar *et al.*, 2011).

ZDON and NC9 treatments increased the number of MDA-MB-231 cells possessing the $CD44^{+}/CD24^{-/low}$ phenotype and significantly decreased the subpopulation of cells with $CD44^{+}/CD24^{+}$ phenotype, implying that the TG2 transamidase activity reduces the oncogenic effect of TG2 and may play a role in the expression of the stemness markers. Consistent with our findings, Kerr et al. found that NC9 inhibits the TG2 transamidase activity by directly interacting with the catalytic domain and locks the protein in its open conformation, inhibiting GTP binding and leading to reduced cancer stem cell survival (Kerr *et al.*, 2017). It is worth

noting that inhibition of transamidase activity and/ or GTPase activity by ZDON or NC9 induced the $CD44^{+}/CD24^{-/low}$ phenotype but silencing of TG2 gene expression reduced the $CD44^{+}/CD24^{-/low}$ phenotype suggesting that TG2 silencing might affect other functions of this enzyme (kinase or PDI activity) that possibly play a role in CSCs formation.

The hypothesis that transamidase activity can reduce stemness was tested in MDA-MB-468 cells which express only the TG2-S isoform in which the catalytic domain is present, but the GTP-binding domain is absent. Treatment of MDA-MB-468 with SAHA, TSA, and RA reduced the expression of the TG2-S compared to untreated control cells resulting in reduced TG2 transamidase activity. Reduction of TG2-S expression in SAHA-, TSA-, and RA-treated MDA-MB-468 cells stimulated stemness as indicated by increased MFE%, CD44 expression, and ALDH activity.

Cells populations of the $CD44^{+}/CD24^{-/low}$ and $CD44^{+}/CD24^{+}$ phenotype isolated from TG2 stably expressing MCF-10 normal breast cells and MCF-7-RT breast cancer cells which overexpress TG2 and are resistant to chemotherapy and re-seeded revealed that $CD44^{+}/CD24^{-/low}$ cells form a higher number of mammospheres through five different serial passages compared to $CD44^{+}/CD24^{+}$ cells. This study concluded that TG2 expression plays an important role in EMT and in conferring stem cell-like features to mammary epithelial cells as well as in transforming them to drug resistant (Kumar *et al.*, 2011). In addition, MCF-10 cells transfected with the catalytically inactive (Cys277) TG2 isoform express 90% and 0.88% of the $CD44^{+}/CD24^{-/low}$ and $CD44^{+}/CD24^{+}$ phenotypes respectively, while cells transfected with the GTP-binding-inactive (Arg580) TG2 isoform express 4% and 92% of the $CD44^{+}/CD24^{-/low}$ and $CD44^{+}/CD24^{+}$ phenotype respectively (Kumar *et al.*, 2012). These findings support the hypothesis that TG2-L and TG2-S exert different functions and differentially affect cancer progression.

The table below summarises the mammosphere forming efficiency and CD44/CD24 phenotype in breast cancer cell lines used in the present study (Table 5.1). Our results suggest that the $CD44^{+}/CD24^{+}$, but not the $CD44^{-}/CD24^{+}$, phenotype is highly associated with MFE% in MCF-7, T47D, and MDA-MB-468. This indicates that increased CD44 expression correlates with CSC features. Inhibition of the TG2 transamidase activity in MDA-MB-231 cells by ZDON,

increased MFE% and was associated with an increased frequency of the $CD44^-/CD24^+$ sub-population, whereas inhibition of the TG2 transamidase and GTPase activities with NC9 reduced MFE% and induced the subpopulation of cells with $CD44^-/CD24^+$ phenotype suggesting that inhibition of GTPase activity is essential to reduce mammosphere formation.

Table 5-1 Summary of mammosphere forming efficiency and CD44/CD24 phenotypes in breast cancer cell lines

		MFE% ± SEM n=3	$CD44^+/CD24^-$ ± SEM n=4	$CD44^+/CD24^+$ ± SEM n=4	$CD44^-/CD24^+$ ± SEM n=4
MCF.7	CTRL	1 ± 0.070	n/a	100	100
	SAHA	1.181 ± 0.22	n/a	100.26 ± 12.97	121.9 ± 51.09
	TSA	1.594 ± 0.105	n/a	103.3 ± 12.32	118.5 ± 52.55
	RA	0.5674 ± 0.13	n/a	91.39 ± 14.43	100.5 ± 58.32
T47D	CTRL	1 ± 0.024	n/a	100	100
	SAHA	0.8881 ± 0.084	n/a	66.47 ± 7.732	154.2 ± 23.7
	TSA	1.026 ± 0.085	n/a	104.6 ± 15.75	105.5 ± 15.76
	RA	0.3829 ± 0.129	n/a	62.51 ± 8.678	149.3 ± 9.878
MDA-MB-468	CRTL	1 ± 0.048	n/a	100	n/a
	SAHA	1.223 ± 0.234	n/a	100.9 ± 0.959	n/a
	TSA	1.404 ± 0.256	n/a	100.7 ± 1.68	n/a
	RA	1.335 ± 0.317	n/a	101.5 ± 1.288	n/a
MDA-MB-231	CTRL	1 ± 0.076	100	100	n/a
	ZDON	1.198 ± 0.096	113.1 ± 5.48	68.73 ± 7.636	n/a
	NC9	0.8577 ± 0.108	112.8 ± 6.76	68.73 ± 7.636	n/a
MDA-MB-231	scr	1 ± 0.156	100	100	n/a
	siTG2	0.7547 ± 0.132	93.05 ± 0.68	150.5 ± 10.39	n/a

Blue colour represents the control, green colour represents an increase over the control, and red colour represents a decrease below the control. n/a indicates a phenotype not expressed in this condition.

5.4.3 Role of TG2 in ALDH activity

It has been reported that $CD44^{high}$ and ALDH1A1-positive subpopulations are enriched in CSC (Yao *et al.*, 2020). Ginestier et al. reported that cells treated with DEAB block the retinoid signaling and increase the mammosphere formation efficiency of the DEAB treated cells compared to the untreated control cells and concluded that ALDH-positive cell lines are more effective in forming mammospheres than ALDH-negative cell lines (Ginestier *et al.*, 2009). In contrast, Ginestier et al. found that primary mammosphere formation is increased in DEAB-treated cells, while cells treated with RA showed decreased ability to form primary mammospheres compared to the control (Ginestier *et al.*, 2009). This study is consistent with our findings, indicating that RA-treated MCF-7 and T47D cells exhibit reduced mammosphere formation ability compared to control cells. However, RA has been reported to induce stemness or cell differentiation in cell type dependent manner (Mezquita and Mezquita, 2019).

RA is a significant regulator of TG2 (Shimada *et al.*, 2001). The gene that encodes TG2 is a transcriptional target of the retinoic acid receptor (RAR). The regulatory region of the TG2 promoter contains a RA-response element (RARE) which is recognized by the RAR retinoid X receptor (RXR) heterodimer (Gundemir *et al.*, 2012). In the absence of RA, the RAR/RXR heterodimer attaches to co-repressors, resulting in histone deacetylation and transcriptional repression. In the presence of RA, the RAR/RXR heterodimer dissociates from the co-repressor complexes and attaches to co-activator complexes that stimulate histone acetylation and gene transcription (Bastien and Rochette-Egly, 2004; Di Masi *et al.*, 2015).

Acute promyelocytic leukaemia patients treated with combination of RA and chemotherapy showed better outcomes compared to patients treated with chemotherapy alone (Fenaux *et al.*, 1992). In addition, RA treatment promotes the differentiation of promyelocytes into neutrophils, resulting in cell-cycle arrest and apoptosis of HL-60 cells (Ozeki and Shively, 2008). RA therapy has been demonstrated to indirectly reduce ALDH1 promoter activity by increasing RA signalling levels (Elizondo *et al.*, 2000). It has also been reported that RA inhibits ALDH1A1 activity and prevents CSCs-mediated resistance to gefitinib in lung cancer (Yao *et al.*, 2020).

The ALDEFLUOR™ assay was used to measure the ALDH1 activity and in particular the ALDH1A1 activity, but it should be noted that ALDH1A3 and ALDH1A7 can also have an impact on cancer cell chemo-resistance and CSCs formation (Marcato *et al.*, 2011). The identification of the ALDH isoform that plays important role in CSCs formation for each cancer cell type is critical. It has been reported for example that the ALDH1 family member ALDH1A3 functions in glioma stem cells as a retinaldehyde dehydrogenase and generates RA from retinal inducing TG2 gene expression thereby linking the ALDH1A3 and TG2 expression to CSCs formation. The higher ALDH activity observed in the RA-treated MCF-7 cells compared to control cells and the lower ALDH activity observed in the RA-treated T47D cells compared to control cells could be explained by the fact that different ALDH isoform is involved in the CSC formation in the two cell lines that cannot be detected by the ALDEFLUOR™.

The highest TG2 protein level was observed in the MDA-MB-231 cells. MDA-MB-231 cells also exhibited the highest ALDH activity level among the cell lines tested in this study and the only cell line that expressed a $CD44^+/CD24^-$ phenotype. Inhibition of TG2 activity by ZDON or NC9 induced the $CD44^+/CD24^-$ sub-population, whereas silencing of TG2 significantly reduced the $CD44^+/CD24^-$ phenotype. The same trend was observed in the ALDH activity measured, suggesting that other TG2 functions, such as kinase or PDI TG2 enzymatic activities, are potentially implicated in CSCs progression. TG2 kinase activity is stimulated only in the presence of low Ca^{2+} levels when TG2 is in its closed conformation and in these conditions it has been shown to phosphorylate the retinoblastoma protein (Min and Chung, 2018). This suggests that NC9 locks the TG2 in its open conformation thereby inhibiting the TG2 kinase activity and inducing CSC characteristics. On the other hand, silencing of the TG2 gene expression down-regulated the levels of TG2-L and TG2-S and consequently reduced the transamidase activity, facilitating GTP-binding and induction of the TG2 closed conformation, which activates the TG2 kinase activity. Phosphorylation of different proteins by TG2 results in CSC inhibition. Therefore, different TG2 enzymatic activities might be up-or down-regulated in TG2 silenced or cells treated with TG2 inhibitors.

5.5 Conclusion

The expression of the CD44 and the CD24 and ALDH activity were investigated in different molecular subtypes of breast cancer cell lines, and our results suggested that their expression was inconsistent even in cell lines having the same molecular subtype. High number of $CD44^{+}/CD24^{-/low}$ and ALDH+ cells were associated with the highly metastatic and aggressive cell line, MDA-MB-231. The $CD44^{+}/CD24^{-/low}$ phenotype was associated with TG2-L high basal expression but not with basal-like carcinomas, MDA-MB-231 and MDA-MB-468, which are both TNBC but express different levels of stemness markers. MCF-7 and T47D formed more stable mammospheres than MDA-MB-231 and MDA-MB-468 cell lines, suggesting that these cells can form mammospheres under non-adherent conditions through serial non-adherent passages. On the other hand, the TNBC cell lines MDA-MB-231 and MDA-MB-468 formed smaller sizes of mammospheres and were easily disrupted by moving the plate. The transamidase inhibitors ZDON induced mammosphere formation and $CD44^{+}/CD24^{-/low}$ phenotype, indicating that the TG2 transamidase activity possibly inhibits the acquisition of stem cell like characteristics. Silencing of the TG2 gene expression by siRNA significantly reduced $CD44^{+}/CD24^{-/low}$ and ALDH+ cells and reduced mammosphere formation but not to a significant level, suggesting that silencing of the TG2 is could be a promising therapeutic target. However, this study used only four breast cancer cell lines and further experiments need to be carried out on additional cell lines in order to draw a clear conclusion. RA-induced expression of both TG2-L and TG2-S in luminal cells and showed beneficial effects on the possession of stemness characteristics indicate that this vitamin A metabolite could be exploited in the design of effective therapies to target pathways that regulate breast cancer cell growth and survival.

Chapter 6

The role of TG2 in cell migration and EMT

6. Chapter 6: The role of TG2 expression in cell migration and EMT

6.1 Introduction

Cell migration occurs normally during embryonic development, tissue regeneration, and wound healing. The epithelial-to-mesenchymal transition (EMT) is the process when epithelial cells lose their epithelial characteristics and gain mesenchymal characteristics (Thiery, 2003; Lim and Thiery, 2012). The EMT process is characterised by changes in expression levels of cadherins where E-cadherin (E-cad) is down-regulated and N-cadherin (N-cad) is up-regulated (Loh *et al.*, 2019). It is associated with cancer progression, metastatic growth, higher expression of stem-cell markers, and a greater ability to form mammospheres, resulting in treatment resistance and recurrence (Mani *et al.*, 2008; Thiery *et al.*, 2009; Wang *et al.*, 2010). Continued activation of EMT is believed to play a significant role in cancer progression by transforming immobile epithelial cells into fibroblast-like cells exhibiting decreased intercellular adhesion, enhanced cell motility, and invasive activity (Thiery *et al.*, 2009; Wang *et al.*, 2010; Lim and Thiery, 2012). Therefore, targeting EMT may act as a promising target for the treatment of metastatic cancers.

TG2 expression in tumour cells or the tumour microenvironment promotes cell adhesion and modulates intracellular pathways (Fesus and Piacentini, 2002b). Sustained expression of TG2 results in constitutive activation of focal adhesion kinase (FAK), AKT (Verma, Guha, Wang, *et al.*, 2008), and nuclear factor kappa B (Mann *et al.*, 2006). These signaling pathways, in turn, can facilitate cancer progression by inducing EMT and stimulating drug resistance and metastasis (Kalluri, 2009; Thiery *et al.*, 2009). Other suggested pathways that govern TG2-induced EMT include transforming growth factor β1 (TGFβ1) (Cao *et al.*, 2012), and Wnt/ β-catenin. In cells lacking TG2 expression TGF-β does not stimulate EMT, indicating that TG2 can activate TGF-β (Nunes *et al.*, 1997), and in turn TGF-β can then up-regulate TG2 expression (Quan *et al.*, 2005). TG2 can also affect extracellular matrix proteins and modify cell-cell and cell-matrix interactions in the extracellular environment (Balklava *et al.*, 2002). In mammary epithelial cells, TG2 has been suggested to enhance drug resistance and invasion by activating EMT (Kumar *et al.*, 2010). Its sustained expression is associated with metastatic breast cancer phenotype and drug resistance (Mehta *et al.*, 2004; Kumar *et al.*, 2010).

In mammary epithelial cells expressing TG2 wild type-catalytically active or mutant domain show the same activity in mediating the degradation of IκBα and activation of NF-κB (Kumar and Mehta, 2012). On the other hand, a significant reduction in TG2 ability to induce EMT activities is exhibited by the mutant GTP-binding (Arg 580) inactive domain (Kumar and Mehta, 2012; Kumar *et al.*, 2012). These results suggest that the GTP binding domain, but not the catalytic binding domain, controls cancer progression and EMT activation.

TG2 expression is associated with loss of E-cad, up-regulation of mesenchymal markers, such as N-cad, vimentin, and fibronectin. TG2 also promotes the expression of different transcriptional repressors, including Snail1, Twist1, Zeb1, and Zeb2 (Kumar *et al.*, 2010). Aberrant expression of TG2 induces EMT, stem cell-like characteristics, and tumour metastasis by activating oncogenic signaling in breast (Kumar *et al.*, 2010; He, Sun and Liu, 2015) and ovarian cancer (Shao *et al.*, 2009) leading to drug resistance.

Taken together these results indicate that different TG2 domains exhibit differential effects on conferring EMT characteristics to cancer cells on a manner dependent on the type of cancer and potentially the stage of the disease.

6.2 Aim of the chapter

In the previous chapters, it has been shown that MDA-MB-231 and MCF-7 cells express different levels of endogenous TG2 isoforms. TG2 is a multifunctional enzyme bearing transamidase, GTPase, protein disulfide isomerase, protein kinase, and protein scaffolding activities (Fesus and Piacentini, 2002b; Mehta and Eckert, 2005). The two most studied functions are the transamidase and GTPase activities. Given that both the TG2-L and TG2-S isoforms carry transamidase enzymatic activity and the TG2-S isoform lacks the Arg580 residue in the GTP binding domain (Tee *et al.*, 2010; Singh *et al.*, 2016). The TG2 isoform that induces cell migration and confers EMT characteristics was investigated in MDA-MB-231 and MCF-7 breast cancer cells. MDA-MB-231 cells express high levels of TG2-L and lower levels of TG2-S, and MCF-7 cells express almost undetectable levels of TG2-L and low levels of TG2-S compared to MDA-MB-231 cells.

The effects of TG2-L and TG2-S on the migration potential of MCF-7 and MDA-MB-231 and whether these TG2 isoforms regulate EMT, or mesenchymal-to-epithelial transition (MET), were investigated following the shift in epithelial and mesenchymal markers' expression, including E-cadherin, N-cadherin, vimentin, and β-catenin.

Objectives:

- Evaluate the effect of the transamidase and GTPase activities of TG2 on the migration potential of breast cancer cell lines.
- Evaluate the relative contributions of the transamidase and GTPase activities of TG2 on the protein expression of the EMT markers.

6.3 Results

6.3.1 The role of TG2 in the regulation of the migratory potential of breast cancer cells

Cell migration was assessed in MCF-7 and MDA-MB-231 using the wound-healing assay (scratch assay). Cells were pre-treated prior to the scratch assay to induce or reduce the expression of the TG2-L and/or TG2-S isoforms. Cells were seeded in a 12-well plate and then MCF-7 cells were treated with either SAHA (0.5 μM), TSA (0.05 μM), or RA (40 μM) for 48 h to induce the expression of the different TG2 isoforms. MDA-MB-231 cells were treated with either ZDON (70 μM) or NC9 (30 μM) for 72h, or transfected with siRNA (siTG2) to silence TG2 expression or a non-targeting control (scramble siRNA) for 96 h.

After cells were incubated with required treatments, were grown to 90% confluent and a 200μl sterile pipette tip was used to create a scratch across the cell monolayer. Cells were incubated in low serum (0.5% FBS) medium. Images were taken at time points of 0, 24h, and 48h for MCF-7 cells and at 0, 6h, and 24h for MDA-MB-231 cells using an Inverted Phase Contrast Microscope (Optika) at 4x objective. Two images were taken per well for two independent wells from three independent experiments. The scratch gap area of these images was analysed on ImageJ software and the average of measurements was calculated. Percentage of cell migration was calculated as the percentage of gap closure with reference to time point 0h, then control sample was arbitrarily set as 100 as described in materials and methods.

6.3.1.1 The role of SAHA, TSA, and RA treatments in the regulation of the MCF-7 cells' migratory activity

The anticancer properties of the HDACIs SAHA and TSA are a result of their ability to inhibit proliferation and induce apoptosis and cell cycle arrest, although their importance and effectiveness in the treatment of breast cancer patients remain controversial (Wawruszak *et al.*, 2015). The migration potential of breast cancer cells has been reported to be inhibited in a dose-dependent manner by SAHA (Wawruszak *et al.*, 2019). RA has also been found to remarkably suppress the proliferation and migration of hepatocarcinoma cells by reversing EMT (Cui *et al.*, 2016).

The gap closure in MCF.7 cells treated with either SAHA (0.5 μM), TSA (0.05 μM), or RA (40 μM) inhibited the MCF.7 cells migratory potential compared to the DMSO (control) treated cells in a time-dependent manner (Figure 6.1A, B). The MCF-7 cell migration in SAHA treated cells was inhibited significantly by 57% and 56% at 24h and 48h, respectively, compared to the control (DMSO) treated cells. Non statistically significant inhibition (by 39% at 24h and 23% at 48h) of MCF.7 cells migration was observed in these cells treated with TSA (0.05 μM) compared to the control (DMSO) treated cells, while RA (40 μM) treatment inhibited MCF.7 cells migration by 50% at 24h and 47% at 48h, respectively.

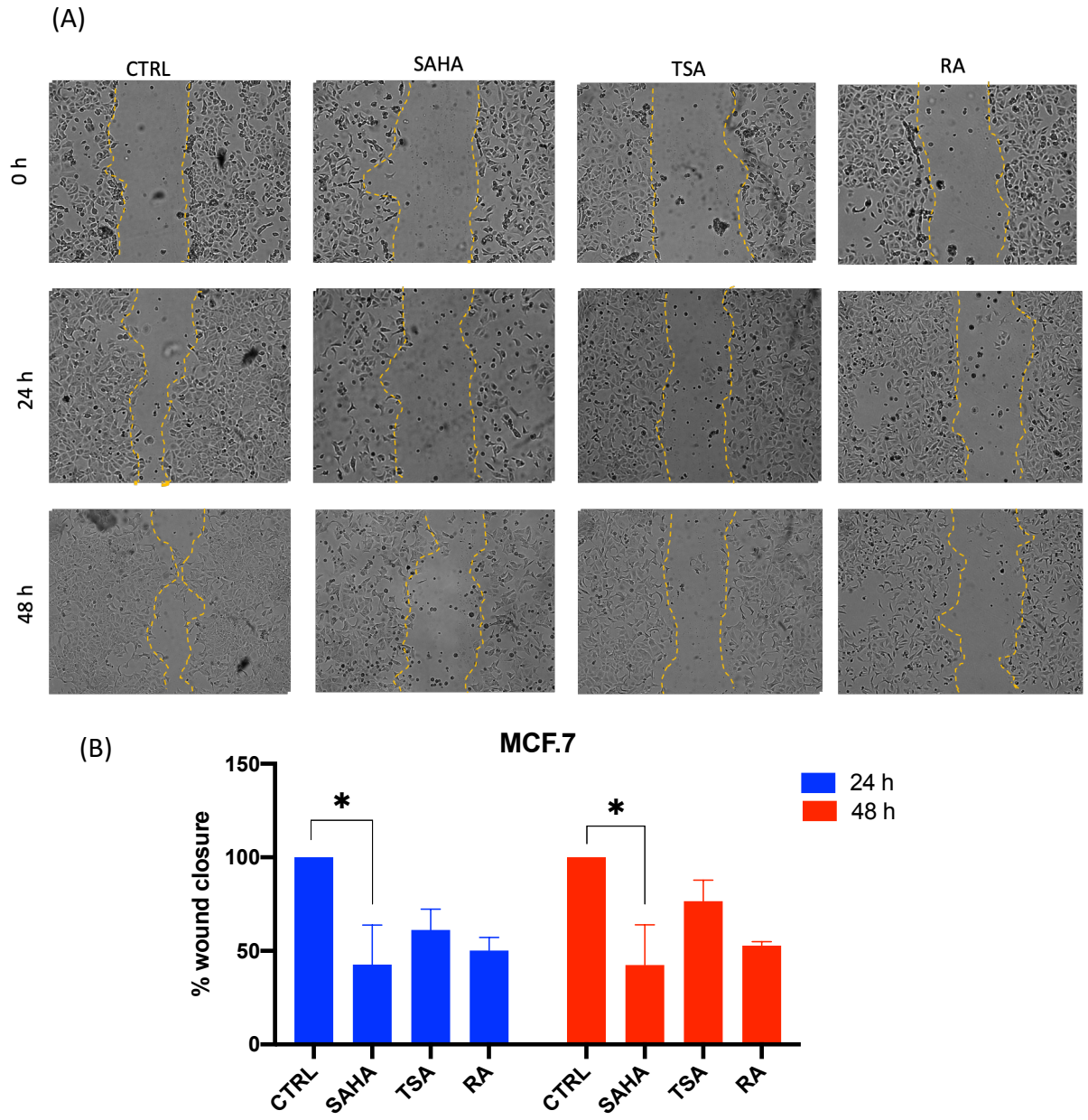

Figure 6-1 The role of SAHA, TSA, and RA treatments in the regulation of the MCF-7 cells migratory potential. Cells were seeded in 12 well plates and treated with DMSO (CTRL), 0.5 µM SAHA, 0.05 µM TSA, or 40 µM RA for 48 hours. Then scratches were generated using a 200µL pipette tip and images were captured using an inverted phase Contrast Microscope (Optika) at 4x objective at times 0h, 24h and 48h. The width of the scratch was measured using Image J software. The distance of the gap was measured and expressed as a percentage of the gap at time 0h. A) Gap closure of MCF-7 cells treated with DMSO (CTRL), 0.5 µM SAHA, 0.05 µM TSA, or 40 µM RA for 48 hours. B) Graph represents the percentage of migration gap in MCF-7 cells after treatment compared to the DMSO treated cells. Data are representative of three independent experiments. Data plotted are the mean ± SEM of three independent experiments each performed in duplicates. Statistical analysis was performed using One-way ANOVA followed by Dunnett's multiple comparison test. Statistical significance is denoted by *p≤0.05. Dashed yellow lines indicate wound edge.

6.3.1.2 The role of TG2 in the regulation of MDA-MB-231 cell migration

MDA-MB-231 cells exhibit higher migration rate than MCF.7 cells. The gaps captured at 48h, were very narrow and difficult to analyse, thus cell migration was captured at 0h, 6h, and 24h to enable differentiation between the gaps in control and cells treated with TG2 inhibitors. Figure 6.2A shows the gap closure for control cells treated with DMSO (control) or ZDON (70 μM), or NC9 (30 μM) at 0h, 6h and 24h. ZDON and NC9 inhibited MDA-MB-231 cell migration in a time-dependent manner compared to the DMSO treated control cells (Figure 6.2A, B).
The MDA-MB-231 cell migration was inhibited by 2% at 6h and 17% at 24h in the ZDON treated cells, compared to the control (DMSO) treated cells. The cell migration of MDA-MB-231 cells treated with NC9 (30 μM), was inhibited by 25% at 6h and by 37% at 24h, compared to the control (DMSO) treated cells but the inhibition observed at 24h was not statistically significant. Statistically significant inhibition of the MDA-MB-231 cells migratory potential was observed at 24h in cells treated with ZDON or NC9. These findings suggest that inhibition of TG2 activities by ZDON or NC9 decreased the migratory potential of the MDA-MB-231 cells.

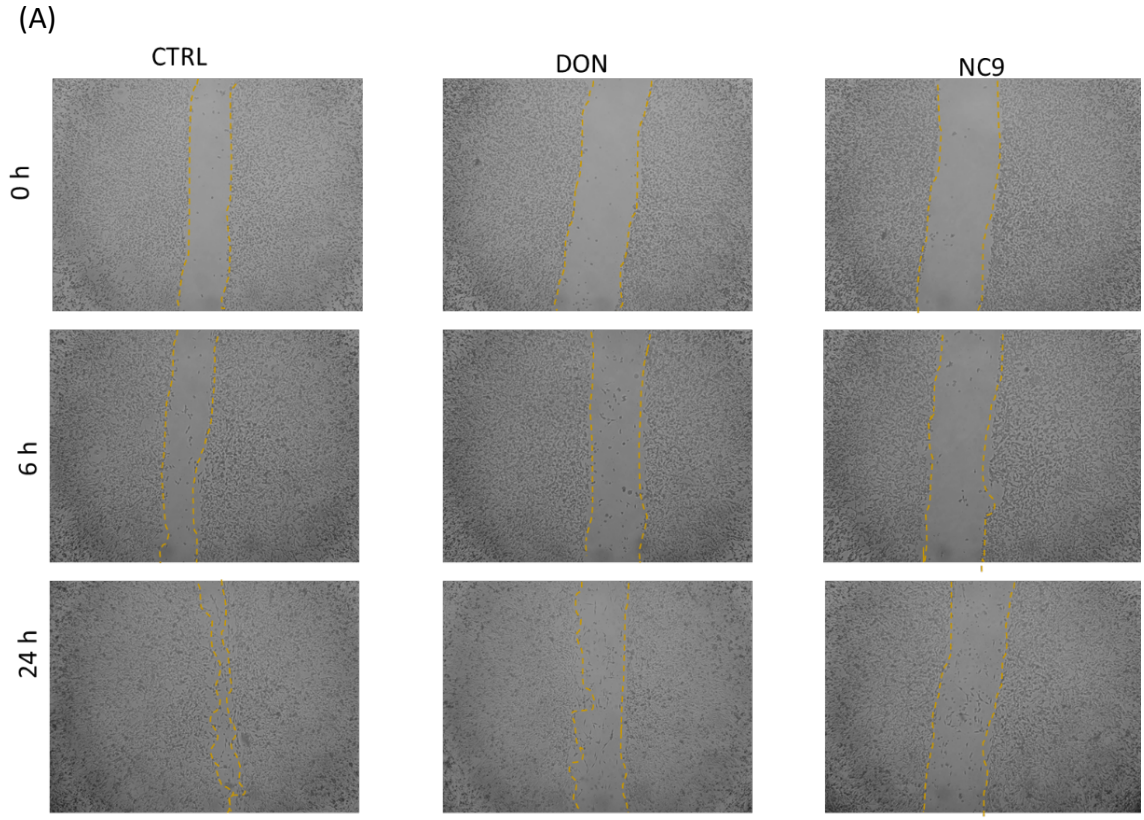

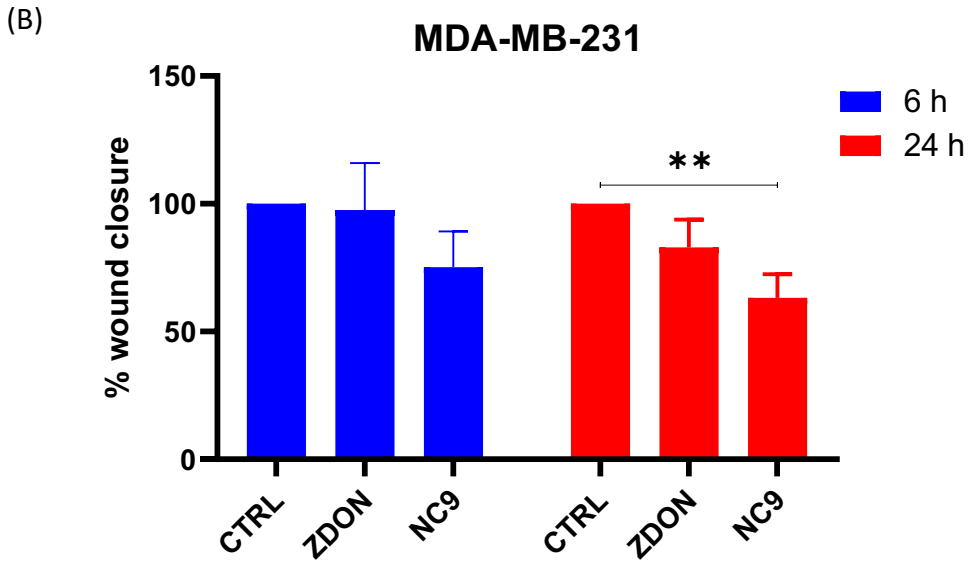

Figure 6-2 The role of TG2 transamidase and GTPase enzymatic activities on the MDA-MB-231 cells migratory potential. Cells were seeded in 12 well plates and treated with DMSO (CTRL), 70 µM ZDON, or 30 µM NC9 for 72 hours. Scratches then were generated using a 200 µL pipette tip and images were captured using an inverted phase Contrast Microscope (Optika) at 4x objective at times 0h, 6h and 24h. The width of the scratch was then measured using the Image J software. The distance of the gap at each time point was measured and

expressed as a percentage of the gap at time 0h. A) Gap closure of MDA-MB-231 cells treated with DMSO (CTRL), 70 µM ZDON, or 30 µM NC9 for 72 hours. B) Graph represents the percentage of migration in MDA-MB-231 cells after treatment compared to the DMSO treated cells. Data are representative of three independent experiments. Data plotted are the mean ± SEM of three independent experiments each performed in duplicates. Statistical analysis was performed using One-way ANOVA followed by Dunnett's multiple comparison test. Statistical significance is denoted by **P<0.01. Dashed yellow lines indicate wound edge.

Our previous findings showed that TG2 silencing by siRNA down-regulated the TG2-L isoform protein levels by approximately 30% and the TG2-S isoform by ~ 90%. TG2-L bears the full protein sequence and contains both the transamidase and GTP binding domains, while the TG2-S isoform lacks the GTP binding domain (Singh *et al.*, 2016). Figure 6.3A shows the gap closure for cells transfected with specific TG2 siRNA (siTG2) or a non-targeting siRNA control (scramble) for 96h. Down-regulation of TG2 protein levels increased the MDA-MB-231 cell migration in a time-dependent manner compared to the non-targeting siRNA control (Figure 6.3A, B). The MDA-MB-231 cell migration in siTG2 transfected cells was significantly increased by 69% at 6h and by 7% at 24h compared to the non-targeting siRNA control.

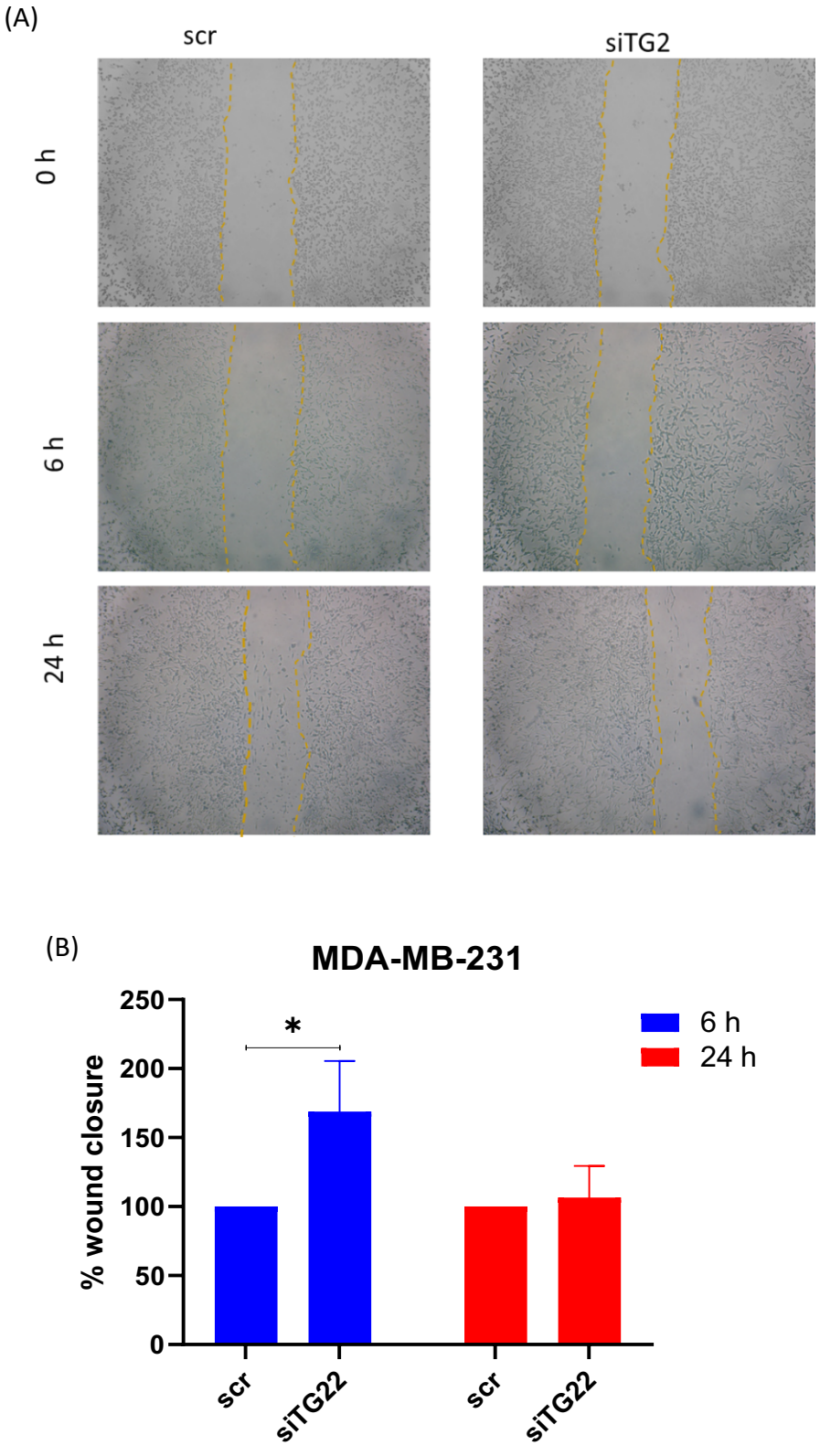

Figure 6-3 The role of the TG2 isoforms in the regulation of the MDA-MB-231 cells migratory potential. Cells were seeded in 12 well plates and transfected with either siRNA (siTG2) or a non-targeting siRNA control (scramble) for 96h. Scratches were then generated using a 200 µL pipette tip and images were captured using an inverted phase Contrast Microscope

(Optika) at 4x objective at times 0h, 6h and 24h. The scratch width was measured using Image J software. The distance of the gap distance was measured and expressed as a percentage of the gap at time 0h. A) Gap closure of MDA-MB-231 cells transfected with siRNA (siTG2) or a non-targeting siRNA control (scramble) for 96h. B) Graph represents the percentage of migration in MDA-MB-231 cells after transfection. Data are representative of three independent experiments. Data plotted are the mean ± SEM of three independent experiments each performed in duplicates. Statistical analysis was performed using t-test. Statistical significance is denoted by **P<0.01. Dashed yellow lines indicate wound edge.

6.3.2 The role of TG2 isoforms in the regulation of EMT markers in breast cancer cells

EMT is considered the major factor in tumour invasion, metastasis, and CSCs formation. The migration potential is associated with EMT, as cells that have acquired mesenchymal phenotype exhibit higher migration rate than epithelial cells (Fan *et al.*, 2012).

Given that SAHA, TSA, and RA treatment of MCF-7 cells induced the TG2-L and TG2-S protein levels the role of TG2-L and TG2-S isoforms in the regulation of the E-cad, N-cad, vimentin, and β-catenin protein levels was investigated in the MCF-7 cells treated with either SAHA, TSA or RA by western blot. On the other hand, in the MDA-MB-231 cells the role of the TG2 transamidase and/or GTPase enzymatic activities are inhibited by treatment of these cells with the TG2 inhibitors ZDON or NC9. Additionally, the role of the TG2-L and TG2-2 isoforms on the EMT markers' protein levels was investigated in MDA-MB-231 cells transfected with siTG2 or scramble siRNA.

MCF-7 cells (5 x 10^5 cells) were seeded in a 6 well plate and treated with SAHA (0.5 μM), TSA (0.05 μM), or RA (40 μM) for 48h to induce the expression of the different TG2 isoforms. MDA-MB-231 cells (2 x 10^5 cells) were seeded in a 6 well plate and treated with ZDON (70 μM) or NC9 (30 μM) for 72 hours or transfected with either specific siRNA (siTG2) or a non-targeting siRNA control (scramble) for 96h. Samples were then subjected to western blot as described in materials and methods to evaluate the protein levels of the EMT markers E-cadherin, N- cadherin, vimentin, and β-catenin.

6.3.2.1 The role of TG2 in the regulation of EMT in MCF-7 cells

MCF-7 cells express E-cadherin but not N-cadherin or vimentin . Our results showed that both SAHA and TSA treatment induced the TG2-L and TG2-S protein levels. However, RA treatment resulted in a significant increase of the TG2-L isoform and exerted a minor effect on TG2-S protein levels (Figure 6.4A and B). Significant reductions in E-cadherin protein levels were recorded in TSA (23%) and RA (46%) treated cells compared to DMSO-treated control cells (Figure 6.4C). β-catenin protein levels were decreased in SAHA-, TSA-, and RA-treated cells by 1%, 9%, and 8%, respectively, compared to the control cells (DMSO) but this decrease was not statistically significant (Figure 6.4D). Increased N-cadherin protein levels were detected in MCF-7 cells treated with SAHA, TSA, or RA by 39%, 65%, and 100%, respectively compared to the control cells (Figure 6.4E). Similar trend was also observed for vimentin protein levels, which were induced by 44%, 74%, and 99% in MCF-7 cells treated with SAHA, TSA, and RA, respectively (Figure 6.4F). No conclusion can be drawn for the N-cadherin and vimentin protein levels as one experiment was carried out.

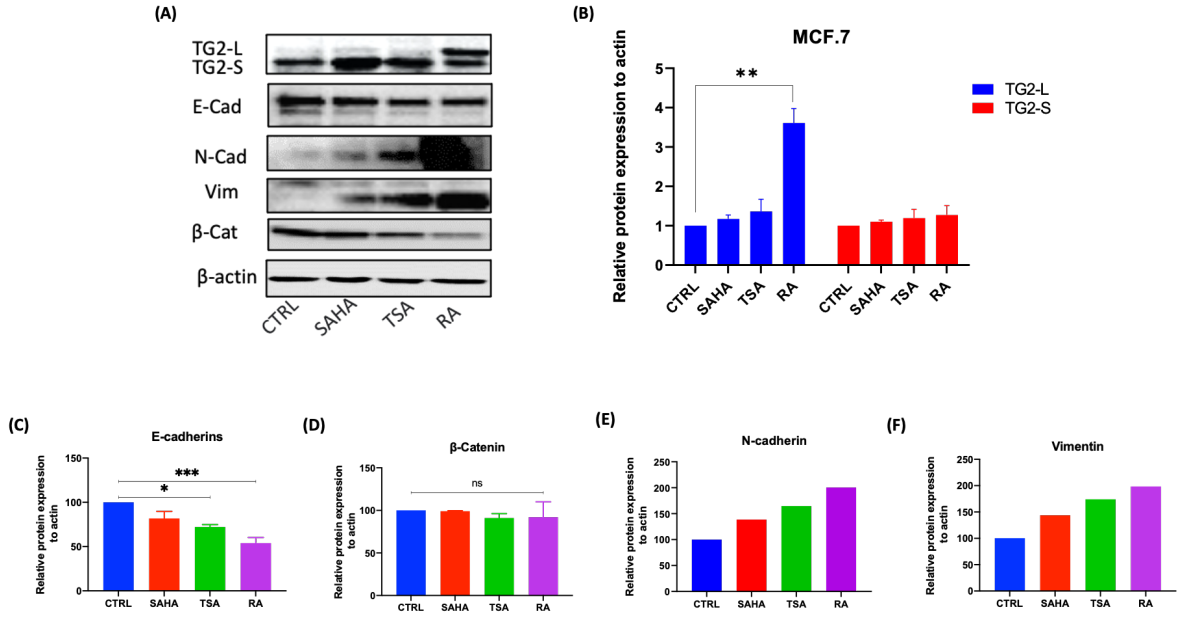

Figure 6-4 Protein levels of EMT markers in MCF-7 cells. MCF-7 cells were treated with DMSO (CTRL), 0.5 µM SAHA, 0.05 µM TSA, or 40 µM RA for 48 hours as indicated. Cells were then lysed, and cellular extract (20 µg protein) was analyzed by western blotting. A) Representative western blot indicating the TG2-L, TG2-S, E-cad, N-cad, vimentin, β-catenin, and β-actin. B) Densitometric analysis of TG2-L (blue bars) and TG2-S (red bars) expression normalized to the

respective β-actin protein levels. C) Densitometric analysis of E-cad expression (n=3). D) Densitometric analysis of β-catenin expression (n=2). E) Densitometric analysis of N-cad expression (n=1). Densitometric analysis of vimentin expression (n=1). Bars represent the mean ± SEM of at least two independent experiments. Statistical analysis was performed using One-way ANOVA followed by Dunnett's multiple comparisons test. Significance is denoted by *p≤0.05, **P<0.01, and ***p<0.005.

6.3.2.2 The role of TG2 transamidase and/or GTPase enzymatic activities in the regulation of the EMT markers protein levels in MDA-MB-231 cells

Increased E-cadherin protein levels were observed in ZDON and NC9 treated cells by 15% and 16%, respectively, compared to the control cells (DMSO) treated cells (Figure 6.5C). No conclusion can be reached for the regulation of the E-cadherin protein levels by the TG2 transamidase and/or GTPase enzymatic activities in MDA-MB-231 cells as one experiment was carried out. Decreased but not statistically significant N-cadherin protein levels were observed in cells treated with either ZDON or NC9 by 20%, or 25%, respectively, compared to the control cells (Figure 6.5D). Lower but not statistically significant vimentin protein levels were also recorded in ZDON and NC9 treated cells by 0.4% and 7%, respectively, compared to the control cells (DMSO) (Figure 6.5E).

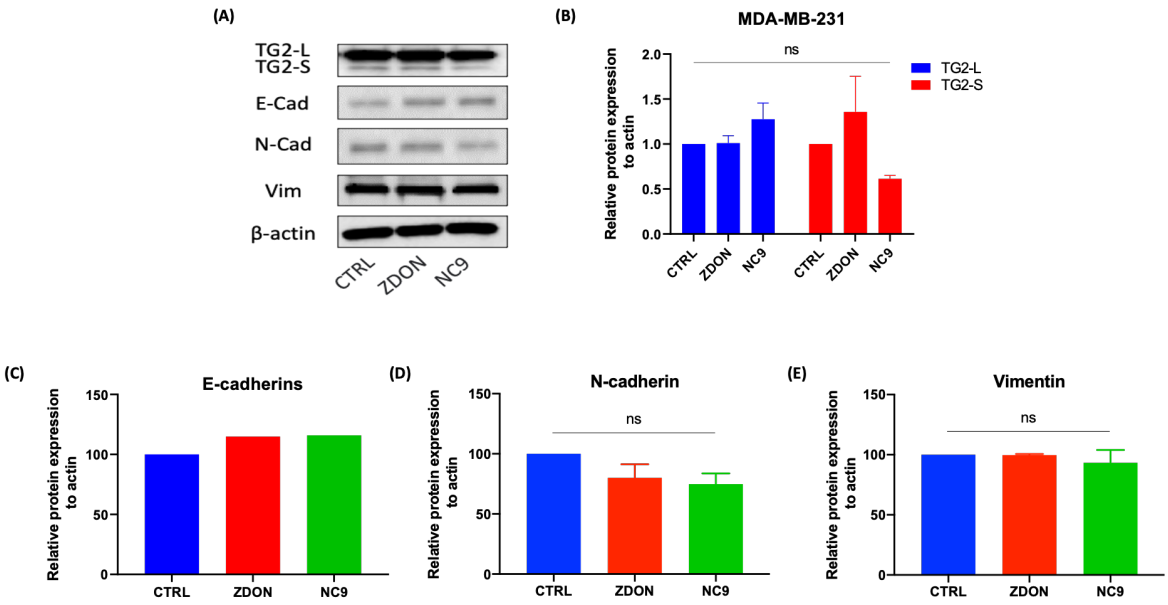

Figure 6-5 Effect of TG2 transamidase and/or GTPase enzymatic activities in the regulation of the EMT markers protein levels in MDA-MB-231. MDA-MB-231 cells were treated with DMSO (CTRL), 70 µM ZDON, or 30 µM NC9 for 72 hours. Cells were then lysed, and cellular

extract (20µg protein) was analyzed by western blotting. A) Representative western blot indicating the TG2-L, TG2-S, E-cad, N-cad, vimentin, β-catenin, and β-actin. B) Densitometric analysis of TG2-L (blue bars) and TG2-S (red bars) protein levels normalized to the respective β-actin. C) Densitometric analysis of E-cad expression (n=1). D) Densitometric analysis of N-cad expression (n=3). E) Densitometric analysis of vimentin expression (n=3). Bars represent the mean ± SEM of at least three independent experiments. Statistical analysis was performed using One-way ANOVA followed by Dunnett's multiple comparisons test. ns= non-significant.

Results shown in previous chapters indicate that TG2 silencing by siRNA down-regulated the TG2-L isoform protein levels by approximately 30% and the TG2-S isoform by ~90% compared to cells transfected with non-targeting scramble siRNA control. Decreased by 28% E-cadherin protein levels were evident in MDA-MB-231 cells transfected with siTG2 compared to scramble transfected cells but only one experiment was performed, therefore no conclusions can be drawn. Decreased by 22% N-cadherin protein levels were observed in cells transfected with siTG2 compared to scramble transfected cells (Figure 6.6D). Vimentin protein levels were not significantly decreased by 14% in the siTG2-transfected cells, compared to the scramble transfected cells (Figure 6.6E) .

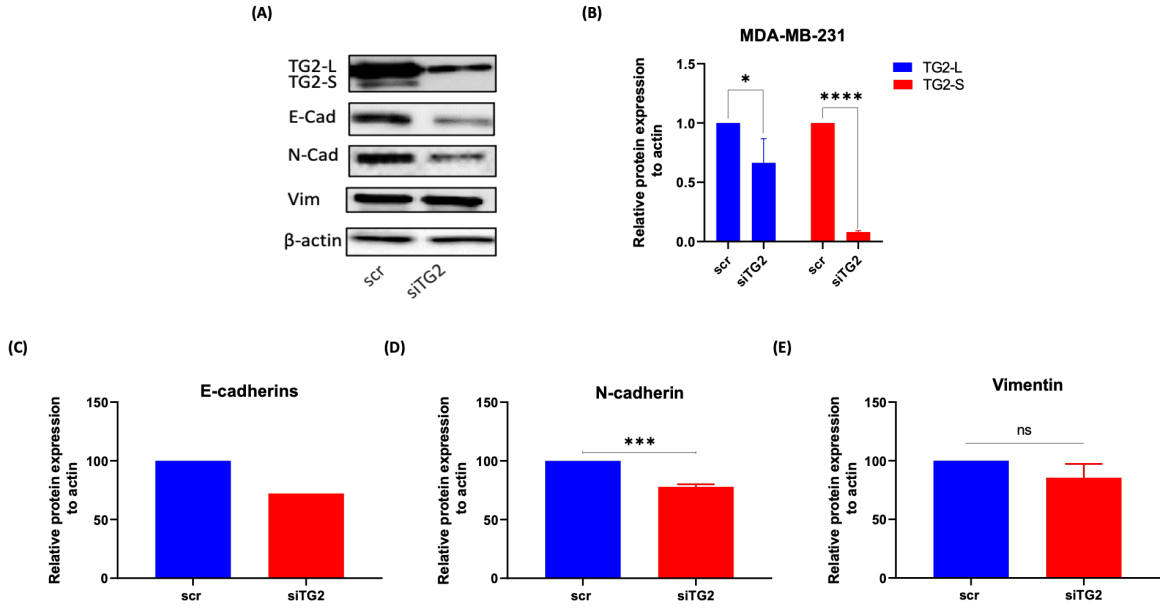

Figure 6-6 Protein levels of EMT markers in MDA-MB-231. MDA-MB-231 cells were transfected with either specific siRNA (siTG2) or a non-specific siRNA control (scramble) for 96h. Cells were then lysed, and cellular extract (20 µg protein) was analyzed by western blotting. A) Representative western blot indicating the TG2-L, TG2-S, E-cad, N-cad, vimentin, β-catenin, and β-actin. B) Densitometric analysis of TG2-L (blue bars) and TG2-S (red bars)

expression normalized to the respective β-actin. C) Densitometric analysis of E-cad expression (n=1). D) Densitometric analysis of N-cad expression (n=3). E) Densitometric analysis of vimentin expression (n=3). Bars for TG2-L, TG2-S and N-cadherin represent the mean ± SEM of at least three independent experiments. Statistical analysis was performed using t-test. Significance is denoted by *p≤0.05, ***p<0.005, and ****p<0.0001. ns= non-significant.

6.4 Discussion

Different pathways are involved in the transformation of primary tumours into metastatic tumours. Metastatic cells leave the initial site of the tumour via the bloodstream and migrate to a distant site, forming a secondary tumour (Woodhouse, Chuaqui and Liotta, 1997). It is important to understand the pathways that allow cells to migrate and produce subsequent tumours since the treatment of metastatic tumours is much more challenging in the clinic. Cancer invasion and metastasis have been associated with EMT. The mesenchymal phenotype facilitates cell migration to distant organs and acquires stemness characteristics (Thiery *et al.*, 2009). Cells with elevated TG2 levels display up-regulation of EMT and high migration and invasion rates (Fisher *et al.*, 2015). To shed light on the role of the different TG2 isoforms on cell migration and acquisition of EMT characteristics different conditions under which the TG2-L and TG2-S isoforms are expressed in MCF-7 and MDA-MB-231 cells were used and migratory potential and EMT markers were followed in these cells.

6.4.1 The role of the TG2 isoforms on the migratory potential of breast cancer cells

6.4.1.1 The effect of TG2 isoforms of the migratory potential of the MCF-7 cells

TG2-L and TG2-S protein levels were up-regulated in SAHA-, TSA-, and RA-treated MCF-7 cells compared to DMSO-treated cells (control). Cell migration was found to be reduced in SAHA, TSA and RA treated MCF-7 compared to the DMSO treated cells. In agreement with these results, published reports have indicated that SAHA treatment reduces migration in MCF-7 cells in a dose-dependent manner, however the concentrations of this HDAC inhibitor used in this study is significantly higher (2 and 5μM) (Wawruszak *et al.*, 2019). The TG2-L and TG2-S protein levels in these concentrations of SAHA have not been studied in the present thesis. In agreement with results reported in this thesis RA treatment inhibits cell growth, migration, and invasion capacity of hepatocarcinoma cells in a dose-dependent manner (Cui *et al.*, 2016).

It has been suggested that RA inhibits cell migration by inhibiting the function of EMT inducers such as the growth factors EGF and heregulin-β1 (Zanetti *et al.*, 2015).

6.4.1.2 The effect of TG2 down-regulation in MDA-MB-231 cell migration

The NC9 locks the TG2 in its open conformation, resulting in inhibition of GTP binding to the GTP-binding domain (Caron *et al.*, 2012; Song *et al.*, 2017). On the other hand, ZDON inhibits the TG2 transamidase activity and possibly inhibits the GTPase activity by locking the enzyme in an open active conformation. However, its role in the regulation of the TG2 GTPase activity is still not clear. Inhibition of the TG2 transamidase activity (ZDON) or transamidase and GTPase activities (NC9) reduced cell migration in MDA-MB-231 cells. NC9 exhibited higher inhibition efficiency compared to ZDON, suggesting that the TG2 GTPase activity plays an important role in the induction of cell migration in the MDA-MB-231 cells.

It has been reported that the TG2 transamidase activity is not required for TG2 carcinogenic effects, and the GTP-binding domain is critical for EMT and CSC formation in mammary epithelial cells (Kumar *et al.*, 2012) and renal cell carcinoma (Ulukan *et al.*, 2020). Migration potential is affected by cell-cell adhesion rates, in which strong cell-cell adhesion reduces cell migration and vice versa (Kedrin *et al.*, 2007; Schaeffer *et al.*, 2014). Therefore, inhibition of TG2 GTPase activity would potentially strengthen the TG2 protein cross-linking activity and facilitate cell-cell adhesion, thereby preventing high migration rate, invasion, and metastasis potential.

6.4.2 The role of TG2 on EMT

6.4.2.1 The effect of TG2 isoforms on EMT in luminal MCF-7 cells

Several reports indicate that the ability of cells to migrate associates with EMT whereas increased migration is not necessary for EMT (Schaeffer *et al.*, 2014). To investigate the association between the TG2-L/TG2-S expression and migratory potential to EMT phenotype the protein levels of the EMT markers E-cadherin, N-cadherin, vimentin, and β-catenin were followed in SAHA, TSA and RA treated MCF-7 cells. Our findings showed that E-cadherin protein levels decreased in SAHA-, TSA-, and RA-treated MCF-7 cells while the N-cadherin

protein levels increased in SAHA-, TSA-, and RA-treated MCF-7 cells compared to control. In agreement with these results SAHA and TSA HDACIs were found to induce the EMT phenotype in prostate cancer cells by reducing of E-cadherin protein level and increasing the protein levels of the mesenchymal markers vimentin and N-cadherin (Kong *et al.*, 2012). It has been suggested that HDACIs mediated increase of the EMT markers protein levels is associated to the hyperacetylation of histone 3 in the promoters of genes inducing EMT such as vimentin, Slug, ZEB1, and MMP2 (Kong *et al.*, 2012). In addition, HDACIs induce the gene expression of the Nanog and Sox2 stem cell markers in a dose-dependent manner thereby stimulating CSC characteristics (Kong *et al.*, 2012). In line with these observations other studies have demonstrated that HDACIs increase the EMT phenotype by up-regulating the protein levels of E-cadherin in pancreatic cancer (Burstin *et al.*, 2009) and in the head and neck squamous cell carcinoma (Bruzzese *et al.*, 2011). Inverse correlation between induction of SAHA-mediated cell death and TG2 protein levels in MCF-7 cells and re-sensitization of cancer cells expressing reduced TG2 levels or activity to SAHA's anti-cancer effects have also been reported (Carbone *et al.*, 2017). On the other hand, treatment of MCF-7 cells with high concentrations of TSA (0.1mM) has been suggested to reverse the EMT process by modulating the activity of transcription factors, such as the zinc finger protein SNAI2 in a time-dependent manner (Wang *et al.*, 2020). Hence, treatment with low concentrations of HDACIs induce EMT whereas treatment with high doses of HDACIs induce the MET process.

In our study, the most distinctive increase in the EMT process was associated with the induction of the expression of the TG2-L isoform in RA-treated MCF-7 cells in which the highest levels of TG2-L were recorded compared to the SAHA, TSA and DMSO treated cells. RA-treated MCF-7 cells exhibited reduced mammoshpere formation efficiency, $CD44^{+}/CD24^{-/low}$ CSCs phenotype and decreased migration potential compared to the DMSO-treated cells (control). Under these conditions reduction of E-cadherin and β-catenin and increase of N-cadherin and vimentin protein levels were observed suggesting that the TG2-L isoform plays a crucial role in the induction of EMT. Consistently with these findings, down-regulation of the epithelial marker E-cadherin has been demonstrated in the normal breast cell line MCF10A which overexpresses RARα (Doi *et al.*, 2015), which in turn induces TG2 up-regulation. In contrast, in RA-treated hepatocarcinoma cells increased E-cadherin expression

and reduced N-cadherin, vimentin, snail, and twist protein levels were observed (Cui *et al.*, 2016) suggesting that the effect of RA-RARα-TG2-L axis on EMT is cell type dependent.

It has also been shown that the EMT phenotype is linked to IL-6 expression in breast cancer cells (Sullivan *et al.*, 2009). IL-6 overexpression is stimulated in stably TG2 transfected MCF-7 cells conferring to these cells stem-cell-like phenotypes, increased invasive ability, and increased metastatic potential coinciding with decreased E-cadherin protein levels (Oh *et al.*, 2016). Furthermore, patients with advanced breast cancer expressing high TG2 and IL-6 levels had shorter metastasis-free survival compared to patients with high IL-6 expression alone [42]. These findings raise the possibility that RA-mediated increase of the TG2-L protein levels in MCF-7 cells and the consequent effects on EMT might be mediated by IL-6.

6.4.2.2 The effect of the TG2 enzymatic activities and isoform protein levels on EMT in MDA-MB-231 cells

MDA-MB-231 are aggressive basal cells with high invasion and metastatic potential. In our study, both ZDON and NC9 reduced EMT in MDA-MB-231 cells compared to DMSO treated control cells. In agreement with these findings, NC9-treatment of the A431 squamous cell carcinoma cells decreased the activity of the mesenchymal markers Snail, Slug, and Twist transcription factors. Reduced levels of these transcription factors coincides with increased levels of E-cadherin and reduced expression of N-cadherin, vimentin, and fibronectin, and decreased cell migration, invasion, and spheroid formation (Fisher *et al.*, 2015).

Our findings showed that high TG2-L expressing MDA-MB-231 cells express low levels of the epithelial marker E-cadherin, but increased levels of the mesenchymal markers N-cadherin and vimentin compared to low TG2-L expressing MCF-7 cells. This is in agreement with studies demonstrating that high TG2-L levels associate with low epithelial marker expression and high mesenchymal marker levels in rat mammary tumor cells (Wang and Griffin, 2013) and colorectal cancer (Ayinde, Wang and Griffin, 2017). Indication that TG2 is essential for EMT, migration, invasion and metastasis has been provided by studies in squamous cell carcinoma (Fisher *et al.*, 2015) and colorectal cancer (Ayinde, Wang and Griffin, 2017; Kang *et al.*, 2018).

Silencing of TG2 gene expression by siRNA in these cancers reduces EMT marker expression and spheroid formation. Furthermore, silencing of TG2 gene expression by siRNA reverses EMT and re-sensitises MDA-MB-231 cells to docetaxel treatment (He, Sun and Liu, 2015). In addition, TG2 mediated constitutive activation of NF-κB in breast cancer (Agnihotri, Kumar and Mehta, 2012) and ovarian cancer (Cao *et al.*, 2008) induces EMT and cell survival. Confirmation that NF-κB activation is an essential downstream mediator of TG2-dependent induction of EMT has been provided by studies in which knocking-down the NF-κB subunit p65 in TG2 expressing cells reversed the EMT phenotype without affecting TG2 levels (Kumar *et al.*, 2012).

6.5 Conclusion

SAHA ,TSA, and RA treatment of MCF-7 cells moderately induced the TG2-L and substantially increased the TG2-S protein levels compared to DMSO treated MCF-7 cells. SAHA, TSA and RA treatment reduced the migratory potential of MCF-7 cells compared to DMSO treated control cells. In addition, SAHA, TSA, and RA treatment reduced the protein levels of this epithelial marker in MCF-7 cells. On the other hand, SAHA, TSA, and RA treatment of MCF-7 cells resulted in the induction of N-cadherin and vimentin and downregulation of the β-catenin protein levels.

In the metastatic breast cancer MDA-MB-231 cells treatment with the small molecule TG2 inhibitor NC9 blocking both the TG2 transamidase and GTPase activities reduced cell migration and EMT by lowering the levels of the mesenchymal markers N-cadherin and vimentin more efficiently than the ZDON. This suggests that the TG2 mediated migratory potential and EMT of the MDA-MB-231 cells are mainly regulated via the TG2 GTP binding domain, where the GTP binds and activates the TG2 GTPase activity, and less via the TG2 catalytic binding domain, where Ca^{2+} binds and activates the TG2 transamidase activity. Silencing of the TG2 gene expression leading to reduction of TG2-L (by 30%) and TG2-S (by 90%) isoforms reversed EMT and induced cell migration supporting the notion that the protein levels of the TG2-L and TG2-S isoforms could serve as prognostic markers in breast carcinogenesis.

Chapter 7

Conclusion and future works

7. Chapter 7: General discussion and future works

7.1 General discussion

Cancer therapy relies on targeting rapidly proliferating tumour cells for tumour suppression. However, cancer stem cells (CSCs) can migrate to other organs and increase the risk of recurrence (Kumar *et al.*, 2011). Targeting CSCs is an essential strategy for treating metastatic cancer that is resistant to conventional treatment. However, the mechanism behind CSCs' metastatic potential and chemoresistance remains unclear. Surviving breast tumour cells in clinical samples following conventional therapy are enriched in sub-populations of cells with both CSC and mesenchymal characteristics, highlighting the correlation between stem cell and EMT phenotype. Several studies indicate that aberrant expression of TG2 is associated with the transition of mammary epithelial cells into a mesenchymal phenotype and the acquisition of CSC traits, as revealed by an increase in $CD44^{+}/CD24^{-/low}$ cells, self-renewal ability, and the ability to form mammosphere in non-adherent conditions (Kumar *et al.*, 2010, 2011). This suggests that TG2-regulated pathways play a significant role in the development of chemoresistance and metastasis by acquiring the EMT-CSC phenotype in mammary epithelial cells (Mangala *et al.*, 2007; Wang and Griffin, 2013; Oh *et al.*, 2016; Tempest *et al.*, 2021).

Inflammation-induced breast cancer progression is facilitated by TG2. It promotes cell survival and invasion by constitutive activation of NF-κB. TG2 binds to NF-κB and the resulting complex regulates transcription by binding to the HIF-1α promoter. Increased expression of HIF-1α stimulates the expression of several transcription factors, such as Snail, Twist, Zeb, and VEGF, that promote angiogenesis, EMT, and stem cell-like traits. The changes in EMT and CSC-related genes affect cell-cell and cell-ECM interaction, resulting in increased cell proliferation in a hypoxic environment, the production of extracellular matrix (ECM) proteins, and invasion and metastasis (Agnihotri, Kumar and Mehta, 2013).

TG2 has received considerable attention in the last few years as a potential therapeutic target for cancer treatment. It has been reported as a promising therapeutic target for the treatment of metastatic breast cancer. TG2 siRNA knockdown or inhibition by small molecule inhibitor has been shown to improve cancer cell sensitivity to chemotherapy-induced cell death as well as suppression of invasion and metastasis (Verma and Mehta, 2007; Hwang *et al.*, 2008; Verma, Guha, Diagaradjane, *et al.*, 2008).

The TG2 structure revealed different domains, each of which is assigned to a specific function. Breast cancer cell lines transfected with GTP-binding-mutant constructs (Arg580) induced epithelial marker expression with E-cadherin and reduced mesenchymal marker expression, such as N-cadherin, vimentin, and FN, compared to cells transfected with wild-type TG2 or transamidating-mutant constructs (Cys277). Transcription repressors, such as Snail1, Zeb 1/2, and Twist 1, are also reduced in the GTP-binding mutant. This suggests that oncogenic functions exerted by TG2 are attributed to GTP-binding (GTPase activity) (Kumar *et al.*, 2011, 2012).

The study hypothesised that breast cancer cells express different TG2 isoforms, and these isoforms contribute differently to breast cancer progression. Understanding their expression and function will allow for more targeted therapeutics and personalised medicine.This study aimed to understand the significance of TG2 isoforms in breast cancer cells. This led us to further characterise the TG2 activities.

Aim of the study:

- Evaluation of TG2-L and TG2-S expression in different breast cancer cell lines.
- Evaluation of the role of TG2 isoforms in CSC characteristics, such as the ability to form mammospheres in non-adherent conditions and assessing the expression of CD24, CD44, and ALDH.
- Evaluation of the role of TG2 in breast cancer cell migration and its role in the EMT phenotype.

7.2 Conclusion

Our results demonstrated that MDA-MB-231 expresses both the TG2-L and TG2-S isoforms. MCF-7 and T47D also express both isoforms but to a very lower extent compared to MDA-MB-231, whereas MDA-MB-468 expresses only the TG2-S isoform. MDA-MB-231 revealed the highest TG2-L and TG2-S basal levels. Increased protein levels of the TG2-L and TG2-S isoforms occur in the SAHA-, TSA-, and RA-treated MCF-7 and T47D cells compared to untreated cells, and TG2 transamidase activity has been induced in all treated cells. TG2-S protein levels decreased in the SAHA, TSA, and RA-treated MDA-MB-468 compared to untreated cells. The reduction of TG2-S expression was associated with decreased transamidase activity in MDA-MB-468 treated cells compared to the control.

Transfection of MDA-MB-231 with siRNA knock-down the expression of TG2-L by approximately 30% and TG2-S by approximately 90%. Inhibition of TG2 transamidase activity by ZDON had no effect on TG2-L but induced TG2-S expression levels. Inhibition of TG2 transamidase and GTPase activities by NC9 increased TG2-L protein levels while decreasing TG2-S protein levels. NC9-treated cells significantly reduced TG2 transamidase activity compared to the untreated control cells, indicating that NC9 mediated induction of TG2-L protein levels induces GTP-binding, thus leading to the inhibition of TG2 transamidase activity. ZDON reduced the TG2 transamidase activity but to a lesser extent compared to that exhibited by the NC9, lending support to the previously described model.

Breast cancer cell lines used in this study expressed different levels of CD24 and CD44 and a CD44/CD24 phenotype. The highly metastatic and aggressive MDA-MB-231 cells have the $CD44^{+}/CD24^{-/low}$ phenotype, high ALDH activity, and the ability to form mammospheres in non-adherent conditions, indicating that stem cell traits are associated with high TG2-L basal expression levels.

The enzymatic transamidase activity assay revealed that NC9 significantly inhibited the transamidase activity to a higher level than ZDON did. Moreover, NC9 induced TG2-L and reduced TG2-S protein expression as confirmed by western blot. ZDON increased the $CD44^{+}/CD24^{-/low}$ phenotype and ALDH activity. NC9 induced $CD44^{+}/CD24^{-/low}$ phenotype and

induced ALDH activity to a higher extent than ZDON, indicating that transamidase activity reduces the oncogenic effect of TG2 and reduces stemness traits. However, ZDON induced mammosphere formation while NC9 reduced it, suggesting that inhibition of GTPase activity is essential to reduce mammosphere formation.

Silencing of the TG2 gene expression by siRNA decreased $CD44^{+}/CD24^{-/low}$ and ALDH+ cells and mammosphere development to a non-significant extent, indicating that TG2 knock-down is a feasible therapeutic target.

The percentage of the $CD44^{+}/CD24^{+}$ sub-population was linked to mammosphere forming ability in MCF.7 and T47D, in which increased $CD44^{+}/CD24^{+}$ sub-population induced mammosphere formation and vice versa. The RA-induced expression of both TG2-L and TG2-S in luminal MCF.7 and T47D cells and reduced stemness features by reducing mammosphere formation and $CD44^{+}/CD24^{+}$ phenotype suggest that this vitamin A metabolite might be used to develop a drug that targets RA signaling pathways that control the growth and survival of breast cancer cells.

In MCF.7, TG2-L and TG2-S up-regulation by SAHA, TSA, and RA suggested to promote EMT by reducing of epithelial marker's expression of E-cadherin and by inducing mesenchymal markers' expression of N-cadherin and vimentin.

NC9 significantly inhibited cell migration and reduced EMT by decreasing the levels of the mesenchymal markers N-cadherin and vimentin more effectively than ZDON, indicating that the TG2-mediated migratory potential and EMT of the MDA-MB-231 cells are predominantly regulated by the TG2 GTP-binding domain and less by the TG2 catalytic binding domain.

Interestingly silencing of the TG2 gene expression by siRNA induced cell migration. On the other hand, it reduced mesenchymal markers' expression of N-cadherin and vimentin, suggesting that protein knock-down affects other TG2 functions that contribute to migration and EMT phenotype and migration potential associated with EMT, whereas increased migration is not essential for EMT.

The study concluded that TG2-L and TG2-S expression are up-regulated in the highly metastatic breast cancer cell line (MDA-MB-231), and are associated with CSC features and the EMT phenotype. Therefore, TG2-L and TG2-S could serve as prognostic markers for the development of a specific molecule inhibitor or gene siRNA transfection. The GTP-binding domain (GTPase activity) of TG2 plays an important role in promoting its carcinogenic effects. The catalytic-binding domain (transamidase activity) reduces the oncogenic effect of TG2, reduces stemness traits, and EMT phenotype.

This thesis showed the differential expression of TG2-L and TG2-S in different breast cancer cell lines. Understanding the link between distinctive isoforms' expression provides the explanation for treatment response and builds the foundation for future research. It also demonstrates the necessity of developing a new TG2 inhibitor that targets specifically GTPase activity.

7.3 Future works

- In physiological conditions, low calcium and high GTP levels lock TG2 in its closed conformation and activate GTPase and kinase activities. In pathological conditions, a disruption in calcium homeostasis and a depletion of GTP stores could activate TG2's open conformation and stimulate transamidation and PDI activities (Hitomi, Kojima and Fesus, 2016; Min and Chung, 2018). Therefore, measuring the Ca^{2+} and GTP levels could determine the TG2 conformation and proposed activated function.

- TG2 is mainly expressed in the cytoplasm, but it is also expressed in the mitochondria, nucleus, and ECM. Therefore, it is essential to determine the TG2 localisation and its effect on TG2 conformation
- Developing transamidase-mutant (Cys277) and GTPase-mutant (Arg580) forms of TG2 could provide further characterisation of the role of the two isoforms in cancer progression

- Transfect the cells with the TG2 mutated forms, then isolate the $CD44^{+}/CD24^{-/low}$ cells by fluorescence-activated cell sorting and re-seed them for further experimentation. This will provide more explanation for the TG2 isoforms' contribution in $CD44^{+}/CD24^{-/low}$ phenotype.

Chapter 8

References

8. Chapter 8: References

Achyuthan, K. E. and Greenberg, C. S. (1987) 'Identification of a guanosine triphosphate-binding site on guinea pig liver transglutaminase. Role of GTP and calcium ions in modulating activity.', *Journal of Biological Chemistry*, 262(4), pp. 1901–1906.

Afornali, A. *et al.* (2013) 'Tripla nanoemulsão potencializa os efeitos do tratamento tópico com retinol microencapsulado e modula processos biológicos relacionados ao envelhecimento da pele', *Anais Brasileiros de Dermatologia*, 88(6), pp. 930–936.

Agnihotri, N., Kumar, S. and Mehta, K. (2012) 'Tissue transglutaminase as a central mediator in inflammation-induced progression of breast cancer', *Breast Cancer Research*, 15(1), pp. 1–9.

Agnihotri, N., Kumar, S. and Mehta, K. (2013) 'Tissue transglutaminase as a central mediator in infl ammation-induced progression of breast cancer', *Breast Cancer Research,* 15(1), p. 202.

Agnihotri, N. and Mehta, K. (2017) 'Transglutaminase-2: evolution from pedestrian protein to a promising therapeutic target', *Amino Acids*, 49(3), pp. 425–439.

Ai, L. *et al.* (2008) 'The transglutaminase 2 gene (TGM2), a potential molecular marker for chemotherapeutic drug sensitivity, is epigenetically silenced in breast cancer', *Carcinogenesis*, 29(3), pp. 510–518.

Akbar, A. *et al.* (2017) 'Structure-Activity Relationships of Potent, Targeted Covalent Inhibitors That Abolish Both the Transamidation and GTP Binding Activities of Human Tissue Transglutaminase', *Journal of Medicinal Chemistry*, 60(18), pp. 7910–7927.

Al-Hajj, M. *et al.* (2003) 'Prospective identification of tumorigenic breast cancer cells', *Proceedings of the National Academy of Sciences*, 100(7), pp. 3983–3988.

Alexander, I. E. *et al.* (1992) 'Expression and Regulation of Retinoic Acid Receptors in Human Breast Cancer Cells', *Cancer Research*, 52(8), pp. 2236–2242.

Antonyak, M. A. *et al.* (2004) 'Augmentation of Tissue Transglutaminase Expression and Activation by Epidermal Growth Factor Inhibit Doxorubicin- induced Apoptosis in Human Breast Cancer Cells *', *Journal of Biological Chemistry*, 279(40), pp. 41461–41467.

Antonyak, M. A. *et al.* (2006) 'Two isoforms of tissue transglutaminase mediate opposing

cellular fates', *Proceedings of the National Academy of Sciences*, 103(49), pp. 18609–18614.

Ayinde, O., Wang, Z. and Griffin, M. (2017) 'Tissue transglutaminase induces Epithelial-Mesenchymal-Transition and the acquisition of stem cell like characteristics in colorectal cancer cells', *Oncotarget*, 8(12), pp. 20025–20041.

Badarau, E., Collighan, R. J. and Griffin, M. (2013) 'Recent advances in the development of tissue transglutaminase (TG2) inhibitors', *Amino Acids*, 44(1), pp. 119–127.

Bagatur, Y. *et al.* (2018) 'Tissue transglutaminase expression is necessary for adhesion, metastatic potential and cancer stemness of renal cell carcinoma', *Cell Adhesion and Migration*. Taylor & Francis, 12(2), pp. 138–151.

Bailey, P. C. *et al.* (2018) 'Single-Cell Tracking of Breast Cancer Cells Enables Prediction of Sphere Formation from Early Cell Divisions', *iScience*. Elsevier Inc., 8, pp. 29–39.

Balklava, Z. *et al.* (2002) 'Analysis of tissue transglutaminase function in the migration of Swiss 3T3 fibroblasts', *Journal of Biological Chemistry*, 277(19), pp. 16567–16575.

Bastien, J. and Rochette-Egly, C. (2004) 'Nuclear retinoid receptors and the transcription of retinoid-target genes', *Gene*, 328, pp. 1–16.

Beatson, G. T. (1896) 'on the Treatment of Inoperable Cases of Carcinoma of the Mamma: Suggestions for a New Method of Treatment, With Illustrative Cases.', *The Lancet*, 148(3803), pp. 162–165.

Begg, G. E., Carrington, L., *et al.* (2006) 'Mechanism of allosteric regulation of transglutaminase 2 by GTP', *Proceedings of the National Academy of Sciences of the United States of America*, 103(52), pp. 19683–19688.

Begg, G. E., Holman, S. R., *et al.* (2006) 'Mutation of a critical arginine in the GTP-binding site of transglutaminase 2 disinhibits intracellular cross-linking activity', *Journal of Biological Chemistry*, 281(18), pp. 12603–12609.

Berger, C. E. *et al.* (2012) 'p53, a target of estrogen receptor (ER) α, modulates DNA damage-induced growth suppression in ER-positive breast cancer cells', *Journal of Biological Chemistry*, 287(36), pp. 30117–30127.

Bernard, P. S. *et al.* (2009) 'Supervised risk predictor of breast cancer based on intrinsic subtypes', *Journal of Clinical Oncology*, 27(8), pp. 1160–1167.

Bland, K. I. *et al.* (2017) *The breast E-book: Comprehensive management of benign and malignant diseases*. Elsevier Health Sciences.

Bruzzese, F. *et al.* (2011) 'HDAC inhibitor vorinostat enhances the antitumor effect of gefitinib in squamous cell carcinoma of head and neck by modulating ErbB receptor expression and reverting EMT', *Journal of Cellular Physiology*, 226(9), pp. 2378–2390.

Budillon, A., Carbone, C. and Di Gennaro, E. (2013) 'Tissue transglutaminase: A new target to reverse cancer drug resistance', *Amino Acids*, 44(1), pp. 63–72.

Burnette, W. N. (1981) '"Western Blotting": Electrophoretic transfer of proteins from sodium dodecyl sulfate-polyacrylamide gels to unmodified nitrocellulose and radiographic detection with antibody and radioiodinated protein A', *Analytical Biochemistry*, 112(2), pp. 195–203.

Burstin, J. von *et al.* (2009) 'E-Cadherin Regulates Metastasis of Pancreatic Cancer In Vivo and Is Suppressed by a SNAIL/HDAC1/HDAC2 Repressor Complex', *Gastroenterology*, 137(1), pp. 361-371.e5.

Butler, L. M. *et al.* (2000) 'Suberoylanilide hydroxamic acid, an inhibitor of histone deacetylase, suppresses the growth of prostate cancer cells in vitro and in vivo', *Cancer Research*, 60(18), pp. 5165–5170.

Campisi, A. *et al.* (2008) 'Effect of growth factors and steroids on transglutaminase activity and expression in primary astroglial cell cultures', *Journal of Neuroscience Research*, 86(6), pp. 1297–1305.

Cao, L. *et al.* (2008) 'Tissue transglutaminase protects epithelial ovarian cancer cells from cisplatin-induced apoptosis by promoting cell survival signaling', *Carcinogenesis*, 29(10), pp. 1893–1900.

Cao, L. *et al.* (2012) 'Tissue transglutaminase links TGF-B, epithelial to mesenchymal transition and a stem cell phenotype in ovarian cancer', *Oncogene*. Nature Publishing Group, 31(20), pp. 2521–2534.

Carbone, C. *et al.* (2017) 'Tissue transglutaminase (TG2) is involved in the resistance of cancer cells to the histone deacetylase (HDAC) inhibitor vorinostat', *Amino Acids*. Springer Vienna, 49(3), pp. 517–528.

Caron, N. S. *et al.* (2012) 'Using FLIM-FRET to Measure Conformational Changes of Transglutaminase Type 2 in Live Cells', *PLoS ONE*, 7(8), p. e44159.

Catalogus, C. (1968) 'Cross-link in Fibrin Polymerized by Factor XIII - ε-(γ-Glutamyl)lysine', *Science*, 160(11), pp. 892–893.

Centritto, F. *et al.* (2015) 'Cellular and molecular determinants of all- trans retinoic acid sensitivity in breast cancer: Luminal phenotype and RAR α expression', *EMBO Molecular Medicine*, 7(7), pp. 950–972.

Chekhun, S. *et al.* (2013) 'Expression of biomarkers related to cell adhesion, metastasis and invasion of breast cancer cell lines of different molecular subtype', *Experimental Oncology*, 35(3), pp. 174–179.

Chen, J. D., Umesono, K. and Evans, R. M. (1996) 'SMRT isoforms mediate repression and anti-repression of nuclear receptor heterodimers', *Proceedings of the National Academy of Sciences of the United States of America*, 93(15), pp. 7567–7571.

Chen, K., Huang, Y. H. and Chen, J. L. (2013) 'Understanding and targeting cancer stem cells: Therapeutic implications and challenges', *Acta Pharmacologica Sinica*. Nature Publishing Group, 34(6), pp. 732–740.

Chen, S. *et al.* (2013) 'The anti-tumor effects and molecular mechanisms of suberoylanilide hydroxamic acid (SAHA) on the aggressive phenotypes of ovarian carcinoma cells', *PLoS ONE*, 8(11), pp. 1–13.

Chiba, T. *et al.* (2004) 'Identification of genes up-regulated by histone deacetylase inhibition with cDNA microarray and exploration of epigenetic alterations on hepatoma cells', *Journal of Hepatology*, 41(3), pp. 436–445.

Chlapek, P. *et al.* (2018) 'Why differentiation therapy sometimes fails: Molecular mechanisms of resistance to retinoids', *International Journal of Molecular Sciences*, 19(1), p. 132.

Choi, S. A. *et al.* (2014) 'Identification of brain tumour initiating cells using the stem cell marker aldehyde dehydrogenase', *European Journal of Cancer*. Elsevier Ltd, 50(1), pp. 137–149.

Cioce, M. *et al.* (2010) 'Mammosphere-forming cells from breast cancer cell lines as a tool

for the identification of CSC-like- and early progenitor-targeting drugs', *Cell Cycle*, 9(14), pp. 2950–2959.

Clarke, D. D. *et al.* (1959) 'The incorporation of amines into protein', *Archives of Biochemistry and Biophysics*, 79(July), pp. 338–354.

Collins, K., Jacks, T. and Pavletich, N. P. (1997) 'The cell cycle and cancer', *Proceedings of the National Academy of Sciences of the United States of America*, 94(7), pp. 2776–2778.

Connolly, R. M., Nguyen, N. K. and Sukumar, S. (2013) 'Molecular pathways: Current role and future directions of the retinoic acid pathway in cancer prevention and treatment', *Clinical Cancer Research*, 19(7), pp. 1651–1959.

Conserva, M. R. *et al.* (2019) 'The pleiotropic role of retinoic acid/retinoic acid receptors signaling: From vitamin A metabolism to gene rearrangements in acute promyelocytic Leukemia', *International Journal of Molecular Sciences*, 20(12), p. 2921.

Costa, A. *et al.* (1994) 'Prospects of chemoprevention of human cancers with the synthetic retinoid fenretinide', *Cancer Research*, 54(7), pp. 2032s-2037s.

Croker, A. K. *et al.* (2009) 'High aldehyde dehydrogenase and expression of cancer stem cell markers selects for breast cancer cells with enhanced malignant and metastatic ability', *Journal of Cellular and Molecular Medicine*, 13(8 B), pp. 2236–2252.

Cui, J. *et al.* (2016) 'All-trans retinoic acid inhibits proliferation, migration, invasion and induces differentiation of hepa1-6 cells through reversing EMT in vitro', *International Journal of Oncology*, 48(1), pp. 349–357.

Davies, P. J. A. *et al.* (1985) 'Retinoic acid-induced expression of tissue transglutaminase in human promyelocytic leukemia (HL-60) cells', *Journal of Biological Chemistry*, 260(8), pp. 5166–5174.

Doi, A. *et al.* (2015) 'Enhanced expression of retinoic acid receptor alpha (RARA) induces epithelial-to-mesenchymal transition and disruption of mammary acinar structures', *Molecular Oncology*, 9(2), pp. 355–364.

Dunn, B. K. and Ford, L. G. (2001) 'From adjuvant therapy to breast cancer prevention: BCPT and STAR', *Breast Journal*, 7(3), pp. 144–157.

Duvic, M. *et al.* (2001) 'Bexarotene is effective and safe for treatment of refractory

advanced-stage cutaneous t-cell lymphoma: Multinational phase II-III trial results', *Journal of Clinical Oncology*, 19(9), pp. 2456–2471.

Eckert, R. L. *et al.* (2014) 'Tran gl amina e Reg la ion of Cell F nc ion', *Physiological Reviews*, 94(2), pp. 383–417.

El-Deiry, W. S. *et al.* (1993) 'WAF1, a potential mediator of p53 tumor suppression', *Cell*, 75(4), pp. 817–825.

Elizondo, G. *et al.* (2000) 'Feedback inhibition of the retinaldehyde dehydrogenase gene ALDH1 by retinoic acid through retinoic acid receptor α and CCAAT/enhancer-binding protein β', *Journal of Biological Chemistry*, 275(50), pp. 39747–39753.

Eramo, A. *et al.* (2008) 'Identification and expansion of the tumorigenic lung cancer stem cell population', *Cell Death and Differentiation*, 15(3), pp. 504–514.

Fan, F. *et al.* (2012) 'Overexpression of Snail induces epithelial-mesenchymal transition and a cancer stem cell-like phenotype in human colorectal cancer cells', *Cancer Medicine*, 1(1), pp. 5–16.

Fearon, E. R. and Dang, C. V. (1999) 'Cancer genetics: Tumor suppressor meets oncogene', *Current Biology*, 9(2), pp. 62–65.

Fenaux, P. *et al.* (1992) 'All-transretinoic acid followed by intensive chemotherapy gives a high complete remission rate and may prolong remissions in newly diagnosed acute promyelocytic leukemia: a pilot study on 26 cases', *Blood*, 80(9), pp. 2176–2181.

Fesus, L. and Piacentini, M. (2002a) 'Transglutaminase 2 : an enigmatic', *TRENDS in Biochemical Sciences*, 27(10), pp. 534–539.

Fesus, L. and Piacentini, M. (2002b) 'Transglutaminase 2: an enigmatic enzyme with diverse functions', *Trends in Biochemical Sciences*, 27(10), pp. 534–539.

Fisher, M. L. *et al.* (2015) 'Type II transglutaminase stimulates epidermal cancer stem cell epithelial-mesenchymal transition', *Oncotarget*, 6(24), pp. 20525–20539.

Fraij, B. M. *et al.* (1992) 'A retinoic acid-inducible mRNA from human erythroleukemia cells encodes a novel tissue transglutaminase homologue', *Journal of Biological Chemistry*, 267(31), pp. 22616–22623.

Fraij, B. M. and Gonzales, R. A. (1996) 'A third human tissue transglutaminase homologue as

a result of alternative gene transcripts', *Biochimica et Biophysica Acta - Gene Structure and Expression*, 1306(1), pp. 63–74.

Fraij, B. M. and Gonzales, R. a (1997) 'Organization and structure of the human tissue transglutaminase gene.', *Biochimica et biophysica acta*, 1354(1), pp. 65–71.

Freemantle, S. J., Spinella, M. J. and Dmitrovsky, E. (2003) 'Retinoids in cancer therapy and chemoprevention: Promise meets resistance', *Oncogene*, 22(47), pp. 7305–7315.

Gentile, V. *et al.* (1991) 'Isolation and characterization of cDNA clones to mouse macrophage and human endothelial cell tissue transglutaminases', *Journal of Biological Chemistry*, 266(1), pp. 478–483.

Georgopoulou, N. and McLaughlin, M. (2001) 'The role of post-translational modification in beta-amyloid precursor protein processing', *Biochemical Society Symposia*, 67(January), pp. 23–36.

Giatromanolaki, A. *et al.* (2011) 'The CD44+/CD24- phenotype relates to "triple-negative" state and unfavorable prognosis in breast cancer patients', *Medical Oncology*, 28(3), pp. 745–752.

Ginestier, C. *et al.* (2007) 'ALDH1 Is a Marker of Normal and Malignant Human Mammary Stem Cells and a Predictor of Poor Clinical Outcome', *Cell Stem Cell*, 1(5), pp. 555–567.

Ginestier, C. *et al.* (2009) 'Retinoid signaling regulates breast cancer stem cell differentiation', *Cell cycle*, 8(20), pp. 3297–3302.

Grabarska, A. *et al.* (2017) 'Histone deacetylase inhibitor SAHA as potential targeted therapy agent for larynx cancer cells', *Journal of Cancer*, 8(1), pp. 19–28.

Grenard, P., Bates, M. K. and Aeschlimann, D. (2001) 'Evolution of transglutaminase genes: Identification of a transglutaminase gene cluster on human chromosome 15q15: Structure of the gene encoding transglutaminase X and a novel gene family member, transglutaminase Z', *Journal of Biological Chemistry*, 276(35), pp. 33066–33078.

Griffn, M., Casadio, R. and Bergamini, C. M. (2002) 'Transglutaminases: Nature's biological glues', *Biochemical Journal*, 368(2), pp. 377–396.

Grosso, H. and Mouradian, M. M. (2012) 'Transglutaminase 2: Biology, relevance to neurodegenerative diseases and therapeutic implications', *Pharmacology and Therapeutics*.

Elsevier Inc., 133(3), pp. 392–410.

Gundemir, S. *et al.* (2012) 'Transglutaminase 2: A molecular Swiss army knife', *Biochimica et Biophysica Acta - Molecular Cell Research*. Elsevier B.V., 1823(2), pp. 406–419.

Guzman, M. L. and Jordan, C. T. (2004) 'Considerations for Targeting Malignant Stem Cells in Leukemia', *Cancer Control*, 11(2), pp. 97–104.

Ha, H. J. *et al.* (2018) 'Structure of natural variant transglutaminase 2 reveals molecular basis of gaining stability and higher activity', *PLoS ONE*, 13(10), p. e0204707.

Hanahan, D. (2022) 'Hallmarks of Cancer: New Dimensions', *Cancer Discovery*, 12(1), pp. 31–46.

Hanahan, D. and Weinberg, R. A. (2000) 'The hallmarks of cancer', *Cell*, 100(1), pp. 57–70.

Hanahan, D. and Weinberg, R. A. (2011) 'Hallmarks of cancer: The next generation', *Cell*. Elsevier Inc., 144(5), pp. 646–674.

Hasegawa, G. *et al.* (2003) 'A novel function of tissue-type transglutaminase: Protein disulphide isomerase', *Biochemical Journal*, 373(3), pp. 793–803.

He, W., Sun, Z. and Liu, Z. (2015) 'Silencing of TGM2 reverses epithelial to mesenchymal transition and modulates the chemosensitivity of breast cancer to docetaxel', *Experimental and Therapeutic Medicine*, 10(4), pp. 1413–1418.

Herschkowitz, J. I. *et al.* (2007) 'Identification of conserved gene expression features between murine mammary carcinoma models and human breast tumors', *Genome Biology*, 8(5), pp. 1–17.

Hitomi, K., Kojima, S. and Fesus, L. (2016) *Transglutaminases: Multiple Functional Modifiers and Targets for New Drug Discovery*. Japan: Springer.

Hiyama, E. and Hiyama, K. (2007) 'Telomere and telomerase in stem cells', *British Journal of Cancer*, 96(7), pp. 1020–1024.

Hobbs, G. A., Der, C. J. and Rossman, K. L. (2016) 'RAS isoforms and mutations in cancer at a glance', *Journal of Cell Science*, 129(7), pp. 1287–1292.

Hsieh, Y. F. *et al.* (2013) 'Transglutaminase 2 contributes to apoptosis induction in jurkat t cells by modulating Ca2+ homeostasis via cross-linking RAP1GDS1', *PLoS ONE*, 8(12), pp. 1–14.

Huang, B. *et al.* (2014) 'Differential expression of estrogen receptor α, β1, and β2 in lobular and ductal breast cancer', *Proceedings of the National Academy of Sciences of the United States of America*, 111(5), pp. 1933–1938.

Huang, L., Xu, A. M. and Liu, W. (2015) 'Transglutaminase 2 in cancer', *American Journal of Cancer Research*, 5(9), pp. 2756–2776.

Huaying, S. *et al.* (2016) 'Transglutaminase 2 Inhibitor KCC009 Induces p53-Independent Radiosensitization in Lung Adenocarcinoma Cells', *Medical Science Monitor: international medical journal of experimental and clinical research*, 22, p. 5041.

Hulin-Curtis, S. L. *et al.* (2018) 'Histone deacetylase inhibitor trichostatin A sensitises cisplatinresistant ovarian cancer cells to oncolytic adenovirus', *Oncotarget*, 9(41), pp. 26328–26341.

Hwang, J. Y. *et al.* (2008) 'Clinical and Biological Significance of Tissue Transglutaminase in Ovarian Carcinoma', *The Journal Of Cancer Research*, 68(14), pp. 5849–5859.

Hyland, K. M. (2008) 'Tumor Suppressor Genes and Oncogenes : Genes that Prevent and Cause Cancer', pp. 292–306.

Iglesias, J. M. *et al.* (2013) 'Mammosphere Formation in Breast Carcinoma Cell Lines Depends upon Expression of E-cadherin', *PLoS ONE*, 8(10), pp. 1–12.

Ivshina, A. V. *et al.* (2006) 'Genetic reclassification of histologic grade delineates new clinical subtypes of breast cancer', *Cancer Research*, 66(21), pp. 10292–10301.

Jang, G. Y. *et al.* (2010) 'Transglutaminase 2 suppresses apoptosis by modulating caspase 3 and NF-κB activity in hypoxic tumor cells', *Oncogene*. Nature Publishing Group, 29(3), pp. 356–367.

Jang, T. H. *et al.* (2014) 'Crystal structure of transglutaminase 2 with GTP complex and amino acid sequence evidence of evolution of GTP binding site', *PLOS ONE*, 9(9), pp. 1–8.

Jeong, E. M. *et al.* (2009) 'Degradation of transglutaminase 2 by calcium-mediated ubiquitination responding to high oxidative stress', *FEBS Letters*, 583(4), pp. 648–654.

Johnson, K. *et al.* (2001) 'Interleukin-1 induces pro-mineralizing activity of cartilage tissue transglutaminase and factor XIIIa', *American Journal of Pathology*, 159(1), pp. 149–163.

Jolly, M. K. *et al.* (2017) 'Inflammatory breast cancer: A model for investigating cluster-based

dissemination', *NPJ Breast Cancer*, 3(1), pp. 1–8.

Jordan, V. C. (2004) 'Selective estrogen receptor modulation: Concept and consequences in cancer', *Cancer Cell*, 5(3), pp. 207–213.

Kalluri, R. (2009) 'EMT: When epithelial cells decide to become mesenchymal-like cells', *Journal of Clinical Investigation*, 119(6), pp. 1417–1419.

Kanchan, K., Fuxreiter, M. and Fésüs, L. (2015) 'Physiological, pathological, and structural implications of non-enzymatic protein-protein interactions of the multifunctional human transglutaminase 2', *Cellular and Molecular Life Sciences*, 72(16), pp. 3009–3035.

Kang, S. *et al.* (2018) 'Transglutaminase 2 regulates self-renewal and stem cell marker of human colorectal cancer stem cells', *Anticancer Research*, 38(2), pp. 787–794.

Karpuj, M. V. *et al.* (2002) 'Prolonged survival and decreased abnormal movements in transgenic model of Huntington disease, with administration of the transglutaminase inhibitor cystamine', *Nature Medicine*, 8(2), pp. 143–149.

Katt, W. P., Antonyak, M. A. and Cerione, R. A. (2015) 'Simultaneously targeting tissue transglutaminase and kidney type glutaminase sensitizes cancer cells to acid toxicity and offers new opportunities for therapeutic intervention', *Molecular Pharmaceutics*, 12(1), pp. 46–55. doi: 10.1021/mp500405h.

Kedrin, D. *et al.* (2007) 'Cell motility and cytoskeletal regulation in invasion and metastasis', *Journal of Mammary Gland Biology and Neoplasia*, 12(2–3), pp. 143–152.

Keillor, J. W., Apperley, K. Y. P. and Akbar, A. (2015) 'Inhibitors of tissue transglutaminase', *Trends in Pharmacological Sciences*, 36(1), pp. 32–40.

Kelly, W. K. *et al.* (2005) 'Phase I study of an oral histone deacetylase inhibitor, suberoylanilide hydroxamic acid, in patients with advanced cancer', *Journal of Clinical Oncology*, 23(17), pp. 3923–3931.

Kerr, C. *et al.* (2017) 'Transamidase site-targeted agents alter the conformation of the transglutaminase cancer stem cell survival protein to reduce GTP binding activity and cancer stem cell survival', *Oncogene*, 36(21), pp. 2981–2990.

Kim, S. and An, S. S. A. (2016) 'Role of p53 isoforms and aggregations in cancer', *Medicine*, 95(26), p. e3993.

Klein, E. S. *et al.* (1996) 'Identification and functional separation of retinoic acid receptor neutral antagonists and inverse agonists', *Journal of Biological Chemistry*, 271(37), pp. 22692–22696.

Kong, D. *et al.* (2012) 'Histone Deacetylase Inhibitors Induce Epithelial-to-Mesenchymal Transition in Prostate Cancer Cells', *PLoS ONE*, 7(9), pp. 1–12.

Kumar, A. *et al.* (2010) 'Tissue transglutaminase promotes drug resistance and invasion by inducing mesenchymal transition in mammary epithelial cells', *PLoS ONE*, 5(10), p. e13390.

Kumar, A. *et al.* (2011) 'Evidence that aberrant expression of tissue transglutaminase promotes stem cell characteristics in mammary epithelial cells', *PLoS ONE*, 6(6), p. e20701.

Kumar, A. *et al.* (2012) 'Evidence that GTP-binding domain but not catalytic domain of transglutaminase 2 is essential for epithelial-to-mesenchymal transition in mammary epithelial cells', *Breast Cancer Research*. BioMed Central Ltd, 14(1), pp. 1–15.

Kumar, S. *et al.* (2014) 'Transglutaminase 2 reprogramming of glucose metabolism in mammary epithelial cells via activation of inflammatory signaling pathways', *International Journal of Cancer*, 134(12), pp. 2798–2807.

Kumar, S. and Mehta, K. (2012) 'Tissue Transglutaminase Constitutively Activates HIF-1α Promoter and Nuclear Factor-κB via a Non-Canonical Pathway', *PLoS ONE*, 7(11), p. e49321.

Kuncio, G. S. *et al.* (1998) 'TNF-alpha modulates expression of the tissue transglutaminase gene in liver cells.', *The American journal of physiology*, 274(2), pp. G240–G245.

Lai, T. *et al.* (2007) 'Identification of two GTP-independent alternatively spliced forms of tissue transglutaminase in human leukocytes, vascular smooth muscle, and endothelial cells', *The FASEB Journal*, 21(14), pp. 4131–4143.

Lai, T. and Greenberg, C. S. (2013) 'TGM2 and implications for human disease: role of alternative splicing', *Front. Biosci*, 18(2), pp. 504–519.

Lane, D. P. (1993) 'Viral Oncogene Binds Host p53 Protein', *Nature*, 278(24), pp. 261–263.

Lapidot, T. *et al.* (1994) 'A cell initiating human acute myeloid leukaemia after transplantation into SCID mice', *Nature*, 367(6464), pp. 645–648.

Lazennec, G. *et al.* (2001) 'ERβ inhibits proliferation and invasion of breast cancer cells', *Endocrinology*, 142(9), pp. 4120–4130.

Lebedeva, M. A., Eaton, J. S. and Shadel, G. S. (2009) 'Loss of p53 causes mitochondrial DNA depletion and altered mitochondrial reactive oxygen species homeostasis', *Biochimica et Biophysica Acta - Bioenergetics*. Elsevier B.V., 1787(5), pp. 328–334.

Lehmann, B. . *et al.* (2011) 'Identification of human triple-negative breast cancer subtypes and preclinical models for selection of targeted therapies', *The Journal of clinical investigation*, 121(7), pp. 2750–2767.

Leygue, E. *et al.* (2000) 'Altered expression of estrogen receptor-α variant messenger RNAs between adjacent normal breast and breast tumor tissues', *Breast Cancer Research*, 2(1), pp. 64–72.

Li, Q. *et al.* (2015) 'Efficacy and safety of bevacizumab combined with chemotherapy for managing metastatic breast cancer: A meta-analysis of randomized controlled trials', *Scientific Reports*, 5(September), pp. 1–11.

Li, W. *et al.* (2017) 'Unraveling the roles of CD44/ CD24 and ALDH1 as cancer stem cell markers in tumorigenesis and metastasis', *Scientific reports*, 7(1), pp. 1–15.

Liang, C. C., Park, A. Y. and Guan, J. L. (2007) 'In vitro scratch assay: A convenient and inexpensive method for analysis of cell migration in vitro', *Nature Protocols*, 2(2), pp. 329–333.

Lim, J. and Thiery, J. P. (2012) 'Epithelial-mesenchymal transitions: Insights from development', *Development (Cambridge)*, 139(19), pp. 3471–3486.

Lim, L. Y. *et al.* (2009) 'Mutant p53 mediates survival of breast cancer cells', *British Journal of Cancer*, 101(9), pp. 1606–1612.

Lim, S. and Kaldis, P. (2013) 'Cdks, cyclins and CKIs: roles beyond cell cycle regulation', *Development*, 140(15), pp. 3079–3093.

Ling, D. *et al.* (2012) 'Enhancing the anticancer effect of the histone deacetylase inhibitor by activating transglutaminase', *European Journal of Cancer*, 48(17), pp. 3278–3287.

Liou, M.-Y. and Storz, P. (2010) 'Reactive oxygen species in cancer', *Free radical research*, 44(5), pp. 479–496.

Liu, S., Cerione, R. a and Clardy, J. (2002) 'Structural basis for the guanine nucleotide-binding activity of tissue transglutaminase and its regulation of transamidation activity.',

Proceedings of the National Academy of Sciences, 99(5), pp. 2743–2747.

Liu, T. *et al.* (2007) 'Activation of tissue transglutaminase transcription by histone deacetylase inhibition as a therapeutic approach for Myc oncogenesis.', *Proceedings of the National Academy of Sciences*, 104(47), pp. 18682–18687.

Loh, C. Y. *et al.* (2019) 'The e-cadherin and n-cadherin switch in epithelial-to-mesenchymal transition: Signaling, therapeutic implications, and challenges', *Cells*, 8(10), pp. 1–33.

Lombardo, Y. *et al.* (2015) 'Mammosphere Formation Assay from Human Breast Cancer Tissues and Cell Lines', *Journal of Visualized Experiments*, 97, p. e52671.

Lotan, R., Lotan, D. and Sacks, P. G. (1990) 'Inhibition of tumor cell growth by retinoids', *Methods in enzymology*, 190, pp. 100–110.

Lowe, S. W. *et al.* (1993) 'P53 is required for radiation-induced apoptosis in mouse thymocytes', *Nature*, 362(6423), pp. 847–849.

Lu, M. *et al.* (2005) 'Expression of estrogen receptor α, retinoic acid receptor α and cellular retinoic acid binding protein II genes is coordinately regulated in human breast cancer cells', *Oncogene*, 24(27), pp. 4362–4369.

Lumachi, F. (2015) 'Current medical treatment of estrogen receptor-positive breast cancer', *World Journal of Biological Chemistry*, 6(3), p. 231.

M Robertson, F. and Chu, K. (2012) 'Genomic Profiling of Pre-Clinical Models of Inflammatory Breast Cancer Identifies a Signature of Epithelial Plasticity and Suppression of TGFβ Signaling', *J Clin Exp Pathol*, 2(5), pp. 2161–0681.

Malkomes, P. *et al.* (2021) 'Transglutaminase 2 promotes tumorigenicity of colon cancer cells by inactivation of the tumor suppressor p53', *Oncogene*, 40(25), pp. 4352–4367.

Mangala, L. S. *et al.* (2007) 'Tissue transglutaminase expression promotes cell attachment , invasion and survival in breast cancer cells', *Oncogene*, 26(17), pp. 2459–2470.

Mani, S. A. *et al.* (2008) 'The Epithelial-Mesenchymal Transition Generates Cells with Properties of Stem Cells', *Cell*, 133(4), pp. 704–715.

Mann, A. P. *et al.* (2006) 'Overexpression of tissue transglutaminase leads to constitutive activation of nuclear factor-κB in cancer cells: Delineation of a novel pathway', *Cancer Research*, 66(17), pp. 8788–8795.

Marcato, P. *et al.* (2011) 'Aldehyde dehydrogenase its role as a cancer stem cell marker comes down to the specific isoform', *Cell Cycle*, 10(9), pp. 1378–1384.

Marchitti, S. A. *et al.* (2008) 'Non-P450 aldehyde oxidizing enzymes: The aldehyde dehydrogenase superfamily', *Expert Opinion on Drug Metabolism and Toxicology*, 4(6), pp. 697–720.

Marks, P. A. and Breslow, R. (2007) 'Dimethyl sulfoxide to vorinostat: Development of this histone deacetylase inhibitor as an anticancer drug', *Nature Biotechnology*, 25(1), pp. 84–90.

Marlétaz, F. *et al.* (2006) 'Retinoic acid signaling and the evolution of chordates', *International Journal of Biological Sciences*, 2(2), pp. 38–47.

Di Masi, A. *et al.* (2015) 'Retinoic acid receptors: From molecular mechanisms to cancer therapy', *Molecular Aspects of Medicine*, 41, pp. 1–115.

McConoughey, S. J. *et al.* (2010) 'Inhibition of transglutaminase 2 mitigates transcriptional dysregulation in models of Huntington's disease', *EMBO Molecular Medicine*, 2(9), pp. 349–370.

Mehta, K. (1994) 'High levels of transglutaminase expression in doxorubicin-resistant human breast carcinoma cells', *International Journal of Cancer*, 58(3), pp. 400–406.

Mehta, K. *et al.* (2004) 'Prognostic Significance of Tissue Transglutaminase in Drug Resistant and Metastatic Breast Cancer', *Clinical cancer research*, 10(23), pp. 8068–8076.

Mehta, K. and Eckert, R. L. (2005) *Transglutaminases: family of enzymes with diverse functions*. Karger Medical and Scientific Publishers.

Mehta, K., Fok, J. Y. and Mangala, L. S. (2006) 'Tissue transglutaminase: from biological glue to cell survival cues.', *Frontiers in bioscience*, 11(3), pp. 173–185.

Mehta, K., Kumar, A. and Kim, H. I. (2010) 'Transglutaminase 2: A multi-tasking protein in the complex circuitry of inflammation and cancer', *Biochemical Pharmacology*, 80(12), pp. 1921–1929.

Mehta, K. and Lopez-Berestein, G. (1986) 'Expression of Tissue Transglutaminase in Cultured Monocytic Leukemia (THP-1) Cells during Differentiation', *Cancer Research*, 46(3), pp. 1388–1394.

Mezquita, B. and Mezquita, C. (2019) 'Two opposing faces of retinoic acid: Induction of stemness or induction of differentiation depending on cell-type', *Biomolecules*, 9(10), p. 567.

Miller, L. D. *et al.* (2005) 'An expression signature for p53 status in human breast cancer predicts mutation status, transcriptional effects, and patient survival', *Proceedings of the National Academy of Sciences of the United States of America*, 102(38), pp. 13550–13555.

Min, A. *et al.* (2015) 'Histone deacetylase inhibitor, suberoylanilide hydroxamic acid (SAHA), enhances anti-tumor effects of the poly (ADP-ribose) polymerase (PARP) inhibitor olaparib in triple-negative breast cancer cells', *Breast Cancer Research*, 17(1), pp. 1–13.

Min, B. and Chung, K. C. (2018) 'New insight into transglutaminase 2 and link to neurodegenerative diseases', *BMB reports*, 51(1), pp. 5–13.

Mishra, S. *et al.* (2006) 'Phosphorylation of histones by tissue transglutaminase', *Journal of Biological Chemistry*, 281(9), pp. 5532–5538.

Mishra, S., Melino, G. and Murphy, L. J. (2007) 'Transglutaminase 2 kinase activity facilitates protein kinase A-induced phosphorylation of retinoblastoma protein', *Journal of Biological Chemistry*, 282(25), pp. 18108–18115.

Mishra, S. and Murphy, L. J. (2004) 'Tissue transglutaminase has intrinsic kinase activity', *Journal of Biological Chemistry*, 279(23), pp. 23863–23868.

Mishra, S. and Murphy, L. J. (2006) 'The p53 oncoprotein is a substrate for tissue transglutaminase kinase activity', *Biochemical and Biophysical Research Communications*, 339(2), pp. 726–730.

Mittal, N. *et al.* (2014) 'Fenretinide: A novel treatment for endometrial cancer', *PLoS ONE*, 9(10), p. e110410.

Molberg, Ø. *et al.* (2001) 'T cells from celiac disease lesions recognize gliadin epitopes deamidated in situ by endogenous tissue transglutaminase', *European Journal of Immunology*, 31(5), pp. 1317–1323.

Monsonego, A. *et al.* (1997) 'Expression of GTP-dependent and GTP-independent tissue-type transglutaminase in cytokine-treated rat brain astrocytes', *Journal of Biological Chemistry*, 272(6), pp. 3724–3732.

MS, T. *et al.* (1997) 'ALL- TRANS -RETINOIC ACID IN ACUTE PROMYELOCYTIC LEUKEMIA', *New England Journal of Medicine*, 337(15), pp. 1021–1028.

Nagy, L. *et al.* (1996) 'Identification and characterization of a versatile retinoid response element (retinoic acid receptor response element-retinoid X receptor response element) in the mouse tissue transglutaminase gene promoter', *Journal of Biological Chemistry*, 271(8), pp. 4355–4365.

Nakaoka, H. *et al.* (1994) 'Gh: A GTP-Binding protein with transglutaminase activity and receptor signaling function', *Science*, 264(5165), pp. 1593–1596.

Nathan, C. and Cunningham-bussel, A. (2013) 'Beyond oxidative stress : an immunologist ' s guide to reactive oxygen species', *Nature Publishing Group*, 13(5), pp. 349–361.

Nogueira, V. and Hay, N. (2013) 'Molecular pathways: Reactive oxygen species homeostasis in cancer cells and implications for cancer therapy', *Clinical Cancer Research*, 19(16), pp. 4309–4314.

Nunes, I. *et al.* (1997) 'Latent transforming growth factor-β binding protein domains involved in activation and transglutaminase-dependent cross-linking of latent transforming growth factor-β', *Journal of Cell Biology*, 136(5), pp. 1151–1163.

Nurminskaya, M. V. and Belkin, A. M. (2012) *Cellular Functions of Tissue Transglutaminase*, *International Review of Cell and Molecular Biology*.

O'Brien, C. A. *et al.* (2007) 'A human colon cancer cell capable of initiating tumour growth in immunodeficient mice', *Nature*, 445(7123), pp. 106–110.

Odii, B. O. and Coussons, P. (2014) 'Biological functionalities of transglutaminase 2 and the possibility of its compensation by other members of the transglutaminase family', *The Scientific World Journal*, 2014, pp. 1–13.

Oh, K. *et al.* (2016) 'IL-1β induces IL-6 production and increases invasiveness and estrogen-independent growth in a TG2-dependent manner in human breast cancer cells', *BMC Cancer*, 16(1), pp. 1–11.

Olsen, E. A. *et al.* (2007) 'Phase IIB multicenter trial of vorinostat in patients with persistent, progressive, or treatment refractory cutaneous t-cell lymphoma', *Journal of Clinical Oncology*, 25(21), pp. 3109–3115.

Olsson, E. *et al.* (2011) 'CD44 isoforms are heterogeneously expressed in breast cancer and correlate with tumor subtypes and cancer stem cell markers', *BMC Cancer*, 11(1), pp. 1–13.

Onyekachi, O., Ebidor, U. and Maxwell, O. (2015) 'The Role of Transglutaminase 2 (TG2) in Definition of Cancer Hallmarks', *British Journal of Medicine and Medical Research*, 6(3), pp. 297–311.

Orfanos, C. E. *et al.* (1997) 'Current use and future potential role of retinoids in dermatology', *Drugs*, 53(3), pp. 358–388.

Ou, H. *et al.* (2000) 'Retinoic acid-induced tissue transglutaminase and apoptosis in vascular smooth muscle cells', *Circulation Research*, 87(10), pp. 881–887.

Ozeki, M. and Shively, J. E. (2008) 'Differential cell fates induced by all-trans retinoic acid-treated HL-60 human leukemia cells', *Journal of Leukocyte Biology*, 84(3), pp. 769–779.

Park, K.-S. *et al.* (2009) 'Increase in transglutaminase 2 expression is associated with NF-κB activation in breast cancer tissues', *Front Biosci*, 14(1), pp. 1945–1951.

Perou, C. M. *et al.* (2000) 'Molecular portraits of human breast tumours', *Nature*, 406(6797), pp. 747–752.

Phaniendra, A., Jestadi, D. B. and Periyasamy, L. (2015) 'Free Radicals: Properties, Sources, Targets, and Their Implication in Various Diseases', *Indian Journal of Clinical Biochemistry*, 30(1), pp. 11–26.

Piacentini, M. *et al.* (1991) 'The expression of "tissue" transglutaminase in two human cancer cell lines is related with the programmed cell death (apoptosis)', *European Journal of Cell Biology*, 54(2), pp. 246–254.

Pietsch, M. *et al.* (2013) 'Tissue transglutaminase: An emerging target for therapy and imaging', *Bioorganic & Medicinal Chemistry Letters*, 23(24), pp. 6528–6543.

Prince, M. E. *et al.* (2007) 'Identification of a subpopulation of cells with cancer stem cell properties in head and neck squamous cell carcinoma', *Pnas*, 104(3), pp. 973–978.

Puduvalli, V. K. *et al.* (1999) 'Fenretinide activates caspases and induces apoptosis in gliomas', *Clinical Cancer Research*, 5(8), pp. 2230–2235.

Quan, G. *et al.* (2005) 'TGF-β1 up-regulates transglutaminase two and fibronectin in dermal fibroblasts: A possible mechanism for the stabilization of tissue inflammation', *Archives of*

Dermatological Research, 297(2), pp. 84–90.

Ray, S. *et al.* (2020) 'A Review on Cell Cycle Checkpoints in Relation to Cancer', *The Journal of Medical Sciences*, 5(4), pp. 88–95.

Recchia, F. *et al.* (2009) 'Beta-interferon, retinoids and tamoxifen in metastatic breast cancer: Long-term follow-up of a phase II study', *Oncology reports*, 21(4), pp. 1011–1016.

Reinert, T. and Barrios, C. H. (2015) 'Optimal management of hormone receptor positive metastatic breast cancer in 2016', *Therapeutic Advances in Medical Oncology*, 7(6), pp. 304–320.

Reynolds, B. A. and Weiss, S. (1992) 'Generation of neurons and astrocytes from isolated cells of the adult mammalian central nervous system', *Science*, 255(5052), pp. 1707–1710.

Rishi, A. K. *et al.* (1996) 'Regulation of the Human Retinoic Acid Receptor x Gene in the Estrogen Receptor', *Cancer research*, 56(22), pp. 5246–5252.

Ritter, S. J. and Davies, P. J. A. (1998) 'Identification of a transforming growth factor-β1/bone morphogenetic protein 4 (TGF-β1/BMP4) response element within the mouse tissue transglutaminase gene promoter', *Journal of Biological Chemistry*, 273(21), pp. 12798–12806.

Rivlin, N. *et al.* (2011) 'Mutations in the p53 tumor suppressor gene: Important milestones at the various steps of tumorigenesis', *Genes and Cancer*, 2(4), pp. 466–474.

Robertson, J. F. R. (1996) 'Oestrogen receptor: A stable phenotype in breast cancer', *British Journal of Cancer*, 73(1), pp. 5–12.

Ross-Innes, C. S. *et al.* (2010) 'Cooperative interaction between retinoic acid receptor-α and estrogen receptor in breast cancer', *Genes and Development*, 24(2), pp. 171–182.

Schaeffer, D. *et al.* (2014) 'Cellular Migration and Invasion Uncoupled: Increased Migration Is Not an Inexorable Consequence of Epithelial-to-Mesenchymal Transition', *Molecular and Cellular Biology*, 34(18), pp. 3486–3499.

Schaertl, S. *et al.* (2010) 'A profiling platform for the characterization of transglutaminase 2 (TG2) inhibitors', *Journal of Biomolecular Screening*, 15(5), pp. 478–487.

Shankar, S. *et al.* (2020) 'Altered RNA splicing by mutant p53 activates oncogenic RAS signaling in pancreatic cancer', *Nature Communications*, 38(2), pp. 1–17.

Shao, M. *et al.* (2009) 'Epithelial-to-mesenchymal transition and ovarian tumor progression induced by tissue transglutaminase', *Cancer Research*, 69(24), pp. 9192–9201.

Shaw, F. L. *et al.* (2012) 'A Detailed Mammosphere Assay Protocol for the Quantification of Breast Stem Cell Activity', *Journal of mammary gland biology and neoplasia*, 17(2), pp. 111–117.

Sheridan, C. *et al.* (2006) 'CD44+/CD24-Breast cancer cells exhibit enhanced invase properties: An early step necessary for metastasis', *Breast Cancer Research*, 8(5), pp. 1–13.

Shimada, J. *et al.* (2001) 'Transactivation via RAR/RXR-Sp1 Interaction: Characterization of Binding Between Sp1 and GC Box Motif', *Cell Regulation*, 15(10), pp. 1677–1692.

Shiohara, M. *et al.* (1996) 'Effects of novel retinoid X receptor-selective ligands on myeloid leukemic differentiation and proliferation in vitro', *Blood*, 87(5), pp. 1977–1984.

Shrestha, B. *et al.* (2014) 'Upregulation of Transglutaminase and ε (γ -Glutamyl)-Lysine in the Fisher-Lewis Rat Model of Chronic Allograft Nephropathy', *BioMed Research International*, 2014(July 2014).

Siegel, D. *et al.* (2009) 'Vorinostat in solid and hematologic malignancies', *Journal of Hematology and Oncology*, 2, pp. 1–11.

Siegel, M. and Khosla, C. (2007) 'Transglutaminase 2 inhibitors and their therapeutic role in disease states', *Pharmacology and Therapeutics*, 115(2), pp. 232–245.

Silva, J. L. *et al.* (2014) 'Prion-like aggregation of mutant p53 in cancer', *Trends in Biochemical Sciences*, 39(6), pp. 260–267.

Singh, G. *et al.* (2016) 'The different conformational states of tissue transglutaminase have opposing affects on cell viability', *Journal of Biological Chemistry*, 291(17), pp. 9119–9132.

Singh, U. S. and Cerione, R. A. (1996) 'Biochemical effects of retinoic acid on GTP-binding protein/transglutaminases in HeLa cells: Stimulation of GTP-binding and transglutaminase activity, membrane association, and phosphatidylinositol lipid turnover', *Journal of Biological Chemistry*, 271(44), pp. 27292–27298.

Smith, P. K. *et al.* (1985) 'Measurement of protein using bicinchoninic acid', *Analytical Biochemistry*, 150(1), pp. 76–85.

Song, M. *et al.* (2017) 'Recent progress in the development of transglutaminase 2 (TGase2)

Inhibitors: Miniperspective', *Journal of Medicinal Chemistry*, 60(2), pp. 554–567.

Storms, R. W. *et al.* (1999) 'Isolation of primitive human hematopoietic progenitors on the basis of aldehyde dehydrogenase activity', *Proceedings of the National Academy of Sciences of the United States of America*, 96(16), pp. 9118–9123.

Sullivan, N. *et al.* (2009) 'Interleukin-6 induces an epithelial–mesenchymal transition phenotype in human breast cancer cells', *Oncogene*, 28(33), pp. 2940–2947.

Sung, H. *et al.* (2021) 'Global Cancer Statistics 2020: GLOBOCAN Estimates of Incidence and Mortality Worldwide for 36 Cancers in 185 Countries', *CA: A Cancer Journal for Clinicians*, 71(3), pp. 209–249.

Suto, N., Ikura, K. and Sasaki, R. (1993) 'Expression induced by interleukin-6 of tissue-type transglutaminase in human hepatoblastoma HepG2 cells', *Journal of Biological Chemistry*, 268(10), pp. 7469–7473.

Szondy, Z. *et al.* (2017) 'Transglutaminase 2 in human diseases', *BioMedicine*, 7(3), p. 15.

Tatsukawa, H. *et al.* (2016) 'Transglutaminase 2 has opposing roles in the regulation of cellular functions as well as cell growth and death.', *Cell death & disease*. Nature Publishing Group, 7(6), p. e2244.

Tatsukawa, H. and Hitomi, K. (2021) 'Role of transglutaminase 2 in cell death, survival, and fibrosis', *Cells*, 10(7), p. 1842.

Tee, A. E. L. *et al.* (2010) 'Opposing effects of two tissue transglutaminase protein isoforms in neuroblastoma cell differentiation', *Journal of Biological Chemistry*, 285(6), pp. 3561–3567.

Tempest, R. *et al.* (2021) 'The biological and biomechanical role of transglutaminase-2 in the tumour microenvironment', *Cancers*, 13, p. 2788.

Theodosiou, M., Laudet, V. and Schubert, M. (2010) 'From carrot to clinic: An overview of the retinoic acid signaling pathway', *Cellular and Molecular Life Sciences*, 67(9), pp. 1423–1445.

Thiery, J. P. (2003) 'Epithelial-mesenchymal transitions in development and pathologies', *Current Opinion in Cell Biology*, 15(6), pp. 740–746.

Thiery, J. P. *et al.* (2009) 'Epithelial-Mesenchymal Transitions in Development and Disease',

Cell, 139(5), pp. 871–890.

Towbin, H., Staehelin, T. and Gordon, J. (1979) 'Electrophoretic transfer of proteins from polyacrylamide gels to nitrocellulose sheets: procedure and some applications.', *Proceedings of the National Academy of Sciences*, 76(9), pp. 4350–4354.

Tsang, J. Y. S. and Tse, G. M. (2020) 'Molecular classification of breast cancer', *Advances in anatomic pathology*, 27(1), pp. 27-35.

Tsuji, N. *et al.* (1976) 'A new antifungal antibiotic, trichostatin', *The Journal of antibiotics*, 29(1), pp. 1–6.

Ulukan, B. *et al.* (2020) 'Role of tissue transglutaminase catalytic and guanosine triphosphate-binding domains in renal cell carcinoma progression', *ACS Omega*, 5(43), pp. 28273–28284.

Di Venere, A. *et al.* (2000) 'Opposite effects of Ca2+ and GTP binding on tissue transglutaminase tertiary structure', *Journal of Biological Chemistry*, 275(6), pp. 3915–3921.

Verma, A. *et al.* (2006) 'Increased Expression of Tissue Transglutaminase in Pancreatic Ductal Adenocarcinoma and Its Implications in Drug Resistance and Metastasis', *Cancer research*, 66(21), pp. 10525–10533.

Verma, A., Guha, S., Diagaradjane, P., *et al.* (2008) 'Therapeutic significance of elevated tissue transglutaminase expression in pancreatic cancer', *Clinical Cancer Research*, 14(8), pp. 2476–2483.

Verma, A., Guha, S., Wang, H., *et al.* (2008) 'Tissue transglutaminase regulates focal adhesion kinase/AKT activation by modulating PTEN expression in pancreatic cancer cells', *Clinical Cancer Research*, 14(7), pp. 1997–2005.

Verma, A. and Mehta, K. (2007) 'Tissue transglutaminase-mediated chemoresistance in cancer cells', *Drug Resistance Updates*, 10(4–5), pp. 144–151.

Veronesi, U. *et al.* (2006) 'Fifteen-year results of a randomized phase III trial of fenretinide to prevent second breast cancer', *Annals of Oncology*, 17(7), pp. 1065–1071.

Vichai, V. and Kirtikara, K. (2006) 'Sulforhodamine B colorimetric assay for cytotoxicity screening', *Nature Protocols*, 1(3), pp. 1112–1116.

Vikram, R. *et al.* (2020) 'Tumorigenic and Metastatic Role of CD44−/low/CD24−/low Cells in

Luminal Breast Cancer', *Cancers*, 12(1239), pp. 1–23.

Vogel, V. G. *et al.* (2003) 'National surgical adjuvant breast and bowel project update: Prevention trials and endocrine therapy of ductal carcinoma in situ', *Clinical Cancer Research*, 9(1 II), pp. 495–501.

Vousden, K. H. and Prives, C. (2009) 'Blinded by the Light: The Growing Complexity of p53', *Cell*, 137(3), pp. 413–431.

Wang, H. *et al.* (2016) 'Bufalin suppresses cancer stem-like cells in gemcitabine-resistant pancreatic cancer cells via Hedgehog signaling', *Molecular Medicine Reports*, 14(3), pp. 1907–1914.

Wang, X. *et al.* (2020) 'Trichostatin A reverses epithelial-mesenchymal transition and attenuates invasion and migration in MCF-7 breast cancer cells', *Experimental and Therapeutic Medicine*, 19(3), pp. 1687–1694.

Wang, Z. *et al.* (2010) 'Acquisition of Epithelial-Mesenchymal Transition phenotype of gemcitabine-resistant pancreatic cancer cells is linked with activation of Notch signaling pathway', *Cancer research*, 69(6), pp. 2400–2407.

Wang, Z. and Griffin, M. (2013) 'The Role of TG2 in Regulating S100A4-Mediated Mammary Tumour Cell Migration', *PLoS ONE*, 8(3), p. e57017.

Warburg, O. (1956) 'Injuring of Respiration the Origin of Cancer Cells', *Science*, 123(3191), pp. 309–14.

Wasielewski, M. *et al.* (2006) 'Thirteen new p53 gene mutants identified among 41 human breast cancer cell lines', *Breast Cancer Research and Treatment*, 99(1), pp. 97–101.

Wawruszak, A. *et al.* (2015) 'Assessment of interactions between cisplatin and two histone deacetylase inhibitors in MCF7, T47D and MDA-MB-231 human breast cancer cell lines - An isobolographic analysis', *PLoS ONE*, 10(11), p. e0143013.

Wawruszak, A. *et al.* (2019) 'Histone deacetylase inhibitors reinforce the phenotypical markers of breast epithelial or mesenchymal cancer cells but inhibit their migratory properties', *Cancer Management and Research*, 11, p. 8345.

Weinberg, R. A. (1995) 'The retinoblastoma protein and cell cycle control', *Cell*, 81(3), pp. 323–330.

Woodhouse, E. C., Chuaqui, R. F. C. and Liotta, L. A. L. (1997) 'General Mechanisms of Metastasis', *Cancer: Interdisciplinary International Journal of the American Cancer Society*, 80(S8), pp. 1529–1537.

Yang, Z. F. *et al.* (2008) 'Significance of CD90+ Cancer Stem Cells in Human Liver Cancer', *Cancer Cell*, 13(2), pp. 153–166.

Yao, W. *et al.* (2020) 'All-trans retinoic acid reduces cancer stem cell-like cell-mediated resistance to gefitinib in NSCLC adenocarcinoma cells', *BMC Cancer*. BMC Cancer, 20(1), pp. 1–9.

Yeh, B. W. *et al.* (2016) 'Histone deacetylase inhibitor trichostatin A resensitizes gemcitabine resistant urothelial carcinoma cells via suppression of TG-interacting factor', *Toxicology and Applied Pharmacology*. Elsevier Inc., 290, pp. 98–106.

York, N. and Clarke, D. D. (1957) 'An enzymically catalyzed incorporation of amines into proteins', *Chemistry Faculty Publications*, 25, pp. 451–452.

Yoshida, M. *et al.* (1990) 'Potent and specific inhibition of mammalian histone deacetylase both in vivo and in vitro by trichostatin A', *Journal of Biological Chemistry*, 265(28), pp. 17174–17179.

Yu, Z. *et al.* (2012) 'Cancer stem cells', *International Journal of Biochemistry and Cell Biology*. Elsevier Ltd, 44(12), pp. 2144–2151.

Zakrzewski, W. *et al.* (2019) 'Stem cells: past, present, and future', *Stem Cell Research & Therapy*, 10(1), pp. 1–22.

Zanetti, A. *et al.* (2015) 'All-trans-retinoic Acid Modulates the plasticity and inhibits the motility of breast cancer cells role of notch1 and transforming growth factor (TGF β)', *Journal of Biological Chemistry*, 290(29), pp. 17690–17709.

Zemskov, E. A. *et al.* (2006) 'The role of tissue transglutaminase in cell-matrix interactions.', *Frontiers in bioscience*, 11(1), pp. 1057–1076.

Zhang, L.-X. *et al.* (1995) 'Evidence for the involvement of retinoic acid receptor RARα-dependent signaling pathway in the induction of tissue transglutaminase and apoptosis by retinoids', *Journal of Biological Chemistry*, 270(11), pp. 6022–6029.

Zhao, Y. *et al.* (2014) 'Anticancer activity of SAHA, a potent histone deacetylase inhibitor, in

NCI-H460 human large-cell lung carcinoma cells in vitro and in vivo', *International Journal of Oncology*, 44(2), pp. 451–458.

Chapter 9

Appendicies

9. Chapter 9: Appendicies

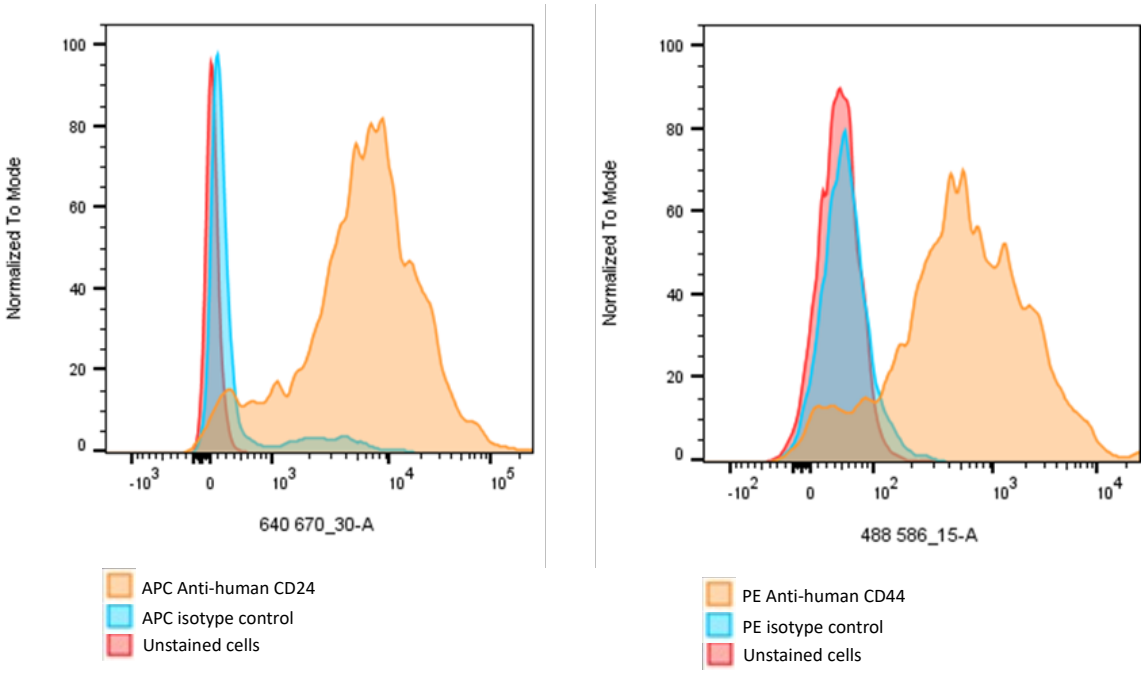

Figure 9-1 Representative flow cytometry plots for CD24 and CD44 isotype control in MCF.7 cells

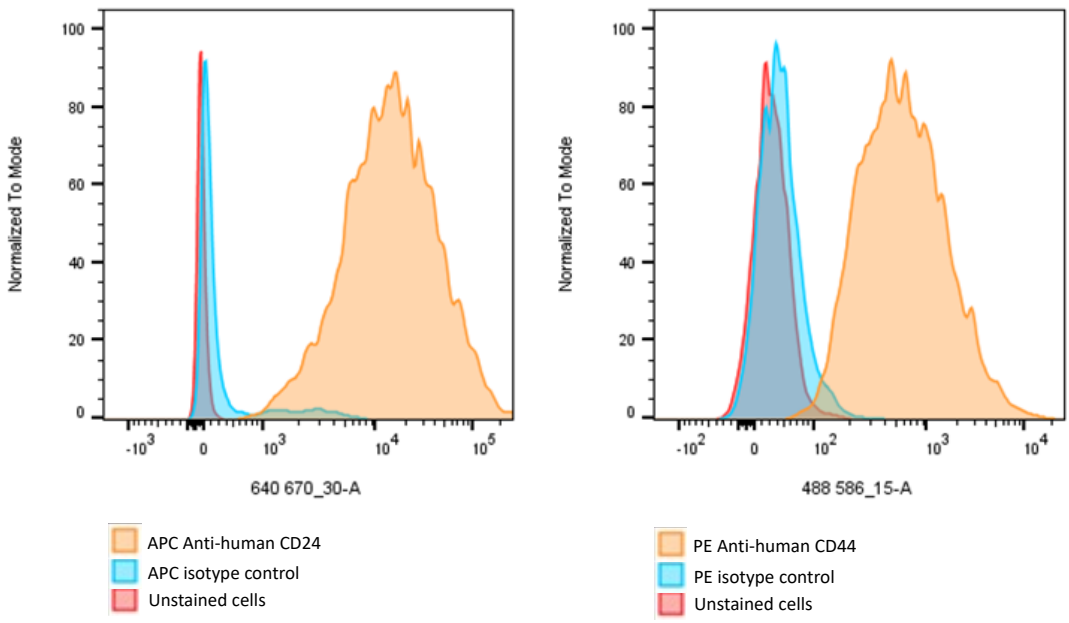

Figure 8-2 Representative flow cytometry plots for CD24 and CD44 isotype control in T47D cells

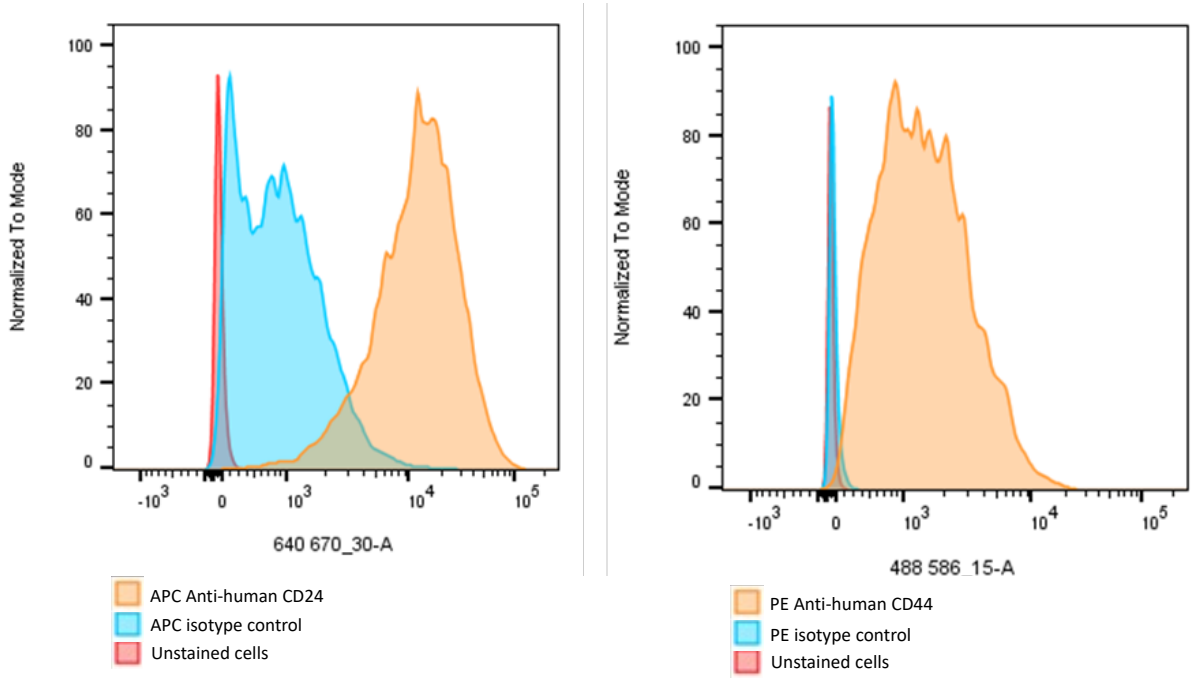

Figure 9-3 Representative flow cytometry plots for CD24 and CD44 isotype control in MDA-MB-468 cells

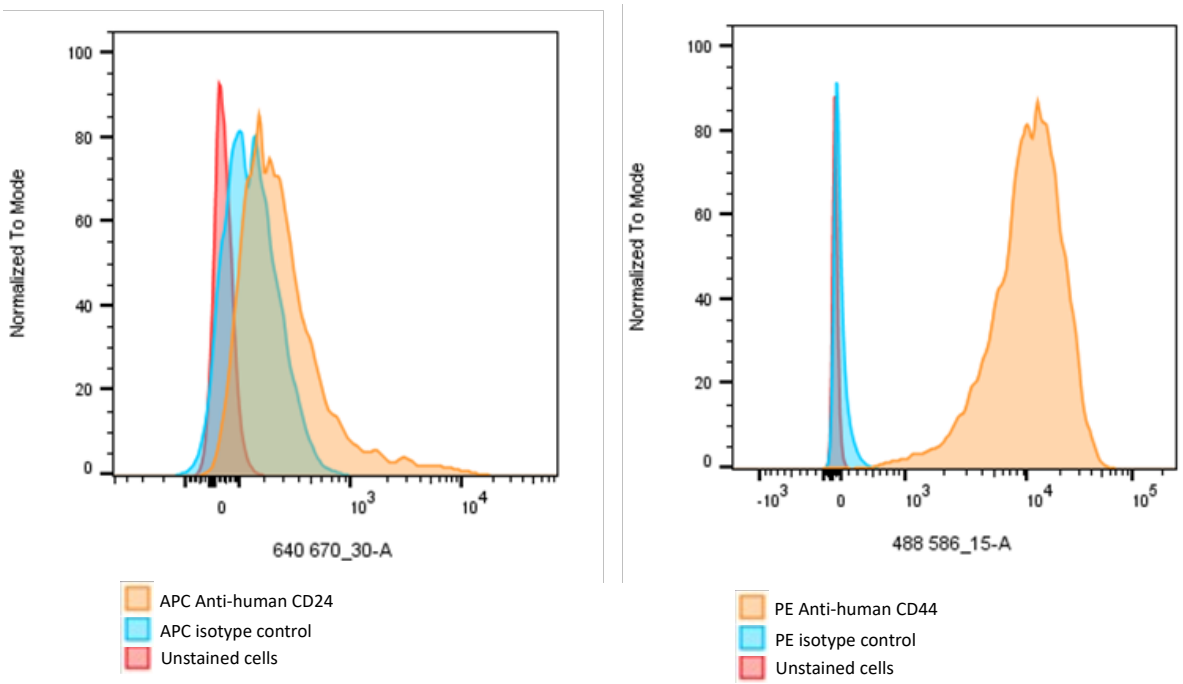

Figure 9-4 Representative flow cytometry plots for CD24 and CD44 isotype control in MDA-MB-231 cells

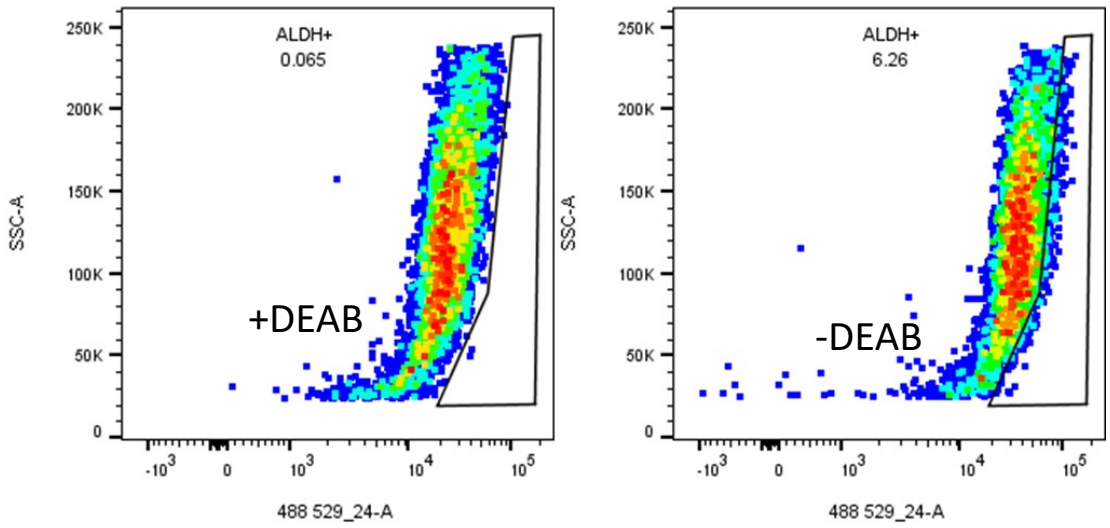

Figure 9-5 Representative flow cytometry plots for ALDH cells in positive control A-549 lung cancer cell line